A metabolomics investigation of selected m.3243A>G mutation phenotypes

K Esterhuizen

orcid.org 0000-0002-1884-8419

Thesis submitted in fulfilment of the requirements for the degree *Doctor of Philosophy in Biochemistry* at the North-West University

Promoter:	Prof R Louw
Assistant Promoter:	Prof JZ Lindeque

Graduation October 2018

20745044

“Through many dangers, toils and snares, I

have already come;

'Tis Grace that brought me safe thus far and

Grace will lead me home.”

Acknowledgements

Taking on a journey like this is not easy. You need lots of support, guidance and love. I was fortunate enough to be blessed with a group of people providing me with just that and more. At the end of this long road I want to acknowledge and thank these important people.

Absolutely nothing would have been possible without **Jesus Christ** in my life. Thank You for the talents You gave me, for giving me the strength to complete this long road and for all the wonderful people You put into my life. Thank You for carrying me when I stumbled. All glory to Your name!

My supervisors, **Prof. Roan Louw** and **Dr. Zander Lindeque**. I will always be grateful for your support and guidance throughout this journey. I have learned valuable lessons from the both of you that I will carry with me for the rest of my life.

My mom and dad, **Suzi** and **Johan**. Thank you for being my biggest cheerleaders, for believing in me when I didn't, for listening to all my stories and for being tough when I needed it the most. Words will never be enough to tell you how much I love you!

My brother and sister-in-law, **Riaan** and **Lané**. Thank you for always looking very interested even if you didn't understand a word I said. Thank you for all of your love and support, but most of all thank you for just being you!

My best friend, **Bianca**. We have walked a long road together and I would have not been able to do it without you by my side. Thank you for being such a big part of my life. Thank you for all the late night coffees, encouragement and cheering up. I am looking forward to this next chapter in our friendship!

To my NWU family, especially **Jaundrie** and **Leonie**. Potchefstroom would have been very boring without you there. Thank you for your support and friendship.

The **National Research Foundation (NRF)**, the **Technology Innovation Agency (TIA)** and **the North-West University (NWU)** for financial support.

There are a few people that I want to mention by name. **Dr. Channa**, thank you for all your support and understanding. **Bronwyn**, thank you for your friendship and being weird with me. **Ron** and **Karinda**, my chosen family. Thank you for being there without you even knowing it!

Finally, my husband, **Dewald**. Where do I start? Thank you for dreaming with me. Thank you for loving me through this crazy adventure and for willingly taking a back seat for the last six years. I am looking forward to living and enjoying life with you. Our time starts now. I love you to the moon and back times infinity plus too much!

Abstract

Mitochondrial disease (MD) is a subgroup of inborn errors of metabolism, which can be caused by a mutation in either the nuclear DNA (nDNA) or mitochondrial DNA (mtDNA). One of the most common mtDNA disease causing mutations is the m.3243A>G point mutation, which affects the incorporation of the amino acid leucine into mitochondrial proteins and thus the oxidative phosphorylation system (OXPHOS) system. This mutation was initially linked to mitochondrial myopathy, encephalopathy lactic acidosis and stroke like episodes (MELAS), but various other phenotypes and symptoms was later linked to this mutation, including progressive external ophthalmoplegia (PEO), maternally inherited diabetes-deafness (MIDD) and myopathy. However, the reason why these patients presents with such a broad spectrum of symptoms, even though they harbor the same mutation, remains unknown. Therefore, the aim of this study was to investigate the urine metabolome of a cohort of m.3243A>G diagnosed patients, presenting with different phenotypes (MELAS, MIDD and myopathy), using a multi-platform metabolomics approach.

This multi-platform metabolomics approach consisted of untargeted as well as targeted analytical methods. The untargeted analyses consisted of gas chromatography–mass spectrometry (GC-MS), nuclear magnetic resonances (NMR) spectroscopy, and liquid chromatography mass spectrometry with ion mobility (LC-IM-MS), in negative as well as positive ionization mode, while the targeted analyses consisted of liquid chromatography tandem-mass spectrometry (LC-MS/MS). Using this multi-platform metabolomics approach enabled us to analyze a larger portion of the metabolome compared to using a single analytical technique.

In the first part of the study, we investigated 9 patients presenting specifically with MELAS and 29 healthy controls. We were able to identify 36 metabolites that were altered in the patient group when compared to healthy controls. When investigating these 36 metabolites further, we were able to link them to redox imbalance as a result of a defective OXPHOS system and stalled fatty acid oxidation. Our investigation also resulted in the first association between MELAS and an intricate web of affected pathways consisting of the one-carbon metabolism, methylation cycle and the transsulfuration pathway. In order to validate the 36 markers identified, a new cohort consisting of two MELAS patients and seven controls were used. We demonstrate complete separation of the MELAS patients and controls using principle component analysis, thus indicating that the 36 markers are not unique to the initial cohort used and thus have potential for diagnosis or treatment monitoring.

In the second part of the study, we expanded on the findings by investigating two additional m.3243A>G associated phenotypes, MIDD (n = 30) and myopathy (n = 18). These two phenotypes, together with the MELAs cohort were compared to healthy controls, and to one another, in order to find not only metabolic similarities between the different phenotypes, but also phenotypic specific perturbations. Our novel findings indicate, especially in the MELAS patients, increased *de novo* fatty acid synthesis (FAS) in the mitochondria. We hypothesize that this increased FAS is probably due to lipoic acid synthesis, an essential cofactor for pyruvate dehydrogenase, 2-ketoglutarate dehydrogenase as well as the glycine cleavage system. Furthermore, we show specific metabolic perturbations in each of the three phenotypes. Investigating the metabolic similarities, we found three metabolites that were perturbed in all three phenotypes, 2-hydroxyglutaric acid, glycolic acid and 4-pentenoic acid. We conclude that these metabolites should be further investigated for diagnostic potential.

The strength of our study was the utilization of different analytical platforms to generate the robust metabolomics data reported here. We show that urine may be a useful source for disease-specific metabolomics data. Our study contributed to the mitochondrial disease research field by providing significant insight into metabolic alterations caused by the m.3243A>G mutation. Firstly, results obtained in both parts of this study showcased the valuable information that could be obtained when implementing metabolomics as investigation tool. Secondly our results highlighted the potential for mitochondrial disease biosignatures for disease mechanistic understanding. Finally, we pointed out several important metabolic pathways affected in these patients that could be investigated in future studies. Ultimately, understanding the m.3243A>G mutation could lead to better diagnostic and treatment options, which both doctors and patients would benefit from immensely.

Keywords: Metabolomics; MELAS; MIDD; myopathy; mitochondrial disease; m.3243A>G

Table of Contents

Acknowledgements ..... **iii**

Abstract ..... **v**

List of Tables ..... **xv**

List of Figures ..... **xvi**

List of Symbols and Abbreviations ..... **xviii**

CHAPTER 1: Introduction **1**

1.1 Background and Motivation **1**

1.2 Aim and Objectives of This Study **2**

1.2.1 Aim 2

1.2.2 Specific objectives 2

1.3 Structure of Thesis **2**

1.4 Outcomes of the Study **4**

1.4.1 Published peer-reviewed article 1 (Chapter 2, Annexure A) 4

1.4.2 Published peer-reviewed article 2 (Chapter 4, Annexure B) 4

1.4.3 Manuscript to be submitted (Chapter 5) 4

1.4.4 Poster presentation 5

1.5 Ethics **5**

1.6 Financial Support **5**

1.7 Author Contribution **5**

CHAPTER 2: Literature Review **8**

2.1 Metabolomics of Mitochondrial Disease 8

2.1.1 Introduction 8

2.1.2 Mitochondrial disease as an inherited metabolic disease 8

2.1.3 Metabolomics: general applications and platforms 9

2.1.4 The application of metabolomics in mitochondrial disease research 11

2.1.4.1 Models 11

2.1.4.2 Defining patient and control groups for metabolomics investigations 12

2.1.4.3 Metabolites and pathways affected by mitochondrial disease 13

2.1.5 Conclusions and future prospects of metabolomics in mitochondrial disease investigations 37

2.2 Mitochondrial Disease Caused by the m.3243A>G Mutation 38

2.2.1 Introduction 38

2.2.2 Mitochondrial bioenergetics 38

2.2.2.1 The mitochondrion 38

2.2.2.2 The OXPHOS system 40

2.2.3 Mitochondrial genetics 40

2.2.3.1 Mitochondrial DNA (mtDNA) 40

2.2.3.2 Replication, transcription, and translation of mtDNA 42

2.2.3.2.1 Introduction 42

2.2.3.2.2 Replication of mitochondrial DNA 42

2.2.3.2.3 Transcription of mtDNA 43

2.2.3.2.4 Translation of mtDNA 44

2.2.4 Mitochondrial disease caused by mtDNA mutations 45

2.2.4.1 Heteroplasmy, threshold effect and mtDNA copy number 45

2.2.4.2 mtDNA mutations (Point mutations, rearrangements and deletions) 46

2.2.4.2.1 Point mutations 46

2.2.4.2.2 Rearrangements (Deletion and duplication) 47

2.2.5 The m.3243A>G mutation 48

2.2.5.1 Background 48

2.2.5.2 Symptoms and phenotypes associated with the m.3243A>G mutation 50

2.2.5.2.1 Mitochondrial encephalopathy, lactic acidosis, and stroke-like episodes (MELAS) 50

2.2.5.2.2 Kearns-Sayre syndrome (KSS) 51

2.2.5.2.3 Maternally inherited diabetes and deafness (MIDD) 51

2.2.5.2.4 Progressive external ophthalmoplegia (PEO) 52

2.2.5.2.5 Leigh syndrome (LS) 52

2.2.5.2.6 Myoclonus epilepsy with ragged red fibers (MERRF) 53

2.2.6 Diagnosis of m.3243A>G patients 54

2.2.6.1 Family history 55

2.2.6.2 Clinical assessments 55

2.2.6.3 Biochemical investigations 56

2.2.6.4 Muscle histochemistry 56

2.2.6.5 Molecular genetic testing 56

2.2.7 Management of m.3243A>G patients 57

2.2.7.1 Genetic counselling 57

2.2.7.2 Supportive therapy 57

2.2.7.3 Pharmacological therapy 58

2.3 Study Design 59

2.4 References 62

CHAPTER 3: Analytical Methods, Bioinformatics and Data Quality 80

3.1 Introduction 80

3.2. Samples and Ethics 80

3.3 Analytical Methods 81

3.3.1 Reagents 81

3.3.2 Preparation of reagents 82

3.3.2.1 Preparation of reagents for creatinine quantification 82

3.3.2.2 Preparation of GC-MS reagents 82

3.3.2.3 Preparation of reagents used for LC analyses 83

3.3.2.4 Preparation of internal standard solutions 83

3.3.3 Osmolality determination 84

3.3.4 Creatine quantification 84

3.3.4.1 Sample preparation 84

3.3.4.2 Instrumentation 84

3.3.5 Gas chromatography mass spectrometry (GC-MS) 84

3.3.5.1 Sample preparation 84

3.3.5.2 Instrumentation 85

3.3.6 Nuclear magnetic resonance (NMR) spectroscopy 85

3.3.6.1 Sample preparation 85

3.3.6.2 Instrumentation 86

3.3.7 Liquid chromatography-tandem mass spectrometry (LC-MS/MS) 86

3.3.7.1 Sample preparation 86

3.3.7.2 Instrumentation 86

3.3.8 Untargeted liquid chromatography - ion mobility - mass spectrometry (LC-IM-MS) 89

3.3.8.1 Sample preparation 89

3.3.8.2 Instrumentation 89

3.4 Batch Composition and Data Quality 91

3.5 Bioinformatics 91

3.6 References 94

CHAPTER 4: A Urinary Biosignature for Mitochondrial Myopathy, Encephalopathy, Lactic Acidosis and Stroke Like Episodes (MELAS) 96

4.1 Introduction 96

4.2 Methods 97

4.2.1 Patients and ethics 97

4.2.2 Metabolic profiling 100

4.2.3 Statistical analyses 100

4.3 Results 102

4.3.1 Exploratory phase 102

4.3.2 Validation phase 104

4.4 Discussion 105

4.5 Conclusion 111

4.6 References 112

4.7 Supplementary Information 115

4.7.1 Urine quality control sample 115

4.7.2 Urine metabolomic analyses 115

4.7.2.1 Gas chromatography mass spectrometry (GC-MS) 115

4.7.2.2 Targeted LC-MS 116

4.7.2.3 Nuclear magnetic resonance (NMR) spectroscopy 117

4.7.2.4 Untargeted liquid chromatography - ion mobility - mass spectrometry (LC-IM-MS) 117

4.7.3 Data pre-processing, normalization and extraction 118

CHAPTER 5: One Mutation, Three Phenotypes: A Metabolic Comparison of MELAS, MIDD and Myopathy Caused by the M.3243A>G Mutation 119

5.1 Introduction 119

5.2 Results and Discussion 120

5.2.1 Patient and control characteristics 120

5.2.2 Metabolic perturbations 123

5.2.2.1 Common metabolic traits of the m.3243A>G mutation 128

5.2.2.2 Metabolic perturbation of MELAS 131

5.2.2.3 Metabolic perturbation of MIDD 136

5.2.2.4 Metabolic perturbation of myopathy 138

5.3 Conclusion 138

5.4 Experimental Procedures 139

5.4.1 Patients and Ethics 139

5.4.2 Metabolic Profiling 139

5.4.3 Data mining and statistical analyses 139

5.4.4 Acknowledgements 140

5.4.5 Supplemental information 140

5.4.6 Author contributions 140

5.4.7 Declaration of interests 141

5.5 References 141

5.6 Supplementary Information 145

5.6.1 Quality control sample and batch composition 145

5.6.2 Analytical platforms and sample analyses 145

5.6.3 Pre-processing, normalization and extraction of data 145

5.6.4 References 148

CHAPTER 6: Conclusion 149

6.1 Introduction 149

6.2 Summary on the Findings from This Study 150

6.2.1 Chapter 2 – Literature review 150

6.2.2 Chapter 4 – Biosignature for MELAS 151

6.2.3 Chapter 5 – Comparing three m.3243A>G phenotypes 152

6.3 Strengths and Limitations of This Study 154

6.3.1 Strengths 154

6.3.1.1 Patient and control samples 154

6.3.1.2 Multi-platform metabolomics approach 154

6.3.2 Limitations 155

6.3.2.1 Identification of features/metabolites from the untargeted metabolomics data 155

6.3.2.2 Number of patients per phenotype 155

6.3.2.3 Medication and supplements 156

6.3.2.4 Normalization of metabolomics data 156

6.4 For Future Studies 157

6.4.1 Pathways affected in different phenotypes 157

6.4.2 Reinvestigate untargeted LC-IM-MS data 158

6.5 Conclusion 158

6.6 References 159

ANNEXURE A 161

ANNEXURE B 176

ANNEXURE C 190

List of Tables

CHAPTER 2

Table 2.1: Metabolites associated with mitochondrial disease when compared to healthy controls 16

Table 2.2: Summary of different organs and symptoms associated with the m.3243A>G mutation 54

Table 2.3: Treatment options for patients with the mitochondrial m.3243A>G mutation 58

CHAPTER 3

Table 3.1: Mobile phase gradient used for separation of metabolites 87

Table 3.2: Precursor/product ion transitions and instrument conditions of metabolites being monitored 87

CHAPTER 4

Table 4.1: Characteristics of the MELAS patients and healthy controls of the Nijmegencohort used in this study 98

Table 4.2: Characteristics of the MELAS patients and healthy controls of the Helsinki cohort used in this study 99

Table 4.3: List of 36 metabolites that differed significantly between MELAS patients and controls in the Nijmegen cohort 101

CHAPTER 5

Table 5.1: Characteristics of the patients and healthy controls used in this study 122

Table 5.2: List of metabolites that differ significantly between m.3243A>G mutation phenotypes and controls 125

List of Figures

CHAPTER 2

Figure 2.1: Summary of the perturbed metabolism detected in different mitochondrial disease models 36

Figure 2.2: Structure of the mitochondrion 40

Figure 2.3: Structure of mitochondrial DNA (mtDNA) 41

Figure 2.4: Replication of mtDNA 43

Figure 2.5: Selected mtDNA point mutations 47

Figure 2.6: Cloverleaf structures of tRNAsLeu (UUR) (m.3243A>G) 49

Figure 2.7: Flow diagram of the analytical approach followed in this study 61

CHAPTER 3

Figure 3.1: Flow diagram of the sample preparation procedure followed in this study 90

CHAPTER 4

Figure 4.1: Differences between Controls and MELAS patients of the exploration (Nijmegen) cohort using the 36 selected variables 103

Figure 4.2: Venn diagram illustrating the contribution of each analytical platform to the detection of the 36 important metabolites 104

Figure 4.3: Differences between Controls and MELAS patients of the validation (Helsinki) cohort using the 36 selected variables 105

Figure 4.4: Schematic representation of the altered metabolism detected in the MELAS patients compared to healthy controls 110

CHAPTER 5

Figure 5.1: PCA score plots of MELAS (A), MIDD (B), and Myopathy (C) patients against Controls 124

Figure 5.2: Volcano plots (A-C) and heat maps (D-F) depicting statistically significant metabolites that discriminate the MELAS (A&D), MIDD (B&E) and myopathy (C&F) patients from the controls. A) MELAS vs controls 127

Figure 5.3: Venn diagram used to identify VIPs that are affected in more than one phenotype 128

Figure 5.4: Quantitative profiling of selected metabolites 130

Figure 5.5: Metabolic charts of the perturbed metabolism detected in MELAS, MIDD and myopathy 136

Figure 5.6: Schematic overview of the study 147

List of Abbreviations and Symbols

↑	increase
↓	decrease
>	greater-than
<	less-than
±	plus-minus
&	and
°C	degree Celsius
°C/min	degree Celsius per minute
× g	times gravity
β	beta
µ	micro
µL	microliter
µm	micrometer
µs	microsecond
%	percent
mg%	milligram per cent
I	one
II	two
III	three
V	five
2-HG	2-hydroxyglutaric acid
A	adenine
A	acceptor site
ACE	angiotensin-converting-enzyme

ADP	adenosine diphosphate
ANOVA	analysis of variance
AMP	adenosine monophosphate
AMPK	adenosine monophosphate-activated protein kinase
ARB	Angiotensin Receptor Blocker
ATP	adenosine triphosphate
ATPase	adenylpyrophosphatase
a-vO2	arteriovenous oxygen
BCKDC	Branched-chain α-ketoacid dehydrogenase complex
BCAA	branched-chain amino acid
BSTFA	O-bis(trimethylsilyl)trifluoro acetamide
C2-carnitine	acetyl-carnitine
C3-carnitine	propionyl-carnitine
C4-carnitine	butanoyl-carnitine
C5-carnitine	isovaleryl-carnitine
C12-carnitine	dodecanoylcarnitine
CI KO	Complex I knockout
CII KO	Complex II knockout
CIII KO	Complex III knockout
CCS	collision cross section
CE	capillary electrophoresis
C. elegans	Caenorhabditis elegans
ChEBI	Chemical Entities of Biological Interest
CID	collision-induced dissociation
CK	creatine kinase
CNS	central nervous system
CoA	Coenzyme A
CoQ10	Coenzyme Q10

COX	cytochrome c oxidase
CS	citrate synthase
CT	computed tomography
CV	coefficient of variation
Cyt b	cytochrome b
D_2O	deuterium oxide
dCMP	deoxycytidine monophosphate
DMSO	dimethyl sulfoxide
DNA	deoxyribonucleic acid
Dnase	deoxyribonuclease
dNTP	deoxynucleotide
dTMP	deoxythymidine monophosphate
E	exit site
ECG	electrocardiography
EDTA	ethylenediaminetetraacetic acid
e.g.	for example
EMG	electromyography
ESI	Electrospray ionization
EtBr	Ethidium bromide
FAD	flavin adenine dinucleotide (quinone form)
$FADH_2$	flavin adenine dinucleotide (hydroquinone form)
FAS	fatty acids synthesis
FDR	false discovery rate
FGF-21	fibroblast growth factor 21
Fmet	N-formylmethionine
FMN	flavin mononucleotide
g	gram
G	guanine

G10	non-G-tract guanine
GC	gas chromatography
GC–MS	gas chromatography–mass spectrometry
GC-TOF-MS	gas chromatography time-of-flight mass spectrometry
GDF-15	growth differentiation factor-15
GI	gastrointestinal
GDP	guanosine diphosphate
GMP	guanosine monophosphate
GTP	guanosine triphosphate
HCl	hydrogen chloride
HDMSe	high-definition mass spectrometry
HMDB	Human Metabolome Database
HREC	Health Research Ethics Committee
HSP	heavy-strand promoter
Hz	hertz
IEM	inborn error of metabolism
kDa	kilodaltons
KH_2PO_4	potassium phosphate monobasic
KOH	potassium hydroxide
KSS	Kearns-Sayre syndrome
LC	liquid chromatography
LC-MS/MS	liquid chromatography tandem-mass spectrometry
LC-MS	liquid chromatography–mass spectrometry
LC-IM-MS	liquid chromatography mass spectrometry with ion mobility
LDH	lactate dehydrogenase
Leu	leucine
LHON	Leber's hereditary optic neuropathy
L/min	liter per minute

LS	Leigh syndrome
LSP	L-strand promotor
LSU	large subunit
MD	mitochondrial disease
MELAS	mitochondrial encephalomyopathy, lactic acidosis, and stroke-like episodes
MERRF	myoclonic epilepsy with ragged red fibers
Met	methionine
MIDD	maternally inherited diabetes and deafness
M	Molar
m	meter
MERRF	myoclonic epilepsy with ragged-red fibers
mg	milligram
mg/L	milligrams per liter
mg/mL	milligrams per milliliter
MHz	megahertz
MIRAS	mitochondrial recessive ataxia syndrome
mL	milliliter
mm	millimeter
mL/min	milliliter per minute
mmol/L	millimoles per liter
mOsm/kg	milliosmoles per kilogram
MOX	methoxyamine hydrochloride
MRI	magnetic resonance imaging
MRM	multiple reaction monitoring
mRNA	messenger RNA
MS	mass spectrometry

mTOR	mammalian target of rapamycin
mtDNA	mitochondrial DNA
mtEFT	mitochondrial elongation factor
mtERF	mitochondrial transcription termination factor
mtIF	mitochondrial translation factor
mtRF	mitochondrial release factor
mtRRF	mitochondrial ribosome recycling factor
mt-SSB	mitochondrial single-stranded binding protein
MT-TF	Mitochondrially encoded tRNA phenylalanine
MT-TL	Mitochondrially Encoded TRNA Leucine 1
m/z	mass-to-charge ratio
N	Normal
N/A	not applicable
NaN_3	sodium azide
NADH	reduced nicotinamide adenine dinucleotide
NAD+	oxidized nicotinamide adenine dinucleotide
NADPH	nicotinamide adenine dinucleotide phosphate
NaOH	sodium hydroxide
NARP	Neuropathy, ataxia, and retinitis pigmentosa
nDNA	nuclear DNA
NDUFS4	NADH: Ubiquinone Oxidoreductase Subunit S4
NIST	National Institute of Standards and Technology
nm	nanometers
NMDAS	The Newcastle Mitochondrial Disease Scale for Adults
NMR	nuclear magnetic resonances
NWU	North-West University
O_H	heavy strand origin site
O_L	light strand origin site

OPA 1	mitochondrial dynamin like GTPase
OXPHOS	oxidative phosphorylation system
P	peptidyl site
Pa	pascal
PCA	principle component analysis
PCR	Polymerase chain reaction
PCr	phosphocreatine
PDHc	pyruvate dehydrogenase complex
PEO	progressive external ophthalmoplegia
POLG	DNA polymerase gamma
POLRMT	RNA polymerase mitochondrial
PPAR	peroxisome proliferator-activated receptors
Q-TOF	quadrupole–time-of-flight
QC	quality control
s	second
SA	South Africa
SAM	S-adenosylmethionine
SDH	Succinate dehydrogenase
SSCP	single strand conformation polymorphism
SSU	small subunit
RC	respiratory chain
RFLP	restriction fragment length polymorphism
RNA	ribonucleic acid
RRF	ragged red fibers
RRM2B	ribonucleoside-diphosphate reductase subunit M2 B
rRNA	ribosomal ribonucleic acid
TCA	tricarboxylic acid
TFAM	transcription activator

TFB2M	transcription factor
THF	tetrahydrofolate
TIA	Technology Innovation Agency
TMA	trimethylamine
TMAO	trimethylamine N-oxide
TMCS	trimethylchlorosilane
TOF	time-of-flight
TPS	trimethylsilyl-2,2,3,3-tetradeuteropropionic acid
TSP	trimethylsilyl-2,2,3,3-tetradeuteropropionic acid
tRNA	transfer RNA
UPLC	ultra performance liquid chromatography
USA	United States of America
V	volt
VIP	important metabolites

Chapter 1

Introduction

1

1.1 BACKGROUND AND MOTIVATION

Mitochondrial disease (MD) is a group of diseases, forming part of inborn errors of metabolism, which can be caused by mutations in either the nuclear DNA (nDNA) or mitochondrial DNA (mtDNA). It affects patients of any age, with manifestation of a wide range of symptoms. One of the most common mtDNA disease causing mutations is the m.3243A>G mutation with an estimated prevalence of 1 in 400 (Manwaring et al., 2007). Initially the mutations were referred to as the MELAS mutation, with patients harboring the mutation presenting with a specific set of symptoms consisting of mitochondrial myopathy, encephalopathy, lactic acidosis and stroke like episodes. Since its discovery in 1990, other symptoms and phenotypes have also been associated with this mutation, adding to the complexity of the disease mutation and its associated pathology.

Even though numerous studies have investigated the m.3243A>G mutation, in order to determine why these patients, harboring the exact same mutation, presented with such a wide range of symptoms and phenotypes, very little metabolomics data are available on this mutation. Since the metabolome is the end product of cellular activity, implementing metabolomics as an investigation tool holds great potential to identify mechanistic differences between the different phenotypes caused by the m.3243A>G mutation.

The motivation for this study came after a series of studies were performed on a South African MD cohort at the Centre for Human Metabolomics (North-West University). The studies investigated the metabolic perturbation caused by the disease, and aimed at establishing a metabolic signature (biosignature) for MD, which can be used in diagnostics as well as monitoring disease progression. However, with the heterogeneous South African cohort, metabolomics investigations proved difficult to establish a reliable biosignature. Due to this heterogeneity and the inability to obtain a more homogenous South African cohort, we obtained a cohort of patients, all diagnosed with the m.3243A>G mutation, fom two international cohort. The patients however presented with different phenotypes, this presented us with the perfect opportunity to not only investigate the metabolic alteration

caused by MD, but also to study possible mechanistic differences involved in the different phenotypes.

1.2 AIM AND OBJECTIVES OF THIS STUDY

1.2.1 AIM:

The **aim** of this study was to investigate the urinary metabolome of three different m.3243A>G mutation phenotypes i.e. MELAS, MIDD and myopathy, using a multi-platform metabolomics approach.

1.2.2 SPECIFIC OBJECTIVES:

a. To **analyze** all patient and control samples on five different analytical platforms.

b. To do data pre-processing and normalization for all analytical platforms before combining the different data sets to **generate a single data matrix.**

c. To perform **statistical analyses** in order to obtain a list of metabolites perturbed in each phenotype.

d. To do **biological interpretation** of the data in order to generate new knowledge on the altered metabolome of the different phenotypes.

1.3 STRUCTURE OF THE THESIS

This thesis is presented in chapter format as per the requirements of the North-West University. It is comprised of six chapters, and includes two peer-reviewed publications as well as a manuscript prepared for submission.

Chapter 1 consists of a short background and motivation for this study as well as the aim and objectives. The structure of the thesis together with the outcomes of the study is discussed in this chapter. The chapter concludes with a signed statement by all co-authors, confirming their individual roles in the study.

Chapter 2 can be divided into four parts. The first section contains a peer-reviewed paper published in *Mitochondrion* (Esterhuizen *et al*., 2017) discussing the use of metabolomics as

an investigative tool in the field of mitochondrial disease. Here, a list of studies investigating mitochondrial diseases using metabolomics are discussed, including the models they used and their findings. This section also visualizes the findings in the form of metabolic pathways. The second part of this chapter provides background on the mitochondrion and OXPHOS system, the involvement of both nDNA and mtDNA in the coding of the different complexes of the OXPHOS system, replication, transcription and translation of mtDNA, and different types of mutations. In the third part of this chapter, more information on the m.3243A>G mutation is provided. This includes, physiological consequences, symptoms and different phenotypes associated with the m.3243A>G mutation as well as the management of affected patients. The chapter concludes with the fourth part containing the experimental approach of the study accompanied by a flow diagram of the analytical approach followed.

In **Chapter 3** an outline of the sample cohort as well as information with regards to sample collection and ethical guidelines adhered to are given. All reagents used in the study are listed together with preparation methods of these reagents. The analytical methods, quality control as well as statistical analyses used in the study are discussed in detail in this chapter.

Chapter 4 contains the second peer-reviewed paper resulting from this study that was published in *Mitochondrion* (Esterhuizen et al., 2018). This paper focused exclusively on mitochondrial myopathy, encephalopathy, lactic acidosis and stroke like episodes (MELAS) caused by the m.3243A>G mutation and describes a biosignature for this phenotype.

Chapter 5 contains a metabolic comparison of three phenotypes associated with the m.3243A>G mutation [MELAS, maternally inherited diabetes and deafness (MIDD) and myopathy]. This chapter is presented as a manuscript prepared for submission to *Cell Reports*. The manuscript focusses on metabolic similarities, as well as differences, between the three phenotypes and how the perturbed metabolites could be linked to the phenotypic symptoms these patients present with.

Chapter 6 of the thesis contains a summary of the study and concluding remarks, strengths and limitations, as well as future research prospects arising.

Annextures: This thesis concludes with Annexures A, B and C, containing the two published papers and the instructions to authors for both *Mitochondrion* and *Cell Reports* (as required by the NWU to be included in the thesis).

1.4 OUTCOMES OF THE STUDY

This study contributes to the field of mitochondrial diseases in the form of two peer-reviewed articles, a manuscript to be submitted as well as one presentation at an international conference.

1.4.1 PUBLISHED PEER-REVIEWED ARTICLE 1 (CHAPTER 2, ANNEXURE A)

Esterhuizen, K., Van der Westhuizen, Francois H., Louw, R., 2017. Metabolomics of mitochondrial disease. ***Mitochondrion***. 35, 97-110.

1.4.2 PUBLISHED PEER-REVIEWED ARTICLE 2 (CHAPTER 4, ANNEXURE B)

Esterhuizen, K., Lindeque, J.Z., Mason, S., van der Westhuizen, Francois H, Suomalainen, A., Hakonen, A.H., Carroll, C.J., Rodenburg, R.J., de Laat, P.B., Janssen, M.C., 2018. A urinary biosignature for mitochondrial myopathy, encephalopathy, lactic acidosis and stroke like episodes (MELAS). ***Mitochondrion***.

Both of the articles were published in the Mitochondrion journal (https://www.journals.elsevier.com/mitochondrion) with an impact factor of 3.704 (2016/2017). The scope of Mitochondrion is broad, reporting on basic science of mitochondria from all organisms and from basic research to pathology and clinical aspects of mitochondrial diseases. Author guidelines (Annexure C) can be accessed at: https://www.elsevier.com/journals/mitochondrion/1567-7249?generatepdf=true

1.4.3 MANUSCRIPT TO BE SUBMITTED (CHAPTER 5)

This manuscript was prepared for submission to ***Cell Reports*** with an impact factor of 8.282. *Cell Reports* is an open-access journal from Cell Press that publishes high-quality papers across the entire life sciences spectrum. The primary criterion for publication in *Cell Reports*, as for all Cell Press journals, is new biological insight. *Cell Reports* publishes thought-provoking, cutting-edge research, with a focus on a shorter, single-point story, called a Report, in addition to a longer Article format. *Cell Reports* also publishes Resources, which highlight significant technical advances and/or major informational data sets. Information for authors are given in Annexure C or can be accessed at: https://www.cell.com/cell-reports/authors

1.4.4 POSTER PRESENTATION

A poster titled “Metabolomics signatures identified for selected mitochondrial 3243 A>G mutation phenotypes” was presented by Prof R. Louw at the EUROMIT 2017: International Meeting on Mitochondrial Pathology held in Cologne, Germany (11th – 15th June).

1.5 ETHICS

Ethical approval was obtained from the Health Research Ethics Committee (HREC) of the North-West University (NWU- 00170-13-A1). The study complied with all applicable institutional guidelines and terms of the Declaration of Helsinki of 1975 (as revised in 2013) for investigation of human participants. All participants in this study gave written informed consent for their urine samples to be used for research purposes.

1.6 FINANCIAL SUPPORT

This study was financially supported by the Technology Innovation Agency (TIA, Grant number 301 Metabol. 01), South Africa.

1.7 AUTHOR CONTRIBUTIONS

Paper I presented in Chapter 2**:** Karien Esterhuizen was involved in the review of the literature and manuscript writing. Francois H. van der Westhuizen and Roan Louw were involved in manuscript writing and supervision.

Paper II presented in Chapter 4: Karien Esterhuizen was involved in the design of the study, analytical work, data analysis and manuscript writing. Shayne Mason was involved in data analyses and manuscript writing (specifically the NMR section). Anu Suomalainen was involved in sample and patient information collection for the Finland cohort as well as manuscript writing. Christopher J. Carroll and Anna H. Hakonen was involved in sample and patient information collection for the Finland cohort. Jan A.M. Smeitink, Richard J. Rodenburg and Mirian C.H. Janssen was involved in sample and patient information collection for the Nijmegen cohort as well as manuscript writing. Paul de Laat was involved in sample and patient information collection for the Nijmegen cohort. J. Zander Lindeque and Roan Louw was involved in the design of the study, data analysis, manuscript writing and supervision.

Submitted manuscript in Chapter 5: Karien Esterhuizen was involved in the design of the study, analytical work, data analysis and manuscript writing. Shayne Mason was involved in data analyses and manuscript writing (specifically the NMR section). Jan A.M. Smeitink, Richard J. Rodenburg and Mirian C.H. Janssen was involved in sample and patient information collection for the Nijmegen cohort as well as manuscript writing. Paul de Laat was involved in sample and patient information collection for the Nijmegen cohort. J. Zander Lindeque and Roan Louw was involved in the design of the study, data analysis, manuscript writing and supervision.

All authors signed the declarations on this page:

As a co-author, I hereby approve and give consent that the mentioned articles and manuscript can be used for the PhD thesis of Karien Esterhuizen. I declare that my role in the study, as indicated above, is a representation of my actual contribution.

Signature: Mrs. K. Esterhuizen

Signature: Dr. C.J. Carroll

Signature: Prof. R. Louw

Signature: Dr. A.H. Hakonen

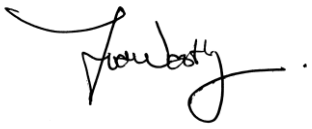

Signature: Prof. F. H. van der Westhuizen

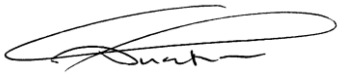

Signature: Prof. J.A.M. Smeitink

Signature: Dr. J.Z. Lindeque

Signature: Dr. M. C.H. Janssen

Signature: Prof. A. Suomalainen

Signature: Dr. R. J. Rodenburg

Signature: Dr. S. Mason

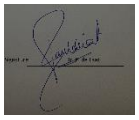

Signature: Dr. P. de Laat

Chapter 2

Literature review

2

2.1 METABOLOMICS OF MITOCHONDRIAL DISEASE

2.1.1 INTRODUCTION

Mitochondrial disease, when defined as disorders resulting from deficiencies in the mitochondrial oxidative phosphorylation (OXPHOS) system, has a current minimum prevalence of one in every 5 000 live births and is therefore considered one of the most common inborn errors of metabolism (Gorman *et al.*, 2015; Schaefer *et al.*, 2004). Although diagnostic methods for mitochondrial disease are available, several studies have highlighted limitations in the diagnostic approach, including overlapping phenotypes, patient selection, disease monitoring and response to treatment, to name but a few (DiMauro and Schon., 2003; Reinecke *et al.*, 2012; Schaefer *et al.*, 2004; Smuts *et al.*, 2013). Metabolomics is one of the more recent additions to the "-omics" family and can be defined as the detection, quantification and identification of all small-molecule metabolites present in a biological sample (Dunn *et al.*, 2005). Since the metabolome is at the end-point of all cellular activity, implementation of metabolomics in a study holds the potential to overcome some of the limitations currently observed in the study of mitochondrial disease. With these limitations in mind, various studies have used a metabolomics approach to study mitochondrial disease and, with significant progress made in recent years, a review of these contributions and the potential they reveal is long overdue. Here we review metabolomics as a relatively novel approach to the field of mitochondrial disease research and diagnostics, with a focus on the instrumental platforms, practicalities and future prospects.

2.1.2 MITOCHONDRIAL DISEASE AS AN INHERITED METABOLIC DISEASE

Since the first inborn error of metabolism (IEM) was identified by Archibald E. Garrod in 1904, diagnosing IEMs has evolved extensively and to date more than 500 IEMs, affecting various metabolic pathways, can be diagnosed using an array of analytical techniques (Kamboj, 2008; Martins, 1999). Diagnosing most IEMs involves targeted analyses, which measures a specific metabolite(s). Altered concentrations of a specific metabolite(s) usually

results from a specific enzyme defect. An example is the case of isovaleric acidemia, in which isovaleric acid coenzyme A (CoA) dehydrogenase is defective, resulting in the accumulation of isovalerylglycine in urine. Another example is propionic acidemia, where propionyl-CoA carboxylase is defective, resulting in the accumulation of propionic acid. Thus, for many IEMs, altered levels of one (or a few) specific metabolite(s) are analyzed in a biological sample and used to diagnose the disease. In contrast, a defect of the OXPHOS system results in insufficient ATP production due to the inhibited flow of electrons through the respiratory chain, resulting in a NAD^+/NADH redox imbalance, oxidative stress and a reduction of the mitochondrial membrane potential. Compared to an IEM where fewer metabolites are usually affected, the redox imbalance ultimately results in a plethora of possible cellular responses, generally affecting a large number of metabolites (Brière *et al.*, 2004; Naviaux, 2014; Reinecke *et al.*, 2009; Smeitink *et al.*, 2006).

For mitochondrial disease, the current gold standard for diagnosis is measuring the activity of the respiratory chain enzymes in tissue biopsies plus complex V and functional tests if fresh samples are available, in combination with other assessments. These assessments includes brain imaging, genetic testing for specific mutations, histochemical investigations as well as exercise stress tests to determine the arteriovenous oxygen difference (a-vO2 difference) (Haas *et al.*, 2008; Menezes *et al.*, 2014; Taivassalo *et al.*, 2003). Over the past 15 years, various scoring systems for mitochondrial disease have been developed (for both pediatric and adult patients) to assist physicians in screening patients for the disease (Bernier *et al.*, 2002; Koene *et al.*, 2016; Parikh *et al.*, 2015; Phoenix *et al.*, 2006; Schaefer *et al.*, 2004; Wolf and Smeitink, 2002). However, the use of metabolite data are very limited in these scoring systems and includes only a few selected metabolites (lactate, pyruvate, alanine, tricarboxylic acid cycle intermediates, ethylmalonic acid, 3-methylglutaconic acid, dicarbonic acids, acylcarnitines) (Parikh *et al.*, 2015; Phoenix *et al.*, 2006; Rasanu *et al.*, 2011; Schaefer *et al.*, 2004; Wolf and Smeitink, 2002). Few studies have used semi-targeted or untargeted metabolomics to study mitochondrial disease, despite the potential of the technology to find metabolites/biomarkers not previously associated with the disease. Such an approach might be useful in understanding and diagnosing the disease, a screening and monitoring of patients.

2.1.3 METABOLOMICS: GENERAL APPLICATIONS AND PLATFORMS

Metabolomics was first defined in 1998 (by Oliver *et al.*, 1998) and has since become a popular investigative tool for research on biological systems and complex disease models, using a wide range of biofluids, tissues and cell cultures (Dunn *et al.*, 2011; Nikolic *et al.*,

2014). Metabolomics usually follow one of three approaches: a *targeted* approach where a group of small metabolites are quantified and identified, a *semi-targeted* approach that focuses on a specific class of metabolite (for example amino acids, organic acids or acylcarnitines), or an *untargeted* approach, which is the unbiased detection and quantification of all the metabolites in a sample using a single- or multiple-platform approach (Álvarez-Sánchez *et al.*, 2010; Dunn *et al.*, 2011; Dunn *et al.*, 2013; Monteiro *et al.*, 2013).
Analytical techniques used in metabolomics studies usually include a technique to separate the metabolites in the biological matrix [gas chromatography (GC), liquid chromatography (LC) or capillary electrophoresis (CE)] coupled with a detection system [mass spectrometry (MS) or nuclear magnetic resonances (NMR)]. To increase the sensitivity of the analytical technique, numerous different combinations of these components are available (Bouatra *et al.*, 2013). It is also important to realize that the specific metabolites detected by metabolomics studies depends on various factors, for example more polar compounds are usually investigated with an LC-system, whereas a GC-system is the preferred technique for more non-polar metabolites. While NMR is not as sensitive as mass spectrometry, it is a useful technique when sample volumes are limited as it is a non-destructive technique. Another factor to take in consideration is the stability of a compound as some metabolites are unstable and therefore more difficult to detect - some of these metabolites might require a derivatization step to increase stability. Data pre-processing and clean-up can also influence the metabolites reported by a study. During the clean-up process, metabolites may be removed from the data matrix for numerous reasons (like a high coefficient of variance in the quality control samples etc.), thus a specific metabolite may not be in the data set to be considered for statistical analyses and is thus not reported on by the study. Another factor to take in account is the availability of spectral libraries for data interpretation. LC-MS and NMR has a limited number of databases available compared to GC-MS, which has a wide range of public as well as commercial spectral libraries available (Monteiro *et al.*, 2013). To summarize, each analytical platform has both advantages and disadvantages that should be taken into account before deciding on an appropriate technique (Fang and Gonzalez, 2014). The use of different combinations of platforms is encouraged to analyze a larger portion of the metabolome, since *the different analytical methods usually complement each other (*Bouatra *et al*., 2013*).*

2.1.4 THE APPLICATION OF METABOLOMICS IN MITOCHONDRIAL DISEASE RESEARCH

2.1.4.1 Models

The use of metabolomics in the field of mitochondrial disease research has been very limited, compared to its use to study other human diseases, such as diabetes and cardiovascular disease. This is probably a result of the relatively small number of well-defined (phenotype–genotype) samples available in mitochondrial disease patient cohorts and the heterogeneous nature of the disease. To address this challenge, numerous models have been developed to study the disease.

One such animal model uses the nematode *Caenorhabditis elegans* (*C. elegans*). This model is favored because the *C. elegans* respiratory chain (RC) subunits are morphologically very similar to the human RC. Using these nematodes, various knockout models have been generated to mimic different mitochondrial diseases, including a complex I knockout (CI KO) model [gas-1(fc21)], a complex II knockout (CII KO) model [mev-1 (kn1), a complex III knockout (CIII KO) model [isp-1(qm150), a tricarboxylic acid (TCA) cycle knockout model (idh-1(ok2832) and coenzyme Q biosynthesis knockout model [clk-1(qm30) (Butler *et al.*, 2013; Falk *et al.*, 2008; Morgan *et al.*, 2015; Vergano *et al.*, 2014). In addition to the nematode, another animal model frequently used in metabolomics studies is a mouse model such as the *Ndufs4* knockout mouse model. Due to the size of complex I, various mutations have been associated with the complex, including a mutation in the *Ndufs4* gene, which is involved in the assembly and stability of complex I. Another mouse model used is a deletor mouse model, which contains a 13 amino acid duplication situated in the mitochondrial helicase Twinkle. This deletor model is used to study adult-onset mitochondrial myopathy also known as progressive external ophthalmoplegia (PEO). Animal models such as these are currently favored in metabolomics studies to investigate the altered metabolism in mitochondrial disease, due in part to the more homogenous nature of experimental animals, compared to the more heterogeneous nature of human samples (Ahola-Erkkilä *et al.*, 2010; Leong *et al.*, 2012; Nikkanen *et al.*, 2016; Tyynismaa *et al.*, 2010). Additionally, due to its controlled environment, animal models are also useful in therapeutic studies, as it is much easier to investigate the effect of potential treatment (Leong *et al.*, 2015).

Although not as commonly used as animal models, a few studies have used cell cultures for the investigation of mitochondrial disease (Bao *et al.*, 2016; Kami *et al.*, 2012; Shaham *et al.*, 2008; Shaham *et al.*, 2010; Sim *et al.*, 2002; Vo *et al.*, 2007). Cell cultures are particular

useful study models, as the metabolite profiling of the extracellular medium provides rich information on the uptake, metabolism and secretion of metabolites. Cell cultures used for the metabolomics investigation of mitochondrial disease includes fibroblasts to investigate Leigh's disease, human embryonic kidney cells to investigate how mitochondrial dysfunction alters the one-carbon metabolism pathways, cybrid cells from 143B osteosarcoma cells to investigate the m.A3243G MELAS mutation and muscle cells to investigate induced complex I and complex III defects with rotenone and antimycin A, respectively.

The application of metabolomics in human biofluids is a major objective of current research in the field as it holds potential to clarify the complex biochemistry and the involved diagnostics. A reason for this is that metabolites are the end products of cellular processes and the variability in their concentrations could be due to changes in biological systems, which could, in turn, be linked to phenotype. Human biofluids that have been used in metabolomics studies investigating mitochondrial disease include plasma, blood and urine. Urine samples have become a favored sample choice for investigating mitochondrial disease, as it is easy to obtain and requires minimal sample preparation (Esteitie *et al.*, 2005; Reinecke *et al.*, 2012; Smuts *et al.*, 2013; Venter *et al.*, 2015). However, when working with human biofluids, the involvement of the gut microbiome should never be underestimated. The metabolites measured in the biofluids are not only due to the human genes, but are also influenced/metabolized by the hundreds of trillions of microbes colonizing the human body, *i.e.* the microbiome (Wikoff *et al.*, 2009).

2.1.4.2 Defining patient and control groups for metabolomics investigations

The outcome of metabolomics investigations are significantly affected by the way patient and control groups are defined, as well as the phenotypic homogeneity of these groups. In most metabolomics studies on mitochondrial disease (MD), the patients were compared to healthy controls to ascertain the effects of the disease on the metabolism. Although this approach could shed light on the basic biochemistry of the disease, it would have been beneficial from a diagnostic point of view to compare patients suffering from MD to a disease control group, the latter being a group of patients with a different disease but displaying similar clinical symptoms. However, only a few metabolomics studies have used disease control groups, such as organic acidemia and fatty acid oxidation defects, to compare to their mitochondrial disease cohorts (Barshop *et al.*, 2004; Sim *et al.*, 2002). One of the latest studies involving metabolomics of mitochondrial disease implemented an alternative control group referred to as clinically referred controls (Venter *et al.*, 2015), *i.e.* individuals who initially presented with symptoms usually associated with mitochondrial disease, but did not display a respiratory

chain deficiency on enzymatic level. The use of this type of control group is of particular value due to the diverse phenotypes of mitochondrial disease, overlapping with other diseases, and the challenges of diagnosing a primary mitochondrial deficiency. In most cases, a physician will have to distinguish mitochondrial disease patients from those who present with similar symptoms, but do not have the disease (DiMauro and Schon, 2003; Schaefer *et al.*, 2004). Due to the limited number of studies comparing other disease control groups to mitochondrial disease cohorts, the rest of this review will focus on metabolomics studies where patients/disease models with a deficient OXPHOS system is compared to healthy controls (Butler *et al.*, 2013; Falk *et al.*, 2008; Falk *et al.*, 2011; Hall *et al.*, 2015; Johnson *et al.*, 2013; Legault *et al.*, 2015; Leong *et al.*, 2012; McCormack *et al.*, 2015; Morgan *et al.*, 2015; Reinecke *et al.*, 2012; Shaham *et al.*, 2008; Shatla *et al.*, 2014; Smuts *et al.*, 2013; Vergano *et al.*, 2014; Vo *et al.*, 2007).

2.1.4.3 Metabolites and pathways affected by mitochondrial disease

Considering the wide-ranging immediate and downstream cellular consequences of any of a number of possible types and levels of deficiencies of the OXPHOS system in different tissues, it is not surprising that the metabolome is not affected in a localized way, as is often the case in other inherited metabolic disorders (Brière *et al.*, 2004; Elstner and Turnbull, 2012; Naviaux 2014; Reinecke *et al.*, 2009). This is clearly demonstrated by the vast number of metabolites, as summarized in Table 2.1, that have been reported in literature as affected by mitochondrial disease. However, an in-depth discussion or understanding of all the mechanisms regulating these metabolic pathways is beyond the scope of this review, and thus only a selected number of prominent and novel findings will further be highlighted, as well as the possible mechanisms responsible for these perturbations.

A fundamental consequence of an OXPHOS deficiency is the disturbance of the redox balance, which modulates a wide-ranging number of cellular processes. This results from a compromised electron transport through the respiratory chain (RC), resulting in leakage of electrons from the RC, poor membrane coupling (with resulting effect on nucleotide phosphorylation state) and a decreased redox state/ratio of the nicotinamide nucleotides and flavin coenzyme. The altered states of these OXPHOS electron carriers along with other nucleotides also modulate the activities of numerous dehydrogenase and other enzymes involved in metabolic reactions (Brière *et al.*, 2004; Naviaux, 2014; Reinecke *et al.*, 2009; Smeitink *et al.*, 2006). The result of this shift, as well as pathways affected by other mechanisms, can be observed in a number of catabolic and anabolic pathways - the most of which are illustrated in Figure 2.1, which summarizes in a number of sections (A-I) the

reported perturbed metabolism in mitochondrial disease. The most well-known perturbation is the conversion of pyruvate to lactate (Figure 2.1A). Under normal circumstances, pyruvate is converted to acetyl-CoA by the pyruvate dehydrogenase complex (PDHc), with the concomitant interconversion of NAD^+ to NADH. However, the decreased NAD^+/NADH ratio caused by an OXPHOS defect inhibits the conversion of pyruvate to acetyl-CoA, resulting in increased pyruvate levels. The latter is then converted to lactate by lactate dehydrogenase (LDH) with the concomitant interconversion of NADH to NAD^+. This is a classic example of how the activity of one dehydrogenase enzyme reaction (PDHc) can be inhibited, while the activity of another dehydrogenase reaction (LDH) can be increased by the same decreased NAD^+/NADH ratio, depending on the direction of the reaction. The conversion of pyruvate to lactate also results in the recycling of NAD+, which allows anaerobic glycolysis to continue in an attempt to recover ATP levels. The lactate/pyruvate ratio is also of great importance as this ratio gives an indication on the cytosolic redox state (Munnich *et al.*, 1996). Furthermore, in the TCA cycle, three dehydrogenases (citrate synthase, isocitrate synthase and α-ketoglutarate dehydrogenase) are inhibited by a high NADH concentration, thus a lowered NAD^+/NADH ratio will lead to a congested TCA cycle, accounting for the increased levels of TCA cycle intermediates, and the metabolites they are subsequently converted to, as commonly reported by metabolomics studies (Figure 2.1A).

Similarly, a frequent observation in mitochondrial disease is elevated alanine, which forms via the transamination of pyruvate by alanine aminotransferase. Together with the mentioned TCA cycle intermediates, as well as lactate (or elevated lactate/pyruvate ratio), alanine is one of the few metabolic markers used in scoring criteria for MD (Wolf and Smeitink, 2002). Thus, it is not surprising that numerous metabolomics studies also detected and reported these markers as important biomarkers as can be seen from Table 2.1. Noteworthy is that these “classic” metabolic markers (of albeit limited sensitivity and specificity) are reported in various models of the disease, e.g. elevated pyruvate was reported in an *Ndufs4* knockout mouse model (Johnson *et al.*, 2013), as well as in patient urine and plasma samples (Legault *et al.*, 2015); elevated lactate was reported in a complex I knockout nematode model (Vergano *et al.*, 2014), in addition to frequent reports in patient urine and plasma samples (Legault *et al.*, 2015; Reinecke *et al.*, 2012; Shaham *et al.*, 2008; Shatla *et al.*, 2014; Smuts *et al.*, 2013). Furthermore, increased alanine was reported in nematode models (Falk *et al.*, 2008; Falk *et al.*, 2011; Vergano *et al.*, 2014), tissue cultures (Bao *et al.*, 2016), mouse models (Tyynismaa *et al.*, 2010), patient plasma (Legault *et al.*, 2015; Shaham *et al.*, 2008; Shatla *et al.*, 2014) and patient urine samples (Smuts *et al.*, 2013). Although the studies listed here also identified possible novel biomarkers, they still

reported the classic markers to be discriminative between MD and controls – something that bolsters the overall metabolomics methodology.

Table 2.1: Metabolites associated with mitochondrial disease when compared to healthy controls.

	Falk *et al.*, 2008			Falk *et al.*, 2011	Butler *et al.*, 2013		Vergano *et al.*, 2014					Morgan *et al.*, 2015		McCormack *et al.*, 2015	Tyynismaa *et al.*, 2005		Ahola-Erkkilä *et al.*, 2010		Leong *et al.*, 2012	Johnson *et al.*, 2013	Nikkanen *et al.*, 2016				Vo *et al.*, 2007	Bao *et al.*, 2016	Shaham *et al.*, 2008	Reinecke *et al.*, 2012	Smuts *et al.*, 2013	Shatla *et al.*, 2014		Legault *et al.*, 2015		Hall *et al.*, 2015	
	CI KO gas-1 (fc21)	CII KO mev-1 (kn1)	CIII KO isp-1 (qm150)	CIII KO isp-1 (qm150)	CII KO mev-1 (kn1)	CIII KO isp-1 (qm150)	CI KO gas-1 (fc21)	CII KO mev-1 (kn1)	CIII KO isp-1 (qm150)	Q10 KO clk-1(qm30)	Krebs KO idh-1(ok2832)	CI KO gas-1 (fc21)	CII KO mev-1 (kn1)	CI KO gas-1 (fc21)	Deletor	Deletor	Deletor	Deletor	*NDUFS4* KO	*NDUFS4* KO	Deletor	Deletor	PEO	PEO	Cell cultures	Cell cultures	Human Plasma	Human urine	Human urine	MD score greater than 4	MD score greater than 4	Urine	Plasma	MELAS	MIDD
	Nematode			Nematode	Nematode		Nematode					Nematode		Nematode	Mouse (Male)	Mouse (Female)	Mouse plasma	Mouse muscle	Mouse	Mouse	Mouse skeletal muscle	Mouse heart muscle	Human Plasma	Human skeletal muscle	Cell cultures	Cell cultures (spent media)	Human Plasma	Human urine	Human urine	Human urine	Human Plasma	Human urine	Human Plasma	Human urine	Human urine
AMINO ACIDS																																			
Alanine	+			+			+									+					+				-	+	+		+		+		+		
Alpha-amino adipic acid																						+				-			+						
Arginine	-							+												-					-	+									
Asparagine					+																+				-	+							-		

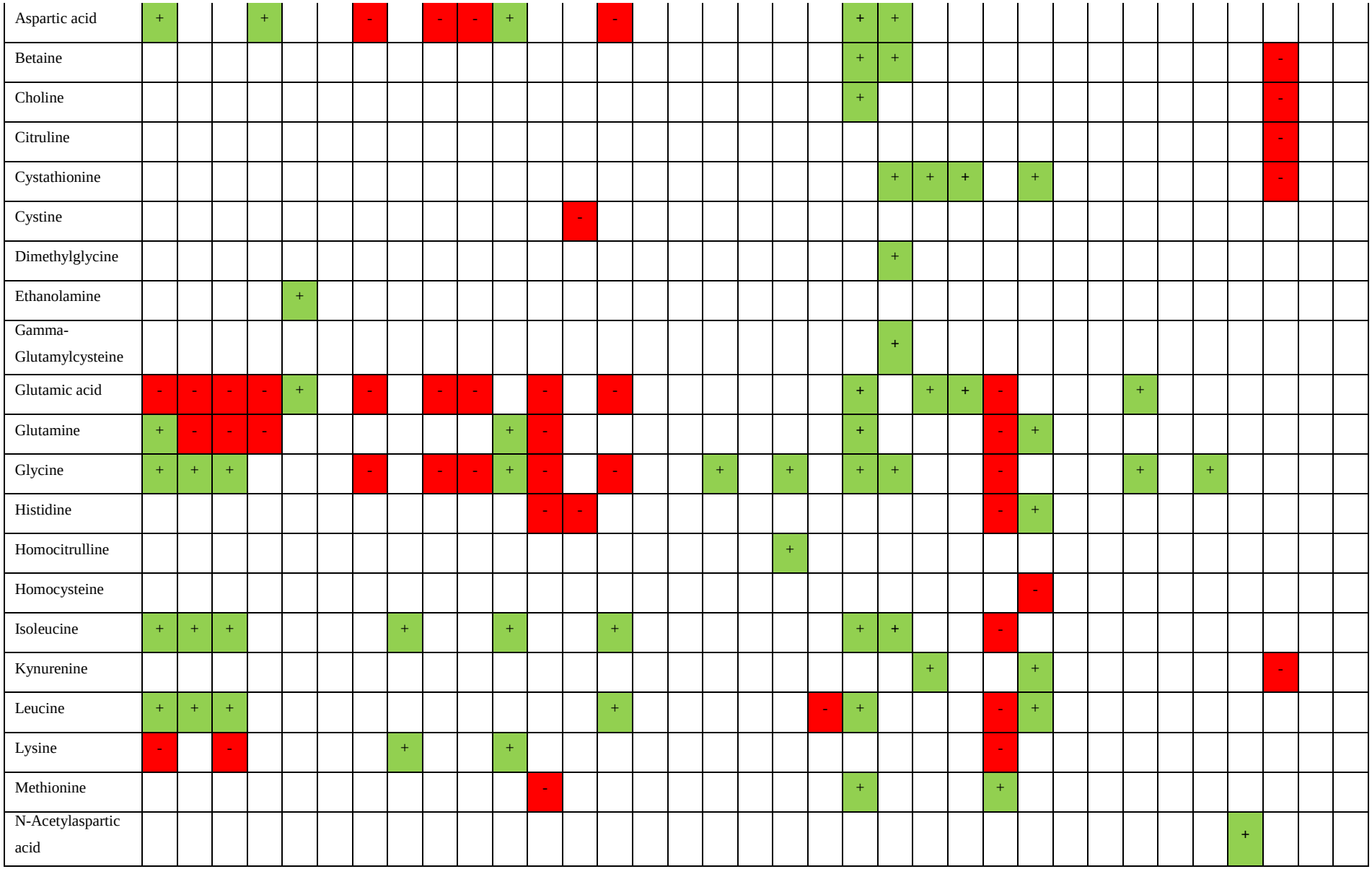
Aspartic acid
Betaine
Choline
Citruline
Cystathionine
Cystine
Dimethylglycine
Ethanolamine
Gamma-Glutamylcysteine
Glutamic acid
Glutamine
Glycine
Histidine
Homocitrulline
Homocysteine
Isoleucine
Kynurenine
Leucine
Lysine
Methionine
N-Acetylaspartic acid

N-Narbamoyl-beta-alanine																										-												
Ornithine		-	-																				+				-											
Phenylalanine	-	+						+				-								+		+				-											
Phosphocholine																						+															
Proline												-										+	+			-								+				
Hydroxyproline																						+															
Serine											+			-	+		+					+	+	+	+	+	+			+							
Homoserine																						+															
Threonine		+	+																			+	+			-											
Tryptophan					+																-		+			-											
Tyrosine	-				+						+	-	-													-				+							
Valine	+	+	+										-	+								+	+		+	-											
FATTY ACIDS PHOPHOLIPIDS AND ACYLCARNITINES																																					
Acetylcarnitine (C2)																										+							+				
Acylcanitine (C0)																																	+				
Arachidylcarnitine																								+	+												
Dihomo-y-linolenic acid (C20:3n-6)																																	+				

Hydroxy-C16:0 acylcarnitine																			+																	
Hydroxy-C18:1 acylcarnitine																			+																	
Hydroxy-C4:0 acylcarnitine																			+																	
Isobutyrylcarnitine																								+										-		
L-Decadieny carnitine (C10:2)																																			+	
L-Dodecanoylcarnitine (C12)																								+												
L-Hexanoylcarnitine (C6)																																			+	
Linoleic acid (C18:2)																				-															+	
L-Malonylcarnitine (C3-DC)																				-																
L-Nonayl carnitine (C9)																																			-	
L-Octenoylcarnitine (C18:1)																																			+	
L-Palmitoylcarnitine (C16)																						+		+											+	
L-Tetradecanoylcarnitine (C14)																																			+	

L-Tetradecenoylcarnitine (C14:1)																																	+			
Myristoylcarnitine																								+												
Oleic acid (C18:1n-7)																																	+			
Phosphatidylcholine																	-	+																		
Propionyl-Carnitine (C3)																																	+			
Sphingomyelin																		+																		
Stearoyl Carnitine																						+														
Triacylglycerol(44:0)																									-											
Triacylglycerol(52:3)																									-											
ORGANIC ACIDS																																				
Acetoacetic acid																																+				
Adipic acid																																+				
Anthranilic acid																										+										
Arachidonic acid																									-											
Citric acid					+		+																			-										
Docosahexaenoic caid																									-											
Fumaric acid					+																							+								
Glutaric acid																												+								

Glycerol																											+										
Glycocholic acid																																		-		
Glycolic acid																																			-	
Hippiruc acid																										-									-	-
Homogentisic acid																										-										
Homovanilic acid																												+								
Isocitric acid																										-		+						+		
Lactic acid							+					-														-	+	+	+	+	+		+	+		
Malic acid					+		+						-																+					+		
Methylmalonic acid																																		-		
Methylsuccinic acid																												+								
Oleic acid																										-										
Palmitic acid																										-										
Pantothenate																											+									
Phenylacetylglutamine																												+								
Propionic acid																												+						+		
Pyroglutamic acid																											+		+							
Stearic acid																										-										
Suberic acid																												+								
Succinic acid							+					-																+	+	+				-		

Taurine																					+					+												
Uracil																						+				+		+										
2-Ethylhydracrylic acid																												+										
2-Hydroxybutyric acid						+																				+		+					+					
2-Hydroxycaproic acid						+																																
2-Hydroxyglutaric acid					+																					+		+	+								
2-Hydroxyisovaleric acid																																						
2-Keto-3-methylvaleric acid						+																																
2-Ketobutyric acid						+																																
2-Ketoglutaric acid					+																																
2-Ketoisocaproic acid						+																																
2-Ketoisovaleric acid						+																													+			
2-Keto-octanoic acid																										+												
2-Methyl-3-hydroxybutyric acid																										+												
3-Hydroxy-3-methylglutaric acid																										+	+											

3-Hydroxyadipic acid																												+										
3-Hydroxyanthranilic acid																																	-				
3-Hydroxybutyric acid																	-													+		+					
3-Hydroxyisobutyric acid																												+	+								
3-Hydroxyisovaleric acid																												+	+								
3-Hydroxysebacic acid																												+									
3-Methyladipic acid																												+									
3-Methylglutaconic acid																												+									
4-Hydroxymandelic acid																																	-				
4-Hydroxyphenyllactic acid																												+									
OTHER																																					
Acetylacetone																											-										
Acetylglycine																												+									
Adenosine																							+														

AMP																				+																		
ATP																									-													
Bisphosphoglyceric acid																				+																	
Creatine																					+	+				+	+		+				+				
Creatinine																					+														-		
Deoxycytidine																										-											
Dopamine																				+																	
dTMP																				+																	
Formate																					-																
Fructose 6-phosphate																				+																	
Fructose-1,6-bisphosphate																				+																	
GABA																					+																
Glucose					+																				-	-							+				
Glucose 6-phosphate																				+																	
Glutathione (reduced)																					+			+		+											
Glyceraldehyde																					+																
Glycerophosphate																										+											
Guanidinoacetic acid																					+																
Guanosine																				+		+															

Hypoxanthine					+																	+																
Indoxysulfate																																			+			
Inosine																							+														
Lactose																										-											
Malondialdehyde																										+									+		
Neopterin																						+															
N-Methylnicotinamide																																				-	-
Phosphoethanolamine																																			+		
Pyruvic acids																					+					-	-							+	+		
S-Methyl-cysteine-sulfoxide																																				-	-
Sorbitol																								+													
Sucrose																									+												
THF																						+															
Thymidine																										-											
Thymine																										-											
Thyroxine																										-											
Trimethylamine-N-Oxide																							+														
Uridine																					+					-											
Xanthine					+																					-											

Xanthosine																						+																
1-Methylhistamine																								+														
2-Aminoisobutyric acid																						+																
4-Cresyl sulfate																																				-	-
5,10-Methylene-THF																					+																
5-Hydroxyindole-3-acetic acid																					+	+															
5-Methyl-THF																					+																
Niacinamide																					+																

As evident from the illustrations in Figure 2.1, the decreased NAD^+/NADH ratio can also account for numerous other metabolites altered by MD. One example is the ketone bodies, acetoacetate and 3-hydroxybutyric acid. Acetoacetate is formed from acetyl-CoA and is converted to 3-hydroxybutyric acid by 3-hydroxybutyric acid dehydrogenase with the concomitant conversion of NADH to NAD^+. Again, the decreased NAD^+/NADH ratio can account for the increased 3-hydroxybutyric acid reported in human urine (Legault *et al.*, 2015; Shatla *et al.*, 2014). However, Ahola-Erkkilä *et al.* (2010) reported decreased levels of 3-hydroxybutyric acid in a mouse model – clear discrepancies between different disease models and studies. While the lactate/pyruvate ratio provides information on the cytosolic redox state of a model, the acetoacetate/3-hydroxybutyric acid ratio is also of great importance as it reflects the mitochondrial redox state of the model (Munnich *et al.*, 1996).
An altered redox balance can also explain observations of a perturbed catabolism of the branched chain amino acids (Figure 2.1B). Firstly, the lowered NAD^+/NADH ratio inhibits the activity of the branched-chain α-ketoacid dehydrogenase complex (BCKDC) responsible for the oxidative decarboxylation of 2-ketoisocaproic acid, 2-keto-3-methylvaleric acid, 2-ketoisovaleric acid in the leucine, isoleucine and valine catabolic pathways, respectively. This leads to increased levels of 2-ketoisocaproic acid, 2-keto-3-methylvaleric acid, 2-ketoisovaleric acid and 2-hydroxycaproic acid reported in nematode models (Butler *et al.*, 2013) and human urine (Legault *et al.*, 2015). In addition, there is evidence that the branched-chain amino acid catabolic pathway (Figure 2.1B) is dysregulated by an altered (decreased) FAD/$FADH_2$ redox state, which can be affected by deficient electron delivery to complex II. This is, for example, evident by the elevated excretion in urine of 3-hydroxyisovaleric acid in MD patients, which in these disorders would implicate a decreased FAD/$FADH_2$ ratio and subsequent inhibition of isovaleryl-CoA dehydrogenase (Reinecke *et al.*, 2012; Smuts *et al.*, 2013). In a similar mechanism in the isoleucine catabolism, 2-methylbutyryl-CoA has been found to be elevated, putatively due to the decreased FAD/$FADH_2$ ratio, resulting in the conversion of 2-methylbutyryl-CoA to 2-ethylhydracrylic acid and the elevated excretion of the latter in patients suffering from MD (Reinecke *et al.*, 2012). In addition to branched-chain amino acids, the catabolism of the ketogenic amino acid, lysine (Figure 2.1C), have frequently been reported in metabolomics investigations to be affected in MD via a similar regulatory mechanism (Bao *et al.*, 2016; Falk *et al.*, 2008; Smuts *et al.*, 2013).

One-carbon metabolism, the methylation cycle and the transsulfuration pathway form an intricate web of pathways that are also regulated by the redox state (Figure 2.1D). Although one-carbon metabolism has previously been identified as a possible cellular response to deficiencies of the OXPHOS system (Naviaux, 2014), it was not until recent metabolomics

studies (Bao *et al.*, 2016; Nikkanen *et al.*, 2016) that altered one carbon metabolism was identified as a major consequence of mitochondrial disease. One-carbon metabolism is a process where serine acts as the major one-carbon donor to the folate cycle. During this cycle, dietary folate enters the system and is converted to tetrahydrofolate (THF). One-carbon units are donated to THF by serine, which results in the formation of 5,10-methylene-THF and glycine. The formed 5,10-methylene-THF can be reduced to 5-methyl-THF, a methyl group donor that is involved in the conversion of homocysteine to methionine in the methylation cycle, with 5-methyl-THF being converted back to THF. The one carbon cycle also forms 10-formyl THF, involved in purine synthesis (Figure 2.1E) as well as 5,10-methylene-THF that is involved in pyrimidine biosynthesis (Figure 2.1F). In the methylation cycle, methionine is converted to S-adenosylmethionine (SAM), a universal methyl donor to reactions that involve numerous methyltransferase reactions, including carnitine and polyamine biosynthesis as well as methylation reactions. The methylation capacity is mostly used for metabolite methylation, of which creatine and phosphatidylcholine synthesis utilizes the vast majority, up to 80% (Mudd *et al.*, 2007). Furthermore, the folate cycle is linked to NADPH biosynthesis; therefore, serine can be considered a one-carbon donor of the generation of NADPH for antioxidant defense (Yang and Vousden, 2016). Nikkanen *et al.* (2016) recently reported that mitochondrial DNA replication defects disturb cellular dNTP pools and remodel one-carbon metabolism, activating *de novo* serine biosynthesis that ultimately drives glutathione synthesis.

Because of the central role that serine and glycine play in the one-carbon metabolism, it is not surprising that numerous metabolomics studies reported variations in glycine and serine levels caused by MD (Table 2.1). Considering glycine, most studies reported that MD elevated glycine levels, including studies on nematodes (Falk *et al.*, 2008), mouse models (Ahola-Erkkilä *et al.*, 2010; Leong *et al.*, 2012; Nikkanen *et al.*, 2016) and humans (Smuts *et al.*, 2013; Shatla *et al.*, 2014). Some studies however reported lower glycine levels in nematodes (McCormack *et al.*, 2015; Morgan *et al.*, 2015; Vergano *et al.*, 2014) – again discrepancies between different studies. For serine, elevated levels were reported in nematode- and mouse models, as well as in tissue cultures and patient samples. Although serine and glycine have previously been linked to MD, it was only recently that a broader metabolomics approach (Bao *et al.*, 2016; Nikkanen *et al.*, 2016) identified disturbed cellular dNTP pools and remodeling of the one-carbon metabolism caused by MD and linked the altered glycine and serine levels to one-carbon metabolism. This again reiterates the value of metabolomics not only as a useful tool in identifying novel biomarkers, but also as indispensable in the elucidation of mechanistic alterations caused by mitochondrial disease.

Other notable metabolic pathways that are influenced by MD include phenylalanine and tyrosine catabolism (Figure 2.1G), sphingomyelin biosynthesis (Figure 2.1H) as well as beta-oxidation (Figure 2.1I), often resembling glutaric aciduria type II. Possibly also a consequence of redox shift, or in the case of phenylalanine catabolism possibly also liver dysfunction (Reinecke *et al.*, 2012), a wide range of metabolites in these pathways have been identified to be affected by MD in numerous studies and models, including mouse models (Johnson *et al.*, 2013; Leong *et al.*, 2012) and patient plasma and urine (Legault *et al.*, 2015; Reinecke *et al.,* 2012). Several of the affected metabolites that can be attributed to increased catabolism of fatty acids and amino acids share a bioenergetics-sensing (hormone-modulated) induction pathway with the serum biomarker FGF-21 and possibly also GDF-15 (Kalko *et al.*, 2014; Smuts *et al.*, 2013; Suomalainen *et al.,* 2011). Another consequence of phenylalanine metabolism is the formation of benzoic acid via cinnamic acid (Figure 2.1G), a reaction that cannot be catalyzed by humans, but is indeed catalyzed by the gut microbiota (Badenhorst *et al.*, 2014). From here the benzoic acid is conjugated with glycine to form hippuric acid, another metabolite reported as perturbed by mitochondrial disease (Bao *et al.*, 2016; Hall *et al.*, 2015).

Clearly, in a complex disease of this kind, predicting the metabolic response *in vivo* at any point in time – considering the number of variables involved – is a systems biology challenge of the highest order as is evident from all the metabolic pathways affected by the disease (Figure 2.1A-I). Even though some of the metabolites, such as citric acid, alanine and isoleucine, are consistently reported as elevated (Butler *et al.*, 2013; Shaham *et al.*, 2008; Smuts *et al.*, 2013; Vergano *et al.*, 2014; Vo *et al.*, 2007), discrepancies are found for other metabolites. While glycine, lysine and glutamic acid were reported as elevated in certain studies, other studies reported decreased levels of the same metabolites (Butler *et al.*, 2013; Falk *et al.*, 2008; Smuts *et al.*, 2013). These contradictions make it difficult for researchers to draw common mechanistic conclusions, as the elevation or decrease of a metabolite can change the flux of a metabolic pathway. Moreover, different altered metabolic profiles were reported for specific study models. In nematode models, Vergano *et al.* (2014) obtained clear metabolic separation between a complex II knockout model and nematodes with complex I and complex III knockouts, due to different metabolic alterations caused by the knockouts. However, no metabolic separation was reported between complex I, complex III and combined complex defects when investigating human urine (Reinecke *et al.*, 2012). Two possible explanations can be offered for this: first, it can be argued that although complex II is part of the respiratory chain, it also forms part of the TCA cycle. This could explain why a complex II metabolic profile would be more similar to the metabolic profile caused by a TCA cycle defect than an OXPHOS defect. A second argument could be that while it is possible

to distinguish different mitochondrial diseases from each other in animal models, this is far more difficult to achieve in human biofluids. The reason for this is that animal models present a more controlled environment and the animals are highly inbred, while patients live in a less controlled environment where external factors could drastically influence the metabolome. Humans are also more genetically diverse, compared to animal models, adding to an increase in variation of the metabolome.

In recent studies, some of the metabolites reported in Table 2.1 showed promising results as potential markers to monitor MD. One example is where a ketogenic diet restored levels of 3-hydroxybutyric acid and phosphatidylcholine in deletor mice (Ahola-Erkkilä *et al.*, 2010). In another study, elevated 2-hydroxybutyrate levels in *Ndufs4* knockout were restored with the help of hypoxic conditions (Jain *et al.*, 2016). In a study using nematodes as a model, McCormack *et al.,* demonstrated that by restoring the redox imbalance (nicotinic acid supplementation), altered sirtuin and PPAR signaling pathways were restored, which resulted in improved longevity in the nematodes with a complex I defect (McCormack *et al.,* 2015). By administering purine or format supplementation, cells that showed growth defects as result of decreased serine levels could also be rescued (Bao *et al.*, 2016). These studies proved that a metabolomics approach not only have the potential to identify diagnostic markers, but possibly also identify metabolic markers that can be used to monitor disease progression or even therapeutic interventions.

Lastly, normalization of metabolomics data remains problematic, especially for urine samples. Unlike plasma, where solute concentrations are tightly controlled, urine volume can vary widely based upon water consumption and other physiological factors. Therefore, the concentrations of endogenous metabolites analyzed in urine vary widely and normalizing for these effects is necessary (Warrack *et al.*, 2009). Normalization approaches commonly used include osmolality, creatinine concentration, and components that are common to all samples (“total useful mass spectrometry signal”). Numerous studies reported on altered creatine concentration in mitochondrial disease, including mouse models (Nikkanen *et al.*, 2016), tissue cultures (Bao *et al.*, 2016), plasma (Legault *et al.*, 2015; Shaham *et al.*, 2008) and urine (Smuts *et al.*, 2013). Due to creatine being converted to creatinine, the use of creatinine for urine normalization in mitochondrial disease studies raises concern and should thus be reconsidered.

A

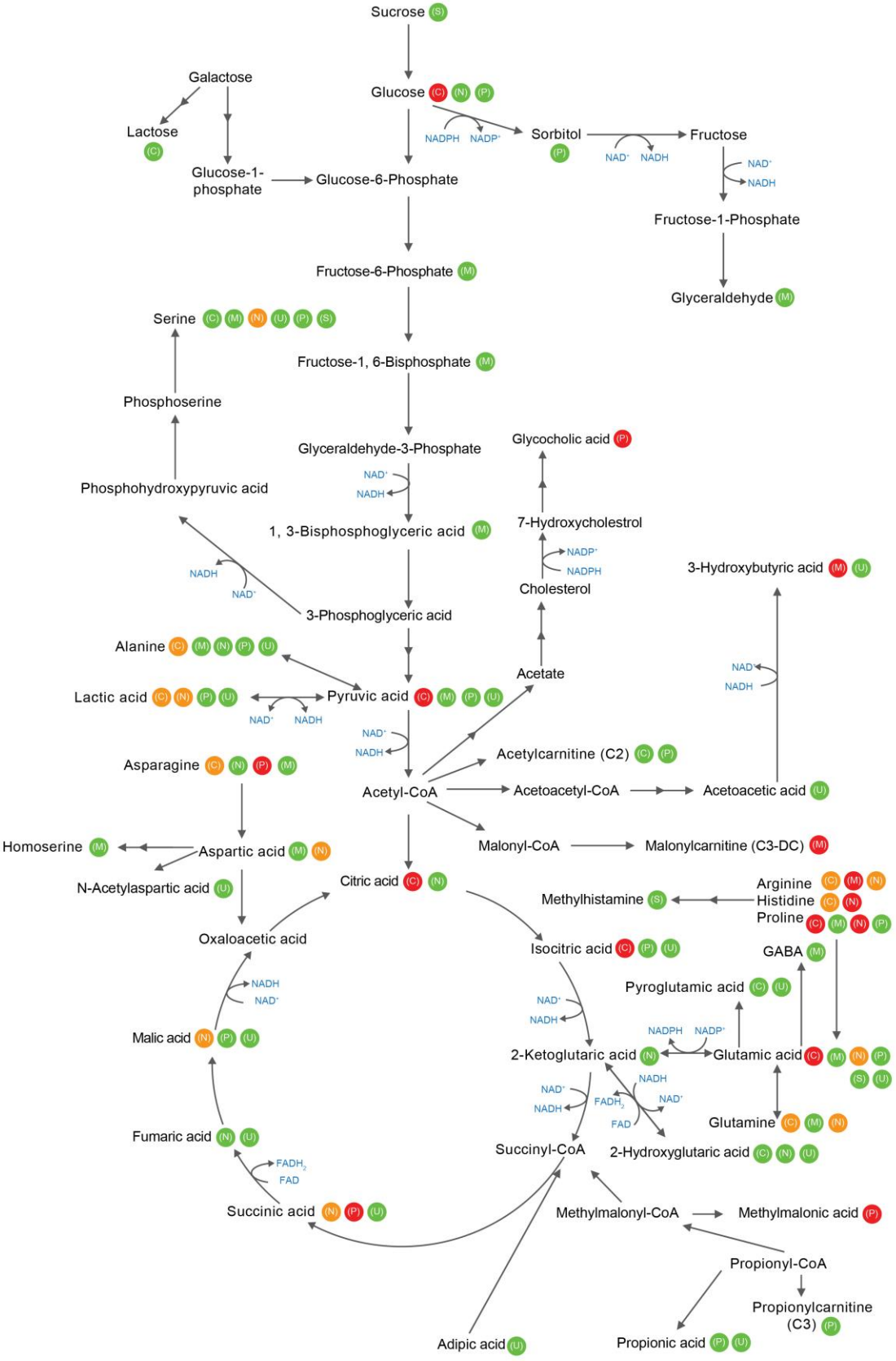
Sucrose (S)
Galactose
Glucose (C) (N) (P)
Lactose (C)
NADPH NADP+
Sorbitol (P)
NAD+ NADH
Fructose
NAD+ NADH
Glucose-1-phosphate
Glucose-6-Phosphate
Fructose-1-Phosphate
Fructose-6-Phosphate (M)
Glyceraldehyde (M)
Serine (C) (M) (N) (U) (P) (S)
Fructose-1, 6-Bisphosphate (M)
Phosphoserine
Glycocholic acid (P)
Glyceraldehyde-3-Phosphate
Phosphohydroxypyruvic acid
NAD+ NADH
7-Hydroxycholestrol
1, 3-Bisphosphoglyceric acid (M)
NADP+ NADPH
3-Hydroxybutyric acid (M) (U)
NADH NAD+
Cholesterol
3-Phosphoglyceric acid
Alanine (C) (M) (N) (P) (U)
NAD NADH
Acetate
Lactic acid (C) (N) (P) (U)
Pyruvic acid (C) (M) (P) (U)
NAD+ NADH
NAD+ NADH
Acetylcarnitine (C2) (C) (P)
Asparagine (C) (N) (P) (M)
Acetyl-CoA
Acetoacetyl-CoA
Acetoacetic acid (U)
Homoserine (M)
Aspartic acid (M) (N)
Malonyl-CoA
Malonylcarnitine (C3-DC) (M)
N-Acetylaspartic acid (U)
Citric acid (C) (N)
Arginine (C) (M) (N)
Histidine (C) (N)
Proline (C) (M) (N) (P)
Methylhistamine (S)
Oxaloacetic acid
Isocitric acid (C) (P) (U)
GABA (M)
Pyroglutamic acid (C) (U)
NADH NAD+
NAD+ NADH
Malic acid (N) (P) (U)
NADPH NADP+
2-Ketoglutaric acid (N)
Glutamic acid (C) (M) (N) (P) (S) (U)
NADH
NAD+ NADH
FADH2 FAD
NAD+
Glutamine (C) (M) (N)
Fumaric acid (N) (U)
Succinyl-CoA
2-Hydroxyglutaric acid (C) (N) (U)
FADH2 FAD
Succinic acid (N) (P) (U)
Methylmalonyl-CoA
Methylmalonic acid (P)
Propionyl-CoA
Propionylcarnitine (C3) (P)
Adipic acid (U)
Propionic acid (P) (U)

B

Leucine
2-Ketoisocaproic acid
2-Hydroxycaproic acid
NAD+
NADH
Isovaleryl-CoA
3-Hydroxyisovaleric acid
FAD
FADH2
3-Methylcrotonyl-CoA
3-Methylglutaconyl-CoA
3-Methylglutaconic acid
3-Hydroxy-3- methylglutaryl-CoA
3-Hydroxy-3-methylglutaric acid
Acetyl-CoA
Acetoacetic acid
Isoleucine
2-Keto-3-methylvaleric acid
2-Methylbutyryl-CoA
2-Ethylhydracrylic acid
Tiglyl-CoA
2-Methyl-3-hydroxbutyryl-CoA
2-Methyl-3-hydroxy butyric acid
2-Methylacetoacetyl-CoA
Acetyl-CoA
Propionyl-CoA
Valine
2-Ketoisovaleric acid
Isobutyrylcamitine
Isobutyryl-CoA
Methacrylyl-CoA
3-Hydroxyisobutyryl-CoA
3-Hydroxyisobutyric acid
Methylmalonic acid semialdehyde
Propionyl-CoA

C

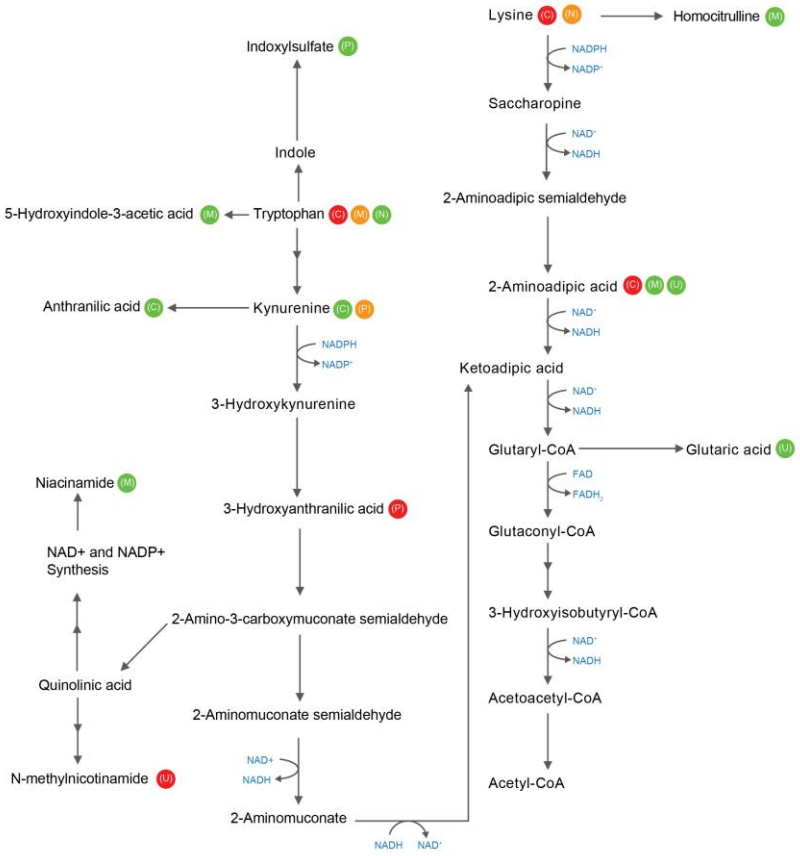
Lysine
Homocitrulline
NADPH
NADP+
Saccharopine
2-Aminoadipic semialdehyde
2-Aminoadipic acid
Ketoadipic acid
Glutaryl-CoA
Glutaric acid
Glutaconyl-CoA
3-Hydroxyisobutyryl-CoA
Acetoacetyl-CoA
Acetyl-CoA
Indoxylsulfate
Indole
5-Hydroxyindole-3-acetic acid
Tryptophan
Anthranilic acid
Kynurenine
3-Hydroxykynurenine
Niacinamide
3-Hydroxyanthranilic acid
NAD+ and NADP+ Synthesis
2-Amino-3-carboxymuconate semialdehyde
Quinolinic acid
2-Aminomuconate semialdehyde
N-methylnicotinamide
2-Aminomuconate

D

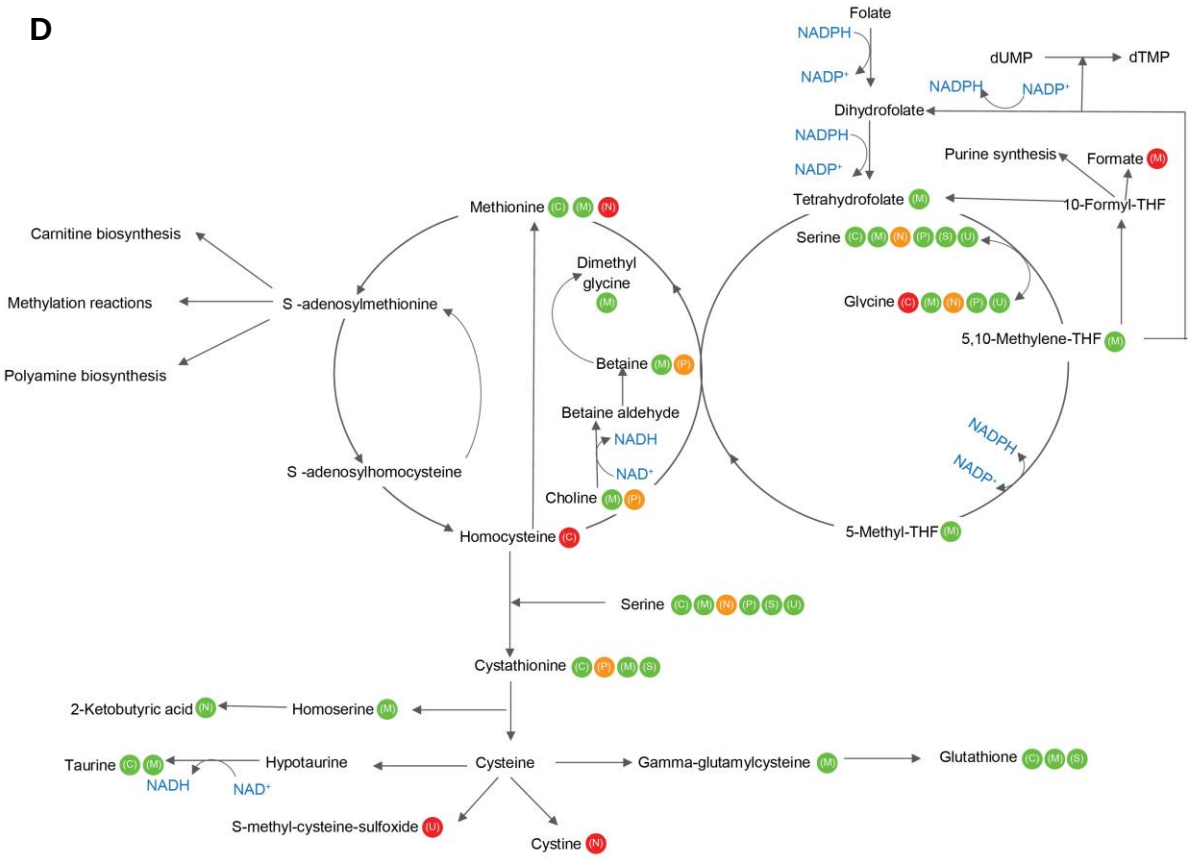
Folate
NADPH
NADP+
dUMP
dTMP
NADPH
NADP+
Dihydrofolate
NADPH
NADP+
Purine synthesis
Formate
Tetrahydrofolate
10-Formyl-THF
Methionine
Serine
Carnitine biosynthesis
Methylation reactions
Polyamine biosynthesis
S -adenosylmethionine
Dimethyl glycine
Glycine
Betaine
5,10-Methylene-THF
Betaine aldehyde
NADH
NAD+
NADPH
NADP+
S -adenosylhomocysteine
Choline
Homocysteine
5-Methyl-THF
Serine
Cystathionine
2-Ketobutyric acid
Homoserine
Taurine
Hypotaurine
NADH
NAD+
Cysteine
Gamma-glutamylcysteine
Glutathione
S-methyl-cysteine-sulfoxide
Cystine

E

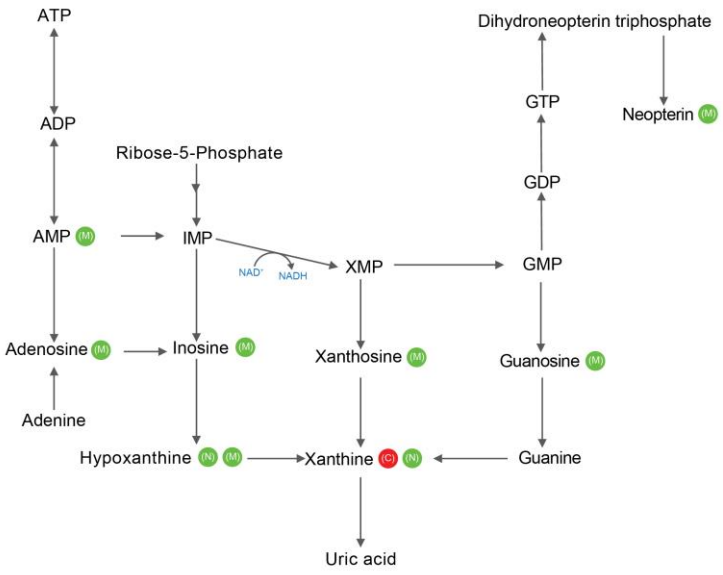
ATP
ADP
Ribose-5-Phosphate
AMP
IMP
NAD+
NADH
XMP
GMP
GDP
GTP
Dihydroneopterin triphosphate
Neopterin
Adenosine
Inosine
Xanthosine
Guanosine
Adenine
Hypoxanthine
Xanthine
Guanine
Uric acid

F

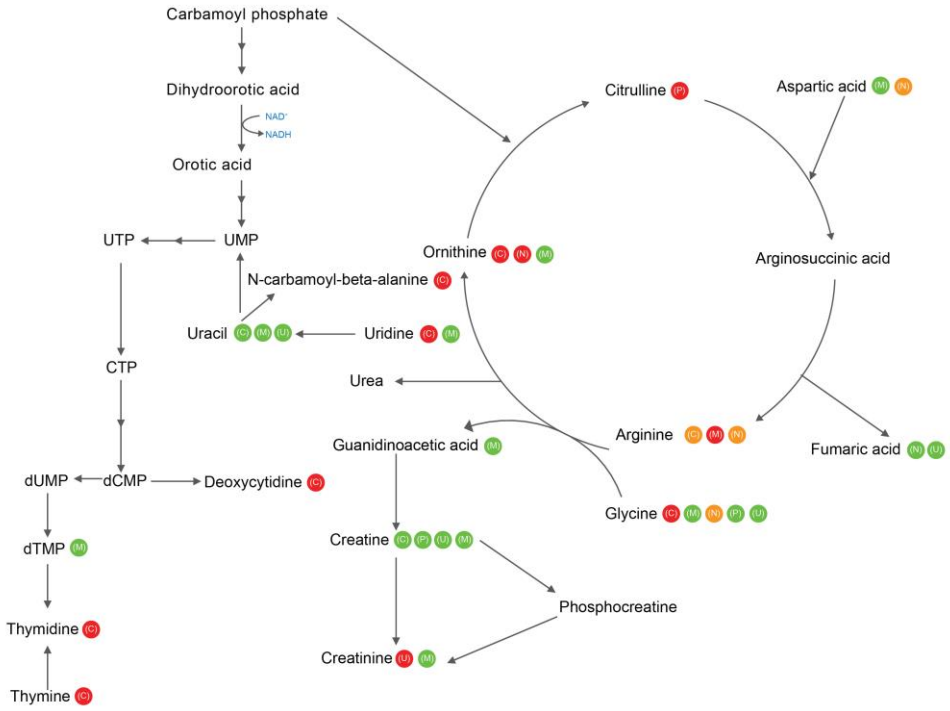
Carbamoyl phosphate
Dihydroorotic acid
NAD+
NADH
Orotic acid
UTP
UMP
CTP
Uracil
Uridine
N-carbamoyl-beta-alanine
Ornithine
Citrulline
Aspartic acid
Arginosuccinic acid
Urea
Arginine
Fumaric acid
Guanidinoacetic acid
Glycine
dUMP
dCMP
Deoxycytidine
dTMP
Thymidine
Thymine
Creatine
Phosphocreatine
Creatinine

G

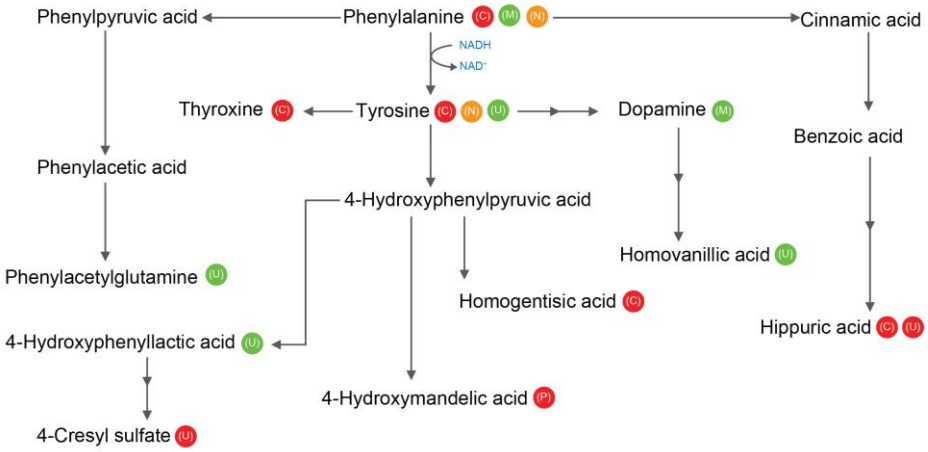
Phenylpyruvic acid
Phenylalanine
Cinnamic acid
NADH
NAD+
Thyroxine
Tyrosine
Dopamine
Benzoic acid
Phenylacetic acid
4-Hydroxyphenylpyruvic acid
Homovanillic acid
Phenylacetylglutamine
Homogentisic acid
Hippuric acid
4-Hydroxyphenyllactic acid
4-Hydroxymandelic acid
4-Cresyl sulfate

H

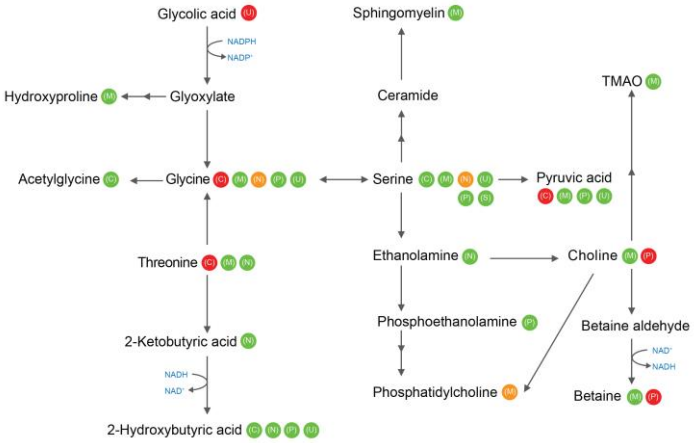
Glycolic acid
NADPH
NADP+
Hydroxyproline
Glyoxylate
Sphingomyelin
Ceramide
TMAO
Acetylglycine
Glycine
Serine
Pyruvic acid
Threonine
Ethanolamine
Choline
Phosphoethanolamine
Betaine aldehyde
2-Ketobutyric acid
NADH
NAD+
Phosphatidylcholine
Betaine
2-Hydroxybutyric acid

I

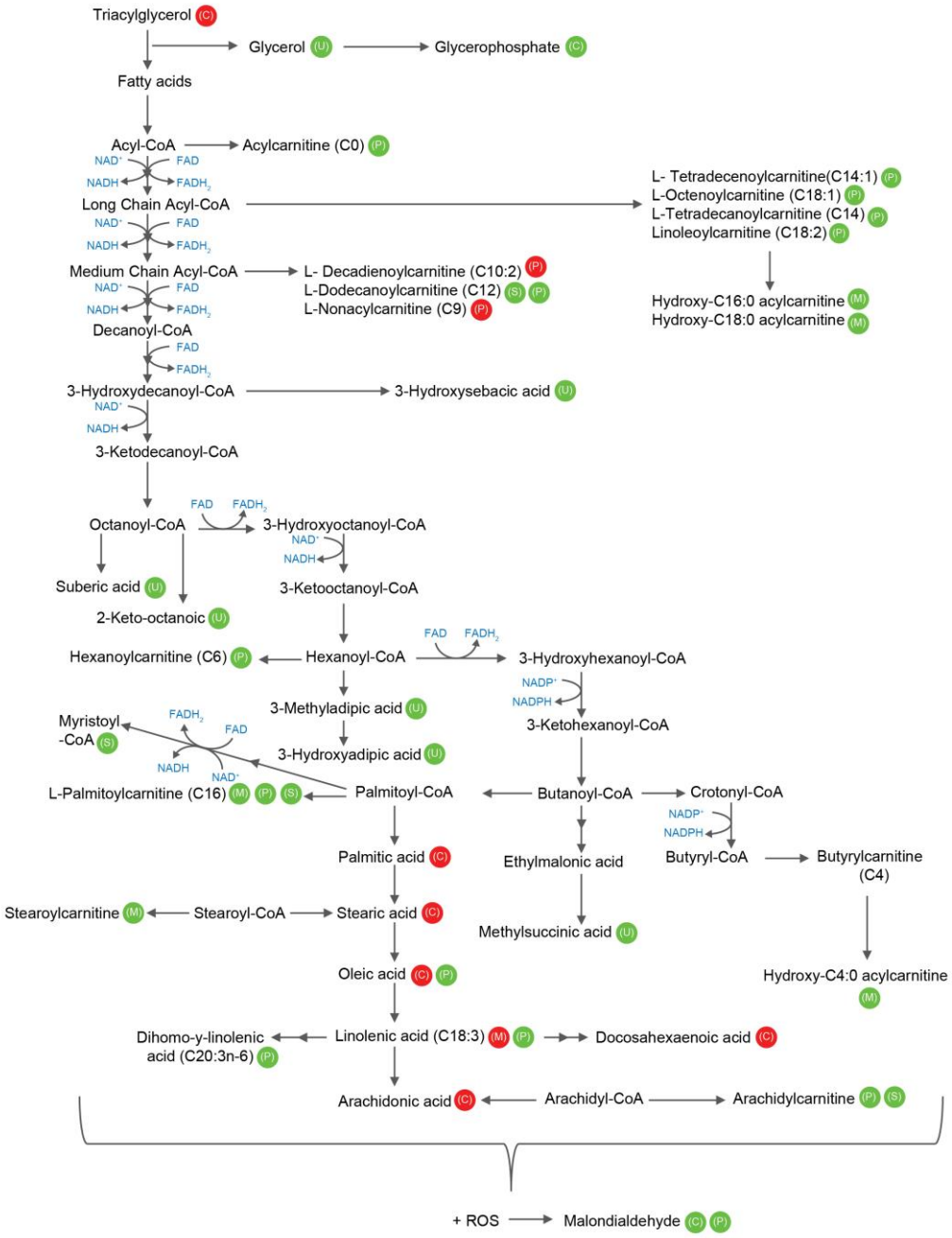

Figure 2.1. Summary of the perturbed metabolism detected in different mitochondrial disease models. A) glycolysis pathway and the TCA cycle; B) branched chain amino acids metabolism; C) tryptophan and lysine metabolism; D) one-carbon metabolism, the methylation cycle and transsulfuration pathway; E) the purine pathway; F) the urea cycle and pyrimidine pathway; G) phenylalanine and tyrosine metabolism; H) glycine, threonine and serine metabolism; I) fatty acid metabolism. This compilation of figures summarizes the findings from numerous studies on the altered metabolic profile caused by mitochondrial disease compared to healthy controls. Abbreviations used for the different models include: N=nematodes, M =mouse, C = tissue cultures, P =human plasma and U =human urine. Metabolites marked in green were reported as elevated (in intensity) in that specific disease model compared to the healthy controls. Metabolites marked in red were reported as decreased (in intensity) in that specific model compared to the healthy controls. When a metabolite is marked yellow, different studies found the specific metabolite as being increased or decreased (in intensity) in that specific disease model, thus for the yellow metabolites, current literature does not have consensus on whether the metabolite is increased or decreased in the disease model. Nicotinamide nucleotides and flavin coenzyme involved in the redox state are marked in blue.

2.1.5 CONCLUSIONS AND FUTURE PROSPECTS OF METABOLOMICS IN MITOCHONDRIAL DISEASE INVESTIGATIONS

It is evident that metabolomics, whether targeted, semi-targeted or untargeted, has been a far more successful tool for generating new information on the biochemical pathways involved in mitochondrial disease, compared to the pre-omics approach. This can be ascribed to the more holistic approach of "-omics", which focuses on all the changes in a system simultaneously to get a better idea of both the pathological and the physiological conditions (Monteiro *et al.*, 2013). As previously mentioned, the current gold standard for diagnosing mitochondrial disease is biochemical analyses performed on muscle biopsies together with other assessments, such as clinical and histochemical assays. However, obtaining muscle biopsies requires anesthesia, is expensive and can be a very traumatic experience in pediatric patients (Smuts *et al.*, 2013). The great strides made with high throughput molecular genetics and the reduction of its cost (notably for exome sequencing) have enabled a significant surge in identifying the mutations affecting MD, even before a patient presents with any symptoms. However, a genetics approach can be expensive, time-consuming, with numerous limitations (DaRe *et al.*, 2013; DiMauro and Schon, 2003; Menezes *et al.*, 2014; Schaefer *et al.*, 2004) and thus be an unattainable process, especially in developing countries. On the other hand, a metabolic *biosignature* (a combination of biomarkers) for MD has the potential to be used as a non-invasive screening method for suspected patients, simplifying the identification of patients who require muscle biopsies (Reinecke *et al.*, 2012; Smuts *et al.*, 2013; Venter *et al.*, 2015).

Another great challenge regarding mitochondrial disease is the monitoring of patients, whether for the progression of the disease or for the response to treatment (Smuts *et al.*, 2013). A non-invasive metabolic biomarker or biosignature could fulfil this purpose, as it would not require a muscle biopsy every time information on the patient's progression or response was needed (Suomalainen, 2011; Zhang *et al.*, 2012). This potential application is of particular interest considering the current drive to find therapeutic drugs for MD. Markers for disease progression can potentially be identified through correlation studies, where the correlation of metabolites with the deterioration of the phenotype is investigated. Once validated, these metabolites could then be used to monitor patients during or without therapies. Although possible in theory, considering its application in other diseases and with the first promising results from animal models of MD, this approach has not yet been attempted or reported in a clinical setting for MD.

In conclusion, it is clear that over a period of more than 15 years, the technology and bioinformatics tools to better identify small molecules on a comprehensive scale have evolved immensely and in a similar way to that of the other -omics tools. The implementation of these techniques in the field of mitochondrial disease has proven to be extremely beneficial and metabolomics has been able to link various potential biomarkers to mitochondrial disease. Considering the scope and mechanistic nature of the metabolic perturbations involved in MD, as reviewed here, it is more likely that a search for a combination of metabolic biomarkers, i.e. a biosignature, may present the best potential for further disclosing the cell biological consequences of this complex disease. Moreover, by targeting blood and urine metabolomics, this holistic approach is likely to provide applications of significant value to mitochondrial medicine.

2.2 MITOCHONDRIAL DISEASE CAUSED BY THE m.3243A>G MUTATION

2.2.1 INTRODUCTION

For functioning of the human body, energy is needed, which is produced in the form of adenosine triphosphate (ATP). For production of this ATP, a series of pathways have to work in combination for satisfactory results. The two main role players involved in human ATP production, namely the mitochondrion and the oxidative phosphorylation (OXPHOS) system, will be discussed in the section below.

2.2.2 MITOCHONDRIAL BIOENERGETICS

2.2.2.1 The mitochondrion

It is hypothesized that approximately two billion years ago, an increase in atmospheric oxygen concentration occurred due to the increase in the activity of the oceanic photosynthetic cyanobacteria. The higher oxygenated atmosphere altered life on earth. The then anaerobic organisms had to adapt to these more aerobic conditions, leading to those organisms that were unable to adapt to become extinct. It is further hypothesized that the adaptions the anaerobic organisms had to undergo included the formation of symbiotic relationships between bacteria, which were able to generate energy in the aerobic environment, and eukaryotic cells. These symbiotic relationships involved the use of the increased oxygen in the eukaryotic cell as an electron acceptor by the electron transport chain. The reactions reduced the oxygen concentrations in the bacteria and produced ATP, which could be used as a source of energy. The possible symbiotic relationship between

bacteria and eukaryotic cells gave rise to theories such as the archezoa and symbiogenesis theory. These theories provided possible explanations for the formation of one of the most important organelles in aerobic cells, known as the mitochondrion (Andersson *et al.*, 2003; Gray *et al.*, 1999).

The mitochondrion, also known as the powerhouse of the cell, is found in almost every eukaryotic cell except for red blood cells. It is an organelle that has a length of approximately 1-2 µm, a width of between 0.1-0.5 µm and consists of five components, which allows for compartmentalization of the metabolism. These components include: an outer membrane, an inner membrane, an intermembrane space, a matrix and finally cristae (Figure 2.2). The outer membrane of the mitochondrion acts as a permeable barrier between the content of the cytoplasm and the organelle itself, and has the same protein to phospholipid ratio as a plasma membrane of the cell. Porins imbedded into the outer membrane allows free diffusion of molecules up to 5 KDa over the membrane. Larger proteins cross the membrane with the help of specific transporters, known as translocases. The inner membrane of the mitochondrion has the highest protein to phospholipid ratio in the mitochondrion, and acts as a chemical barrier and an electrical insulator. The latter can be ascribed to the low permeability this membrane has for ions. The inner membrane also consists of infoldings, referred to as cristae. Between these cristae and the outer membrane, the mitochondrial matrix is situated. Inside the mitochondrial matrix, enzymes of the TCA cycle and β-oxidation can be found. These enzymes produce and utilize acetyl-CoA, as a substrate for the production of the NADH and $FADH_2$. These electron carriers are then further used in the OXPHOS system for ATP formation (Bolisetty and Jaimes, 2013). Although the mitochondrion's most important function is serving as the powerhouse of aerobic organisms, it is also involved in ageing, cell signaling, programmed cell death, and calcium homeostasis (Koshiba *et al.*, 2011).

The dysfunction of this organelle has been linked to neurodegenerative disorders (Alzheimer's, Parkinson's and Huntington's disease), cardio vascular diseases and cancer. Whether this dysfunction is as a result of the disease itself or if the mitochondrial dysfunction contributes to the disease formation and progression is still debatable, as there is literature to support both these views (Filosto *et al.*, 2011; Griffiths *et al.*, 2012).

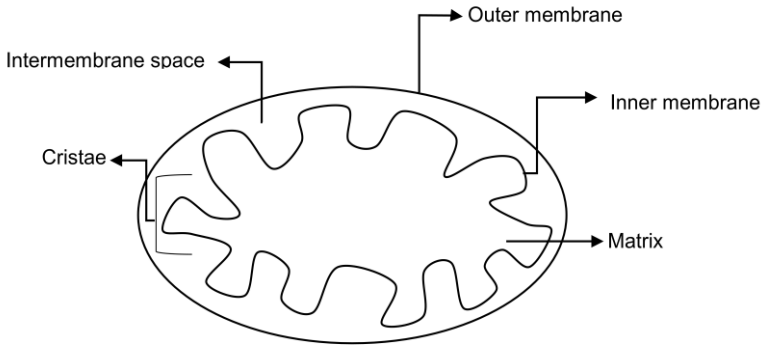

Figure 2.2. Structure of the mitochondrion. Each mitochondrion consists of five components, which ensure compartmentalization of the metabolism. These components are: an outer membrane, an inner membrane, an intermembrane space, cristae and the matrix.

2.2.2.2 The OXPHOS system

As previously mentioned, the inner mitochondrial membrane has a higher protein content than any other membrane in the mitochondrion, as it houses the OXPHOS system. Studies on the OXPHOS system began as far back as the early 1920's when the Polish scientist David Keilin published an article titled "*On cytochrome, respiratory pigment, common to animals, yeast and higher plants*" (Keilin, 1925; Slater, 2003). This paper set the ball rolling for future OXPHOS system research. The OXPHOS system consists of four complexes (complex I - IV), collectively known as the RC, ATPase (complex V) and two electron carriers, ubiquinone and cytochrome c. These electron carriers are responsible for the transportation of electrons between complexes. Through the transfer of electrons through the complexes, protons are pumped from the intermembrane space into the mitochondrial matrix, creating an electrochemical potential. This electrochemical potential is then used to drive ATP synthase to phosphorylate adenosine diphosphate (ADP) to ATP (Saeed and Singer, 2013).

2.2.3 MITOCHONDRIAL GENETICS

2.2.3.1 Mitochondrial DNA (mtDNA)

mtDNA is maternally inherited double stranded circular DNA which consists of 16 569 base pairs (Figure 2.3). This piece of circular DNA was first discovered in 1960 by Margit M. K. Nass and Sylvan Nass by means of electron microscopy and was described as DNase-sensitive thread inside mitochondria (Manev *et al.*, 2012). Twenty years later mtDNA proved

to be of great significance as it was the first human genetic material to be sequenced by Sanger and colleagues for which they were awarded a Nobel Prize (Anderson *et al.*, 1981; Brownlee, 2013; Durham *et al.*, 2003).

The mtDNA encodes 37 genes. Of these 37 genes, 22 encodes for transfer RNA (tRNA) and 2 encodes for ribosomal RNA (rRNA), involved in the translation of the mtDNA. The remaining 13 genes encodes for different subunits of the OXPHOS system. Apart from mtDNA, nuclear DNA (nDNA) contributes the majority of the subunits for the OXPHOS system. When considering the complexes of the OXPHOS system individually, complex I is the largest and consists of 44 subunits of which 14 serves as core subunits. Seven (ND1-ND6, ND4L) of these 14 subunits are encoded by mtDNA while the other seven subunits are encoded by nDNA. The remaining 30 subunits serves as “supportive” subunits for complex stability. These supportive subunits are encoded by nDNA as well. Complex II consists of four subunits, all of which are encoded by nDNA. Complex III comprises of 11 subunits, one (Cyt b) encoded by mtDNA and 10 subunits encoded by nDNA. Complex IV consist of 11 nDNA encoded subunits and three mtDNA encoded subunits (COX I - COX III). The final complex in the OXPHOS system, complex V consists of 19 subunits, of which two subunits (A6 and A8) are encoded by mtDNA and 17 by nDNA (Chinnery and Hudson, 2013; DiMauro and Schon, 2003). nDNA also encodes several proteins that are needed for the assembly of complex I (11 proteins), complex III (two proteins), complex IV (18 proteins) and complex V (four proteins) (Chinnery and Hudson, 2013).

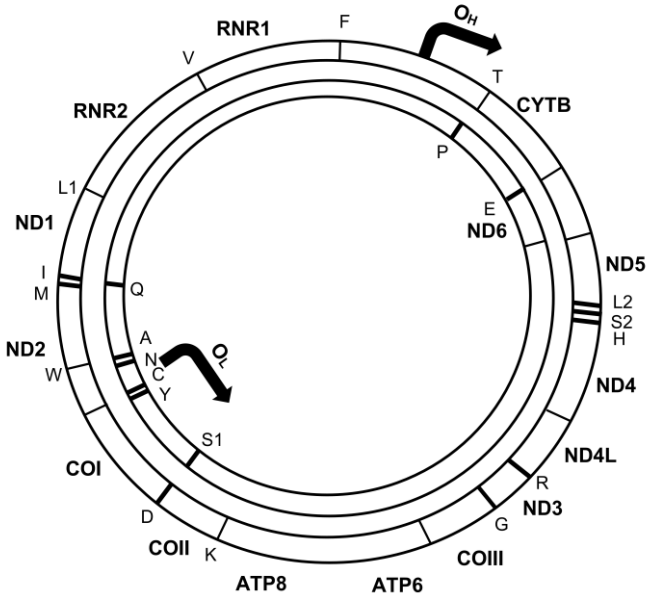

Figure 2.3. Structure of mitochondrial DNA (mtDNA). mtDNA is maternally inherited, double stranded circular DNA which encodes for 37 genes. Of these 37 genes, 22 encodes for transfer RNA (tRNA) and 2 encodes for ribosomal RNA (rRNA). The remaining 13 genes encodes for different subunits of the OXPHOS system. Seven of the 13 genes encode for subunits of complex I (ND1-ND6, ND4L). One gene encodes for a subunit in complex III (Cyt b). Three genes encode for subunits of complex IV (COX I-COX III), while two genes encodes for Complex V (A6 and A8).

2.2.3.2 Replication, transcription, and translation of mtDNA

2.2.3.2.1 Introduction

mtDNA follow the same central dogma of molecular biology as nDNA, therefore the process of how information retrieved from genes are ultimately expressed as proteins is similar. In order to convert the information from these genes into proteins, several steps are involved, namely replication, transcription, and translation (Tuppen *et al.*, 2010). These steps will be discussed in the following section.

2.2.3.2.2 Replication of mitochondrial DNA

Mitochondrial DNA replication occurs independently from nDNA and from the cell cycle. This notion is supported by the fact that mtDNA replication has been observed in postmitotic tissues (e.g., brain, skeletal muscle). Even though the replication mechanism for mtDNA is not yet fully understood, two theories are currently suggested: 1) strand-displacement replication and 2) coupled leading-lagging strand DNA replication.

As indicated by Figure 2.4, the traditional strand-displacement replication suggests that replication start at the heavy strand origin site (O_H). This results in the dissociation of the light strand from the heavy strand. The light strand will then stay disconnected from the heavy strand as a single strand while the heavy strand undergoes replication until the light strand origin site (O_L) is revealed. Once the O_L is revealed, synthesis of the light strand can commence in the opposite direction (Brown *et al.*, 2005; Clayton, 2003; Holt and Reyes, 2012; Tuppen *et al.*, 2010). In the coupled leading and lagging strand DNA replication theory, replication starts at the heavy strand origin O_H, however in contrast to strand-displacement replication, synthesis of the lagging light strand is initiated shortly after replication of the heavy strand begun. This results in the formation of short Okazaki ribonucleotide fragments, which is then converted into DNA (Brown *et al.*, 2005; Clayton, 2003; Holt and Reyes, 2012; Tuppen *et al.*, 2010). In all likelihood, both of these theories are used in different situations in the cell, depending on the cell's requirement. For example, steady state cells could use coupled leading-lagging strand DNA replication while cells that requires rapid mtDNA synthesis will rather make use of strand-displacement replication (Tuppen *et al.*, 2010).

Even though mtDNA replications occurs independently from nDNA, it still requires nuclear-encoded factors. These factors include: 1) DNA polymerase gamma (POLG), which consists

of PolgA and PolgB. PolgA contains the 5′–3′ exonuclease activity, while PolgB serves as the processivity subunit, 2) Twinkle, which is a helicase and 3) mitochondrial single-stranded binding protein (mt-SSB) (Tuppen *et al.*, 2010).

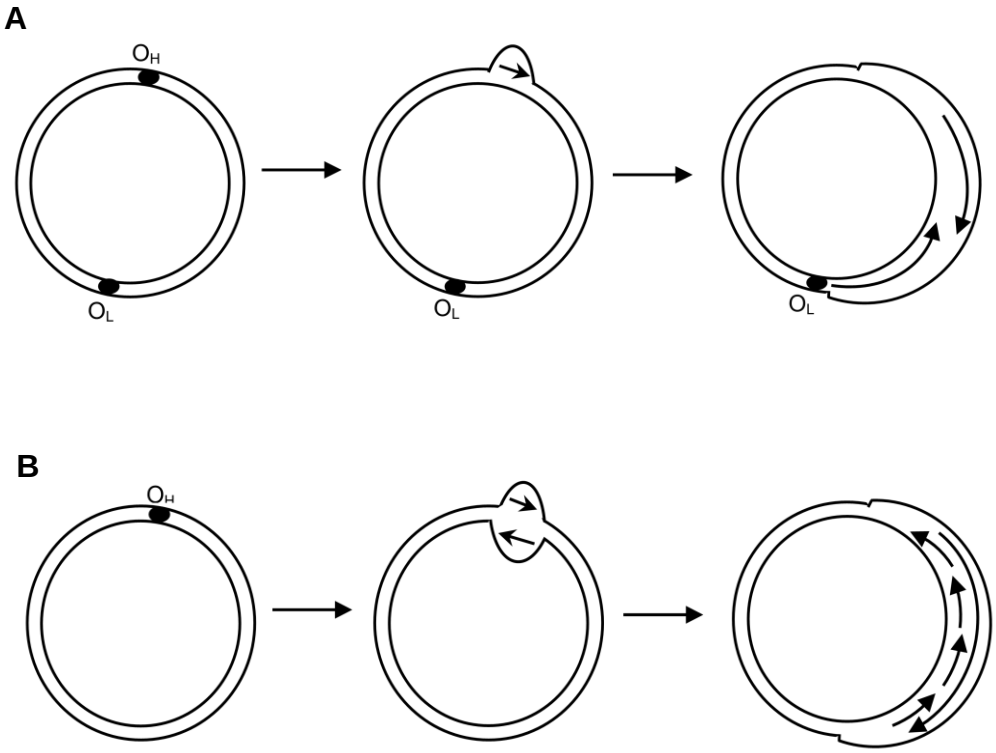

Figure 2.4. Replication of mtDNA. Replication of mtDNA can either occur by using a) Strand-displacement replication or b) Coupled leading-lagging strand DNA replication (Adapted from Clayton, 2003).

2.2.3.2.3 Transcription of mtDNA

In the transcription process, information from the genes are converted to messenger RNA (mRNA) molecules. Transcription can be initiated from three promoters situated on various positions on the mtDNA: one situated on the L-strand (LSP) and two situated on the H-strand (HSP1 and HSP2). These promoters are located at different positions and have different functions. HSP2 is situated in the *MT-RNR1* gene closest to the 5′ end, while the LSP is found in the D-loop. Transcription initiated from both these promoters will result in the formation of almost genome-length polycistronic transcripts, which are ultimately cleaved to individual mRNA and tRNA molecules. Transcription from the promoter on the light strand also produces RNA primers that is required for the initiation of mtDNA replication of the heavy strand. The remaining promoter in the heavy strand, HSP1 is situated upstream of the *MT-TF* gene. Transcription from this promoter results in the formation of only two rRNAs

(12S and 16S) and two mt-tRNAs (mt-tRNA^{Phe} and mt-tRNA^{Val}) (Smits *et al.*, 2010; Tuppen *et al.*, 2010).

As with replication, various nuclear-encoded factors are required for transcription to occur, including: 1) the RNA polymerase (POLRMT), 2) the transcription activator (TFAM), 3) the transcription factor (TFB2M) and 3) the termination factor (mtERF) (Taylor and Turnbull, 2005; Tuppen *et al.*, 2010).

2.2.3.2.4 Translation of mtDNA

During the translation step, mRNA molecules will serve as templates for the synthesis of peptides that form part of complexes I, III, IV and V of the OXPHOS system. Similar to replication and transcription, translation also requires various nuclear-encoded factors to take place. The mitoribosome consists of two rRNAs and 81 mitochondrial ribosomal proteins (Diodato *et al.*, 2014; Smits *et al.*, 2007; Smits *et al.*, 2010).

The translation step of mtDNA can be subdivided into different phases: the initiation phase, the elongation phase and then finally the termination phase (Arava *et al.*, 2005; Christian and Spremulli, 2012; Smits *et al.*, 2010). During the initiation phase, mitochondrial translation factor (mtIF3) initiates the dissociation of the mitoribosome into its two subunits, the 28S small subunit (SSU) and the 39S large subunit (LSU). This dissociation is followed by the attachment of the mRNA to the SSU, with the start codon (AUG) situated at the peptidyl (P) site of the subunit (Christian and Spremulli, 2010; Diodato *et al.*, 2014; Smits *et al.*, 2010). In the next step of the initiation phase, fMet-tRNA binds to the SSU with the assistance of mtIF2. The latter requires GTP for binding. After the binding of fMet-tRNA and mtIF2, the two subunits recombine. This recombining of subunits results in the release of the mtIF3, and mtIF2, with the fMet-tRNA remaining bound to the start codon at the P site. Initiation is now complete (Diodato *et al.*, 2014; Smits *et al.*, 2010).

During the elongation phase, elongation factor (mtEFTu) combines with GTP and an aminoacylated tRNA, to form a tertiary complex. This complex is then transported to the SSU, specifically the acceptor (A) site, where the mRNA is decoded by a codon-anticodon recognition process (Grosjean *et al*., 2010; Smits *et al*., 2010) After codon-anticodon recognition, GTP hydrolysis results in the releasing of mtEFTu·GDP, leaving the aminoacyl-tRNA attached to the A site. Here peptide bond formation occurs, resulting in the addition of an amino acid to the growing peptide chain. mtEFTu-GDP is then converted back to mtEFTu-GTP by means of the nucleotide exchange protein mtEFTs (Gindulyte *et al.*, 2006;

Mai *et al.*, 2017; Smits *et al.*, 2010). The elongation phase ends with an elongation factor-GTP complex (mtEFG1-GTP), imitating the movement of the bound tRNAs from the A and P sites on to the P and exit (E) sites located on the mitoribosome. This movement shifts the mRNA up by one codon, resulting in a tRNA being released at the E site. A new cycle of elongation can then begin (Mai *et al.*, 2017; Smits *et al.*, 2010).

Finally, the translation of mtDNA is ended with a termination phase. This termination is initiated when a stop codon (UAA, UAG, AGA or AGG) is found at the A site (Lightowlers and Chrzanowska-Lightowlers, 2010; Nozaki *et al.*, 2008; Smits *et al.*, 2010). This will result in the identification of the stop codon by the mitochondrial release factor (mtRF1). The action will dissociate the protein that is attached to the last tRNA at the P site (Duarte *et al.*, 2012; Smits *et al.*, 2010). After the protein is released from the last tRNA, ribosome recycling factor (mtRRF) and mtEFG2·GTP will result in the uncoupling of the mitoribosomal subunits, the tRNA and the mRNA, making these components available for a next cycle of protein formation (Inokuchi *et al.*, 2000; Smits *et al.*, 2010).

2.2.4 MITOCHONDRIAL DISEASE CAUSED BY mtDNA MUTATIONS

2.2.4.1 Heteroplasmy, threshold effect and mtDNA copy number

In the field of mitochondrial disease, the terms mtDNA copy number, heteroplasmy/mutation load and threshold are often used. mtDNA copy number refers to the number of mtDNA molecules measured in a cell or tissue, while heteroplasmy refers to the presence of both mutated, and normal mtDNA in a cell or tissue. Mutation load is then used to describe the ratio or percentage of mutated mtDNA to normal DNA. The threshold effect is used to refer to the occurrence of phenotypic manifestations, due to the fact the number of mutated mtDNA (heteroplasmy/mutation load), has reached a level at which the OXPHOS system cannot produce sufficient energy any more. The threshold is the lowest in cells or tissue with a high-energy demand, like brain, heart, skeletal muscles, retina, renal tubules and endocrine glands. The threshold is significantly higher in cells or tissue that can make use of anaerobic glycolysis for survival, like smooth muscle. Threshold levels usually ranges between 60-90% before phenotypic manifestations occur (Al-Enezi *et al.*, 2008; Tuppen *et al.*, 2010).

When determining mutation load in patients, whether it is for diagnostic purposes or disease management, it is important to take into account the type of sample where the mutation load is measured when interpreting the results. For some tRNA mutations, including the

m.3243A>G mutation, the use of blood for mutation load determinations is not ideal as studies have indicated a decline in mutation load over time, as a result of negative selection (Cree *et al.*, 2009; Mehrazin *et al.*, 2009; Sallevelt *et al.*, 2017; Whittaker *et al.*, 2009). This decline in mutation load could result in a low, or even undetectable mutation load, even when a patient is severely affected. The latter will then result in a false negative diagnosis (de Laat *et al.*, 2012; Rahman *et al.*, 2001).

In order to decrease the possibility of false negative diagnosis, various studies have investigated the most suitable sample type for mutation load determination. They indicated that epithelial cells in urine showed the most promising results, having higher mutation load levels, when compared to other samples types such as blood, buccal mucosa and skin fibroblasts (O'Callaghan *et al.*, 2015; Shanske *et al.*, 2004).

2.2.4.2 mtDNA mutations (Point mutations, rearrangements and deletions)

Since the OXPHOS system is encoded by both nDNA and mtDNA, mutations in any one of these genomes can result in mitochondrial dysfunction. Because the focus of this study is on the m.3243A>G mutation, only the different mtDNA mutations is discussed in the following section.

2.2.4.2.1 Point mutations

Point mutations in mtDNA are the most common mutations responsible for mitochondrial disease development, with a prevalence of one in 200 (Burr *et al.*, 2018; Elliott *et al.*, 2008). Point mutations involve the substitution of a base with another base at a specific position of the mtDNA. These point mutations are maternally inherited, heteroplasmic and can either be located in tRNA and rRNA encoding genes or it can be situated in protein encoding genes. Point mutations in the tRNA or rRNA encoding genes will ultimately affect the mitochondrial protein synthesis. Due to this more global effect, these point mutations usually result in multiple deficiencies of the OXPHOS system. Point mutations have been identified in all of the mtDNA genes with more than 50 of these associated with tRNAs. Patients affected by these tRNA mutations usually present with symptoms related to neuromuscular phenotypes, as tRNA genes harbor approximately 80 neuromuscular associated mutations (Tryoen-Toth *et al.*, 2003; von Kleist-Retzow *et al.*, 2003). Patients affected by point mutations in rRNA encoding genes have been linked to aminoglycoside-induced non-syndromic deafness as these antibiotics are known to affect protein synthesis (Bates *et al.*, 2012; Bindu and Reddy, 2008; Hao and Moraes, 1997; Yano *et al.*, 2014; Zhong *et al.*, 2013). In contrast, mutations

situated in protein encoding genes have a more targeted effect as these mutations affect specific proteins. The latter result in a defective complex of the OXPHOS system containing the affected protein subunit. Mutations situated in protein encoding genes have been reported in subunits of complex I (ND1, ND2, ND4 and ND6), cytochrome b, complex IV (CO I, CO II, CO III) and complex V (ATP6) of the OXPHOS system (Alston *et al.*, 2017; Tuppen *et al.*, 2010; von Kleist-Retzow *et al.*, 2003). Some mtDNA point mutations and their respective position on the mtDNA are illustrated in Figure 2.5.

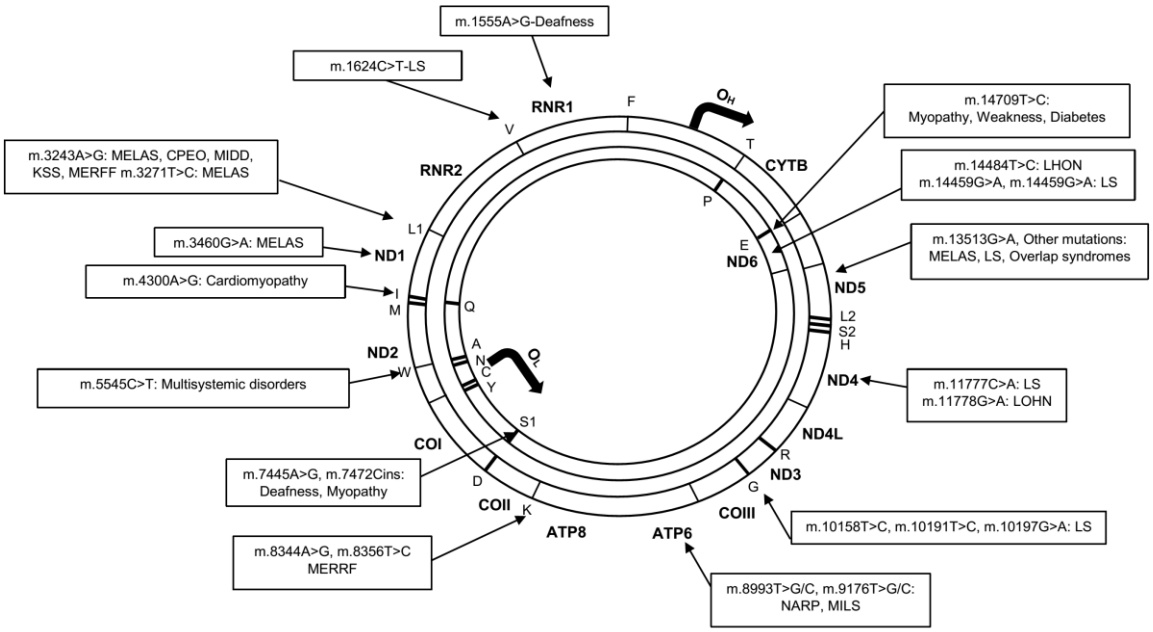

Figure 2.5. Selected mtDNA point mutations. This figure summarizes some mtDNA point mutations by giving its position on the mtDNA and its possible effect. Mitochondrial encephalomyopathy, lactic acidosis, and stroke-like episodes (MELAS), Kearns–Sayre syndrome (KSS), Leigh syndrome (LS), Leber's hereditary optic neuropathy (LHON), myoclonic epilepsy with ragged red fibers (MERRF), maternally inherited diabetes and deafness (MIDD), maternally inherited Leigh syndrome (MILS), neuropathy, ataxia, and retinitis pigmentosa), progressive external ophthalmoplegia (PEO).

2.2.4.2.2 Rearrangements (Deletion and duplication)

In contrast to point mutations, which are maternally inherited, mtDNA mutations caused by rearrangements are formed *de novo* during embryonic development and has a prevalence of around 1.5 in 100 000 (Alston *et al.*, 2017; Gorman *et al.*, 2015). mtDNA rearrangement can exist as deletions where numerous tRNA and protein coding genes are removed in various sizes (1.3 to 8kb), where a segment of the mtDNA is deleted, or as duplications, where a

segment of mtDNA has been inserted into wild-type mtDNA. Even though mtDNA rearrangements have different origins, they do have some common characteristics. First, they take place between the heavy strand and light strand origin site. Secondly, they are surrounded by short direct repeats. Finally, it is also hypothesized that their formation is the same and independent of the symptoms being presented. How these deletions are formed is still a debated topic. Some researches propose that deletions occur during the replication phase of mtDNA, while other researchers suggest that deletions are formed as a result of the repairing of damage mtDNA. Important factors that are believed to be connected to the varied manifestation of symptoms and the severity of them is: 1) the size of the deletion, 2) the location of the deletion, 3) the amount of deletions and 4) distribution of the deletion in the tissue (Grady *et al*., 2014; Pitceathly *et al.*, 2012; Tuppen *et al.*, 2010). The three main phenotypes associated with large scale deletion/rearrangements are chronic PEO, KSS and Pearson syndrome (Alston *et al.*, 2017; Grady *et al*., 2014).

2.2.5 The m.3243A>G MUTATION

2.2.5.1 Background

The m.3243A>G mutation was first discovered in 1990, where it was linked to mitochondrial myopathy, encephalopathy, lactic acidosis and stroke like episodes (MELAS). The mutation is a point mutation on position 3243 of the mtDNA, where an adenine base is substituted with a guanine base in the *MT-TL1* [Mitochondrially Encoded TRNA Leucine 1 (UUA/G)] gene. This gene encodes for a transfer RNA (tRNA), which recognizes the codons UUA, and UUG, for the amino acid leucine (Figure 2.6). However, when the adenine base is substituted with a guanine base, several physiological effects occur: firstly, it affects the stability of the tRNA structure. Although the mutation allows the folding of the acceptor branch of the tRNA, it also allows the folding of an unstable anti-codon branch. This unstable anti-codon branch results in decreased structural stability, which causes incorrect tRNA processing, and enzyme formation. Secondly, the m.3243A>G mutation can cause undermethylation of the isolated non-G-tract guanine (G10) region. Undermethylation of this region could result in impaired function of the coding of mitochondrial enzymes encoded by nDNA. Thirdly, the m.3243A>G mutation results in reduced activity of the enzyme leucyl-tRNA synthetase. This enzyme is responsible for the attachment of the correct amino acid to its corresponding tRNA. When impaired, it will lead to decreased amino-acylation capacity, which will result in reduced amounts of leucine attached to tRNA. Finally, the m.3243A>G mutation affects the taurine modification of the wobble position (Figure 2.6). This process enables the anti-codon to exclusively bind to a specific codon. In the case of leucine, this

codon will be either UUA or UUG. If the uracil is unable to undergo modification, it loses its restriction to only bind to UUA/UUG and then can also recognize the codons UUU and UUC. The latter is the codons for the amino acid phenylalanine (Jacobs and Holt, 2000; Kirino *et al.*, 2004). Losing the ability to undergo taurine modification could lead to the misincorporation of leucine in the position of phenylalanine in the mitochondrial proteins. This could result in deficient decoding, termination of polypeptide elongation, production of premature proteins, decreased enzyme function and decreased level of protein synthesis, all of which can affect the OXPHOS system's ability to perform its normal functions (Finsterer, 2007; Jacobs and Holt, 2000).

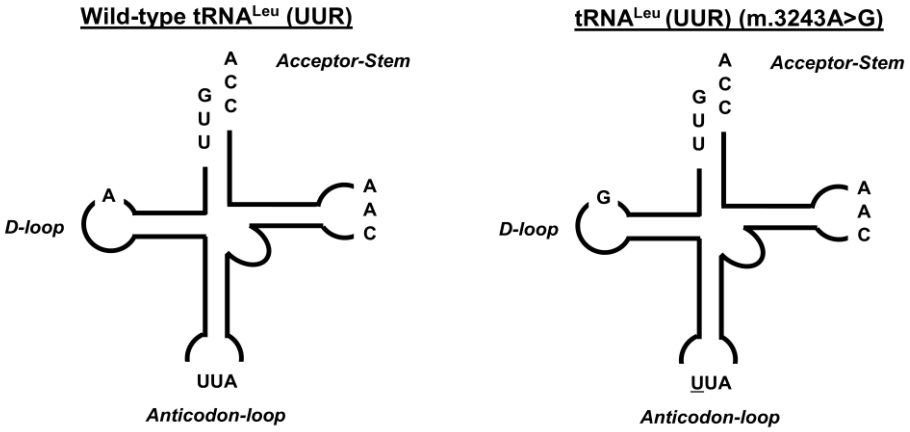

Figure 2.6 Cloverleaf structures of tRNAs^{Leu} (UUR) (m.3243A>G). Illustration of a cloverleaf structure of the a) wild-type tRNAs^{Leu} (UUR), and b) a mutated version, where the adenine is substituted with guanine base on position 3243 of the mitochondrial DNA (Adapted from Kirino *et al.*, 2004).

The prevalence of the m.3243A>G mutation has been determined in different populations using different types of samples, including hair follicles, blood, skeletal muscle and buccal-epithelial cells (Chinnery *et al.*, 2001; Majamaa *et al.*, 1998; Manwaring *et al.*, 2007). Currently the estimated prevalence for the m.3243A>G mutation in the different populations are 7.59/ 100 000 in North England, 16.3/ 100 000 in Finland and 236/100 000 in Australia. The high prevalence of the m.3243A>G mutation determined by Manwaring *et al.,* (2007) can be ascribed to the analyses of samples collected from a general community, rather than just patient referrals used by the other populations. This higher prevalence confirms the underestimation of the prevalence of the mutation, highlighting the possible existence of a large amount of asymptomatic patients in need of future care (de Laat *et al.*, 2012; de Laat et al., 2013; Testai and Gorelick, 2010).

2.2.5.2 Symptoms and phenotypes associated with the m.3243A>G mutation

The m.3243A>G mutation is not specific to only one complex of the OXPHOS system since it is a tRNA mutation, essential to incorporate leucine in multiple areas across the OXPHOS system. However, due to the size of complex I and the high prevalence of the UUG codon in subunit six (NADH dehydrogenase 6) of this complex, phenotypes caused by the m.3243A>G mutation often mimic symptoms associated with a complex I defect (Kami *et al.*, 2012). Harboring the m.3243A>G mutation can result in various symptoms affecting a wide range of organs/ systems, including the central nervous system, dermis, ear, endocrine system, eye, gastrointestinal tract, cardiovascular, renal and peripheral nervous system (Table 2.2) (Baertling *et al.*, 2014; Hernández-Luis *et al.*, 2007; Mignarri *et al.*, 2015; Santa, 2010). Patients diagnosed with the m.3243A>G mutation can be classified into three major groups: asymptomatic, syndromic and non-syndromic (Hoptasz *et al.*, 2014; Vivero *et al.*, 2013). Asymptomatic patients harbor the m.3243A>G mutation, but do not present with any symptoms at the time of examination. These patients could potentially, over time, start to present with symptoms. Non-syndromic patients present with a number of symptoms, but are not associated with a specific pathological phenotype linked to the mutation. And finally, syndromic patients present with a specific set of symptoms associated with a specific phenotype. As previously mentioned, the m.3243A>G mutation was initially associated with MELAS, however, with time, more and more phenotypes have been associated with the m.3243A>G mutation. These phenotypes include for example: maternally inherited diabetes and deafness (MIDD), PEO, LS, myoclonus epilepsy with ragged red fibers (MERRF), and KSS (Finsterer, 2009).

2.2.5.2.1 Mitochondrial encephalopathy, lactic acidosis, and stroke-like episodes (MELAS)

Known to be the first and most common phenotype associated with the m.3243A>G mutation, MELAS was first diagnosed in 1984 as a "*neurodegenerative disease caused by the decreased ability of cells to produce sufficient energy in the form of ATP*" (Pavlakis *et al.*, 1984). It was only six years later that the m.3243A>G mutation was discovered and linked to MELAS (Goto *et al.*, 1990).

MELAS affects patients of all ages and they can present with a wide range of symptoms which varies in severity. The most common symptoms associated with MELAS are, stroke-like episodes, dementia, epilepsy, lactic academia, myopathy, recurrent headaches, hearing impairment, diabetes and short stature (El-Hattab *et al.*, 2015).

Although nearly 80% of MELAS cases are caused by the m.3243A>G mutation, other tRNA mutations (m.583G>A, m.1642G>A, m.3252A>G, m.3260A>G, m.3271T>C, m.3291T>C, and m.5814A>G) have also been associated with this phenotype. Additionally, several mutations in genes encoding for OXPHOS subunits [T9957C (COX), G13513A (ND5)] and single large scale deletions have also been associated with MELAS (Finsterer, 2009; Pinto and Moraes, 2014).

2.2.5.2.2 Kearns-Sayre syndrome (KSS)

KSS is a mitochondrial disease that was first described in 1958, seven years before mtDNA was discovered as "*a rare neuromuscular disorder defined by a characteristic triad of, pigmentary retinopathy, atrioventricular block and cerebellar ataxia*". It has a prevalence of about 1–3 per 100 000 and even though KSS is in most caused by a single large scale deletion in most cases, some cases there has been reports where no single deletion could be detected, but rather point mutations such as the m.3243A>G or m.3249G>A mutations were found to be the cause of the disease (Finsterer and Zarrouk-Mahjoub, 2016; Khambatta *et al.*, 2014; Leal *et al.*, 2016; Seneca *et al.*, 2001).

Patients diagnosed with KSS develops retinitis pigmentosa and PEO before the age of 20. This is accompanied by neurological symptoms such as cerebellar ataxia, cognitive impairment and deafness. These patients can also present with non-neurological symptoms such as cardiomyopathy, short stature, endocrinopathies, and dysphagia (Tuppen *et al.*, 2010).

2.2.5.2.3 Maternally inherited diabetes and deafness (MIDD)

MIDD was the second phenotype associated with the m.3243A>G mutation, which was first described in 1992 (Donovan and Severin, 2006). It is a rare form of diabetes, accounting for up to 1% of all diabetes cases (Gilbert *et al.*, 2017). The main symptoms these patients present with are diabetes and deafness, however they can also present with various additional symptoms ranging in severity. These symptoms are usually general symptoms associated with the m.3243A>G mutation and manifest in organs that are highly energy depended. The symptoms include: myopathy, congestive heart failure, muscular dystrophy, short stature, constipation and malabsorption as well as cerebellar and cerebral atrophy (Murphy *et al.*, 2008).

Nearly 85 % of all MIDD cases are as a result of the m.3243A>G mutation. However other mutations have also been associated with this phenotype which includes: m.3264T>C, m.14709T>C and m.10003T>C (Wang *et al.*, 2016).

2.2.5.2.4 Progressive external ophthalmoplegia (PEO)

PEO is another common phenotype associated with the m.3243A>G mutation was first described in 1868 by von Graefe as "*slowly progressive weakness of ocular muscles*" (Danta *et al.*, 1975; Rüegga *et al.*, 2005). It has a current minimum prevalence of 1 in 30 000 (Yu-Wai-Man *et al.*, 2014).

One of the first signs that a patient is possibly suffering from PEO, is the manifestation of ptosis (drooping of eye lid) and ophthalmoplegia. Even though PEO mostly manifests in adulthood, cases have been reported of manifestation during childhood or adolescence. Other symptoms also associated with PEO are weakness or paralysis of the eye muscles, weakening of muscles in the arms, legs and neck, hearing loss, peripheral neuropathy, diabetes mellitus and lipomatosis (Pinto and Moraes, 2014; Rowland, 1993).

Although most PEO cases are caused by the m.3243A>G mutation, deletions in various other genes have also been reported to result in the manifestation of PEO. These genes include: POLG (encodes the catalytic subunit of DNA polymerase γ), SLC25A4 (encodes the mitochondrial adenine nucleotide translocator ANT1), PEO1 (encodes T7 gene-4-like protein with intramitochondrial nucleoid localization), Twinkle (mitochondrial protein that acts as a helicase), POLG2 (encodes the p55 accessory subunit of DNA polymerase γ), OPA1 (encodes optic atrophy 1) and *RRM2B* (encodes the small subunit of the ribonucleotide reductase) (Park *et al.*, 2011; Ronchi *et al*., 2011; Sommerville *et al*., 2014).

2.2.5.2.5 Leigh syndrome (LS)

LS is another phenotype associated with the m.3243A>G mutation and was first described in 1951 by Dr. Dennis Leigh as a *"progressive neurodegenerative disorder typically beginning in infancy or childhood and is characterized by symmetrical necrosis in the brain stem, basal ganglia, and thalamus*" (Chae *et al.*, 2008). Even though LS was already described in 1951, it was only many years later in 1996, after linking it to the m.3243A>G mutation, that a set of diagnostic criteria was proposed. This criterion consisted of the following: 1) progressive neurologic disease with motor and intellectual developmental delay, 2) signs and symptoms of brainstem and/or basal ganglia disease, 3) elevated lactate concentration in blood and/or

cerebrospinal fluid, 4) typical nervous system tissue changes in patient and similarly manifested in a sibling (Rahman *et al.*, 1996).

LS is usually diagnosed in the first year of a patient's life and progresses at a rapid pace. LS diagnosis has to meet three criteria: 1) the patient must present with a neurodegenerative phenotype; 2) mitochondrial dysfunction must be present; 3) bilateral CNS lesions must be detected (Baertling *et al.*, 2014; Gerards, 2014). Patients present with developmental delay, failure to thrive and feeding difficulties. They also present with neurodegenerative symptoms such as muscular hypertonia or spasticity, dystonia, seizures, ataxia, dysphagia, ptosis and abnormal eye movements. Episodes of lactic acidosis is also present which effects the patient's respiratory and kidney function (Baertling *et al.*, 2014).

Even though LS has been associated with the m.3243A>G mutation, it can also be caused by a wide range of other tRNA and rRNA mutations. These mutations include: m.8344 A>G, m.1644 G>T, m.3537 Tins, m.3243 A>G, m.10410 T>A, m.5523 T>G m.896 A>G 12S rRNA and m.270 A>G 16S rRNA.63. In addition to these tRNA and rRNA mutations, LS can also be caused by mutations encoding for proteins associated with a specific section of the OXPHOS system. These genes are of nDNA and mtDNA origin and affect all the complexes and the electron carriers coenzyme Q10 and cytochrome c (Ruhoy and Saneto, 2014).

2.2.5.2.6 Myoclonus epilepsy with ragged red fibers (MERRF)

MERRF is a rare mitochondrial disease with an estimated prevalence of approximately 1/400,000 in Northern Europe. It was first described in 1973 after a family presented with myoclonus epilepsy that was associated with ragged red fibers and abnormal high blood lactate and pyruvate levels (Lorenzoni et al., 2014; Shoffner *et al*., 1990; Tsaris, 1973). A more accurate diagnostic criteria was described a few years later in 1980 when a second case of MERRF was reported. Patients diagnosed with MERRF usually present with myoclonus, generalized epilepsy, cerebellar ataxia and ragged red fibers that can be observed when investigating a muscle biopsy (Lorenzoni *et al.*, 2014; Park *et al.*, 2017).

Even though 80-90% of MERFF cases are caused by the A8344G mutation, other mutations have also been associated with this phenotype, including m.3243A>G. Apart from m.3243A>G, other mutations reported to result in the manifestation of MERRF includes:m.611G>A, m.3255G>A, m.3291T>C, m.4284G>A, m.5521G>A, m.7512T>C, m.8344A>G, m.8356T>C, m.8361G>A, m.8363G>A, m.12147G>A, m.12300G>A, m.3042A>T, m.15967G>A and multiple deletions (Lorenzoni *et al.*, 2014).

Table 2.2: Summary of different organs and symptoms associated with the m.3243A>G mutation (Finsterer, 2007; Santa, 2010).

Organ/System	Symptoms	
Central nervous system	• Apathy • Autism • Basal ganglia calcification • Cerebral lactazidosis • Cerebral atrophy • Cerebral microangiopathy • Cerebellar ataxia • Cerebellar atrophy • Cluster headaches	• Cognitive decline • Headache • Lethargy • Migraine • Neuropsychological deficits • Parkinson syndrome • Seizures • Striatal lesions • Stroke like episodes
Dermal	• Asymmetric vascular dilatation • Atopic dermatitis	• Lipoma • Local melanoderma
Ear	• Protruding ears	• Sensorineural hearing loss
Endocrine system	• Abortion • Addison's disease • Diabetes mellitus • Goitre • Hashimoto thyroiditis	• Hypoparathyroidism • Miscarriage • Multihormonal hypopituitarism • Ovarian failure • Short stature
Eye	• Hypertelorism • Macula dystrophy • Optic atrophy	• Pigmentary retinopathy • Visual field defects
Gastrointestinal tract	• Abdominal pain • Constipation • Cyclic/episodic vomiting • Diarrhoea • Dysphagia	• Epigastralgia • Gastric dysmotility • Intestinal pseudo-obstruction • Nausea • Sialoadenitis
Cardiovascular	• Aortic rupture • Arterial hypertension	• Hypertrophic cardiomyopathy • Left ventricular hypertrabeculation
Renal	• Nephrotic syndrome • Renal cysts	• Segmental glomerulosclerosis • Tubular dysfunction
Peripheral nervous system	• Anarthria • Easy fatigability • Exercise intolerance • Facial and limb weakness • General wasting • Hypotonia	• Muscle cramps • Myopathy • Ophthalmoparesis • Polyneuropathy • Ptosis • Respiratory muscle weakness

2.2.6 DIAGNOSIS OF m.3243A>G PATIENTS

Diagnosis of a patient affected by the m.3243A>G mutation, involves a multidisciplinary approach which includes: family history assessments, clinical and biochemical investigations, muscle histochemistry and finally molecular genetic testing.

2.2.6.1 Family history

During the diagnosis of a patient with mitochondrial disease, taking an extensive family history is of great importance. When dealing with a mutation such as the m.3243A>G mutation, manifesting with such a wide range of symptoms ranging in severity, even between family members, these detailed family histories could point out maternally inherited patterns that could have been overlooked otherwise. These patterns could then serve as motivation for molecular and genetic investigations of the mtDNA for confirmation of a suspected mtDNA mutation (Vento and Pappa, 2013).

2.2.6.2 Clinical assessments

Due to heterogeneity in the manifested phenotypes, it is essential to do a thorough clinical workup of patients to make the best possible diagnosis. Apart from a physical examination, these assessments included electrocardiography (ECG) for the investigation of cardiac functioning and electromyography (EMG), for muscle functioning. Computed tomography (CT) scans are used to evaluate the intracranial volumes and to look for the presence of basal ganglia calcification. Magnetic resonance imaging (MRI) is a non-specific assessment tool, used to detect structural change in the brain, which is very useful when diagnosing a MD patient. These structural findings depend on the phenotype, degree of severity of symptoms and the age of the patient.Some of the phenotype-specific MRI findings include: 1) progressive signal abnormalities mainly present in patients suffering from LS. These abnormalities are most prominent in the lentiform and caudate nuclei, however are also seen in the thalamus, periaquiductal gray, tegmentum as well as in the red and dentate nuclei. Other common MRI finding associated with LS includes; spongiform changes in the gray matter, cerebral organic acidurias and global atrophy including a decrease in the volume of the basal ganglia; 2) MELAS patients present with temporary stroke-like lesions as well as lesions affecting the gray matter, which is not restricted to the vascular territories. Although not common MELAS patients can also present with white matter lesions; 3) KSS most often shows cerebral and cerebellar atrophy accompanied by bilateral lesions in the subcortical white matter, thalamus, basal ganglia and brainstem; 4) abnormal signal intensities found in both the brainstem and subtentorial nuclei together with a lactate peak is often associated with complex I deficiencies (Saneto *et al*., 2008; Khan *et al.*, 2015).

2.2.6.3 Biochemical investigations

Currently there is no specific biochemical biomarker used for diagnoses of patients presenting with a phenotype associated with the m.3243A>G mutation. However various biochemical investigations can be used to narrow down the possibilities to the presence of a possible mitochondrial disease. These biochemical investigations include the measurement of metabolites such as lactate, pyruvate, alanine, tricarboxylic acid cycle intermediates, ethylmalonic acid, 3-methylglutaconic acid, dicarboxylic acids, acylcarnitines and creatine kinease. In addition to these specific metabolites, total blood count, thyroid and liver function, bone chemistry and random blood glucose is also measured. Even though the biochemical investigation does not always give a clear diagnosis, valuable information can always be gained, such as the lactate/ pyruvate ratio that can be used as a cytosolic redox state indicator. Similarly, insight can be obtaind as to why lactate levels are in most cases elevated more in patients affected by MELAS and LS, compared to patients presenting with PEO (Esterhuizen *et al.*, 2017; Finsterer, 2007; Khan *et al.*, 2015).

2.2.6.4 Muscle histochemistry

Histochemical investigation forms another important part of the diagnosis process of m.3243A>G affected patients, even though it may be normal in some (Wang and Le, 2015). Measuring the activity of the OXPHOS system in muscle biopsies remains the method of choice for many diagnostics laboratories. Staining of samples are usually done to gather histochemical information with regards to tissue type, morphological changes that occurs and structural information. One of the most well know histochemical observations linked to mitochondrial disease is the presence of ragged red fibers. Other morphological changes that has been associated with the m.3243A>G mutation includes the presence of speckled, patchy, heterogeneous or negative cytochrome c-oxidase staining, and increased activity of succinate dehydrogenase (SDH) (Finsterer, 2007; Khan *et al.*, 2015).

2.2.6.5 Molecular genetic testing

Over recent years whole-exome sequencing has received a lot of attention as a single analysis could identity both nDNA and mtDNA pathogenic mutations. It has become so popular that some laboratories already use it as a first-line screening tool for mitochondrial disease. This means that most investigations could be bypassed, which could help to diagnose and treat the patient much faster. The disadvantage of whole-exome sequencing is that it is still very expensive limiting its accessibility to everyone (Griffin *et al.*, 2014).

Although not as effective, but a lot cheaper, other molecular analyses could still be performed, in combination with other investigations (family history, clinical, histochemical, biochemical) to diagnose a mitochondrial disease. These analyses include: 1) direct manual or automatic sequencing; 2) single strand conformation polymorphism (SSCP); 3) restriction fragment length polymorphism (RFLP); 4) combination of PCR and RFLPs; 5) temporal temperature gradient gel electrophoresis and 6) denaturing gradient gel electrophoresis (Khan *et al.*, 2015).

2.2.7 MANAGEMENT OF m.3243A>G PATIENTS

As with all mitochondrial diseases, no cure exists for patients suffering from the m.3243A>G mutation. However, their symptoms can be managed to give them a better quality of life. Management of patients affected by m.3243A>G phenotypes could be divided into three categories: 1) genetic counselling and prenatal diagnosis, 2) supportive therapy and 3) pharmacological therapy.

2.2.7.1 Genetic counselling

Forming part of the management of patients suffering from a mitochondrial disease, is the participation of genetic counselling. Once the m.3243A>G mutation has been identified, the genetic counsellor will then serve as mediator, providing families with information with regards to the disease, the inheritance of the mutations. The counsellor mayalso provide advice on the topic of family planning if it is required (Vento and Pappa, 2013).

2.2.7.2 Supportive therapy

In an attempt to improve the patient's quality of live, doctors often make supportive therapies part of patients' management plans. These therapies could include: physical, speech, respiratory and hydrotherapy, which is implemented to improve the patient's strength, mobility and overall functioning (Parikh *et al.*, 2009). In addition to these different therapies, it has also been suggested that patients affected by mitochondrial disease make exercise part of their daily routine. Studies have indicated that not only does exercise improve the functioning of the healthy mitochondria, but it also decreases the burden imposed by the mutated mtDNA (Jeppesen *et a*l., 2006). Also forming part of supportive therapy, is various strategies that could help at-risk couples prevent the passing on of a mtDNA mutation on to their offspring. These preventative strategies includes oocyte and mitochondrial donation as well as prenatal and preimplantation genetic diagnosis (Craven *et al*., 2017).

2.2.7.3 Pharmacological therapy

Pharmacological therapy forms part of the usual treatment plans used to improve these patients' quality of life. Plans usually consist of a combination of vitamins, supplements and medications which are customized according to each patient's presentation of symptoms.

Some of the most common pharmaceuticals given to patients affected by m.3243A>G includes: 1) coenzyme Q10, this is given to act as a scavenger of reactive oxygen species produced by the dysfunctional mitochondria; 2) creatine, given to patients as a source of high-energy phosphate; 3) L-arginine is given, especially in MELAS patients that presents with stroke like episodes, for an increase in the production of nitric oxide. The latter is known to result in vasodilation of arteries, which could decrease stroke episodes; 4) patients are also given carnitine, a compound involved in beta-oxidation, for increased production of acetyl-CoA, utilized in the TCA cycle to produce ATP; 5) dichloroacetate is given to decrease the levels of lactic acid. This pharmaceutical inhibits pyruvate dehydrogenase, preventing the conversion of pyruvic acid to lactic acid and by doing so, lowers the levels of lactic acid in the body. Table 2.3 summarizes the different treatment options, their general action, and their possible effect (Parikh et al., 2015; Santa, 2010).

Table 2.3: Treatment options for patients with the mitochondrial m.3243A>G mutation (Parikh *et al*., 2015; Santa, 2010)

Treatment	Action	Possible effect
Arginine	• Vasodilation • Increases nitric oxide synthesis	• Improves stroke like episodes
Ascorbic Acid (vitamin C)	• Antioxidant • Electron acceptor	• Symptomatic improvement • Increases energy • Improves exercise tolerance
Cytochrome c	• Electron carrier • Increases RC function	• Improves fatigue • Improves motor disability • Improves severity of stroke like episodes
Coenzyme Q10	• Stabilizes the RC complexes by acting as antioxidant • Electron carrier from complex I and II to complex IV	• Improves exercise tolerance • Improves cognitive function • Improves muscle strength
Corticosteroids	• Stabilizes mitochondrial membrane • Inhibits phospholipase	• Improves mitochondrial cytopathy

Creatine	• Phosphate donor to regenerate ATP	• Increases muscle strength • Increases exercise tolerance
Idebenone	• Antioxidant • Electron carrier	• Improves stroke like episodes
Levocarnitine	• Transporter of fatty acids into mitochondria	• Improves myopathy and encephalopathy
Meadione (vitamin K1)	• Electron acceptor • Stimulates oxygen utilization in mitochondria	• Symptomatic improvement • Increases energy • Improves exercise tolerance
Nicotinamide (vitamin B3)	• Converted to NAD+, which functions as a cofactor for electron transport to complex I	• Improves cognitive function • Improves exercise tolerance
Riboflavin (Vitamin B2)	• Converted to FMN and FAD, which functions as a cofactor for electron transport to complex II	• Improves neurologic symptoms • Improves exercise capacity
Sodium dichloroacetate	• Decrease conversion of pyruvate to lactic acid	• Improves lactic acidosis
Succinate	• Increases RC function by stimulating electron flow from complex II onto complex III and IV	• Prevents further stroke like episodes
Thiamine (Vitamin B1)	• Cofactor for electrons transported in RC • Essential in carbohydrate metabolism, as it is a coenzyme responsible for the decarboxylation of pyruvate to acetyl-CoA	• Improves neurologic symptoms
Thiocitic acid	• Antioxidant	• Decreases lipid peroxidation • Increases mitochondrial membrane potential
α-Tocopherol	• Free radical scavenger • Maintains membrane integrity by inhibiting lipid peroxidation	

2.3 STUDY DESIGN

For this study, urine samples from genetically confirmed m.3243A>G mutation patients, and healthy controls, were received from two international cohorts (Nijmegen, the Netherlands and Helsinki, Finland). All the patient samples received from the Nijmegen cohort harbor the m.3243A>G mutation, while the Helsinki cohort comprised patients affected by the m.3243A>G mutation and other nDNA mutations. Since the focus of this study was exclusively on the 3243A>G mutation, the majority of the Finland samples were not used in

this study, with only two Finland MELAS patients and a Finland control group that were used in a validation part of this study (Chapter 4).

Patient samples were divided into phenotypes associated with the m.3243A>G mutation, i.e. MELAS, MIDD and myopathy. Quality control (QC) samples were prepared by combining a small aliquot form each sample. Patient and control samples were randomized and analyzed on five analytical platforms, i.e. GC-MS, NMR, LC-MS/MS, LC-IM-MS positive ionization mode and LC-IM-MS negative ionization mode (Chapter 3). The data from each analytical platform were then pre-processed and normalized individually, before it was combined into one single data matrix. Data filtering and a log transformation was then applied to the combined data matrix, before it was used for univariate and multivariate statistical analyses. Findings from these statistical analyses were then used for biological interpretation (Chapters 4 and 5). Visualization of this experimental strategy is illustrated in Figure 2.7.

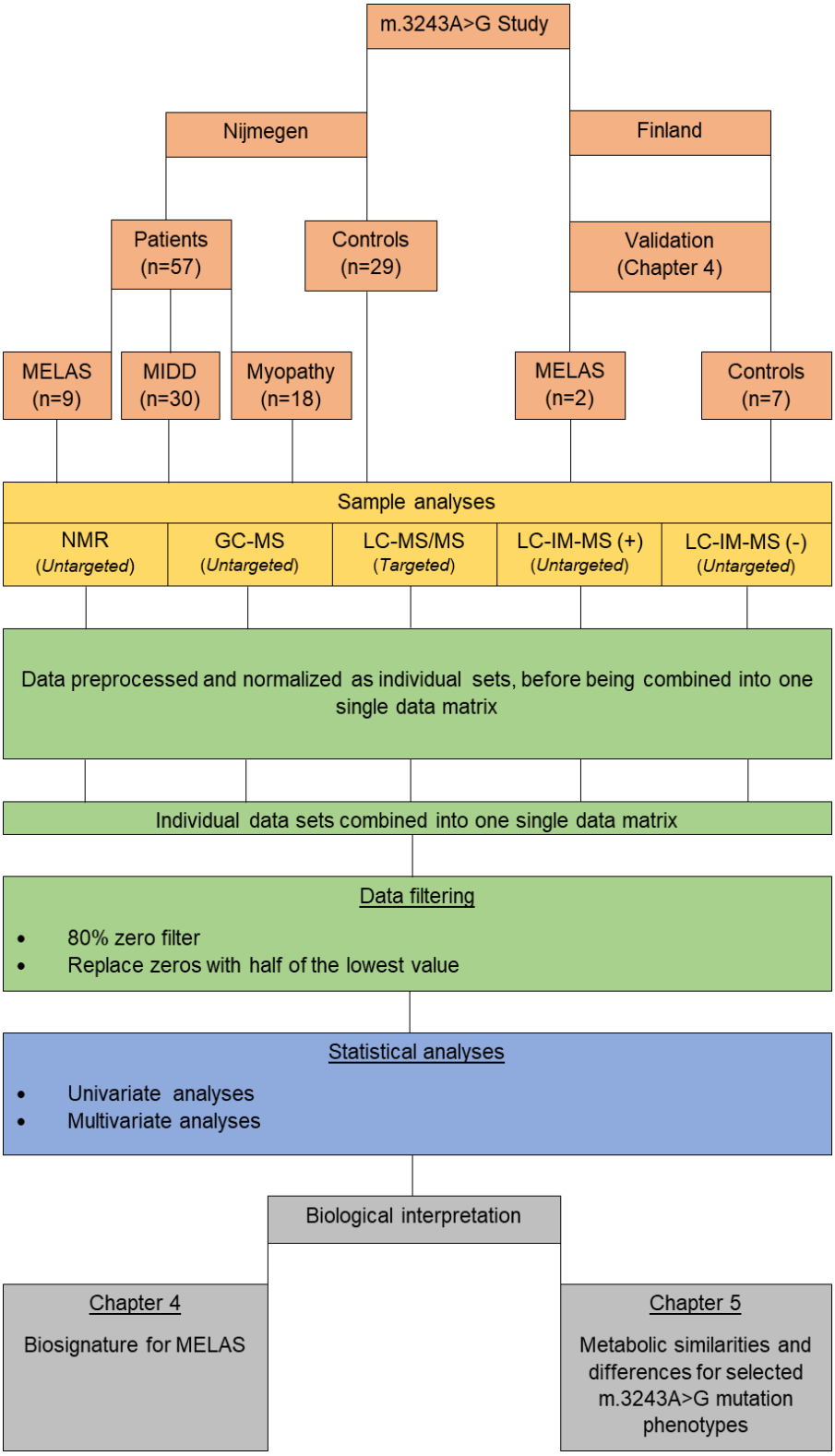

Figure 2.7. Flow diagram of the analytical approach followed in this study. Each cohort's samples were divided into patients and controls. The patients were future divided into phenotypes associated with m.3243A>G mutation. All samples were analyzed on the five analytical platforms. Data was pre-processed individually, after which it was combined into one data matrix for statistical analyses. Data was log transformed, filtered and used for univariate and multivariate analyses. Biological interpretations were made.

2.4 REFERENCES

Ahola-Erkkila, S., Carroll, C.J., Peltola-Mjosund, K., Tulkki, V., Mattila, I., SeppanenLaakso, T., Oresic, M., Tyynismaa, H., Suomalainen, A., 2010. Ketogenic diet slows down mitochondrial myopathy progression in mice. *Human Molecular Genetics.* 19 (10), 1974–1984.

Al-Enezi, M., Al-Saleh, H., Nasser, M., 2008. Mitochondrial disorders with significant ophthalmic manifestations. *Middle East African Journal of Ophthalmology.* 15 (2), 81-86.

Alston, C.L., Rocha, M.C., Lax, N.Z., Turnbull, D.M., Taylor, R.W. 2017. The genetics and pathology of mitochondrial disease. *The Journal of Pathology*. 241 (2), 236-250.

Álvarez-Sánchez, B., Priego-Capote, F., Luque de Castro, M., 2010. Metabolomics analysis I. Selection of biological samples and practical aspects preceding sample preparation. *Trends in Analytical Chemistry*. 29 (2), 111–119.

Anderson, S., Bankier, A.T., Barrell, B.G., De Bruijn, M.H., Coulson, A.R., Drouin, J., Eperon, I.C., Nierlich, D.P., Roe, B.A., Sanger, F., 1981. Sequence and organization of the human mitochondrial genome. *Nature*. 290 (5806), 457-465.

Andersson, S.G., Karlberg, O., Canback, B., Kurland, C.G., 2003. On the origin of mitochondria: a genomics perspective. Philosophical transactions of the Royal Society of London. *Series B, Biological sciences*. 358 (1429), 165-77.

Arava, Y., Boas, F.E., Brown, P.O., Herschlag, D., 2005. Dissecting eukaryotic translation and its control by ribosome density mapping. *Nucleic Acids Research*. 33 (8), 2421-2432.

Badenhorst, C.P.S., Erasmus, E., van der Sluis, R., Nortje, C., van Dijk, A.A., 2014. A new perspective on the importance of glycine conjugation in the metabolism of aromatic acids. *Drug Metabolism Reviews*. 46 (3), 343–361.

Baertling, F., Rodenburg, R.J., Schaper, J., Smeitink, J.A., Koopman, W.J., Mayatepek, E., Morava, E., Distelmaier, F., 2014. A guide to diagnosis and treatment of Leigh syndrome. *Journal of Neurology, Neurosurgery, and Psychiatry*. 85 (3), 257-265.

Bao, X.R., Ong, S.E., Goldberger, O., Peng, J., Sharma, R., Thompson, D.A., Vafai, S.B., Cox, A.G., Marutani, E., Ichinose, F., Goessling, W., Regev, A., Carr, S.A., Clish, C.B., Mootha, V.K., 2016. Mitochondrial dysfunction remodels one-carbon metabolism in human cells. *eLife* 5, e10575.

Barshop, B.A., 2004. Metabolomic approaches to mitochondrial disease: correlation of urine organic acids. *Mitochondrion.* 4 (5), 521–527.

Bates, M.G., Bourke, J.P., Giordano, C., d'Amati, G., Turnbull, D.M., Taylor, R.W., 2012. Cardiac involvement in mitochondrial DNA disease: clinical spectrum, diagnosis, and management. *European Heart Journal*. 33 (24), 3023-3033.

Bernier, F.P., Boneh, A., Dennett, X., Chow, C.W., Cleary, M.A., Thorburn, D.R., 2002. Diagnostic criteria for respiratory chain disorders in adults and children. *Neurology.* 59 (9), 1406–1411.

Bindu, L.H., Reddy, P., 2008. Genetics of aminoglycocide-induced and prelingual non-syndromic mitochondrial hearing impairment: a review. *International Journal of Audiology*. 47 (11), 702-707.

Bolisetty, S., Jaimes, E.A., 2013. Mitochondria and reactive oxygen species: physiology and pathophysiology. *International Journal of Molecular Sciences*. 14 (3), 6306-6344.

Bouatra, S., Aziat, F., Mandal, R., Guo, A.C., Wilson, M.R., Knox, C., Bjorndahl, T.C., Krishnamurthy, R., Saleem, F., Liu, P., 2013. The human urine metabolome. *PloS One*. 8 (9), e73076.

Brière, J., Chrétien, D., Bénit, P., Rustin, P., 2004. Respiratory chain defects: what do we know for sure about their consequences in vivo? *Biochimica et Biophysica Acta (BBA) - Bioenergetics*. 1659 (2), 172–177.

Brown, T.A., Cecconi, C., Tkachuk, A.N., Bustamante, C., Clayton, D.A., 2005. Replication of mitochondrial DNA occurs by strand displacement with alternative light-strand origins, not via a strand-coupled mechanism. *Genes & Development*. 19 (20), 2466-2476.

Brownlee, G.G., 2013. Frederick Sanger (1918-2013). *Current Biology*. 23 (24), R1074-R1076.

Burr, S.P., Pezet, M., Chinnery, P.F., 2018. Mitochondrial DNA heteroplasmy and purifying selection in the mammalian female germ line. *Development, Growth & Differentiation*. 60 (1), 21-32.

Butler, J.A., Mishur, R.J., Bhaskaran, S., Rea, S.L., 2013. A metabolic signature for long life in the Caenorhabditis elegans mit mutants. *Aging Cell.* 12 (1), 130–138.

Chae, J.H., Lee, J.S., Kim, K.J., Hwang, Y.S., Hirano, M., 2008. Biochemical and genetic analysis of Leigh syndrome patients in Korea. *Brain & Development*. 30 (6), 387-390.

Chinnery, P.F., Hudson, G., 2013. Mitochondrial genetics. *British Medical Bulletin*. 106 (1), 135-159.

Chinnery, P.F., Turnbull, D.M., 2001. Epidemiology and treatment of mitochondrial disorders. *American Journal of Medical Genetics*. 106 (1), 94-101.

Christian, B.E., Spremulli, L.L., 2010. Preferential selection of the 5'-terminal start codon on leaderless mRNAs by mammalian mitochondrial ribosomes. *The Journal of Biological Chemistry*. 285 (36), 28379-28386.

Christian, B.E., Spremulli, L.L., 2012. Mechanism of protein biosynthesis in mammalian mitochondria. *Biochimica et Biophysica Acta (BBA)-Gene Regulatory Mechanisms*. 1819 (9), 1035-1054.

Chrzanowska-Lightowlers, Z.M., Pajak, A., Lightowlers, R.N., 2011. Termination of protein synthesis in mammalian mitochondria. *The Journal of Biological Chemistry*. 286 (40), 34479-34485.

Clayton, D., 2003. Mitochondrial DNA replication: what we know. *International Union of Biochemistry and Molecular Biology*. 55 (4-5), 213-217.

Craven, L., Alston, C.L., Taylor, R.W., Turnbull, D.M., 2017. Recent advances in mitochondrial disease. *Annual review of genomics and human genetics*. 18, 257-275.

Cree, L., Samuels, D., Chinnery, P., 2009. The inheritance of pathogenic mitochondrial DNA mutations. *Biochimica et Biophysica Acta (BBA)-Molecular Basis of Disease*. 1792 (2), 1097-

1102.Danta, G., Hilton, R., Łynch, P., 1975. Chronic progressive external ophthalmoplegia. *Brain*. 98 (3), 473-492.

DaRe, J.T., Vasta, V., Penn, J., Tran, N.B., Hahn, S.H., 2013. Targeted exome sequencing for mitochondrial disorders reveals high genetic heterogeneity. *BMC Medical Genetics*. 14 (1), 118.

de Laat, P., Koene, S., van den Heuvel, L.P., Rodenburg, R.J., Janssen, M.C., Smeitink, J.A., 2012. Clinical features and heteroplasmy in blood, urine and saliva in 34 Dutch families carrying the m. 3243A> G mutation. *Journal of Inherited Metabolic Disease*. 35 (6), 1059-1069.

de Laat, P., Koene, S., vd Heuvel, L.P., Rodenburg, R.J., Janssen, M.C., Smeitink, J.A., 2013. Inheritance of the m. 3243A> G mutation. *JIMD Reports*. 8, 47-50.

DiMauro, S., Schon, E.A., 2003. Mitochondrial respiratory-chain disease. *New England Journal of Medicine*. 348 (26), 2656–2668.

Diodato, D., Ghezzi, D., Tiranti, V., 2014. The mitochondrial aminoacyl tRNA synthetases: genes and syndromes. *International Journal of Cell Biology*. 2014, 1-11.

Donovan, L.E., Severin, N.E., 2006. Maternally inherited diabetes and deafness in a North American kindred: tips for making the diagnosis and review of unique management issues. *The Journal of Clinical Endocrinology & Metabolism*. 91 (12), 4737-4742.

Duarte, I., Nabuurs, S.B., Magno, R., Huynen, M., 2012. Evolution and diversification of the organellar release factor family. *Molecular Biology and Evolution*. 29 (11) 3497-3512.

Dunn, W.B., Bailey, N.J.C., Johnson, H.E., 2005. Measuring the metabolome: current analytical technologies. *Analyst.* 130, 606–625.

Dunn, W.B., Broadhurst, D.I., Atherton, H.J., Goodacre, R., Griffin, J.L., 2011. Systems level studies of mammalian metabolomes: the roles of mass spectrometry and nuclear magnetic resonance spectroscopy. *Chemical Society Reviews.* 40 (1), 387–426.

Dunn, W.B., Erban, A., Weber, R.J., Creek, D.J., Brown, M., Breitling, R., Hankemeier, T., Goodacre, R., Neumann, S., Kopka, J., 2013. Mass appeal: metabolite identification in mass spectrometry-focused untargeted metabolomics. *Metabolomics.* 9 (1), 44–66.

Durham, S., Krishnan, K., Betts, J., Birch-Machin, M., 2003. Mitochondrial DNA damage in non-melanoma skin cancer. *British Journal of Cancer*. 88 (1), 90-95.

El-Hattab, A.W., Adesina, A.M., Jones, J., Scaglia, F., 2015. MELAS syndrome: Clinical manifestations, pathogenesis, and treatment options. *Molecular Genetics and Metabolism*. 116 (1), 4-12.

Elliott, H.R., Samuels, D.C., Eden, J.A., Relton, C.L., Chinnery, P.F., 2008. Pathogenic mitochondrial DNA mutations are common in the general population. *The American journal of Human Genetics*. 83 (2), 254-260

Elstner, M., Turnbull, D.M., 2012. Transcriptome analysis in mitochondrial disorders. *Brain Research Bulletin*. 88 (4), 285–293.

Esteitie, N., Hinttala, R., Wibom, R., Nilsson, H., Hance, N., Naess, K., Teär-Fahnehjelm, K., Von Döbeln, U., Majamaa, K., Larsson, N., 2005. Secondary metabolic effects in complex I deficiency. *Annals Of Neurology*. 58 (4), 544–552.

Esterhuizen, K., van der Westhuizen, F.H., Louw, R., 2017. Metabolomics of mitochondrial disease. *Mitochondrion*. 35, 97-110.

Falk, M., Zhang, Z., Rosenjack, J., Nissim, I., Daikhin, E., Nissim, I., Sedensky, M.,Yudkoff, M., Morgan, P., 2008. Metabolic pathway profiling of mitochondrial respiratory chain mutants in C. elegans. *Molecular Genetics and Metabolism*. 93 (4), 388–397.

Falk, M.J., Rao, M., Ostrovsky, J., Daikhin, E., Nissim, I., Yudkoff, M., 2011. Stable isotopic profiling of intermediary metabolic flux in developing and adult stage Caenorhabditis elegans. *Journal of Visualized Experiments.* (48), e2288.

Fang, Z., Gonzalez, F.J., 2014. LC–MS-based metabolomics: an update. *Archives of Toxicology*. 88 (8), 1491–14502.

Filosto, M., Scarpelli, M., Cotelli, M.S., Vielmi, V., Todeschini, A., Gregorelli, V., Tonin, P., Tomelleri, G., Padovani, A., 2011. The role of mitochondria in neurodegenerative diseases. *Journal of Neurology*. 258 (10), 1763-1774.

Finsterer, J., 2007. Genetic, pathogenetic, and phenotypic implications of the mitochondrial A3243G tRNALeu (UUR) mutation. *Acta Neurologica Scandinavica*. 116 (1), 1-14.

Finsterer, J., 2009. Manifestations of the mitochondrial A3243G mutation. *International Journal of Cardiology*. 137 (1), 60-62.

Finsterer, J., Zarrouk-Mahjoub, S., 2016. Diagnosing Kearns-Sayre syndrome requires genetic confirmation. *Chinese Medical Journal*. 129 (18), 2267-2268.

Gerards, M., 2014. Leigh syndrome: the genetic heterogeneity story continues. *Brain*. 137 (11), 2872-2873.

Gilbert, R.D., Hind, E., Vadgama, B., 2017. Diabetes and nephrotic syndrome: answers. *Pediatric Nephrology*. 32 (10), 1887-1889.

Gindulyte, A., Bashan, A., Agmon, I., Massa, L., Yonath, A., Karle, J., 2006. The transition state for formation of the peptide bond in the ribosome. *Proceedings of the National Academy of Sciences of the United States of America*. 103 (36), 13327-13332.

Goto, Y., Nonaka, I., Horai, S., 1990. A mutation in the tRNALeu (UUR) gene associated with the MELAS subgroup of mitochondrial encephalomyopathies. *Nature*. 348 (6302), 651-653.

Grady, J.P., Campbell, G., Ratnaike, T., Blakely, E.L., Falkous, G., Nesbitt, V., Schaefer, A.M., McNally, R.J., Gorman, G.S., Taylor, R.W., 2013. Disease progression in patients with single, large-scale mitochondrial DNA deletions. *Brain*. 137 (2), 323-334.

Gray, M.W., Burger, G., Lang, B.F., 1999. Mitochondrial evolution. *Science (New York).* 283 (5407), 1476-1481.

Griffin, H.R., Pyle, A., Blakely, E.L., Alston, C.L., Duff, J., Hudson, G., Horvath, R., Wilson, I.J., Santibanez-Koref, M., Taylor, R.W., 2014. Accurate mitochondrial DNA sequencing using off-target reads provides a single test to identify pathogenic point mutations. *Genetics in Medicine*. 16 (12), 962-971.

Griffiths, E.J., 2012. Mitochondria and heart disease. *Advances in Mitochondrial Medicine*. 942, 249-267.

Grosjean, H., de Crécy-Lagard, V., Marck, C., 2010. Deciphering synonymous codons in the three domains of life: co-evolution with specific tRNA modification enzymes. *FEBS Letters*. 584 (2), 252-264.

Haas, R.H., Parikh, S., Falk, M.J., Saneto, R.P., Wolf, N.I., Darin, N., Wong, L., Cohen, B.H., Naviaux, R.K., 2008. The in-depth evaluation of suspected mitochondrial disease. *Molecular Genetics and Metabolism*. 94 (1), 16–37.

Hall, A.M., Vilasi, A., Garcia-Perez, I., Lapsley, M., Alston, C.L., Pitceathly, R.D., McFarland, R., Schaefer, A.M., Turnbull, D.M., Beaumont, N.J., 2015. The urinary proteome and metabonome differ from normal in adults with mitochondrial disease. *Kidney International*. 87 (3), 610–622.

Hao, H., Moraes, C.T., 1997. A disease-associated G5703A mutation in human mitochondrial DNA causes a conformational change and a marked decrease in steady-state levels of mitochondrial tRNA(Asn). *Molecular and cellular biology*. 17 (12), 6831-6837.

Hernández-Luis, C., García-Morán, E., Rubio-Sanz, J., Fernández-Avilés, F., 2007. Kearns-Sayre syndrome: recurrent syncope and atrial flutter. *Revista Española de Cardiología (English Edition).* 60 (1), 89-90.

Holt, I.J., Reyes, A., 2012. Human mitochondrial DNA replication. *Cold Spring Harbor Perspectives in Biology*. 4 (12), a012971.

Hoptasz, M., Szczuciński, A., Losy, J., 2014. Heterogeneous phenotypic manifestations of maternally inherited deafness associated with the mitochondrial A3243G mutation. Case report. *Neurologia i Neurochirurgia Polska*. 48 (2), 150-153.

Inokuchi, Y., Hirashima, A., Sekine, Y., Janosi, L., Kaji, A., 2000. Role of ribosome recycling factor (RRF) in translational coupling. *The EMBO Journal*. 19 (14), 3788-3798.

Jacobs, H.T., Holt, I.J., 2000. The np 3243 MELAS mutation: damned if you aminoacylate, damned if you don't. *Human Molecular Genetics.* 9 (4), 463-465.

Jain, I.H., Zazzeron, L., Goli, R., Alexa, K., Schatzman-Bone, S., Dhillon, H., Goldberger, O., Peng, J., Shalem, O., Sanjana, N.E., Zhang, F., 2016. Hypoxia as a therapy for mitochondrial disease. *European Journal of Pharmacology*. 352 (6281), 54–61.

Jeppesen, T.D., Schwartz, M., Olsen, D.B., Wibrand, F., Krag, T., Dunø, M., Hauerslev, S., Vissing, J., 2006. Aerobic training is safe and improves exercise capacity in patients with mitochondrial myopathy. *Brain*. 129 (12), 3402-3412.

Johnson, S.C., Yanos, M.E., Kayser, E.B., Quintana, A., Sangesland, M., Castanza, A., Uhde, L., Hui, J., Wall, V.Z., Gagnidze, A., Oh, K., Wasko, B.M., Ramos, F.J., Palmiter, R.D., Rabinovitch, P.S., Morgan, P.G., Sedensky, M.M., Kaeberlein, M., 2013. mTOR inhibition alleviates mitochondrial disease in a mouse model of Leigh syndrome. *Science.* 342 (6165), 1524–1528.

Kalko, S.G., Paco, S., Jou, C., Rodríguez, M.A., Meznaric, M., Rogac, M., Jekovec-Vrhovsek, M., Sciacco, M., Moggio, M., Fagiolari, G., De Paepe, B., De Meirleir, L., Ferrer, I., Roig-Quilis, M., Munell, F., Montoya, J., López-Gallardo, E., Ruiz-Pesini, E., Artuch, R., Montero, R., Torner, F., Nascimento, A., Ortez, C., Colomer, J., Jimenez-Mallebrera, C., 2014. Transcriptomic profiling of TK2 deficient human skeletal muscle suggests a role for the p53 signalling pathway and identifies growth and differentiation factor-15 as a potential novel biomarker for mitochondrial myopathies. *BMC Genomics*. 15, 91.

Kamboj, M., 2008. Clinical approach to the diagnoses of inborn errors of metabolism. *Pediatric Clinics of North America*. 55 (5), 1113–1127.

Kami, K., Fujita, Y., Igarashi, S., Koike, S., Sugawara, S., Ikeda, S., Sato, N., Ito, M., Tanaka, M., Tomita, M., 2012. Metabolomic profiling rationalized pyruvate efficacyin cybrid cells harboring MELAS mitochondrial DNA mutations. *Mitochondrion.* 12 (6), 644–653.

Keilin, D., 1925. On cytochrome, a respiratory pigment, common to animals, yeast, and higher plants. *Proceedings of the Royal Society of London. Series B*. 98 (690), 312-339.

Khambatta, S., Nguyen, D.L., Beckman, T.J., Wittich, C.M., 2014. Kearns-Sayre syndrome: a case series of 35 adults and children. *International Journal of General Medicine*. 7, 325-332.

Khan, N.A., Govindaraj, P., Meena, A.K., Thangaraj, K., 2015. Mitochondrial disorders: challenges in diagnosis & treatment. *The Indian Journal of Medical Research*. 141 (1), 13-26.

Kirino, Y., Yasukawa, T., Ohta, S., Akira, S., Ishihara, K., Watanabe, K. & Suzuki, T., 2004. Codon-specific translational defect caused by a wobble modification deficiency in mutant tRNA from a human mitochondrial disease. *Proceedings of the National Academy of Sciences of the United States of America*. 101 (42), 15070-15075.

Koene, S., Hendriks, J.C.M., Dirks, I., de Boer, L., de Vries, M.C., Janssen, M.C.H., Smuts, I., Fung, C.-W., Wong, V.C.N., de Coo, I.R.F.M., Vill, K., Stendel, C., Klopstock, T., Falk, M.J., McCormick, E.M., McFarland, R., de Groot, I.J.M., Smeitink, J.A.M., 2016. *International Pediatric Mitochondrial Disease Scale.* 39, 705–712.

Koshiba, T., Holman, H.A., Kubara, K., Yasukawa, K., Kawabata, S., Okamoto, K., MacFarlane, J., Shaw, J.M., 2011. Structure-function analysis of the yeast mitochondrial Rho GTPase, Gem1p: implications for mitochondrial inheritance. *The Journal of Biological Chemistry*. 286 (1), 354-362.

Leal, M., Dhoble, C., Lee, J., Lopez, D., Menéndez, L.S., 2016. A rare case of Kearns–Sayre syndrome in a 17-year-old Venezuelan male with bilateral ptosis as the initial presentation. *Oxford Medical Case Reports*. 2016 (3), 34-36.

Legault, J.T., Strittmatter, L., Tardif, J., Sharma, R., Tremblay-Vaillancourt, V., Aubut, C., Boucher, G., Clish, C.B., Cyr, D., Daneault, C., 2015. A metabolic signature of mitochondrial dysfunction revealed through a monogenic form of Leigh syndrome. *Cell Reports*. 13 (5), 981–989.

Leong, D.W., Komen, J.C., Hewitt, C.A., Arnaud, E., McKenzie, M., Phipson, B., Bahlo, M., Laskowski, A., Kinkel, S.A., Davey, G.M., Heath, W.R., Voss, A.K., Zahedi, R.P., Pitt, J.J., Chrast, R., Sickmann, A., Ryan, M.T., Smyth, G.K., Thorburn, D.R., Scott, H.S., 2012. Proteomic and metabolomic analyses of mitochondrial complex I-deficient mouse model generated by spontaneous B2 short interspersed nuclear element (SINE) insertion into NADH dehydrogenase (ubiquinone) Fe-S protein 4 (Ndufs4) gene. *The Journal of Biological Chemestry*. 287 (24), 20652–20663.

Leong, X.F., Ng, C.Y., Tardif, J., Jaarin, K., 2015. Animal models in cardiovascular research: hypertension and atherosclerosis. *BioMed Research International*. 2015, 1–11.

Lightowlers, R.N., Chrzanowska-Lightowlers, Z.M., 2010. Terminating human mitochondrial protein synthesis: a shift in our thinking. *RNA Biology*. 7 (3), 282-286.

Lorenzoni, P.J., Scola, R.H., Kay, C.S.K., Silvado, C.E.S., Werneck, L.C., 2014. When should MERRF (myoclonus epilepsy associated with ragged-red fibers) be the diagnosis? *Arquivos de Neuro-Psiquiatria*. 72 (10), 803-811.

Mai, N., Chrzanowska-Lightowlers, Z.M., Lightowlers, R.N., 2017. The process of mammalian mitochondrial protein synthesis. *Cell and Tissue Research*. 367 (1), 5-20.

Majamaa, K., Moilanen, J.S., Uimonen, S., Remes, A.M., Salmela, P.I., Kärppä, M., Majamaa-Voltti, K.A., Rusanen, H., Sorri, M., Peuhkurinen, K.J., 1998. Epidemiology of A3243G, the mutation for mitochondrial encephalomyopathy, lactic acidosis, and strokelike episodes: prevalence of the mutation in an adult population. *The American Journal of Human Genetics*. 63 (2), 447-454.

Manev, H., Dzitoyeva, S., Chen, H., 2012. Mitochondrial DNA: a blind spot in neuroepigenetics. *Biomolecular Concepts*. 3 (2), 107-115.

Manwaring, N., Jones, M.M., Wang, J.J., Rochtchina, E., Howard, C., Mitchell, P., Sue, C.M., 2007. Population prevalence of the MELAS A3243G mutation. *Mitochondrion*. 7 (3), 230-233.

Martins, A.M., 1999. Inborn errors of metabolism: a clinical overview. *Sao Paulo Medical Journal*. 117 (6), 251-265.

McCormack, S., Polyak, E., Ostrovsky, J., Dingley, S.D., Rao, M., Kwon, Y.J., Xiao, R., Zhang, Z., Nakamaru-Ogiso, E., Falk, M.J., 2015. Pharmacologic targeting of sirtuin and PPAR signaling improves longevity and mitochondrial physiology in respiratory chain complex I mutant Caenorhabditis elegans. *Mitochondrion.* 22, 45–59.

Menezes, M.J., Riley, L.G., Christodoulou, J., 2014. Mitochondrial respiratory chain disorders in childhood: insights into diagnosis and management in the new era of genomic medicine. *Biochimica et Biophysica Acta (BBA) - General Subjects*. 1840 (4), 1368–1379.

Mignarri, A., Cenciarelli, S., Da Pozzo, P., Cardaioli, E., Malandrini, A., Federico, A., Dotti, M.T., 2015. Mitochondrial recessive ataxia syndrome: a neurological rarity not to be missed. *Journal of the Neurological Sciences*. 349 (1-2), 254-255.

Monteiro, M., Carvalho, M., Bastos, M., Guedes de Pinho, P., 2013. Metabolomics analysis for biomarker discovery: advances and challenges. *Current Medicinal Chemistry*. 20 (2), 257–271.

Morgan, P., Higdon, R., Kolker, N., Bauman, A., Ilkayeva, O., Newgard, C., Kolker, E., Steele, L., Sedensky, M., 2015. Comparison of proteomic and metabolomic profiles of mutants of the mitochondrial respiratory chain in Caenorhabditis elegans. *Mitochondrion.* 20, 95–102.

Mudd, S.H., Brosnan, J.T., Brosnan, M.E., Jacobs, R.L., Stabler, S.P., Allen, R.H., Vance, D.E., Wagner, C., 2007. Methyl balance and transmethylation fluxes in humans. *American Journal of Clinical Nutrition*. 85, 19–25.

Munnich, A., Rötig, A., Chretien, D., Saudubray, J., Cormier, V., Rustin, P., 1996. Clinical presentations and laboratory investigations in respiratory chain deficiency. *European Journal of Pediatrics*. 155, 262–274.

Murphy, R., Turnbull, D., Walker, M., Hattersley, A., 2008. Clinical features, diagnosis and management of maternally inherited diabetes and deafness (MIDD) associated with the 3243A> G mitochondrial point mutation. *Diabetic Medicine*. 25 (4), 383-399.

Naviaux, R.K., 2014. Metabolic features of the cell danger response. *Mitochondrion.* 16, 7–17.

Nikkanen, J., Forsström, S., Euro, L., Paetau, I., Kohnz, R.A., Wang, L., Chilov, D., Viinamäki, J., Roivainen, A., Marjamäki, P., 2016. Mitochondrial DNA replication defects disturb cellular dNTP pools and remodel one-carbon metabolism. *Cell Metabolism*. 23 (4), 635–648.

Nikolic, S.B., Sharman, J.E., Adams, M.J., Edwards, L.M., 2014. Metabolomics in hypertension. *Journal of Hypertension*. 32 (6), 1159–1169.

Nozaki, Y., Matsunaga, N., Ishizawa, T., Ueda, T., Takeuchi, N., 2008. HMRF1L is a human mitochondrial translation release factor involved in the decoding of the termination codons UAA and UAG. *Genes to Cells*. 13 (5), 429-438.

Oliver, S.G., Winson, M.K., Kell, D.B., Baganz, F., 1998. Systematic functional analysis of the yeast genome. *Trends in Biotechnology*. 16 (9), 373–378.

Parikh, S., Goldstein, A., Koenig, M.K., Scaglia, F., Enns, G.M., Saneto, R., Anselm, I., Cohen, B.H., Falk, M.J., Greene, C., Gropman, A.L., 2015. Diagnosis and management of mitochondrial disease: a consensus statement from the Mitochondrial Medicine Society. *American College of Medical Genetics and Genomics.* 17 (9), 689–701.

Parikh, S., Saneto, R., Falk, M.J., Anselm, I., Cohen, B.H., Haas, R., 2009. A modern approach to the treatment of mitochondrial disease. *Current Treatment Options in Neurology.* 11 (6), 414-430.

Park, K., Kim, H., Kim, E., Park, Y., Lee, C., Kim, D., 2011. SLC25A4 and C10ORF2 mutations in autosomal dominant progressive external ophthalmoplegia. *Journal of Clinical Neurology*. 7 (1), 25-30.

Park, S.Y., Kim, S.H., Lee, Y., 2017. Molecular diagnosis of myoclonus epilepsy associated with ragged-red fibers syndrome in the absence of ragged red fibers. *Frontiers in Neurology*. 8, 520.

Phoenix, C., Schaefer, A.M., Elson, J., Morava, E., Bugiani, M., Uziel, G., Smeitink, J., Turnbull, D., McFarland, R., 2006. A scale to monitor progression and treatment of mitochondrial disease in children. *Neuromuscular Disorders*. 16 (12), 814–820.

Pierce, K.M., Hoggard, J.C., Hope, J.L., Rainey, P.M., Hoofnagle, A.N., Jack, R.M., Wright, B.W., Synovec, R.E., 2006. Fisher ratio method applied to third-order separation data to identify significant chemical components of metabolite extracts. *Analytical Chemistry*. 78 (14), 5068-5075.

Pinto, M., Moraes, C.T., 2014. Mitochondrial genome changes and neurodegenerative diseases. *Biochimica et Biophysica Acta (BBA)-Molecular Basis of Disease*. 1842 (8), 1198-1207.

Pitceathly, R.D., Rahman, S., Hanna, M.G., 2012. Single deletions in mitochondrial DNA--molecular mechanisms and disease phenotypes in clinical practice. *Neuromuscular Disorders*. 22 (7), 577-586.

Rahman, S., Blok, R., Dahl, H., Danks, D., Kirby, D., Chow, C., Christodoulou, J., Thorburn, D., 1996. Leigh syndrome: clinical features and biochemical and DNA abnormalities. *Annals of Neurology*. 39 (3), 343-351.

Rahman, S., Poulton, J., Marchington, D., Suomalainen, A., 2001. Decrease of 3243 A→ G mtDNA mutation from blood in MELAS syndrome: a longitudinal study. *The American Journal of Human Genetics*. 68 (1), 238-240.

Rasanu, T., Mehedinti, T., Hancu, A., Damian, I., Mihailov, C., Rasanu, I., 2011. Mitochondrial myopathies: current diagnosis (ii). *Romanian Journal of Neurology and Psychiatry.* 10 (1), 12.

Reinecke, C.J., Koekemoer, G., van der Westhuizen, F.H., Louw, R., Lindeque, J.Z., Mienie, L.J., Smuts, I., 2012. Metabolomics of urinary organic acids in respiratory chain deficiencies in children. *Metabolomics.* 8 (2), 264–283.

Reinecke, F., Smeitink, J.A., Van Der Westhuizen, F.H., 2009. OXPHOS gene expression and control in mitochondrial disorders. *iochimica et Biophysica Acta (BBA) - Molecular Basis of Disease*. 1792 (12), 1113–1121.

Ronchi, D., Fassone, E., Bordoni, A., Sciacco, M., Lucchini, V., Di Fonzo, A., Rizzuti, M., Colombo, I., Napoli, L., Ciscato, P., 2011. Two novel mutations in PEO1 (Twinkle) gene associated with chronic external ophthalmoplegia. *Journal of the neurological sciences*. 308 (1-2), 173-176.Rowland, L.P., 1993. Progressive external ophthalmoplegia. *Handbook of Clinical Neurology*. 22, 177-202.

Rüegga, S., Hagen, M.L., Hohl, U., Kappos, L., Fuhr, P., Plasilov, M., Muller, H., Heinimann, K., 2005. Oculopharyngeal muscular dystrophy-an under-diagnosed disorder? *Swiss Medical Weekly*. 135 (39-40), 574-586.

Saeed, S., Singer, M., 2013. Mitochondria—key roles in sepsis. *Réanimation*. 22 (2), 352-358.

Sallevelt, S.C., de Die-Smulders, C.E., Hendrickx, A.T., Hellebrekers, D.M., de Coo, I.F., Alston, C.L., Knowles, C., Taylor, R.W., McFarland, R., Smeets, H.J., 2017. De novo mtDNA point mutations are common and have a low recurrence risk. *Journal of Medical Genetics*. 54 (2), 73-83.

Saneto, R.P., Friedman, S.D., Shaw, D.W., 2008. Neuroimaging of mitochondrial disease. *Mitochondrion*. 8 (5), 396-413.

Santa, K.M., 2010. Treatment options for mitochondrial myopathy, encephalopathy, lactic acidosis, and stroke-like episodes (MELAS) syndrome. *Pharmacotherapy: The Journal of Human Pharmacology and Drug Therapy*. 30 (11), 1179-1196.

Scaglia, F., Northrop, J.L., 2006. The mitochondrial myopathy encephalopathy, lactic acidosis with stroke-like episodes (MELAS) syndrome: a review of treatment options. *CNS Drugs*. 20 (6), 443-464.

Schaefer, A.M., Taylor, R.W., Turnbull, D.M., Chinnery, P.F., 2004. The epidemiology of mitochondrial disorders—past, present and future. *Biochimica et Biophysica Acta (BBA) – Bioenergetics.* 1659 (2), 115–120.

Seneca, S., Verhelst, H., De Meirleir, L., Meire, F., Ceuterick-De Groote, C., Lissens, W., Van Coster, R., 2001. A new mitochondrial point mutation in the transfer RNALeu gene in a patient with a clinical phenotype resembling Kearns-Sayre syndrome. *Archives of Neurology*. 58 (7), 1113-1118.

Shaham, O., Wei, R., Wang, T.J., Ricciardi, C., Lewis, G.D., Vasan, R.S., Carr, S.A., Thadhani, R., Gerszten, R.E., Mootha, V.K., 2008. Metabolic profiling of the human response to a glucose challenge reveals distinct axes of insulin sensitivity. *Molecular Systems Biology*. 4, 214.

Shanske, S., Pancrudo, J., Kaufmann, P., Engelstad, K., Jhung, S., Lu, J., Naini, A., DiMauro, S., De Vivo, D.C., 2004. Varying loads of the mitochondrial DNA A3243G mutation in different tissues: implications for diagnosis. *American Journal of Medical Genetics Part A*. 130 (2), 134-137.

Shatla, H.M., Tomoum, H.Y., Elsayed, S.M., Elagouza, I.A., Shatla, R.H., Mohsen, M.M., Hamed, A.N., 2014. Role of plasma amino acids and urinary organic acids in diagnosis of mitochondrial diseases in children. *Pediatric Neurology*. 51 (6), 820–825.

Shoffner, J.M., Lott, M.T., Lezza, A.M., Seibel, P., Ballinger, S.W., Wallace, D.C., 1990. Myoclonic epilepsy and ragged-red fiber disease (MERRF) is associated with a mitochondrial DNA tRNALys mutation. Cell. 61 (6) 931-937.

Sim, K.G., Carpenter, K., Hammond, J., Christodoulou, J., Wilcken, B., 2002. Acylcarnitine profiles in fibroblasts from patients with respiratory chain defects can resemble those from patients with mitochondrial fatty acid [beta]-oxidation disorders. *Metabolism* 51 (3), 366–371.

Sims, K.B., Mootha, V.K., 2010. A plasma signature of human mitochondrial disease revealed through metabolic profiling of spent media from cultured muscle cells. *Proceedings of the National Academy of Sciences of the United States of America*. 107 (4), 1571–1575.

Slater, E.C., 2003. Keilin, cytochrome, and the respiratory chain. *The Journal of Biological Chemistry*. 278 (19), 16455-16461.

Smeitink, J.A., Zeviani, M., Turnbull, D.M., Jacobs, H.T., 2006. Mitochondrial medicine: a metabolic perspective on the pathology of oxidative phosphorylation disorders. *Cell Metabolism*. 3 (1), 9–13.

Smits, P., Smeitink, J., van den Heuvel, L., 2010. Mitochondrial translation and beyond: processes implicated in combined oxidative phosphorylation deficiencies. *Journal of Biomedicine Biotechnology*. 2010, 737385.

Smits, P., Smeitink, J.A., van den Heuvel, L.P., Huynen, M.A., Ettema, T.J., 2007. Reconstructing the evolution of the mitochondrial ribosomal proteome. *Nucleic Acids Research*. 35 (14), 4686-4703.

Smuts, I., van der Westhuizen, Francois H., Louw, R., Mienie, L.J., Engelke, U.F., Wevers, R.A., Mason, S., Koekemoer, G., Reinecke, C.J., 2013. Disclosure of a putative biosignature for respiratory chain disorders through a metabolomics approach. *Metabolomics.* 9 (2), 379-391.

Sommerville, E.W., Chinnery, P.F., Gorman, G.S., Taylor, R.W., 2014. Adult-onset mendelian PEO associated with mitochondrial disease. *Journal of neuromuscular diseases*. 1(2), 119-133.

Suomalainen, A., 2011. Biomarkers for mitochondrial respiratory chain disorders. *Journal of Inherited Metabolic Disease.* 34, 277–282.

Taivassalo, T., Ayyad, K., Haller, R.G., 2012. Increased capillaries in mitochondrial myopathy: implications for the regulation of oxygen delivery. *Brain*. 135 (1), 53-61.

Taylor, R.W., Turnbull, D.M., 2005. Mitochondrial DNA mutations in human disease. *Nature Reviews Genetics*. 6 (5), 389-402.

Testai, F.D., Gorelick, P.B., 2010. Inherited metabolic disorders and stroke part 1: Fabry disease and mitochondrial myopathy, encephalopathy, lactic acidosis, and strokelike episodes.*Archives of Neurology*. 67(1), 19-24.

Tuppen, H.A., Blakely, E.L., Turnbull, D.M., Taylor, R.W., 2010. Mitochondrial DNA mutations and human disease. *Biochimica et Biophysica Acta (BBA)-Bioenergetics*. 1797 (2), 113-128.

Tsaris, P., 1973. Familial myoclonic epilepsy syndrome associated with skeletal muscle mitochondrial abnormalities.Neurology. 23, 408.

Tyynismaa, H., Carroll, C.J., Raimundo, N., Ahola-Erkkila, S., Wenz, T., Ruhanen, H., Guse, K., Hemminki, A., Peltola-Mjosund, K.E., Tulkki, V., Oresic, M., Moraes, C.T., Pietilainen, K., Hovatta, I., Suomalainen, A., 2010. Mitochondrial myopathy induces a starvation-like response. *Human Molecular Genetics*. 19 (20), 3948–3958.

Venter, L., Lindeque, Z., van Rensburg, P.J., van der Westhuizen, F., Smuts, I., Louw, R., 2015. Untargeted urine metabolomics reveals a biosignature for muscle respiratory chain deficiencies. *Metabolomics.* 11 (1), 111–121.

Vento, J.M., Pappa, B., 2013. Genetic counselling in mitochondrial disease. *Neurotherapeutics*. 10 (2), 243-250.

Vergano, S.S., Rao, M., McCormack, S., Ostrovsky, J., Clarke, C., Preston, J., Bennett, M.J., Yudkoff, M., Xiao, R., Falk, M.J., 2014. In vivo metabolic flux profiling with stable isotopes discriminates sites and quantifies effects of mitochondrial dysfunction in C. elegans. *Molecular Genetics and Metabolism*. 111 (3), 331–341.

Vivero, R.J., Ouyang, X., Kim, Y.G., Liu, W., Du, L., Yan, D., Liu, X.Z., 2013. Audiologic and genetic features of the A3243G mtDNA mutation. *Genetic Testing and Molecular Biomarkers*. 17 (5), 383-389.

Vo, T.D., Lee, W.P., Palsson, B.O., 2007. Systems analysis of energy metabolism elucidates the affected respiratory chain complex in Leigh's syndrome. *Molecular Genetics and Metabolism*. 91(1), 15–22.

Von Kleist-Retzow, J., Schauseil-Zipf, U., Michalk, D.V., Kunz, W.S., 2003. Mitochondrial diseases-an expanding spectrum of disorders and affected genes. *Experimental Physiology*. 88 (1), 155-166.

Wang, Y.X., Le, W.D., 2015. Progress in Diagnosing Mitochondrial Myopathy, Encephalopathy, Lactic Acidosis, and Stroke-like Episodes. Chinese medical journal. 128(13), 1820-1825.

Wang, M., Liu, H., Zheng, J., Chen, B., Zhou, M., Fan, W., Wang, H., Liang, X., Zhou, X., Eriani, G., Jiang, P., Guan, M.X., 2016. A deafness- and diabetes-associated tRNA mutation causes deficient pseudouridinylation at Position 55 in tRNAGlu and mitochondrial dysfunction. *The Journal of Biological Chemistry*. 291 (40), 21029-21041.

Warrack, B.M., Hnatyshyn, S., Ott, K., Reily, M.D., Sanders, M., Zhang, H., Drexler, D.M. 2009. Normalization strategies for metabonomic analysis of urine samples. *Journal of Chromatography B*. 877 (5-6), 547-552.

Whittaker, R.G., Blackwood, J.K., Alston, C.L., Blakely, E.L., Elson, J.L., McFarland, R., Chinnery, P.F., Turnbull, D.M., Taylor, R.W., 2009. Urine heteroplasmy is the best predictor of clinical outcome in the m.3243A>G mtDNA mutation. *Neurology*. 72 (6), 568-569.

Wikoff, W.R., Anforab, A.T., Liub, J., Schultzb, P.G., Lesleyb, S.A., Petersb, E.C., Siuzdaka, G., 2009. Metabolomics analysis reveals large effects of gut microflora on mammalian blood metabolites. *Proceedings of the National Academy of Sciences of the United States of America.* 106 (10), 3698–3703.

Wolf, N.I., Smeitink, J.A., 2002. Mitochondrial disorders: a proposal for consensus diagnostic criteria in infants and children. *Neurology.* 59 (9), 1402–1405.

Yang, M., Vousden, K.H., 2016. Serine and one-carbon metabolism in cancer. *Nature Reviews Cancer.* 16 (10), 650–662.

Yano, T., Nishio, S., Usami, S., 2014. Frequency of mitochondrial mutations in non-syndromic hearing loss as well as possibly responsible variants found by whole mitochondrial genome screening. *Journal of Human Genetics*. 59 (2), 100-106.

Yu-Wai-Man, P., l Clements, A., Nesbitt, V., Griffiths, P.G., Gorman, G.S., Schaefer, A.M., Turnbull, D.M., Taylor, R.W., McFarland, R., 2014. A national epidemiological study of chronic progressive external ophthalmoplegia in the United Kingdom-molecular genetic features and neurological burden. *Investigative Ophthalmology & Visual Science*. 55 (13), 5109-5109.

Zhang, X., Clausen, M.R., Zhao, X., Zheng, H., Bertram, H.C., 2012. Enhancing the power of liquid chromatography–mass spectrometry-based urine metabolomics in negative ion mode by optimization of the additive. *Analytical Chemistry*. 84 (18), 7785–7792.

Zhong, L.X., Kun, S., Jing, Q., Jing, C., Denise, Y., 2013. Non-syndromic hearing loss and high-throughput strategies to decipher its genetic heterogeneity. *Journal of Otology*. 8 (1), 6-24.

Chapter 3

Analytical methods, bioinformatics and data quality

3

3.1 INTRODUCTION

Untargeted metabolomics has become a popular research tool in systems biology-based investigations, especially in investigations involving complex diseases. Untargeted metabolomics techniques provide us with a comprehensive set of data of all the measurable small compounds present in a sample, which include both known metabolites as well as unknown compounds (Roberts *et al*., 2013). However, this comprehensive view of the metabolome is only attainable with a multi- platform approach, as different analytical techniques are biased toward a certain part of the metabolome (Bouatra *et al*., 2013). Therefore, for this metabolomics investigation, we used five different analytical platforms to comprehensively study the urine metabolome of patients harboring the m.3243A>G mutation, compared to healthy controls. This multi-platform metabolomics approach consisted of untargeted as well as targeted analytical methods. Untargeted analytical methods comprised of gas chromatography mass spectrometry (GC-MS), nuclear magnetic resonance (NMR) spectroscopy and liquid chromatography – ion mobility – mass spectrometry (LC-IM-MS) in positive as well as negative ionization mode, while targeted methods included liquid chromatography-tandem mass spectrometry (LC-MS/MS).

3.2 SAMPLES AND ETHICS

For this study we used urine samples from a genetically confirmed m.3243A>G mutation cohort from the Radboud University Medical Center, Nijmegen, The Netherlands. The patients were divided into a MELAS (n=9), MIDD (n=30) or a myopathy group (n=18) as well as healthy controls (n=29). For the validation phase of this study (Chapter 4), we used urine samples from a genetically confirmed m.3243A>G mutation cohort from the University of Helsinki, Finland. We obtained samples from two MELAS patients and seven healthy controls. To ensure homogeneity, the following samples were excluded: 1) controls that received either medication or supplementation at the time of sample collection; 2) controls with a medical condition (such as diabetes, hypertension); 3) patients that received an organ

transplant (kidney, liver). Due to ethical considerations, treatment (medication and supplementation) of the patients could not be stopped.

Samples were couriered on dry ice respectively from Nijmegen and Finland to the North-West University (Potchefstroom, South Africa). The samples were then aliquoted into various 1.5 mL polypropylene tubes and stored at -80 °C until use.

The study complied with all Institutional guidelines and terms of the Declaration of Helsinki of 1975 (as revised in 2013) for investigation of human participants. Ethical approval was obtained from the Health Research Ethics Committee (HREC) of the North-West University, South Africa (NWU-00170-13-A1). All the patients as well as the controls provided written informed consent for their urine samples to be used for research purposes.

3.3 ANALYTICAL METHODS

All analytical methods used in this study was previously standardized at the Centre of Human Metabolomics. Visualization of the sample preparation procedure for the different analytical platforms is given in Figure 3.1.

3.3.1 REAGENTS

The following high grade reagents were purchased from various suppliers. Acetonitrile (BJ015CS), methanol (BJ230C) and water (BJ365CS) were supplied by Anatech Instruments (Pty) Ltd [Olivedale, South Africa (SA)]. Formic acid (06440), 3-phenylbutyric acid (116807), pyridine (270970), O-bis(trimethylsilyl)trifluoro acetamide (BSTFA) with trimethylchlorosilane (TMCS) (33155), methoxyamine hydrochloride (226904), picric acid (80456), sodium hydroxide (NaOH) (795429), deuterium oxide (D_2O) (151882), potassium phosphate monobasic (KH_2PO_4) (795488), trimethylsilyl-2,2,3,3-tetradeuteropropionic acid (TSP) (71911), potassium hydroxide (KOH) (P1767), sodium azide (NaN3) (S2002), ethylenediaminetetraacetic acid (EDTA) tetrasodium salt hydrate (E26290) and creatinine (C4255) were purchased from Sigma-Aldrich (Kempton Park, SA). Tween 20 (polyoxyethylenesorbitan monolaurate) (822184) was purchased from Merck (Pty) Ltd (Modderfontein, SA). Deuterated amino acids isotopes: [d3]-methyl-L-methionine (CDLM9289), [d5]-ring-L-phenylalanine (IND625P) and [d8]-L-valine (CDNLM6817) were obtained from Cambridge Isotope Laboratories, (Tewksbury, USA). Deuterated acylcarnitines: [4,4,4-d3]butyryl-L-carnitine.HCl (C4_IS), [8,8,8-d3]octanoyl-L-carnitine.HCl (C8_IS) and [16,16,16-d3]hexadecanoyl-L-carnitine.HCl (C16_IS) were obtained from Dr.

H.J. ten Brink (Free University Hospital, Amsterdam, The Netherlands). Leucine enkephaline (186006013) was supplied by Microsep (Bramley, SA).

3.3.2 PREPERATION OF REAGENTS

3.3.2.1 Preparation of reagents for creatinine quantification

Creatinine standard 50 mg/100 mL (50 mg%)

Creatinine standard was prepared by adding 50 mg pure creatinine in 100 mL Milli-Q water. This standard was kept at 2 – 8 °C.

100 x Tween 20 dilution

To prepare the 100 x Tween 20 dilution, 10 µL Tween 20 was added to 990 µL Milli-Q water. This reagent was kept at 2 – 8 °C.

Reagent A

Reagent A was prepared by adding 1,6 g NaOH and 50 mg EDTA to 100 mL Milli-Q water. This reagent was kept at 2 – 8 °C.

Reagent B

Reagent B was prepared by adding 500 µl DMSO and 200 µL 100 x Tween 20 dilution to 100 mL water 100 mL Milli-Q water. This reagent was kept at 2 – 8 °C.

Working solution for creatinine quantification

The volume of working solution prepared was determined by the number of samples being analyzed. To prepare working solution sufficient for analyzing 50 samples, 2.5 mL reagent A was combined with 2 mL reagent B. To this, 500 µL picric acid and 5 mL Milli-Q water was added. The working solution was always prepared freshly before each analysis.

3.3.2.2 Preparation of GC-MS reagents

Methoxyamine hydrochloride (MOX) in pyridine solution (20mg/ml pyridine)

A methoxyamine hydrochloride solution (MOX solution) was prepared by dissolving 20 mg methoxyamine hydrochloride in 1 mL pyridine.

BSTFA with 1% TMCS

BSTFA solution was prepared by adding 100 µL TMCS to 1 mL BSTFA. This solution was stored at 2 – 8 °C.

3.3.2.3 Preparation of reagents used for LC analyses

Butanolic HCl

Butanolic hydrogen chloride (HCl) was prepared by adding 1 unit of acetyl chloride dropwise to 3 units of ice cold 1-butanol solution.

3.3.2.4 Preparation of internal standard solutions

3-Phenylbutyric acid internal standard solution (100 mg/L)

The 3-phenylbutyric acid internal standard was prepared as a 10 000 mg/L stock solution. This was achieved by adding 120 mg 3-phenylbutyric acid to 12 mL methanol. This stock solution was then used to prepare a 1000 mg/L working solution by adding 4 mL 10 000 mg/L to 36 mL water. This 1000 mg/L working solution was then used to prepare the final 100 mg/L internal standard solution by adding 5 mL 1000 mg/L to 45 mL of water. Both the stock solution as well as the dilutions were stored in the fridge at 4 °C.

Isotope solution (10 mg/mL)

A mixed isotope solution was prepared by combining 8.26 mL [d3]-methyl-L-methionine (60.5 mg/L), 2.49 mL [d8]-L-valine (200.4027 mg/L), 2.46 mL [d5]-ring-L-phenylalanine (203.1558 mg/L), 5.81 mL [4,4,4-d3]butyryl-L-carnitine.HCl (C4_IS) (86 mg/L), 9.09 mL [8,8,8-d3]octanoyl-L-carnitine.HCl (C8_IS) (55 mg/L), 7.63 mL [16,16,16-d3]hexadecanoyl-L-carnitine.HCl (C16_IS) (65.5 mg/L) and 14.26 mL of water. This solution was stored in the fridge at 4 °C.

NMR buffer solution

To prepare 100 mL 1.5 M KH_2PO_4 buffer solution, 20.4 g KH_2PO_4 was dissolved in 80 mL of D_2O. In a separate volumetric flask, 100 mg TSP and 13 mg NaN_3 were dissolved in 10 mL D_2O. The two solutions were combined and sonicated to ensure complete mixture of the two solutions. The pH was adjusted to 7.4 by adding KOH. The volume was topped up to 100 mL with D_2O.

3.3.3 OSMOLALITY DETERMINATION

Osmolality was determined by Ampath Laboratories on the Advanced Osmometer (IEPSA Diagnostics, South Africa).

3.3.4 CREATINE QUANTIFICATION

3.3.4.1 Sample preparation

For creatinine analyses, urine sample aliquots were thawed overnight at 4 °C and centrifuged at 15 700 x *g* at room temperature for 2 minutes to remove any crystals. 10 µl of sample was transferred to a 96 well plate. To this 90 µl Milli-Q water was added. The diluted sample was then transferred, in triplicate, to another clean 96 well plate. To each diluted sample, 200 µl of the working solution was added with a multi-channel pipette and inserted into the microplate reader.

3.3.4.2 Instrumentation

Samples were analyzed on a Synergy Multi-Mode microplate Reader from BioTek (Winooski, Vermont, United States). The absorbance was measured every minute for 5 minutes at 510 nm. A calibration, ranging from 0-50 mg%, was used for quantification of creatinine. In case a sample's concentration read lower than 4 mg%, 10 µL of the undiluted sample was reanalyzed.

3.3.5 GAS CHROMATOGRAPHY MASS SPECTROMETRY (GC-MS)

3.3.5.1 Sample preparation

For untargeted GC-MS analyses, an adapted version of a minimal sample preparation method published by Venter *et al*., (2015) was used. Urine sample aliquots, which were stored at -80 °C, were thawed overnight at 4 °C. The samples were centrifuged at 15 700 x *g* at room temperature for 2 minutes. This was done to ensure the removal of any sediment and crystals. A calculated volume for each sample (totaling 0.25 µmoles of creatinine) were transferred into clean vials. To each sample, 50 µL 3-phenylbutyric acid (end concentration 50 mg/L) was added. Samples were then evaporated under a stream of nitrogen gas at 37 ˚C. Evaporated samples were derivatized using a two-step derivatization process. First, samples were oximated by adding 50 µL of methoxyamine HCl (20 mg/mL pyridine), after

which it was incubated at 60 °C for 60 minutes. After the oximation step, samples were silylated by adding 50 µL BSTFA containing 1% TMCS, after which they were again incubated for 60 °C for 60 minutes. Derivatized samples were then transferred to vials with flat bottom inserts for analysis.

3.3.5.2 Instrumentation

Samples were analyzed on a GC-TOF-MS-system consisting of an Agilent 7890 GC system coupled to a Leco Pegasus HT mass analyzer and an Agilent 7693 auto sampler, with helium being used as carrier gas. Metabolites were separated using a Restek RXi® - 5Sil MS column (30 m X 0.25 mm X 0.25 µm). 1 µL of sample was injected per run in a 1:10 split mode at a flow rate of 1.50 mL per minute, with front inlet temperature being kept at a constant 250 °C. To enhance separation of metabolites, the oven temperature was ramped up from 70 °C to 300 °C over a period of 13 minutes. The initial oven temperature started and was kept at 70 °C for 1 minute. The oven temperature was increased to 120 °C at a rate of 7 °C per minute. Thereafter the temperature was again increased to 230 °C at 10 °C per minute and then to 300 °C at 13 °C per minute, where it was kept for one minute before returning to the starting temperature. The transfer line was maintained at 225 °C, while the ion source temperature was kept at 200 °C for the entire run. Data was captured with an acquisition rate of 20 spectra (50 – 950 m/z) per second, with the detector voltage kept at 1450 V. Total run time added up to 13 minutes. For extraction of GC-MS data, ChromaTOF (Leco) was used. Compound peaks were identified through spectral and retention time matching using both a commercial library (NIST11) as well as an in-house library (Reinecke *et al*., 2012).

3.3.6 NUCLEAR MAGNETIC RESONANCE (NMR) SPECTROSCOPY

3.3.6.1 Sample preparation

For NMR analyses, 500 µL urine aliquots were thawed overnight at 4 °C and centrifuged at room temperature for 5 minutes at 12 000 x *g*. After the samples were centrifuged, 450 µL of it was transferred to a new micro-centrifuge tube. To the aliquoted samples, 45 µL NMR buffer solution (pH 7.4, KH_2PO_4 with TSP, in D_2O) was added. Samples were vortexed and transferred into standard 5 mm NMR tubes.

3.3.6.2 Instrumentation

Analyses were performed at 500 MHz on a Bruker Avance III HD NMR spectrometer (Bruker Biospin, Rheinstetten, Germany), fitted with a triple resonance inverse (TXI) ^{1}H {^{15}N, ^{13}C} probe head as well as x, y, z gradient coils. ^{1}H spectra were obtained using the following acquisition paramaters: 28 transients in 32K data points, with a spectral width of 6002 Hz. Water resonance was suppressed by single-frequency irradiation with a relaxation delay of 4 seconds, and a 90° excitation pulse of 8 µs. Automatic shimming occurred on the deuterium signal. Resonance widths for both the TSP and metabolite peaks were less than 1 Hz. Automatic Fourier transformation as well as phase and baseline correction was done. For NMR spectral processing, Bruker Topspin, and for identification and quantification Bruker AMIX (Ellinger *et al*., 2013) was used respectively.

3.3.7 LIQUID CHROMATOGRAPHY - TANDEM MASS SPECTROMETRY (LC-MS/MS)

3.3.7.1 Sample preparation

Sample aliquots, stored at -80 °C, were thawed overnight at 4 °C and centrifuged at 15 700 x *g* at room temperature for 2 minutes to remove any crystals. A calculated volume for each sample (totaling 0.25 µmoles of creatinine) was transferred to clean vials. To each sample, 100 µL of an internal standard solution containing phenylalanine-, methionine- valine-, C4 carnitine-, C8 carnitine- and C16 carnitine isotopes (end concentration 10 mg/L) as well as 50 µL 3-phenylbutyric acid (end concentration 50 mg/L) were added. Samples were then evaporated under a stream of nitrogen gas at 37 ˚C. Samples were derivatized with the addition of 300 µL butanolic HCl after which they were incubated for 60 minutes at 50 °C. Samples were then again dried under a stream of nitrogen gas at 37 ˚C. To reconstitute the samples, 100 µL mobile phase (50% acetonitrile, 50% water, 0.1% formic acid) was added to each sample and left at room temperature for 30 minutes to ensure that the dried samples were completely dissolved. The samples were then vortexed and transferred to vials with tapered inserts.

3.3.7.2 Instrumentation

Samples were analyzed on a 1200 infinity LC connected to a 6410 triple quadrupole mass analyzer (Agilent Technologies, Santa Clara, CA, USA) in positive ionization mode. The sample injection volume was 1 µL which was separated on a C18 column (ZORBAX SB-Aq,

2.1 x 150 mm, 3.5 µm, Agilent Technologies, Santa Clara, CA, USA), using a flow rate of 0.2 mL per minute with mobile phases A (water and 0.1% formic acid) and B (acetonitrile and 0.1% formic acid). To enhance metabolite separation, a mobile phase gradient was used (Table 3.1). Samples were analyzed in multiple reaction monitoring mode (MRM) for maximum sensitivity, with specific precursor and product ions for target amino acids and acylcarnitines being monitored (Table 3.2). Gas (nitrogen) temperature was kept at 300 °C, with a flow rate of 7.5 L per minute and a capillary voltage of 3500 V. Total run time added up to 33 minutes, which included a post run time of 10 minutes.

Table 3.1: Mobile phase gradient used for separation of metabolites.

Time (minutes)	Flow	% Mobile phase B
0	0.2	5
1	0.2	5
5	0.2	18
8	0.2	18
15	0.3	100
20	0.3	100
23	0.2	5

Table 3.2: Precursor/product ion transitions and instrument conditions of metabolites being monitored.

Compound name	Precursor Ion	Product Ion	Dwell	Frag (V)	CE (V)
3-Nitro-Tyrosine	283	181	45	98	12
3-Nitro-Tyrosine	283.1	181.1	45	103	12
Alanine	146.1	90.1	45	65	4
Arginine	231.2	70.1	45	103	32
Asparagine	189.1	144.1	45	89	8
Aspartic acid	246.2	144.1	45	98	8
C0	218	103	45	103	16
C0	218	103	45	89	16
C10	372.3	85	45	122	24
C12	400.3	85	45	117	32
C14	428.4	85.1	45	150	28
C2	260.2	85	45	108	20
C3	274.1	85.1	45	128	20
C4	288.2	85.1	45	108	20
C4_IS	291.2	160.9	45	108	20
C5	302.2	85.1	45	128	20
C6	316	85.1	45	113	20
C8	344.3	85.1	45	123	24

C8_IS	347.2	85.2	45	105	24
Citrulline	232.2	70.1	45	103	32
Creatine	188	90.1	45	89	16
Creatine	188	90.1	45	103	16
Cystathionine	335.2	190.1	45	97	13
Cysteine	178.1	76	45	185	16
Cysteine	178.1	76	45	84	16
Cystine	353	130	45	118	16
Cystine	297	151.9	45	89	12
Cystine	297	151.9	45	103	12
Cystine	297	74.1	45	98	32
GABA	160.1	87.1	45	79	8
Glutamic acid	260.2	84.1	45	89	24
Glutamine	203.1	84.1	45	161	20
Glycine	132.1	76.1	45	65	4
Histidine	212.1	110.1	45	89	16
Homocysteine	192.1	90.1	45	161	12
Homocysteine	192.1	90.1	45	69	12
Homocystine	381.2	192.1	45	98	8
Homocystine	381.2	192.1	45	89	8
Leucine_Isoleucine	188.2	86.2	45	89	8
Lysine	203.2	84.1	45	89	20
Methionine	206.1	104.1	45	94	8
Methionine _IS	209.1	107.2	45	94	8
N,N-Dimethylphenylalanine	250.1	148.1	45	85	20
N,N-Dimethylphenylalanine	250.1	148.1	45	103	20
Ornithine	189.2	70.2	45	89	20
Phenylalanine	222.2	120.1	45	108	16
Phenylalanine_IS	227.2	125.1	45	108	16
Proline	172.1	70.2	45	79	20
Proline	172.1	70.2	45	94	20
Pyroglutamic acid	186	84.1	45	161	16
Pyroglutamic acid	186	84.1	45	103	16
Serine	162	60.1	45	79	12
Taurine	182.1	107.9	45	185	28
Threonine	176	74.2	45	94	12
Tryptophane	261.2	159.1	45	94	16
Tyrosine	238.2	136.1	45	94	12
Valine	174.2	72.2	45	89	12
Valine_IS	182.2	80.2	45	89	12
C16	456.4	85.1	45	152	32
C16_IS	459.4	85.1	45	152	32

3.3.8 UNTARGTED LIQUID CHROMATOGRAPHY - ION MOBILITY - MASS SPECTROMETRY (LC-IN-MS)

3.3.8.1 Sample preparation

A calculated volume of each sample (totaling 0.25 µmoles of creatinine) was transferred into clean vials. To each sample, 100 µL of an internal standard solution containing stable isotopes for phenylalanine, methionine, valine, C4-, C8- and C16-carnitines (end concentration 10 mg/L) as well as 50 µL 3-phenylbutyric acid (end concentration 50 mg/L) was added and then dried under a stream of nitrogen gas. To reconstitute the samples, 100 µL mobile phase (50% acetonitrile, 50% water, 1% formic acid) was added to each sample and left at room temperature for 30 minutes to ensure that the evaporated samples were completely dissolved. The samples were then vortexed and transferred to vials with tapered inserts for analyses.

3.3.8.2 Instrumentation

Samples were analyzed on a Synapt G2-Si (hybrid ion mobility-MS) system (Waters) containing an Acquity UPLC system equipped with ESI source. Five µL sample was injected and separated on a Waters T3 column (2.1 x 100 mm, 1.8 µm), kept at 30 °C, using water with 1% formic acid as mobile phase A and acetonitrile with 1% formic acid as mobile phase B. The mobile phase gradient reported elsewhere (Venter *et al*., 2018) was used for LC separation. The nebulization gas was set to 650 L per minute at a temperature of 500 °C, and the cone gas was set to 30 L per minute. The capillary voltage and cone voltage was set at 2000 V and 30 V, respectively. The Q-TOF acquisition rate was 0.1 s, with argon used as the collision gas at a pressure of 7.066×10^{-3} Pa. Data was captured in HDMSe mode where the collision-induced dissociation (CID) energy for the first (low energy) channel was set at 0 V and those for the second (high energy) channel was set to ramp between 10 and 40 V. Leucine-encephalin (m/z 556.2771 in positive and m/z 554.2615 in negative ionization) was used as lock mass to monitor (and correct) accurate mass measurements in positive and negative ionization modes. Collision cross section (CCS) values were automatically calculated from the ion mobility drift time based on a poly-alanine calibration. Progenesis QI (Nonlinear Dynamics) was used to process the data and to identify compounds using several public databases.

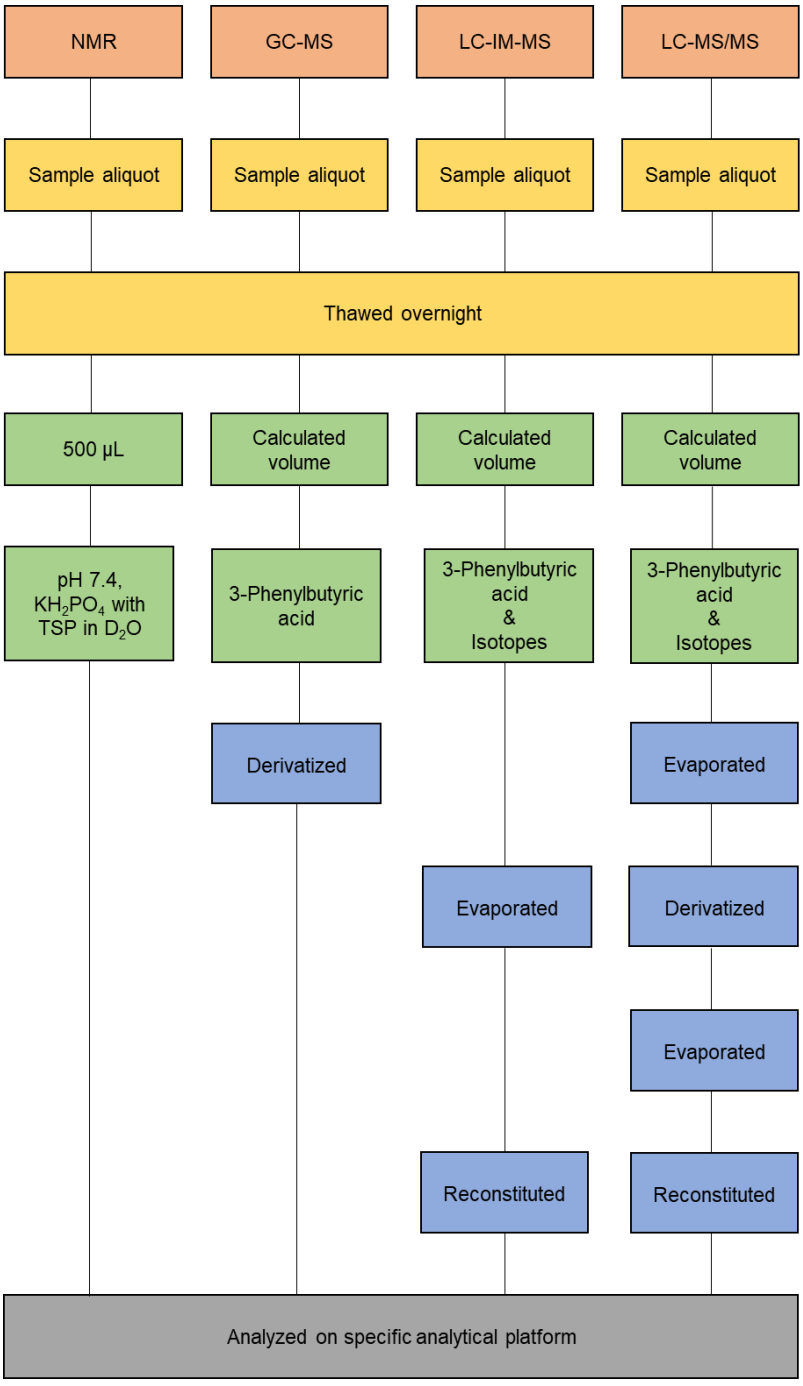

Figure 3.1. Flow diagram of the sample preparation procedure followed in this study. For NMR analyses, 500 µL samples was used whereas the other platforms used a calculated volume based on creatinine concentration. Each analytical platform used different internal standards. For NMR analyses a buffered solution containing TSP was used (pH 7.4, KH_2PO4 with TSP, in D_2O), while GC-MS used only 3-phenylbutyric acid. Both the LC-MS platforms used a combination of 3-phenylbutyric acid as well as deuterated isotopes. NMR samples were analyzed as is, whereas the GC-MS samples first had to be derivatized before analyses. The LC-IM-MS samples was first evaporated before analyses. Samples analyzed on the LC-MS/MS was first evaporated after which it was derivatized and again dried (and reconstituted) before analyses.

3.4 BATCH COMPOSITION AND DATA QUALITY

In order to monitor the reliability and quality of the analyses, quality control (QC) samples were used for all the analytical platforms. These QC samples were prepared by pooling equal volumes of urine (500 µL) from all of the patient as well as control samples. This pooled urine QC sample was then aliquoted into smaller volumes and stored at -80 °C until it was used. Due to the large number of samples, batches containing 30 to 50 samples were run depending on the analytical platform. These batches contained randomized samples, consisting of both patient and control samples. When the batches were analyzed on each platform, a number of QC aliquots were introduced into each batch and were treated in the same manner as the control and patient samples. Each platform contained a different number of QCs. For the LC-MS analyses (untargeted and targeted), three QCs were included in the beginning of a batch, each of them analyzed twice, and then another QC aliquot was included after every five samples. For GC-MS analyses, two QC aliquots were included at the beginning of a batch and then after every 10th sample. For the NMR analyses, only one QC sample was included in the beginning of the batch, with no other QC's included in the rest of the batch. Not all QC samples were used to investigate the quality of the data as the first four QCs (2 aliquots analyzed twice) for LC-MS and the first QC analyzed on the GC-MS were used to equilibrate the analytical system and therefore not utilized in monitoring data quality.

The quality of the data was evaluated in several steps and tests: firstly, the data including the QCs, were visualized with principle component analysis (PCA) to get an overview of the data. Large or obvious grouping patterns can point to strong batch effects which meant that the analyses had to be repeated. Since no pertinent batch-related grouping was observed (using a PCA-approach), the quality of the data was then also checked on univariate level with the help of coefficient of variance (CVs) and visualization with heatmaps and scatter plots (of individual metabolites against run order). Compounds with QC CV >50 were removed as they were not reliably detected. Statistically speaking, it is common to remove about 30% of the metabolites in untargeted methods as the method cannot reliably detect all metabolites.

3.5 BIOINFORMATICS

Data normalization as done in two steps. First the data from each platform was normalized against the specific internal standard used for the specific analysis, then it was normalized

against creatinine (Chapter 4) and osmolality (Chapter 5). When investigating urine metabolites, normalization usually is done against creatinine as it is excreted at a constant rate by the kidneys. However, in diseases where the kidneys are compromised, this constant excretion is altered, which ultimately could affect the normalization of the data. In cases where creatinine can not be used for normalization, other normalization methods should be considered. One of these methods is the use of osmolality, measured in mOsm/kg. Osmolality can be defined as the measurement of the number of dissolved particles per unit of water in the urine which gives an indication of how concentrated or diluted a sample is. When investigating the urine creatinine concentrations of our MELAS patient cohort (Chapter 4), a strong significant correlation was observed between the urine creatinine concentration (measured in mmol/L) and the measured osmolality (mOsm/kg). Due to this strong correlation, it was decided that the urine metabolic data can be normalized to either creatinine or osmolality in this part of the study. We therefore decided to use the data normalized against creatinine as this would be more appropriate to the reader working in the field of mitochondrial disease diagnostics (most diagnostic laboratories normalize all patient data against creatinine and are thus not familiar with data normalized to osmolality). However, when the creatinine values of the two additional phenotypes (MIDD and myopathy) investigated in Chapter 5 were evaluated, creatinine concentration in the MIDD group was not comparable to that of the controls and the other two phenotypes. This indicated the possibility of potential kidney impairment in the MIDD group. Thus, even though the data was normalized against creatinine in Chapter 4 (MELAS patients against controls), it was decided to normalize the data for this second part of the study, including the MELAS dataset (Chapter 5), against osmolality in order to be able to compare all three phenotypes to the controls and one another.

After normalization of the data, an 80% zero filter was applied, where a specific feature had to be detected/quantified in 80% of the samples in at least one of the sample groups (controls, MELAS, MIDD or myopathy), otherwise it was removed from the data set. Next a 50 % coefficient of variation (CV) filter was applied. The QC samples were used to determine the CV of a given metabolic feature/analyte and if the CV was above 50%, the feature was considered poorly quantified under the set experimental conditions and removed from the dataset. An additional filtering step was included when all the phenotypes were compared (Chapter 5) - the Fisher ratio method was used as a low variance/noise filter (Pierce *et al*., 2006), where features with a ratio of <0.05 were removed. Finally missing/zero values were replaced by half of the lowest value in the data set before the data was log transformed. The individually pre-processed data sets from the different analytical platforms were then combined into one single data matrix and used for all further statistical analyses.

Univariate statistical analyses were used to determine important metabolites that differed significantly between each phenotype group and the healthy controls. For a metabolite to be considered important, it had to be statistically (T-test; FDR corrected $p < 0.05$) and practically (Effect size; $d > 0.8$) significant. In Chapter 5, T-test p-values were evaluated at both the 5% and 10% significance level after correcting for multiple testing using the Bonferroni-Holm approach (Holm, 1979; McLaughlin and Sainani, 2014). Principle component analyses (PCA), volcano plots and heat maps were then used to visualize the natural grouping/separation of the respective groups with regards to these important metabolites, performed using MetaboAnalyst 3.0 (Xia *et al*. 2016). Using the important metabolites identified in each phenotype, a Venn diagram was constructed to identify metabolic similarities and differences between the three phenotypes (MELAS, MIDD and myopathy). Finally, one-way ANOVA was used to identify the metabolites that differed significantly between the phenotypes. The metabolic differences were visualized in the form of metabolic pathways and box-plots to highlight the specific differences.

The important features that differed markedly between the control and respective phenotypes were identified using platform specific tools and information. The important features detected with GC-MS were identified by spectral and retention index matching using the NIST11 commercial library as well as an in-house library (Reinecke *et al*. 2012). Spectral matches without retention time/index confirmation were considered Level 3 identities (tentative candidates) while spectral and retention time/index matching resulted in Level 1 identities (confirmed candidates), according to the levels described by Schymanski *et al.,* (2014). The important features detected with untargeted LC-IM-MS were identified by matching the high resolution mass, isotope pattern and MS/MS spectra to an in-house library and several public databases, which included: CheBI (www.ebi.ac.uk/chebi), HMDB (www.hmdb.ca), Lipid maps (http://www.lipidmaps.org), Drug bank (http://www.drugbank.ca), and Metlin (http://metlin.scripps.edu). *In silico* fragmentation spectra of compounds without published spectra were generated and used within Progenesis QI to aid identification. The confidence of the identities based on spectral, accurate mass and isotope matching were considered Level 3 (tentative candidates). The collisional cross section (CCS) values from ion mobility were also used to identify compounds using the Waters CCS library. The additional matching of CCS values increased the confidence of the metabolite identities (Level 1). The important features/bins detected with NMR were identified by matching to spectra of authentic chemical standards compiled in an in-house and Bruker's reference library. Most of the identities of the NMR features were considered Level 1 or 2. Due to the targeted nature of the LC-MS/MS platform, these metabolite identities were considered Level 1.

3.6 REFERENCES

Bouatra, S., Aziat, F., Mandal, R., Guo, A.C., Wilson, M.R., Knox, C., Bjorndahl, T.C., Krishnamurthy, R., Saleem, F., Liu, P., 2013. The human urine metabolome. *PloS One*. 8 (9), e73076.

Ellinger, J.J., Chylla, R.A., Ulrich, E.L., Markley, J.L., 2013. Databases and software for NMR-based metabolomics. Current Metabolomics. 1 (1), 28-40.

Holm, S., 1979. A Simple Sequentially Rejective Multiple Test Procedure. *Scandinavian Journal of Statistics*. 6 (2), 65-70.

McLaughlin, M.J. and Sainani, K.L., 2014. Bonferroni, Holm, and Hochberg corrections: fun names, serious changes to p values. *Physical Medicine and Rehabilitation*. 6 (6), 544-546.

Pierce, K.M., Hoggard, J.C., Hope, J.L., Rainey, P.M., Hoofnagle, A.N., Jack, R.M., Wright, B.W., Synovec, R.E., 2006. Fisher ratio method applied to third-order separation data to identify significant chemical components of metabolite extracts. *Analytical Chemistry*. 78 (14), 5068-5075.

Reinecke, C.J., Koekemoer, G., van der Westhuizen, F.H., Louw, R., Lindeque, J.Z., Mienie, L.J., Smuts, I., 2012. Metabolomics of urinary organic acids in respiratory chain deficiencies in children. *Metabolomics*. 8 (2), 264–283.

Roberts, L.D., Souza, A.L., Gerszten, R.E., Clish, C.B., 2012. Targeted metabolomics", *Current protocols in molecular biology*. 98 (1), 30.2.1-30.2.24.

Schymanski, E.L., Jeon, J., Gulde, R., Fenner, K., Ruff, M., Singer, H.P., Hollender, J., 2014. Identifying Small Molecules via High Resolution Mass Spectrometry: Communicating Confidence. *Environmental Science & Technology*. 48, 2097–2098.

Venter, L., Lindeque, Z., van Rensburg, P.J., van der Westhuizen, F., Smuts, I., Louw, R., 2015. Untargeted urine metabolomics reveals a biosignature for muscle respiratory chain deficiencies. *Metabolomics.* 11 (1), 111–121.

Venter, L., Loots, D.T., Mienie, L.J., Jansen van Rensburg, P.J., Mason, S., Vosloo, A., Lindeque, J.Z., 2018. The cross-tissue metabolic response of abalone (Haliotis midae) to functional hypoxia. *Biology open*. 7 (3) 10.1242/bio.031070.

Xia, J., Wishart, D.S., 2016. Using MetaboAnalyst 3.0 for comprehensive metabolomics data analysis. *Current Protocols in Bioinformatics*. 55, 10-14.

Chapter 4

4

A urinary biosignature for mitochondrial myopathy, encephalopathy, lactic acidosis and stroke like episodes (MELAS)

4.1 INTRODUCTION

Mitochondrial diseases are one of the most common inborn errors of metabolism, with a minimum prevalence of 1:5000 (Gorman *et al*., 2015; Schaefer *et al*., 2008). Mitochondrial myopathy, encephalopathy, lactic acidosis and stroke like episodes, better known as MELAS (MIM 540000), is one such a mitochondrial disease and was first described in 1984 as a "neurodegenerative disease caused by the decreased ability of cells to produce sufficient energy in the form of ATP" (Pavlakis *et al*., 1984). In 1990, the MELAS phenotype was associated with a specific mutation, now known as the m.3243A>G mutation (Goto *et al*., 1990). This mutation is a point mutation on position 3243 of the mitochondrial DNA (mtDNA), where an adenine (A) is substituted with a guanine (G) in the *MT-TL1* gene. The latter gene encodes for a transfer ribonucleic acid (tRNA), which recognizes the codons UUA and UUG for the amino acid leucine in mitochondrial translation (Scaglia and Northrop, 2006; Kami *et al*., 2012). The mutation thus disturbs mitochondrial protein synthesis, ultimately affecting Complexes I, III, IV and V of the oxidative phosphorylation (OXPHOS) system. Although almost 80% of all MELAS cases are caused by the m.3243A>G mutation, other mtDNA mutations have later been associated with the MELAS phenotype, including the m.3244G>A, m.3258T>C, m.3271T>C, m.3291T>C and m.8356T>C mutation (Ruiz-Pesini *et al*., 2007; Scaglia and Northrop, 2006).

Patients diagnosed with MELAS can also present with a wide range of symptoms, varying in degree of prevalence and severity. However, in this study, a MELAS phenotype was defined as a patient carrying the m.3243A>G mutation and that had at least one stroke like episode. Although late onset MELAS does occur, these patients were not included in this study. Initially, the m.3243A>G mutation was specifically associated with MELAS, however, over time various other phenotypes have also been linked to this mutation, including maternally inherited diabetes and deafness (MIDD), progressive external ophthalmoplegia (PEO) and

mitochondrial recessive ataxia syndrome (MIRAS) (Scaglia and Northrop, 2006; Manwaring *et al*., 2007).

A recent study attempted to identify mechanistic differences between different m.3243A>G phenotypes using nuclear magnetic resonance (NMR) spectroscopy. With this single metabolomics technique, the authors were able to identify six urinary metabolites (all decreased in the patients, compared to the controls) that were able to distinguish MELAS patients from controls (Hall *et al*., 2015). The markers included N-methylnicotinamide, hippurate, creatinine, 4-cresyl sulfate, glycolate, and a marker with unconfirmed identity, possibly 4-hydroxyphenylacetic acid. Although these markers point towards altered phenylalanine and tyrosine metabolism, arginine metabolism (creatinine) and a connection to gut microbial metabolism (4-cresyl sulfate and glycolate), the exact mechanism(s) for these changes remains elusive. Here we aimed to extend these findings on MELAS by investigating the urine metabolome of MELAS patients using a multi-platform metabolomics approach. With a larger metabolome coverage, additional metabolites affected in the MELAS patients, compared to healthy controls, can potentially be identified. This can potentially provide a more extensive and improved biochemical understanding of the metabolic perturbations resulting from this specific phenotype.

4.2 METHODS

4.2.1 PATIENTS AND ETHICS

Urine samples of two cohorts of genetically confirmed m.3243A>G MELAS patients and healthy controls were obtained from the Radboud University Medical Center in Nijmegen, The Netherlands and the University of Helsinki, Finland. To ensure group homogeneity, exclusion criteria were applied to the original cohorts, namely, 1) controls that received either medication or supplementation at the time of sample collection; 2) controls with a medical condition (such as diabetes, hypertension, etc.) Characteristics of the patients and controls are summarized in Tables 4.1 and 4.2, including data on the urinary epithelial cell m.3243A>G mutation load measured in the patients.

The study complied with all applicable institutional guidelines and terms of the Declaration of Helsinki of 1975 (as revised in 2013) for investigation of human participants. Ethical approval was obtained from the Health Research Ethics Committee (HREC) of the North-West University (NWU-00170-13-A1). All the patients as well as the controls provided written informed consent for their urine samples to be used for research purposes.

Table 4.1: Characteristics of the MELAS patients and healthy controls of the Nijmegen cohort used in this study (means ± standard deviation).

Characteristic	Patients	Controls
Total, N	9	29
Age, y	31.4 ± 11.6	34.8 ± 19.8
Male	6	10
Female	3	19
Creatinine [mmol/L)	7.2 ± 5.2	13.2 ± 7.1
Osmolality(mOsm/kg)	570.2 ± 279.4	765.6 ± 271.7
NMDAS Score	44.9 ± 18.7	N/A
% m.3243A>G	81 ± 0.19	N/A
Symptoms (Number of patients presenting with symptoms)		
Cardiomyopathy	3 (33.3%)	N/A
Epilepsy	7 (77.8%)	N/A
Myopathy	9 (100%)	N/A
Strokes	9 (100%)	N/A
GI dysmotility	7 (77.8%)	N/A
Diabetes	5 (55.6%)	N/A
Renal insufficiency	0 (0%)	N/A
Hearing loss	9 (100%)	N/A
Medication (Number of patients exposed)		
Acetylsalicylic acid	1 (11.1%)	N/A
Angiotensin-converting-enzyme inhibitor (ACE inhibitor)	1 (11.1%)	N/A
Anticoagulant	2 (22.2%)	N/A
Antiepileptic	7 (77.8%)	N/A
Angiotensin Receptor Blockers (ARBs)	1 (11.1%)	N/A
Beta blockers	2 (22.2%)	N/A
Calcium antagonist	1 (11.1%)	N/A
Diuretic	1 (11.1%)	N/A
Insulin	4 (44.4%)	N/A
Laxative	1 (11.1%)	N/A
Statin	1 (11.1%)	N/A
Sulfanylurea derivative	1 (11.1%)	N/A
Supplements (Number of patients exposed)		
Arginine	2 (22.2%)	N/A
B12 carnitine	1 (11.1%)	N/A
Carnitine	1 (11.1%)	N/A
Coenzyme Q10	2 (22.2%)	N/A
Folic acid	1 (11.1%)	N/A
Riboflavin	2 (22.2%)	N/A

The m.3243A>G mutation load was determined in urinary epithelial cells as described earlier (de Laat *et al.*, 2012).

Table 4.2: Characteristics of the MELAS patients and healthy controls of the Helsinki cohort used in this study (means ± standard deviation).

Characteristic	Patients	Controls
Total, N	2	7
Age, y	54.7 ± 2.2	38.5 ± 13.6
Creatinine [mmol/L)	7.4 ± 2.4	16.2 ± 2.9
Osmolality(mOsm/kg)	504.5 ± 187.4	755.0 ± 69.2
% m.3243A>G urine	71.5 ± 20.5	N/A
% m.3243A>G blood	21.5 ± 9.2	N/A
Symptoms (Number of patients presenting with symptoms)		
Ataxia	1 (50%)	N/A
Cardiomyopathy	2 (100%)	N/A
Depression	2 (100%)	N/A
Diabetes	2 (100%)	N/A
Hearing loss	2 (100%)	N/A
Hyperaldosteronism	1 (50%)	N/A
Myopathy	1 (50%)	N/A
Migraine-type headache	1 (50%)	N/A
Ptosis	1 (50%)	N/A
Medication (Number of patients exposed)		
Acetylsalicylic acid	1 (50%)	N/A
Angiotensin-converting-enzyme inhibitor (ACE inhibitor)	1 (50%)	N/A
Beta blocker	1 (50%)	N/A
Benzodiazepines	2 (100%)	N/A
Insulin	2 (100%)	N/A
Metformin	1 (50%)	N/A
Sulfanylurea derivative	1 (50%)	N/A
Supplements (Number of patients exposed)		
Calcium	1 (50%)	N/A
Coenzyme Q10	1 (50%)	N/A
Iron	1 (50%)	N/A
Magnesium	2 (100%)	N/A
Omega	2 (100%)	N/A
Vitamin B	1 (50%)	N/A
Vitamin D	1 (50%)	N/A

The m.3243A>G mutation load was determined in urinary epithelial cells.

4.2.2 METABOLIC PROFILING

A multi-platform metabolomics approach, which consisted of targeted as well as untargeted techniques, was used to analyze the urine samples of the MELAS patients and healthy controls in order to obtain an extensive metabolomics data set. Targeted analyses consisted of liquid chromatography tandem-mass spectrometry (LC-MS/MS) while untargeted analyses consisted of gas chromatography–mass spectrometry (GC–MS), nuclear magnetic resonance (NMR) spectroscopy and liquid chromatography mass spectrometry with ion mobility (LC-IM-MS) — in positive and negative ionization mode. The protocols for the metabolomics techniques and sample preparation used are discussed in detail in the SI.

4.2.3 STATISTCAL ANALYSES

Data matrixes obtained from the GC–MS, LC-MS/MS, NMR and the two LC-IM-MS platforms were pre-processed individually and were then combined into one single metabolomics data set (pre-processing details are given in the SI). The data were normalized to creatinine, as discussed in the SI. The data was then log-transformed before univariate and multivariate statistical analyses. Univariate analyses (student t–test and effect size) were performed in Excel 2013 (Microsoft Inc.), while the multivariate analyses [principle component analysis (PCA) and heatmaps] were done using Matlab (Mathworks, Natick, Ma) and MetaboAnalyst 3.0 (www.metaboanalyst.ca), respectively. A feature with a t-test P value of <0.05 and an effect size d value of >0.8 was considered important, thus showing statistical significant and practical differences between the patient group and the healthy controls. The covariance and discriminatory power of the important metabolites were visualized with PCA, heatmaps and a volcano plot. The identity of the important features were determined from matching the spectral information (NMR), retention time, high resolution mass and/or fragmentation spectra (MS) to in-house and commercial libraries as well as public databases. Confidence levels for each identity were included (Fiehn *et al*., 2007) as well as the analytical platform used to detect the metabolite (Table 4.3).

Table 4.3: List of 36 metabolites that differed significantly between MELAS patients and controls in the Nijmegen cohort.

	Direction	P-Value (Student t-test)	D-Value (Effect size)	Level of identification	Platform
AMINO ACIDS					
Alanine	↑	0.001	1.258	1	NMR (LC-MS/MS)
Arginine	↑	0.015	0.962	1	LC-MS/MS
Aspartic acid	↑	0.019	0.872	1	LC-MS/MS
Cysteine	↑	0.001	1.244	1	LC-MS/MS
Isoleucine	↑	0.001	1.050	1	NMR
Leucine	↑	0.004	1.007	1	NMR
Lysine	↑	0.014	0.895	1	NMR
N2-Succinyl-L-glutamic acid 5-semialdehyde	↑	0.004	1.052	3	LC-IM-MS (+)
N-Acetyltryptophan	↑	0.003	1.118	3	LC-IM-MS (+)
Proline	↑	0.004	1.123	1	NMR
Sarcosine	↓	0.031	0.853	1	GC-MS
Taurine	↑	0.014	0.924	3	GC-MS
Trimethylglycine (Betaine)	↑	0.003	1.100	1	NMR
ORGANIC ACIDS					
3-Hydroxybutyric acid	↑	0.011	0.993	1	GC-MS
4-Hydroxyglutaric acid	↑	0.007	1.033	3	GC-MS
Acetoacetic acid	↑	0.037	0.810	1	NMR
Butyric/valeric acid	↑	0.000	1.107	2	NMR
Caproic/caprylic acid	↑	0.000	1.225	2	NMR
Citric acid	↑	0.004	1.134	1	NMR
Glycerol	↓	0.002	1.183	3	GC-MS
Lactic acid	↑	0.004	1.085	1	GC-MS (NMR)
Pyruvic acid	↑	0.014	0.987	1	NMR (GC-MS)
CARNITINES					
Carnitine	↑	0.000	1.068	1	NMR
C2-Carnitine	↑	0.000	1.083	1	LC-MS/MS
C3-Carnitine	↑	0.000	1.017	1	LC-MS/MS

C4-Carnitine	↑	0.002	0.923	1	LC-MS/MS
C5-Carnitine	↑	0.000	0.895	1	LC-MS/MS
OTHER					
6-Azathymine	↓	0.006	0.973	3	GC-MS
2,3-Butanediol glucoside	↑	0.002	1.139	3	LC-IM-MS (+)
Butanal	↑	0.015	0.834	3	GC-MS
Glucose	↑	0.000	1.225	1	NMR
Hydroxylamine	↓	0.002	1.081	3	GC-MS
Resolvin D2	↑	0.015	0.877	3	LC-IM-MS (+)
TMAO	↑	0.004	0.844	1	NMR
Urea	↑	0.024	0.878	1	NMR
Xanthine	↑	0.011	0.856	1	NMR

If a metabolite was detected as significant by more than one analytical platform, the second platform is indicated in the table in brackets. ↑ means the metabolite is increased in the MELAS patients, relative to the Controls. ↓ means the metabolite is decreased in the MELAS patients, relative to the Controls.

4.3 RESULTS

4.3.1 EXPLORATORY PHASE

The Nijmegen cohort were utilized for the exploratory phase, i.e. searching for a biosignature for MELAS. Univariate measures — student's t-test ($P < 0.05$) and effect size ($d > 0.8$) — highlighted 36 metabolites that differed significantly between the MELAS patients and healthy controls (Table 4.3). All but four of the 36 urinary metabolites were increased in the MELAS patients (Figure 4.1B + C), with only sarcosine, glycerol, hydroxylamine and 6-azathymine being decreased. The visualized covariance of these metabolites (Figure 4.1A) resulted in separate grouping of the MELAS patients and controls (albeit with some overlap). The PCA scores plot show that the MELAS patients are more homogenous than the controls – indicating a more defined metabolic profile in comparison to the controls. A Venn diagram (Figure 4.2) illustrates the contribution of each analytical platform used in this study towards the final 36 important metabolites detected. Although a large number of features were detected using each analytical platform, only those metabolites that differed significantly between the MELAS and control groups and could be identified/partially identified were considered — forming the final metabolic fingerprint.

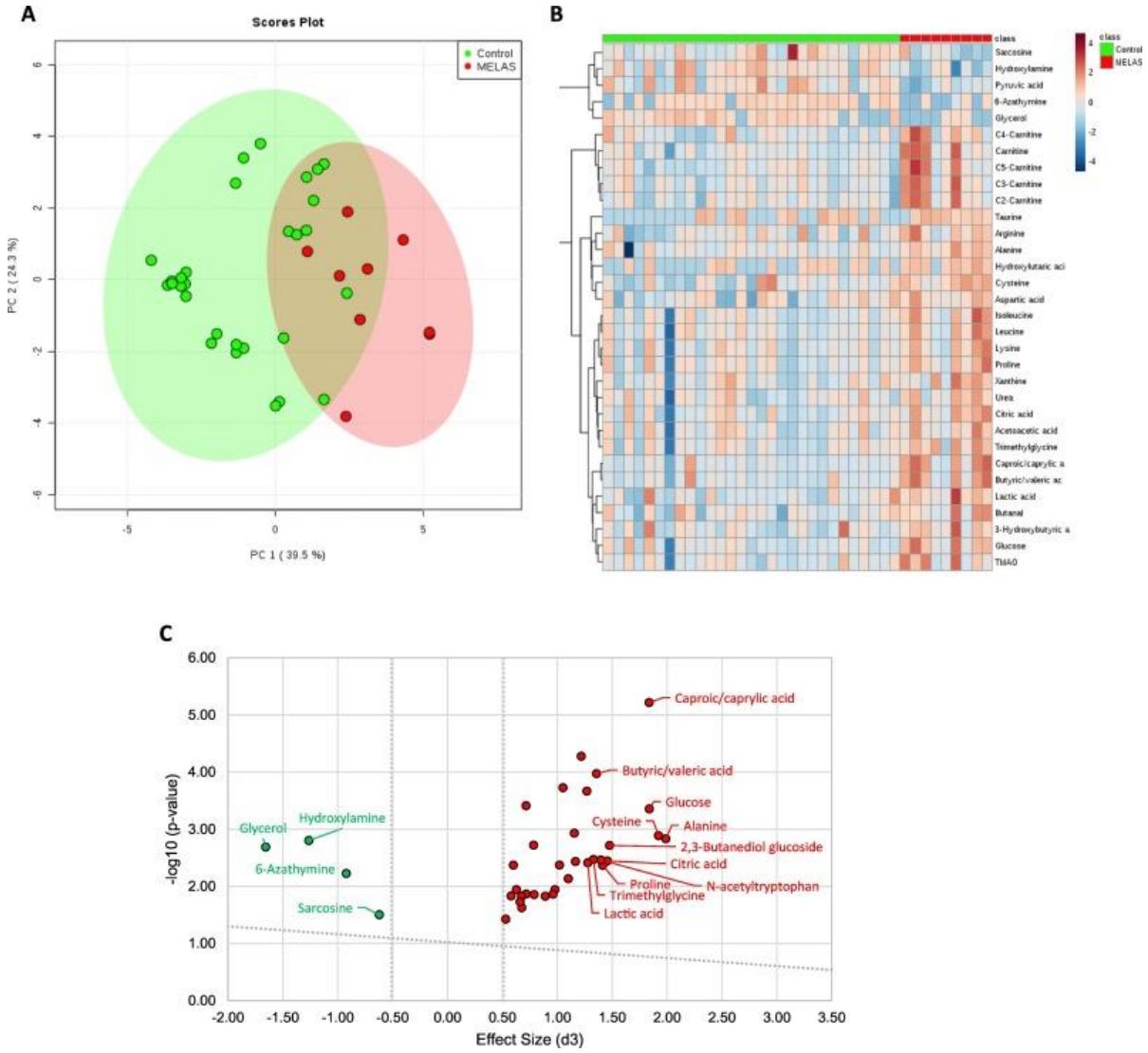

Figure 4.1. Differences between Controls and MELAS patients of the exploration (Nijmegen) cohort using the 36 selected variables. A) Principal component analysis score (PCA) plot. Sample grouping are shown in the PCA with 90% confidence ellipses; B) heatmap; C) volcano plot.

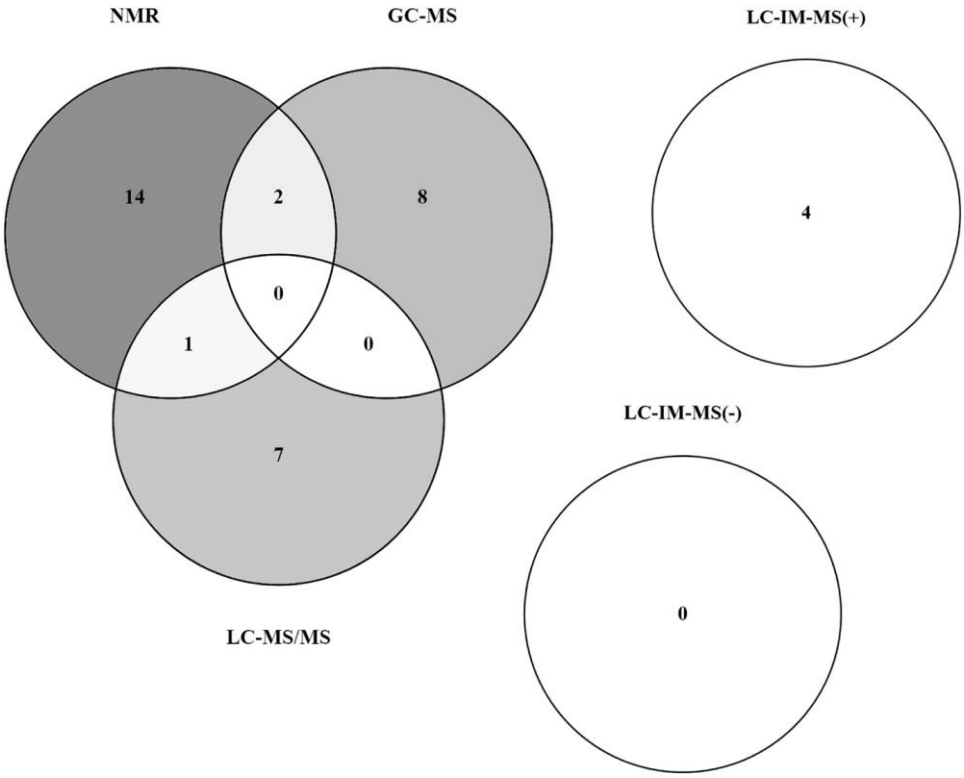

Figure 4.2. Venn diagram illustrating the contribution of each analytical platform to the detection of the 36 important metabolites. Five analytical platforms were used to analyze the metabolome of the MELAS patients and controls. Although a large number of features were detected using each platform, only the metabolites that differed significantly between the MELAS and controls groups and that could be identified/partially identified were considered as "important", thus forming part of the final metabolic fingerprint consisting of 36 metabolites.

4.3.2 VALIDATION PHASE

The Helsinki cohort were used for the validation phase of this study. After identifying the 36 metabolites for MELAS using the Nijmegen cohort during the exploratory phase, data on the same 36 metabolites were extracted from the Helsinki cohort and used for the validation phase. The visualized covariance of these metabolites (Figure 4.3) showed that the 36 metabolite fingerprint strongly separated MELAS patients from controls in a different sample set.

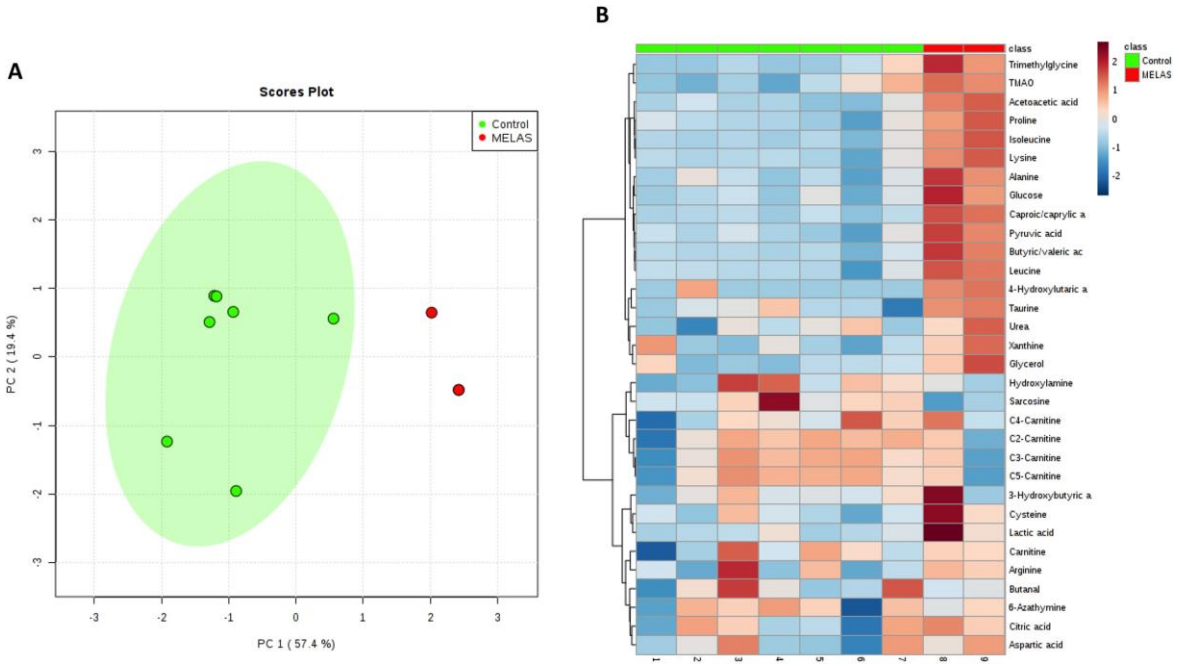

Figure 4.3. Differences between Controls and MELAS patients of the validation (Helsinki) cohort using the 36 selected variables. A) Principal component analysis score (PCA) - since this cohort only contains two MELAS samples, an ellipse could not be drawn for the patient group, although the two samples clearly grouped well away from the controls, indicating natural separation. Sample grouping are shown in the PCA with 90% confidence ellipses; B) heatmap.

4.4 DISCUSSION

We report here a multi-platform metabolomics investigation of the urinary metabolome of MELAS patients carrying the m.3243A>G mutation. We show that urine may be a useful source for disease-specific metabolomics data. Furthermore, we identified a 36 metabolite fingerprint that partially-separated the patients from the controls in two separate cohorts, suggesting usefulness of these 36 separate markers as a diagnostic set.

Several of the affected pathways identified by our metabolomics approach was disturbed by redox-status (Figure 4.4), with increased levels of lactic acid, pyruvic acid, acetoacetic acid and the branched chain amino acids (leucine, isoleucine). These metabolites have previously been linked to mitochondrial diseases in various studies, using different mitochondrial disease models (Esterhuizen *et al*., 2017) and fits with an altered NAD+/NADH ratio, now considered key in the development of mitochondrial disease (Khan *et al*., 2014). Cofactors NADH and $FADH_2$ are formed in the tricarboxylic acid (TCA) cycle and serve as electron carriers onto the complexes of the OXPHOS system. When a defect in any one of the components of the OXPHOS system occurs, the flow of electrons along this chain is

hindered. This perturbed flow results in altered levels of oxidized cofactors (NAD+, FADH) to reduced cofactors (NADH, $FADH_2$), i.e. a redox imbalance (Brière *et al*., 2004; Khan *et al*., 2014; Naviaux, 2014; Reinecke *et al*., 2012; Smeitink *et al*., 2006), affecting dehydrogenase enzymes. A redox imbalance could explain the altered lactic and pyruvic acid levels detected as lactate dehydrogenase, a redox dependent enzyme, is responsible for the interconversion of these two metabolites. The lactate/pyruvate ratio, an indicator of cytosolic redox state (Munnich *et al*., 1996) was slightly increased in the urine of MELAS patients, compared to the controls, although not statistically significant ($P = 0.2$). Furthermore, since branched chain amino acids are ultimately metabolized to their respective α-keto acids through the branched-chain α-keto acid dehydrogenase complex (BCKDC), altered BCKDC activity, caused by a redox imbalance, could elucidate the accumulation of the isoleucine and leucine detected in the MELAS cohort. Another point of interest was the ketone body acetoacetic acid, which is converted to 3-hydroxybutyric acid by 3-hydroxybutyric acid dehydrogenase. Since the activity of this enzyme is also dependent on the redox balance, an altered redox balance caused by MELAS could explain the increased levels of acetoacetic acid found in our MELAS patient group. Thus our findings suggest that urine reflects the overall redox-balance of the body.

Currently receiving a lot of attention in the field of mitochondrial disease research is an intricate web of pathways consisting of one-carbon metabolism, the methylation cycle and the trans-sulfuration pathway. It has been hypothesized that these pathways could be affected in defective OXPHOS systems, but it was not until recent studies that this intricate web of pathways was positively associated with the disease (Bao *et al*., 2016; Nikkanen *et al*., 2016). In addition to a redox imbalance, our data are also supportive of alterations in this cluster of pathways, with increased levels of, cysteine, trimethylglycine (betaine), taurine, and trimethylamine N-oxide (TMAO) detected (Figure 4.4D and Table 4.3). Firstly, cysteine is metabolized to taurine through a cofactor-dependent reaction, thus influencing the taurine levels detected in the MELAS patients. Secondly, during the methylation cycle, homocysteine is converted to methionine through a reaction where choline is converted to trimethylglycine (betaine), ultimately producing dimethylglycine. Finally, choline additionally produces trimethylamine (TMA), which is further broken down to TMAO and dimethylamine. Thus, the results reported here not only indicate affected one-carbon metabolism, but also an altered trans-sulfuration pathway and methylation cycle, explaining the altered levels of all these metabolites observed in this study.

Another component of the metabolism that seems to be strongly affected by MELAS is fatty acid oxidation. We hypothesize that stalled beta-oxidation is responsible for the altered

levels of glycerol, butyric/valeric acid (short chain fatty acid), caproic/caprylic acid (medium chain fatty acid), carnitine, acetyl-carnitine (C2) and butanoyl-carnitine (C4). The altered levels of isovaleryl-carnitine (C5) and propionyl-carnitine (C3) are indicative of altered uneven-chain fatty acid and/or altered amino acid catabolism. From the volcano plot (Figure 4.1C), some of the most discriminatory (statistically significant) metabolites in the MELAS patients can be linked to stalled fatty acid catabolism/beta-oxidation. Many carnitine conjugates also increased in the MELAS group, however, the question arose as to how free carnitine can be increased as well in the MELAS group while it is used for detoxification and hence excreted in elevated levels as conjugates. For this to be possible, increased carnitine biosynthesis is needed. However, such a scenario would require one-carbon units in the form of s-adenosylmethionine for the synthesis of carnitine via trimethyllysine. We thus speculate that due to the increased carnitine conjugates excreted in the urine of MELAS patients, one-carbon metabolism is affected in an effort to replenish the diminished carnitines. Thus, although many of the effected metabolites we report here can be linked to a redox imbalance and one-carbon metabolism, methylation and transsulfuration, our results indicate that stalled fatty acid oxidation was severely affected in this MELAS cohort.

Other metabolites detected as increased can be linked to different metabolic pathways. Increased amino acid catabolism (possibly through the activation of AMPK due to low energy levels) is supported by the increased levels of arginine, N2-succinyl-l-glutamic acid 5-semialdehyde, aspartic acid, and urea. Even though some of the patients received carnitine (n = 1) and arginine (n = 2) supplementation, our data was still supportive of stalled beta-oxidation (Figure 4.4C) and increased amino acid catabolism (Figure 4.4B), even when the patients receiving supplementation were excluded from the data analysis (data not shown). Altered levels of xanthine is supportive of affected purine pathway. Lastly, 2,3-butandiol would normally be associated with high level of alcohol consumption; however, this metabolite can also be expected in urine when high level of glucose (as detected in the MELAS patients) are present as it is further metabolized by the gut microbes (Elshaghabee *et al*., 2016; Venkataraman *et al*., 2014). Additionally, the increased levels of 4-hydroxyvaleric acid could also be ascribed to gut microbial metabolism. Since seven of the nine MELAS patients demonstrated GI dysmotility, the altered levels of 2,3-butandiol and 4-hydroxyvaleric acid could indeed be due to altered gut metabolism on the measured urinary metabolome.

A study in 2015 (Hall *et al*., 2015) of renal involvement in mitochondrial disease included a cohort of 14 patients with the MELAS phenotype; NMR was utilized to identify six potential urinary markers (N-methylnicotinamide, hippurate, creatinine, 4-cresyl sulfate, glycolate, and

a marker with unconfirmed identity, possibly 4-hydroxyphenylacetic acid). In our study, we detected and quantified N1-methylnicotinamide, hippurate, creatinine, glycolate, but none of these markers were significantly affected by MELAS ($P > 0.05$ and $d < 0.8$) in our cohort. Lastly, our multi-platform approach resulted in the detection of 36 metabolites perturbed by MELAS compared to the six reported by Hall *et al*., (2015), whom only used a single analytical platform.

The strength of our study was the utilization of five different analytical platforms to generate the robust metabolomics data reported here. Of the five platforms employed, only three (GC–MS, NMR and LC-MS/MS) contributed to the majority of our metabolite list as illustrated in Figure 4.2. Although many discriminatory features were detected with untargeted LC-IM-MS, only four metabolites (in positive ionization mode) was identified with moderate confidence while none of the discriminatory features in negative ionization mode could be identified. Nevertheless, some of the 36 important metabolites were detected and identified as important by more than one platform (Figure 4.2) due to their overlapping coverage of the metabolome, giving more credibility to the metabolite as being critical in the disease. One important metabolite was detected by both the NMR and LC-MS/MS (alanine) while the overlap between the GC–MS and NMR was two metabolites (lactic acid and pyruvic acid). In the light of these findings, we recommend using a multi-platform approach to analyze the metabolome in mitochondrial disease studies as the multiple platforms complement each other, rather than substitute for each other.

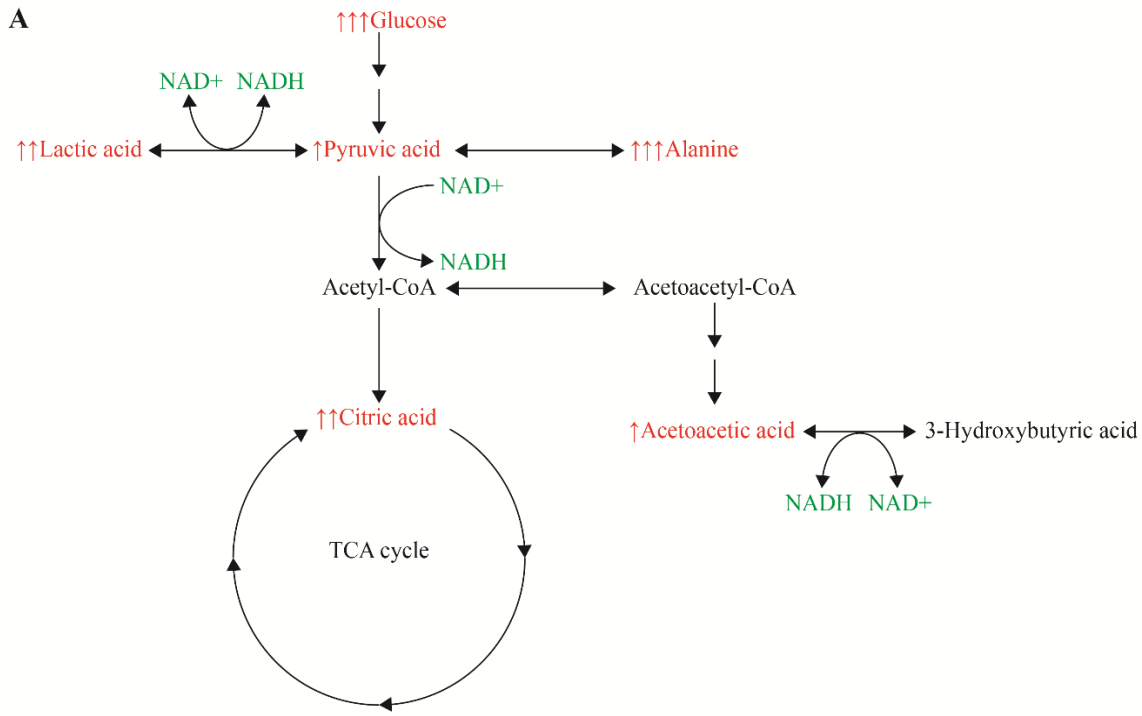
A
↑↑↑Glucose
NAD+ NADH
↑↑Lactic acid
↑Pyruvic acid
↑↑↑Alanine
NAD+
NADH
Acetyl-CoA
Acetoacetyl-CoA
↑↑Citric acid
↑Acetoacetic acid
3-Hydroxybutyric acid
NADH NAD+
TCA cycle

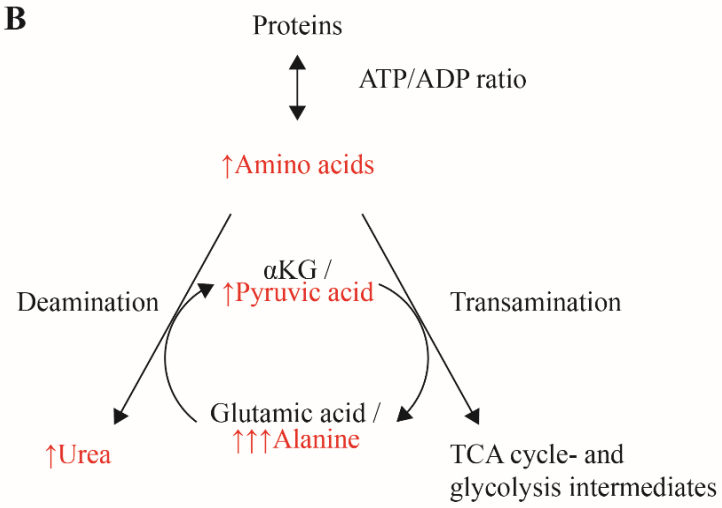
B
Proteins
ATP/ADP ratio
↑Amino acids
αKG /
↑Pyruvic acid
Deamination
Transamination
Glutamic acid /
↑↑↑Alanine
↑Urea
TCA cycle- and
glycolysis intermediates

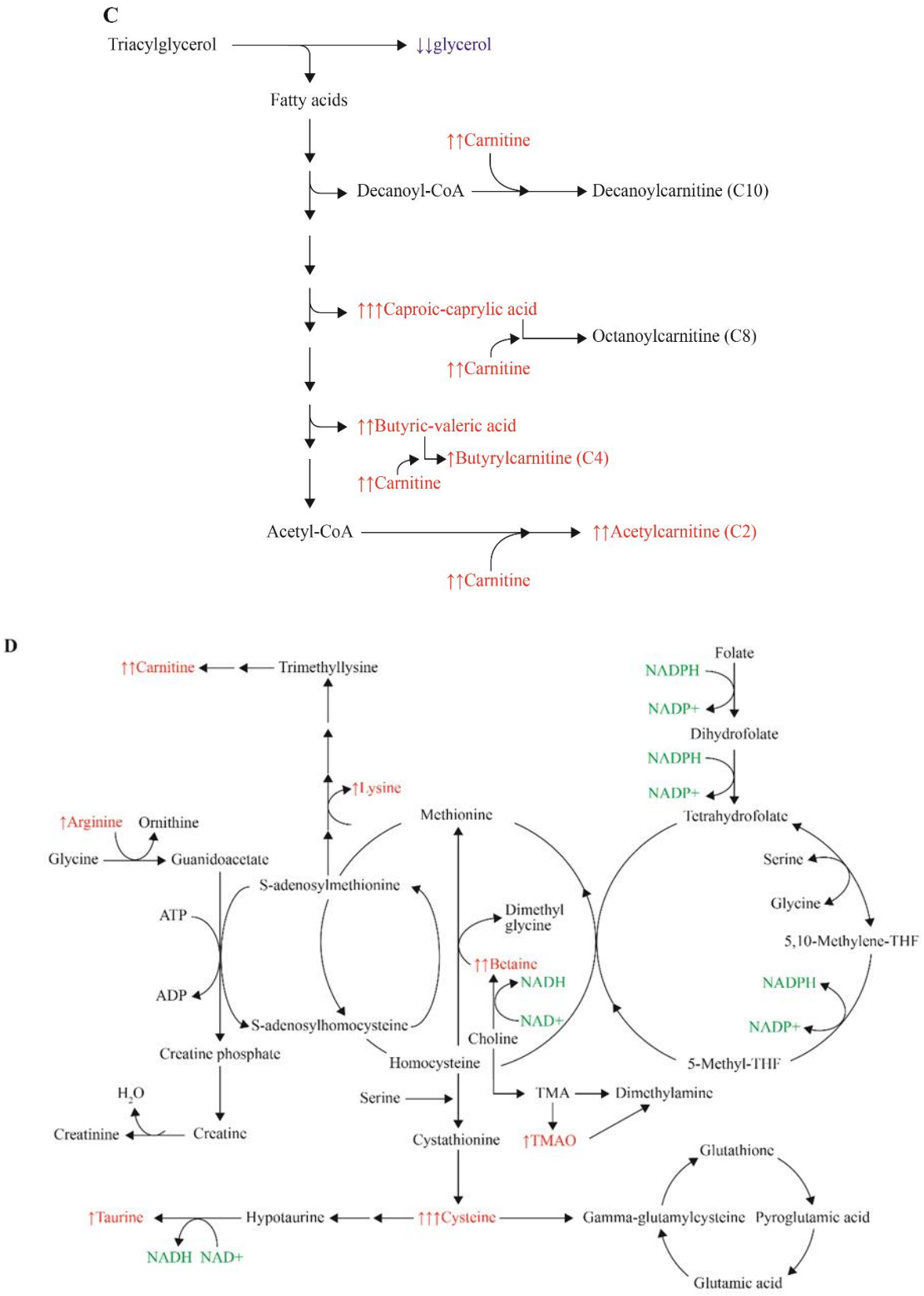

Figure 4.4. Schematic representation of the altered metabolism detected in the MELAS patients compared to healthy controls. A) Altered glucose metabolism, B) protein catabolism, C) lipid catabolism, D) one-carbon metabolism, methylation cycle and the transsulfuration route. Metabolites significantly increased by MELAS (compared to the controls) are indicated in red, those significantly decreased are indicated in blue. ↑ = metabolite is increased (d < 1.0); ↑↑ = moderate increase (d < 1.2); ↑↑↑ = highly increase (d > 1.2) and ↓↓ = moderate decrease (d < 1.2). Cofactor dependent reactions are indicated in green.

4.5 CONCLUSION

We have performed a multi-platform metabolomics investigation on two MELAS cohorts in order to better understand the metabolic alterations caused by the disease. To our knowledge, this is the first multi-platform metabolomics investigation of the MELAS phenotype. By combining the metabolic data sets generated with the multi-platform analytical approach, we were able to cover a larger part of the metabolome, which led to the identification of 36 metabolites (during the exploratory phase) that differed significantly between the patient and control group, compared to the six markers previously reported for the disease (Hall *et al*., 2015). During the validation phase, the 36 selected metabolites were able to separate a validation cohort of two MELAS patients completely from their respective control group.

Upon further investigation of our data, most of the disturbed metabolites could be explained by a redox imbalance caused by a defective OXPHOS system while stalled fatty acid oxidation prevailed as being particularly perturbed in the MELAS phenotype. Furthermore, the intricate web of pathways consisting of the one-carbon metabolism, methylation cycle and trans-sulfuration pathway — previously linked to PEO (Bao *et al*., 2016; Nikkanen *et al*., 2016) – can now, with our data, also be linked to the MELAS phenotype. Although redox imbalance has previously been associated with mitochondrial disease (Brière *et al*., 2004; Khan *et al*., 2014; Naviaux, 2014; Reinecke *et al*., 2012; Smeitink *et al*., 2006), our data confirms the global impact of mitochondrial disease on the metabolism, further contributing to its complexity.

The small number of MELAS patients used in this study (nine MELAS patients for the exploratory phase and only two patients for the validation phase) is a limitation of the study. Larger numbers of patients would have been preferential, although it was not available to this study. Also, all the MELAS patients used in this study had the m.3243A>G mutation – none had any of the numerous other MELAS-causing mutations. Thus the biosignature suggested here is specific for this single phenotype. Although further research is warranted, this study is the first to follow a comprehensive metabolomics analysis approach to identify metabolites altered by the MELAS phenotype. Understanding the metabolic alterations of MELAS could further our understanding of the disease and might lead to better treatment options.

4.6 REFERENCES

Bao, X.R., Ong, S.E., Goldberger, O., Peng, J., Sharma, R., Thompson, D.A., Vafai, S.B., Cox, A.G., Marutani, E., Ichinose, F., Goessling, W., Regev, A., Carr, S.A., Clish, C.B., Mootha, V.K., 2016. Mitochondrial dysfunction remodels one-carbon metabolism in human cells. *eLife*. e10575.

Brière, J., Chrétien, D., Bénit, P., Rustin, P., 2004. Respiratory chain defects: what do we know for sure about their consequences in vivo? *Biochimica et Biophysica Acta (BBA) - Bioenergetics*. 1659 (2), 172–177.

de Laat, P., Koene, S., van den Heuvel, L.P.W.J., Rodenburg, R.J.T., Janssen, M.C.H., Smeitink, J.A.M., 2012. Clinical features and heteroplasmy in blood, urine and saliva in 34 Dutch families carrying the m.3243A > G mutation. *The Journal of Inherited Metabolic Disease*. 35, 1059–1069.

Ellinger, J.J., Chylla, R.A., Ulrich, E.L., Markley, J.L., 2013. Databases and software for NMR-based metabolomics. *Current Metabolomics*. 1 (1), 28-40.

Elshaghabee, F.M., Bockelmann, W., Meske, D., de Vrese, M., Walte, H.G., Schrezenmeir, J., Heller, K.J., 2016. Ethanol Production by Selected Intestinal Microorganisms and Lactic Acid Bacteria Growing under Different Nutritional Conditions. *Frontiers in microbiology*. 7, 47

Esterhuizen, K., van der Westhuizen, F.H., Louw, R., 2017. Metabolomics of mitochondrial disease. *Mitochondrion*. 35, 97-110.

Fiehn, O., Robertson, D., Griffin, J., van der Werf, M., Nikolau, B., Morrison, N., Sumner, L.W., Goodacre, R., Hardy, N.W., Taylor, C., Fostel, J., Kristal, B., Kaddurah-Daouk, R., Mendes, P., van Ommen, B., Lindon, J.C., Sansone, S., 2007. The metabolomics standards initiative (MSI). *Metabolomics*. 3, 175–178.

Gorman, G.S., Schaefer, A.M., Ng, Y., Gomez, N., Blakely, E.L., Alston, C.L., Feeney, C., Horvath, R., Yu-Wai-Man, P., Chinnery, P.F., 2015. Prevalence of nuclear and mitochondrial DNA mutations related to adult mitochondrial disease. *Annals of Neurology*. 77 (5), 753–759.

Goto, Y., Nonaka, I., Horai, S., 1990. A mutation in the tRNA (Leu (UUR)) gene associated with the MELAS subgroup of mitochondrial encephalomyopathies. *Nature*. 348 (6302), 651-653.

Hall, A.M., Vilasi, A., Garcia-Perez, I., Lapsley, M., Alston, C.L., Pitceathly, R.D., McFarland, R., Schaefer, A.M., Turnbull, D.M., Beaumont, N.J., 2015. The urinary proteome and metabonome differ from normal in adults with mitochondrial disease. *Kidney International*. 87 (3), 610–622.

Kami, K., Fujita, Y., Igarashi, S., Koike, S., Sugawara, S., Ikeda, S., Sato, N., Ito, M., Tanaka, M., Tomita, M., 2012. Metabolomic profiling rationalized pyruvate efficacy in cybrid cells harboring MELAS mitochondrial DNA mutations. *Mitochondrion*. 12 (6), 644–653.

Khan, N.A., Auranen, M., Paetau, I., Pirinen, E., Euro, L., Forsström, S., Pasila, L., Velagapudi, V., Carroll, C.J., Auwerx, J., Suomalainen, A., 2014. Effective treatment of mitochondrial myopathy by nicotinamide riboside, a vitamin B3. *EMBO Molecular Medicine*. 6 (6), 721-731.

Manwaring, N., Jones, M.M., Wang, J.J., Rochtchina, E., Howard, C., Mitchell, P., Sue, C.M., 2007. Population prevalence of the MELAS M.3243A>G mutation. *Mitochondrion*. 7 (3), 230-233.

Munnich, A., Rötig, A., Chretien, D., Saudubray, J., Cormier, V., Rustin, P., 1996. Clinical presentations and laboratory investigations in respiratory chain deficiency. *The European Journal of Pediatrics*. 155, 262–274.

Naviaux, R.K., 2014. Metabolic features of the cell danger response. *Mitochondrion*. 16, 7–17.

Nikkanen, J., Forsström, S., Euro, L., Paetau, I., Kohnz, R.A., Wang, L., Chilov, D., Viinamäki, J., Roivainen, A., Marjamäki, P., 2016. Mitochondrial DNA replication defects disturb cellular dNTP pools and remodel one-carbon metabolism. *Cell Metabolism*. 23 (4), 635–648.

Pavlakis, S.G., Phillips, P.C., DiMauro, S., De Vivo, D.C., Rowland, L.P., 1984. Mitochondrial myopathy, encephalopathy, lactic acidosis, and strokelike episodes: a distinctive clinical syndrome. *Annals of Neurology*. 16 (4), 481-488.

Reinecke, C.J., Koekemoer, G., van der Westhuizen, F.H., Louw, R., Lindeque, J.Z., Mienie, L.J., Smuts, I., 2012. Metabolomics of urinary organic acids in respiratory chain deficiencies in children. *Metabolomics*. 8 (2), 264–283.

Ruiz-Pesini, E., Lott, M.T., Procaccio, V., Poole, J.C., Brandon, M.C., Mishmar, D., Yi, C., Kreuziger, J., Baldi, P., Wallace D.C., 2007. An enhanced MITOMAP with a global mtDNA mutational phylogeny. *Nucleic Acids Research*. 35, 823–828.

Scaglia, F., Northrop, J.L., 2006. The mitochondrial myopathy encephalopathy, lactic acidosis with stroke-like episodes (MELAS) syndrome: a review of treatment options. *CNS Drugs*. 20 (6), 443-464.

Schaefer, A.M., McFarland, R., Blakely, E.L., He, L., Whittaker, R.G., Taylor, R.W., Chinnery, P.F. Turnbull, D.M., 2007. Prevalence of mitochondrial DNA disease in adults. *Annals of Neurology*. 63 (1), 35-39.

Smeitink, J.A., Zeviani, M., Turnbull, D.M., Jacobs, H.T., 2006. Mitochondrial medicine: a metabolic perspective on the pathology of oxidative phosphorylation disorders. *Cell Metabolism*. 3 (1), 9–13.

Venkataraman, A., Rosenbaum, M.A., Werner, J.J., Winans, S.C. Angenent, L.T., 2014. Metabolite transfer with the fermentation product 2,3-butanediol enhances virulence by Pseudomonas aeruginosa. *The ISME journal*. 8 (6), 1210-1220.

Venter, L., Lindeque, Z., van Rensburg, P.J., van der Westhuizen, F., Smuts, I., Louw, R., 2015. Untargeted urine metabolomics reveals a biosignature for muscle respiratory chain deficiencies. *Metabolomics.* 11 (1), 111–121.

Venter, L., Loots, D.T., Mienie, L.J., Jansen van Rensburg, P.J., Mason, S., Vosloo, A., Lindeque, J.Z., 2018. The cross-tissue metabolic response of abalone (Haliotis midae) to functional hypoxia. *Biology open*. 7 (3) 10.1242/bio.031070.

4.7 SUPPLEMENTARY INFORMATION

4.7.1 URINE QUALITY CONTROL SAMPLE

Quality control (QC) sample were prepared by pooling equal amounts of urine from all of the patient as well as control samples. Theses pooled urine QC sample were then aliquoted into smaller volumes, stored – 80 °C until use and were prepared in the same manner as the samples. For GC-MS analyses two QC samples were analyzed in the beginning of each batch and then after every 10 samples. For NMR analyses only one QC in the beginning of the batch, and for the LC analyses (targeted and untargeted) three in the beginning of the batch, each of them twice, and then after every 5 samples. Creatinine was determined by using the QuantiChromTM Creatinine Assay Kit from BioAssay Systems. Osmolality was determined by Ampath Laboratories on the Advanced Osmometer (IEPSA Diagnostics, South Africa).

4.7.2 URINE METABOLOMIC ANALYSES

4.7.2.1 Gas chromatography mass spectrometry (GC-MS)

For untargeted GC-MS analyses an adapted version of a minimal sample preparation method published by Venter el al., 2015 was used. Sample aliquots, which were stored at -80°C, were thawed overnight at 4°C and centrifuged at 15 700 x g at room temperature for 2 minutes to remove any crystals. A calculated volume of each sample (totaling 0.25 µmoles of creatinine) was transferred into clean vials. To each sample, 50 µL 3-phenylbutyric acid (end concentration 50 mg/L) was added. Samples were then evaporated under a stream of nitrogen gas at 37 ˚C. Evaporated samples were derivatized using a two-step derivatization process. First samples were oximated by adding 50 µL of methoxyamine HCl (20 mg/mL pyridine), after which it was incubated at 60°C for 60 minutes. After the oximation step, samples were silylated by adding 50 µL BSTFA containing 1 % TMCS after which they were again incubated for 60°C for 60 minutes. Derivatized samples were then transferred to vials with flat bottom inserts.

Samples were analyzed on a GC-TOF-MS-system consisting of an Agilent 7890 GC system coupled to a Leco Pegasus HT mass analyzer and an Agilent 7693 auto sampler, with helium gas being used as carrier gas. Metabolites were separated using a Restek RXi® - 5 column (10 m X 0.2 mm X 0.18 µm). 10 µL of sample was injected per run in a 1:10 split mode at a flow rate of 1.50 mL/min, with front inlet temperature being kept at a constant

250°C. To enhance separation of metabolites the oven temperature was ramped from 70°C to 300°C over a period of 13 minutes. The initial oven temperature started at 70°C and was increased to 120 °C at a flow rate of 7°C/min. Thereafter the temperature was again increased to 230°C at 10°C / min and then to 300°C at 13°C /min. The transfer line was maintained at 225 °C, while the ion source temperature was kept at 200 °C for the entire run. Data was captured with an acquisition rate of 20 spectra (50 – 950 m/z) per second, with the detector voltage kept at 1450 V. Total run time added up to 13 minutes. For extraction of GC-MS data, ChromaTOF (Leco). To identify compounds spectral matching was done by using both a commercial library (NIST11) as well as an in-house created library (Reinecke *et al*., 2012).

4.7.2.2 Targeted LC-MS

Sample aliquots, which were stored at -80°C, were thawed over night at 4°C and centrifuged at 15 700 x g at room temperature for 2 minutes to remove any crystals. A calculated volume for each sample (totaling 0.25 µmoles of creatinine) were transferred into clean vials. To each sample 100, µL of an internal isotope solution containing phenylalanine, methionine valine C4, C8 and C 16 (end concentration 10 mg/L) as well as 50 uL 3-phenylbutyric acid (end concentration 50 mg/L) were added. Samples were then evaporated under a stream of nitrogen gas at 37 ˚C. Samples were then derivatized by adding 300 µL N-butanol:acetyl chloride after which they were incubated for 50 min at 60°C. Samples were then again evaporated under a stream of nitrogen gas at 37 ˚C. To reconstitute samples, 100 µL mobile phase (50% acetonitrile, 50% water) were added to each sample and left at room temperature for 30 minutes to ensure that the evaporated samples was completely dissolved. The samples were then vortexed and transferred to vials with tapered inserts.

Samples were analyzed on 1290 infinity LC from the 1200 infinity series connected to a 6460 triple quadrupole mass analyzer (Agilent Technologies, Santa Clara, CA, USA) in positive ionization mode. The sample injection volume was 5 µL which was separated on a C18 column (ZORBAX SB-Aq, 2.1 x 150 mm, 3.5 µm, Agilent Technologies, Santa Clara, CA, USA), using a flow rate of 0.2 mL/min with mobile phases A (Milli-Q water and 0.1% formic acid) and B (acetonitrile and 0.1 % formic acid). To enhance separation a mobile phase gradient was used. Samples were analyzed in multiple reaction monitoring mode (MRM) for maximum sensitivity, with specific precursor and product ions for the various amino acids and carnitines being monitored. Gas temperature was kept at 300 °C, with a flow rate of 7.5 L/min and a capillary voltage of 3500 V. Total run time added up to 33 minutes, which included a post run time of 10 minutes.

4.7.2.3 Nuclear magnetic resonance (NMR) spectroscopy

For NMR analyses, 500 µL urine aliquots were thawed over night at 4°C and centrifuged at room temperature for 5 minutes at 12 000 x g. After the samples were centrifuged, 450 µL were aliquoted into a new micro-centrifuge tube. To the aliquoted samples 50 µL NMR buffer solution (pH 7.4, KH2PO4 with TSP, in D2O) were added. Samples were vortexed and transferred into standard 5-mm NMR tubes.

Analyses were performed at 500 MHz on a Bruker Avance III HD NMR spectrometer (Bruker Biospin, Rheinstetten, Germany), fitted with a triple resonance inverse (TXI) 1H {15N, 13C} probe head as well as x, y, z gradient coils. 1H spectra was obtained 28 transients in 32K data points, with a spectral width of 6002 Hz. Water resonance was pre-saturated by single-frequency irradiation with a relaxation delay of 4 seconds, and a 90° excitation pulse of 8 µs. Automatic shimming occurred on the deuterium signal. Resonance widths for both the TSP and metabolite peaks were less than 1 Hz. Automatic Fourier transformation as well as phase and baseline correction was done. For NMR spectral processing Bruker Topspin, and for identification and quantification Bruker AMIX (Ellinger *et al*., 2013) was used.

4.7.2.4 Untargeted liquid chromatography – ion mobility – mass spectrometry (LC-IM-MS)

A calculated volume for each sample (totaling 0.25 µmoles of creatinine) were transferred into clean vials. To each sample 100, µL of an internal isotope solution containing stable isotopes for phenylalanine, methionine, valine, C4-, C8- and C16-carnitines (end concentration 10 mg/L) as well as 50 uL 3-phenylbutyric acid (end concentration 50 mg/L) were added and then dried under a stream of nitrogen gas. To reconstitute samples, 100 µL mobile phase (50% acetonitrile, 50% water) were added to each sample and left at room temperature for 30 minutes to ensure that the evaporated samples was completely dissolved. The samples were then vortexed and transferred to vials with tapered inserts.

Samples were also analyzed on the Synapt G2-Si (hybrid ion mobility-MS system) (Waters) containing an Acquity UPLC system equipped with ESI source. Five µL sample was injected and separated on a Waters T3 column (2.1 x 100 mm, 1.8 µm) kept at 30 °C, using water with 1 % formic acid as mobile phase A and acetonitrile with 1 % formic acid as mobile phase B. The mobile phase gradient reported elsewhere (Venter *et al*., 2018) were used for LC separation. The nebulization gas was set to 650 L/min at a temperature of 500°C, and the cone gas was set to 30 L/min. The capillary voltage and cone voltage were set at 2000 V

and 30 V, respectively. The Q-TOF acquisition rate was 0.1 s, with argon used as the collision gas at a pressure of 7.066 × 10−3 Pa. Data was captured in HDMSe mode where the collision-induced dissociation (CID) energy for the first (low energy) channel was set at 0 V and those for the second (high energy) channel was set to ramp between 10 and 40 V. Leucine-encephalin (m/z 556.2771 in positive and 554.2615 in negative ionization) was used as lock mass to monitor (and correct) accurate mass measurements in positive and negative ionization modes. Collision cross section (CCS) values were automatically calculated from the ion mobility drift time based on a poly-alanine calibration. Progenesis QI (Nonlinear Dynamics) was used to process the data and to identify compounds using several public databases.

4.7.3 DATA PRE-PROCESSING, NORMALIZATION AND EXTRACTION

The extracted GC-MS, LC-QQQ as well as NMR data sets were inspected for between-batch effects occurring. No significant batch effects could be observed in any of the data sets, therefore no batch corrections were applied. For normalization, each data set was normalized against its own internal standard. The data was then normalized to the creatinine concentration as determined using the QuantiChromTM Creatinine Assay Kit).

The three, normalized datasets were then combined to generate a single data matrix. Using this combined data set, an 80% zero filter rule was applied, where a metabolite had to be present in 80% of the controls and/or patients sample, otherwise it was removed from the data set. Next, zero values were replaced by half of the lowest value in the data set after which it was log transformed. This log transformed data set was then used for all further statistical analyses (Student t-test, effect size and PCA).

Chapter 5

5

One mutation, three phenotypes: a metabolic comparison of MELAS, MIDD and myopathy caused by the m.3243A>G mutation

5.1 INTRODUCTION

The m.3243A>G mitochondrial DNA (mtDNA) mutation is one of the most common mitochondrial disease (MD) causing mutations, with population studies indicating a carrier rate as high as 1:400 (Manwaring *et al*., 2007). This point mutation affects the MT-TL1 gene, substituting adenine with guanine at position 3243 on the mtDNA. As a leucine tRNA encoding gene, a mutation in this gene results in the incorporation of incorrect amino acids in the subunits of the OXPHOS system encoded by the mtDNA (Kami *et al*., 2012; Scaglia and Northrop, 2006). The consequence is a dysfunctional OXPHOS system, which can have catastrophic physiological effects (Finsterer, 2007).

The m.3243A>G mutation was initially described in the mitochondrial encephalomyopathy, lactic acidosis, and stroke-like episodes (MELAS) syndrome (Goto *et al*., 1990). However, with the improvement of analytical and diagnostic techniques over the years, phenotypes have progressively been linked to this mutation (Manwaring *et al*., 2007; Scaglia and Northrop, 2006). Patients of all ages are affected by this mutation, resulting in the manifestation of a wide range of symptoms, varying in severity (Kaufmann *et al*., 2009). Patients harboring the m.3243A>G mutation can either be classified as asymptomatic (manifestation of no symptoms - dormant carriers), non-syndromic (manifestation of a number of symptoms, not associated with a specific phenotype) and then finally syndromic (manifestation of specific sets of symptoms associated with a specific phenotype) (Finsterer, 2007). The latter includes phenotypes such as MELAS, maternally inherited diabetes and deafness (MIDD), progressive external ophthalmoplegia (PEO), Leigh syndrome (LS), myoclonus epilepsy with ragged red fibers (MERRF), Kearns-Sayre syndrome (KSS) and floppy infant syndrome (Finsterer, 2007; Manwaring *et al*., 2007; Scaglia and Northrop, 2006).

Although the m.3243A>G mutation has been investigated for many years, the question still remains why do patients, harboring the same mutation, present with such a broad spectrum of symptoms? Clearly heteroplasmy levels alone cannot explain this phenomenon. In an effort to study this conundrum, Hall *et al*. (2015) investigated metabolic differences between three phenotypes (MELAS, MIDD, MERRF) associated with the m.3243A>G mutation, using a single analytical technique (nuclear magnetic resonance (NMR) spectroscopy). The metabolic alterations described by Hall *et al*. (2015) were, however, limited by (1) their use of a single analytical platform with (2) inherent lower sensitivity, compared to mass spectrometry (MS) (Markley *et al*., 2017). It is well known that no single analytical platform can analyze the entire metabolome, due to the complexity of the metabolome and the diverse chemical properties of metabolite classes like lipids, amino acids, peptides, organic acids, vitamins, thiols and carbohydrates (Zhang *et al*., 2012). But since NMR and MS are highly complementary, combining the two techniques will likely improve the overall outcome of a study and enhance the coverage of the metabolome (Marshall and Powers, 2017).

We therefore used a multiplatform metabolomics approach to compare metabolic profiles of groups of patients harboring the m.3243A>G mutation, with different phenotypes – MELAS, MIDD and myopathy. Since we have previously shown that urine is a useful source for disease-specific metabolomics data (Esterhuizen *et al*., 2018), this approach can potentially shed light on the biochemical mechanisms involved in different phenotypes, and ultimately help to answer the question as to why patients, harboring the same mutation, present with such a broad spectrum of symptoms.

5.2 RESULTS AND DISCUSSION

5.2.1 PATIENT AND CONTROL CHARACTERISTICS

In this study we performed a urinary metabolomics investigation on different m.3243A>G mutation phenotypes as well as a control group. Our study design is depicted in Figure. 5.6 and described under Experimental Procedures. Firstly, the cohort (n=86) was divided into different phenotypes: Control (n=29), MELAS (n=9), MIDD (n=30) and Myopathy (n=18). Secondly, samples were randomized and analyzed along with quality control samples (QCs, described in the supplementary document) on three complementary, analytical platforms, LC-MS/MS, GC-TOF-MS and NMR. Due to the complexity of the metabolome (in terms of compound classes and dynamic concentration ranges), no single analytical platform can

analyze the entire metabolome (Zhang *et al*., 2012). Our multiplatform approach enhances the coverage of the metabolome (Marshall and Powers, 2017), therefore increasing the number of metabolites that can be analyzed in the urine samples. Thirdly, the data from each platform were individually pre-processed (inspected for batch effects, normalized to osmolality, 80% zero filter applied, 50% CV filter applied, low variance/noise filter applied and missing value imputation) before the data were log transformed and combined in a single dataset (illustrated in Figure 5.6). Fourthly, the data from each phenotype were separately compared to the control group and univariate statistics (T-test with FDR as well as effect size) were used to identify discriminatory metabolites. Fifthly, these metabolites were used to deduce the metabolic perturbation caused by the m.3243A>G mutation in the respective phenotypes [illustrated using principle component analyses (PCAs) and heat maps]. Lastly, metabolic differences between the disease phenotypes were investigated with analyses of variance (ANOVA) by testing the identified discriminatory metabolites for relative concentration differences between the phenotypes.

Table 5.1 summarizes the characteristics of the patient and control groups and contains valuable information that was taken into consideration during data interpretation. The age of the control, MELAS and myopathy groups did not differ significantly with an average of 34.8, 31.4 and 33.8 years old, respectively. However, the MIDD patient group, with an average age of 50.0 years old was significantly ($p<0.05$) older than the other groups, including the control group. The latter is, however, consistent with literature reporting MIDD having a later onset of symptoms compared to more serious phenotypes such as MELAS (Lorenzoni *et al*., 2015). This difference in age was taken into consideration when interpreting the results. The gender representation per phenotype differed between the groups. But since gender is not a confounding factor in mitochondrial disease (Reinecke *et al*., 2012), this was not considered problematic to our study design. Osmolality, measured as milliosmoles/kg (mOsm/kg) of solvent, resembles the degree to which urine is concentrated or diluted. Evaluation of the urinary osmolality of our three patient groups compared to the control group, revealed no statistical difference (ANOVA, $p>0.05$). This indicated that osmolality was unaffected by the mutation and that it could be used for normalization of the urinary data.

An important factor that had to be taken in consideration was the use of medication and supplementation. In order to obtain a homogenous control group, we excluded any participant as a control that used medication or supplementations prior to sample collection. However, most of the patients were taking some sort of medication and/or supplementation

in order to treat their symptoms. Due to ethical considerations, the use of these medications and supplementations could not be stopped before urine sample collection. Furthermore, excluding patients based on the use of medication and/or supplementation was not considered due to the low number of patients, which would negatively impact the statistical power of the results. Table 5.1 demonstrates that the percentage of patients in a given phenotype taking a specific medication and/or supplementation is relatively low, except for the MELAS group taking antiepileptics (67%) and the MIDD patients taking insulin (73%). Apart from these two, the percentage of patients in each group exposed to one specific medication or supplementation was low, thus not considered to influence the group's metabolic alterations significantly. Also, the data were inspected carefully for metabolites known to be of medication or supplementation origin. These were removed from the dataset before further statistical analyses.

Table 5.1: Characteristics of the patients and healthy controls (means ± standard deviation)

Characteristic	**Controls**	**MELAS**	**MIDD**	**Myopathy**
Total, n	29	9	30	18
Age, y	34.8 ± 19.8	31.4 ± 11.6	50.0 ± 9.6	33.8 ± 14.5
Gender (F=female, M=male)	F=19, M=10	F=3, M=6	F=21, M=9	F=16, M=2
m.3243A>G mutation load in urinary epithelial cells	0	80.6 ± 19.2	58.4 ± 18.6	56.5 ± 24.2
Osmolality (mOsm/kg)	765.6 ± 271.8	570.2 ± 279.5	668.8 ± 205.6	587.8 ± 273.6
Symptoms: Number of patients (and percentage) presenting with symptoms	**Controls**	**MELAS**	**MIDD**	**Myopathy**
Stroke	0	9 (100%)	0	0
Epilepsy	0	7 (78%)	3 (10%)	0
Diabetes	0	5 (56%)	30 (100%)	0
Cardiomyopathy	0	3 (33%)	5 (17%)	1 (6%)
Gastro intestinal complaints	0	7 (78%)	10 (33%)	6 (33%)
Hearing loss	0	9 (100%)	30 (100%)	1 (6%)
Renal failure	0	0	0	0
Medication: Number of patients (and percentage)	**Controls**	**MELAS**	**MIDD**	**Myopathy**
Acetylsalicylic acid	0	1 (11%)	7 (23%)	2 (11%)
Angiotensin Receptor Blockers (ARBs)	0	1 (11%)	1 (3%)	0
Angiotensin-converting-enzyme inhibitor (ACE inhibitor)	0	1 (11%)	10 (33%)	0
Anticoagulant	0	2 (22%)	0	0
Antiepileptic	0	6 (67%)	3 (10%)	2 (11%)
Beta blockers	0	2 (22%)	2 (7%)	1 (6%)
Calcium antagonist	0	1 (11%)	3 (10%)	0
Diuretic	0	1 (11%)	2 (7%)	0

Insulin	0	3 (33%)	22 (73%)	0
Laxative	0	1 (11%)	4 (13%)	4 (13%)
Metformin	0	0	2 (7%)	0
Proton pump inhibitor	0	1 (11%)	1 (3%)	1 (6%)
Psychiatric medication	0	1 (11%)	7 (23%)	4 (13%)
Statin	0	1 (11%)	8 (27%)	0
Sulfanylurea derivative	0	1 (11%)	10 (33%)	0
Vitamins and supplements: Number of patients (and percentage) use	**Controls**	**MELAS**	**MIDD**	**Myopathy**
Arginine	0	2 (22%)	1 (3%)	0
Carnitine	0	1 (11%)	1 (3%)	0
Folic acid	0	1 (11%)	0	0
Riboflavin	0	1 (11%)	1 (3%)	0
Coenzyme Q_{10}	0	2 (22%)	1 (3%)	2 (11%)
Vitamin B	0	1 (11%)	1 (3%)	0
Vitamin C	0	0	1 (3%)	0
Vitamin E	0	0	0	1 (6%)
Vitamins (not specified)	0	0	0	2 (11%)

5.2.2 METABOLIC PERTURBATIONS

The main aim of this study was to investigate why do patients, harboring the same m.3243A>G mutation, present with different phenotypes? After our recent report on the urine metabolome of the MELAS phenotype (Esterhuizen *et al*., 2018), we recognized the potential that urine has to provide us with disease-specific data. Unraveling the metabolic perturbation of each m.3243A>G mutation phenotype might be the first step to ultimately solving the single-mutation-different-phenotype conundrum. Principle component analyses (PCA) on all the data (thus before feature selection) were used to visualize the natural separation of the MELAS, MIDD and myopathy groups, respectively, from the controls (Figure 5.1). Most of the samples from the diseased groups separated from the control samples using principle component analyses (PCA) (Figure 5.1), albeit with some overlap, indicating metabolic differences between the respective phenotypes and controls.

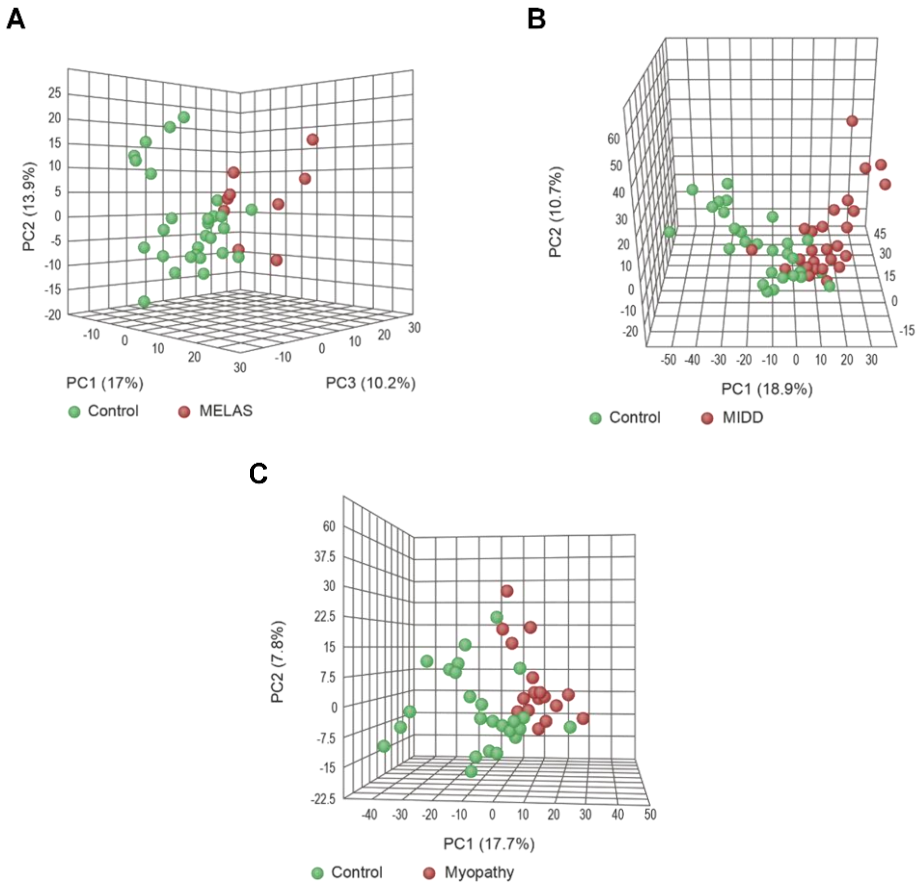

Figure 5.1. PCA score plots of MELAS (A), MIDD (B), and Myopathy (C) patients against Controls. PCAs were performed with all the metabolites detected by the three analytical platforms (after data pre-processing) to illustrate the natural separation of the data; thus, before feature selection.

With univariate statistical analyses (Student's t-test (p value) and effect size (d value)), we were able to identify important metabolites (VIPs) that differed significantly between each of the cohort's phenotypes and the healthy controls (Table 5.2). For the MELAS phenotype, 29 VIPs were discovered, 22 for MIDD and 5 for myopathy. Volcano plots and heat maps (Figure 5.2) were used to visualize the important metabolites detected for each phenotype. From these figures one can not only gather information on which metabolites are increased or decreased, but also to what degree a given metabolite is affected by the disease.

Table 5.2: List of metabolites that differ significantly between m.3243A>G mutation phenotypes and controls.

Phenotype	Metabolite	ID level	t-test *p*	Effect size *d*	Direction	Platform
MELAS	Caproic/caprylic acid	2	<0.001*	1.04	↑	NMR
	Hydroxylamine	3	<0.001*	1.13	↓	GC-TOF-MS
	Pyruvic acid	2	<0.001*	1.48	↓	GC-TOF-MS
	Butyric/valeric/2-hydroxybutyric/3-methyl-2-oxovaleric acid	2	0.001**	0.93	↑	NMR
	Propionylcarnitine	1	0.001**	0.85	↑	LC-MS/MS
	Glycerol	1	0.001**	1.29	↓	GC-TOF-MS
	Glycolic acid	1	0.002**	1.05	↓	GC-TOF-MS
	Acetylcarnitine	1	0.002**	0.88	↑	LC-MS/MS
	6-Azathymine	3	0.004**	1.05	↓	GC-TOF-MS
	Fumaric acid	1	0.004**	1.11	↓	GC-TOF-MS
	Acetic acid	1	0.004**	0.84	↑	NMR
	2,5-Furandicarboxylic acid	3	0.005**	1.13	↓	GC-TOF-MS
	Pseudo uridine	3	0.005**	1.10	↓	GC-TOF-MS
	Sarcosine	1	0.005**	1.01	↓	GC-TOF-MS
	Arabinose	2	0.008*	1.02	↓	GC-TOF-MS
	Glycine	1	0.008*	0.92	↓	LC-MS/MS
	3-Amino-isobutyric acid	3	0.010*	1.00	↓	GC-TOF-MS
	Pyroglutamic acid	1	0.011*	0.98	↓	GC-TOF-MS
	2-Hydroxyglutaric acid	3	0.012*	0.96	↑	GC-TOF-MS
	Threonine	1	0.012*	0.89	↓	LC-MS/MS
	Cystine	1	0.013*	0.96	↓	LC-MS/MS
	Dodecanoylcarnitine	1	0.014*	0.98	↓	LC-MS/MS
	Tyrosine	1	0.015*	0.87	↓	GC-TOF-MS
	4-Amino-butyric acid	1	0.018*	0.84	↓	LC-MS/MS
	4-Pentenoic acid	3	0.018*	0.89	↑	GC-TOF-MS
	Homocysteine	1	0.018*	0.94	↓	LC-MS/MS
	3-Deoxytetronic acid	3	0.019*	0.89	↓	GC-TOF-MS
	Taurine	3	0.024*	0.84	↑	GC-TOF-MS
	Cystathionine	1	0.025*	0.81	↓	LC-MS/MS
Phenotype	**Metabolite**	**ID level**	**t-test *p***	**Effect size *d***	**Direction**	**Platform**
MIDD	Myo-Inositol	2	<0.001*	1.39	↑	GC-TOF-MS
	Glycolic acid	1	<0.001*	1.40	↓	GC-TOF-MS
	1,2-Ethandiol	3	<0.001*	1.35	↓	GC-TOF-MS
	Sarcosine	1	<0.001*	1.39	↓	GC-TOF-MS
	2-Hydroxyglutaric acid	3	<0.001*	1.04	↑	GC-TOF-MS
	3,6,9,12,15,18-hexaoxaicosane-1,20-dioate	3	<0.001*	0.98	↓	GC-TOF-MS

	4-Pentenoic acid	3	<0.001*	0.98	↑	GC-TOF-MS
	Homocysteine	1	<0.001*	1.12	↓	LC-MS/MS
	2,5-Furandicarboxylic acid	3	<0.001*	1.12	↓	GC-TOF-MS
	Glucose	1	<0.001*	0.88	↑	NMR
	Pseudo uridine	3	<0.001*	1.10	↓	GC-TOF-MS
	Aucubin	2	<0.001*	0.90	↓	GC-TOF-MS
	Arabinose	2	<0.001*	1.11	↓	GC-TOF-MS
	2-Ethylhydracrylic acid	3	<0.001*	0.87	↑	GC-TOF-MS
	Pyroglutamic acid	1	<0.001*	1.03	↓	GC-TOF-MS
	Vanillylmandelic acid	3	<0.001*	0.94	↓	GC-TOF-MS
	Glucuronic acid	2	<0.001*	0.94	↑	GC-TOF-MS
	4-Nitrophenyl-galacturonide	3	<0.001*	0.82	↑	GC-TOF-MS
	Dodecanoylcarnitine	1	0.001**	0.88	↓	LC-MS/MS
	2-Hydroxyisovaleric acid	2	0.001**	0.91	↑	GC-TOF-MS
	4-Deoxythreonic acid	2	0.001**	0.82	↓	GC-TOF-MS
	3-Hydroxyisobutyric acid	1	0.001**	0.86	↑	GC-TOF-MS
Phenotype	**Metabolite**	**ID level**	**t-test *p***	**Effect size *d***	**Direction**	**Platform**
Myopathy	2-Hydroxyglutaric acid	3	<0.001*	1.08	↑	GC-TOF-MS
	2-Ethylhydracrylic acid	3	0.003*	0.81	↑	GC-TOF-MS
	4-Pentenoic acid	3	0.003*	0.85	↑	GC-TOF-MS
	Glycolic acid	1	0.005*	0.89	↓	GC-TOF-MS
	Creatine	1	0.010*	0.80	↑	LC-MS/MS

Confidence level of metabolite identities according to the ranking system proposed by Schymanski *et al*. (2014). ** FDR-corrected p value of < 0.05. * FDR-corrected p value of < 0.10.

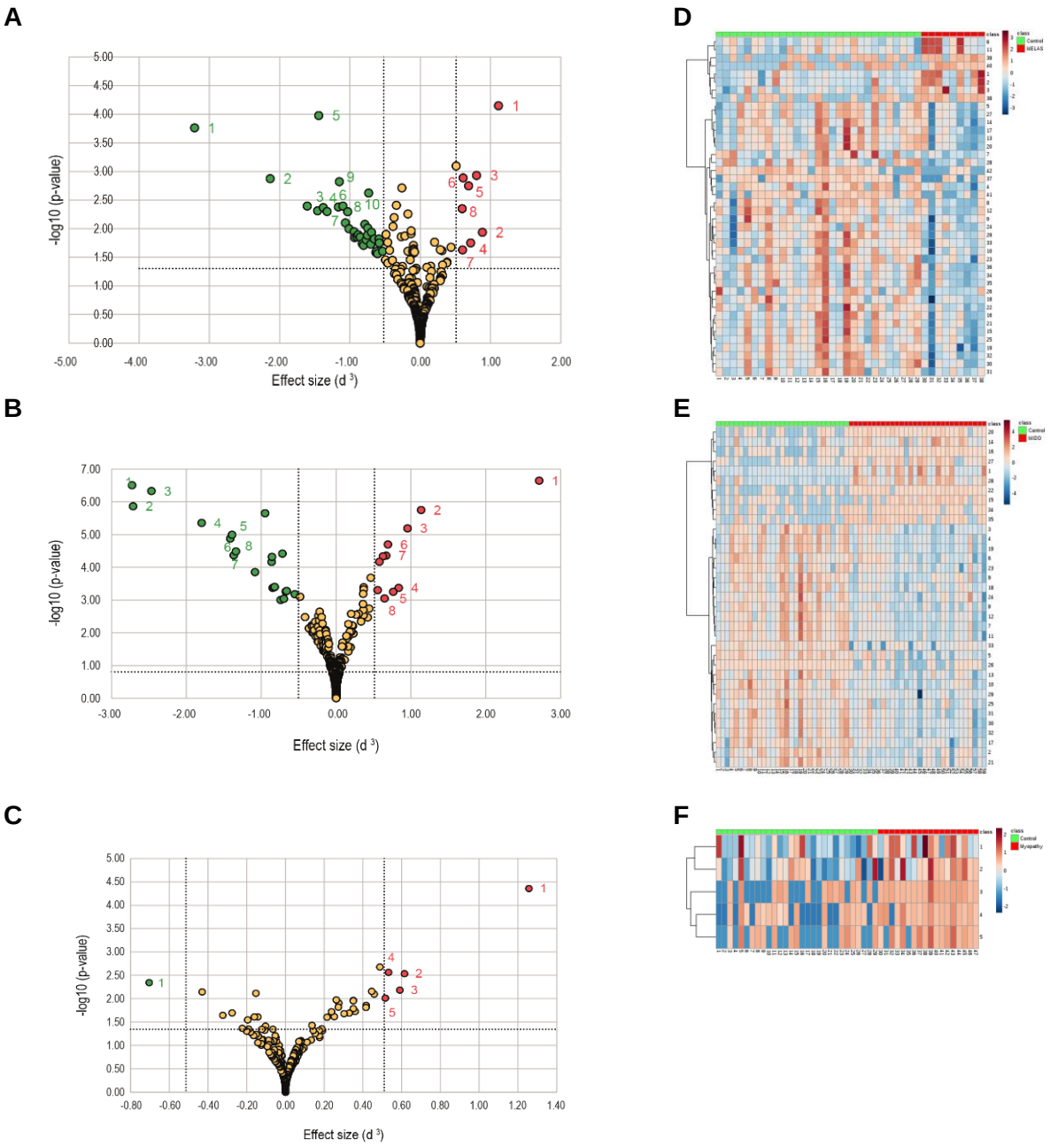

Figure 5.2. Volcano plots (A-C) and heat maps (D-F) depicting statistically significant metabolites that discriminate the MELAS (A&D), MIDD (B&E) and myopathy (C&F) patients from the controls. A) MELAS vs controls: Increased (RED): 1) caproic/caprylic acid, 2) 2-hydroxyglutaric acid, 3) butyric/valeric/2-hydroxybutyric/3-methyl-2-oxovaleric acid, 4) 4-pentenoic acid, 5) acetylcarnitine, 6) propionylcarnitine, 7) taurine, 8) acetic acid. Decreased (GREEN): 1) pyruvic acid, 2) glycerol, 3) carbamate, 4) 2,5-furandicarboxylic acid, 5) hydroxylamine, 6) fumaric acid, 7) pseudo uridine, 8) 6-azathymine, 9) glycolic acid, 10) arabinose. **B) MIDD vs controls**: Increased (RED): 1) myo-inositol, 2) 2-hydroxyglutaric acid, 3) 4-pentenoic acid, 4) glucuronic acid, 5) 2-hydroxyisovaleric acid, 6) glucose, 7) 2-ethylhydracrylic acid, 8) 3-hydroxyisobutyric acid. Decreased (GREEN): 1) glycolic acid, 2) sarcosine, 3) 1,2-ethandiol, 4) 3-methylphenol, 5) 2,5-furandicarboxylic acid, 6) homocysteine, 7) arabinose, 8) pseudo uridine. **C) Myopathy vs controls**. Increased (RED): 1) 2-hydroxyglutaric acid, 2) 4-pentenoic acid, 3) 3-methylphenol, 4) 2-ethylhydracrylic acid, 5) creatine. Decreased (GREEN): 1) glycolic acid

5.2.2.1 Common metabolic traits of the m.3243A>G mutation

The first question that we asked in this metabolomics investigation was "*do the different phenotypes have any kind of similarity in their metabolic response to the mutation?*" Secondly we asked "*can any phenotype-specific metabolic perturbations be identified from the data?*" A Venn diagram (Figure 5.3) was thus used to identify important metabolites that are affected in more than one phenotype. Commonly affected in all three phenotypes (illustrated in Figure. 5.4A-C), were 2-hydroxyglutaric acid, glycolic acid and 4-pentenoic acid. While 2-hydroxyglutaric acid and 4-pentenoic acid were elevated in the patients, compared to the controls, and glycolic acid was markedly decreased in all the phenotypes, compared to the controls.

Figure 5.3. Venn diagram used to identify VIPs that are affected in more than one phenotype. Only three metabolites were affected in all three phenotypes (2-hydroxyglutaric acid, 4-pentenoic acid and glycolic acid). 2-Ethylhydracrylic acid was elevated in MIDD and myopathy. An additional seven metabolites (pseudo-uridine, sarcosine, arabinose, pyroglutamic acid, dodecanoylcarnitine, homocysteine and 2,5-furandicarboxylic acid) were affected in both MELAS and MIDD.

The conversion of 2-ketoglutatric acid (Figure 5.4A), a critical tricarboxylic acid (TCA) cycle intermediate, to 2-hydroxyglutaric acid (2-HG), is driven by a higher NADH/NAD+ ratio in mitochondrial disease as illustrated in Figure 5.5A. Although 2-HG acid has previously been identified as perturbed in mitochondrial disease (Bao *et al*., 2016, Reinecke *et al*., 2012, Smuts *et al*., 2013), our data reconfirm this perturbed metabolite in all phenotypes investigated, hence we identify 2-HG as a possible marker for mitochondrial disease that should be further investigated. But, 2-HG is not simply formed and excreted, it also plays a critical role in the metabolism – 2-HG actively inhibits ATP synthase (complex V of the OXPHOS system) as well as the mammalian target of rapamycin (mTOR) pathway

(Chin *et al*., 2014). Since mTOR can be considered a master regulator in the cell (it integrates nutrients, growth factors and cellular energy status to control protein synthesis, cell growth, survival and metabolism), even a small inhibition might have a huge effect on the cell. Inhibition of mTOR has been shown to alleviate mitochondrial disease in a mouse model of Leigh syndrome (Johnson *et al*., 2013). Thus the effect of elevated 2-HG on a cell suffering low energy levels (mitochondrial disease) is of notable interest for further investigations. However, 2-HG also inhibits ATP synthase, actively enhancing the cell's energy crisis. Furthermore, as 2-HG accumulates, it initiates a negative feedback loop to limit additional NADH production by glycolysis. Thus 2-HG, a mitochondrial metabolite, actively inhibits cytoplasmic NADH production to modulate cellular redox homeostasis. Therefore our finding on the elevated 2-HG in all three m.3243A>G mutation phenotypes warrants further research on the role of this critical metabolite in mitochondrial disease.

Although decreased levels of glycolic acid (Figure 5.4B) have previously been reported in urine of MELAS patients (Hall *et al*., 2015), our study found this metabolite highly decreased in all three phenotypes investigated: MELAS, MIDD and myopathy. Previously we have linked this metabolite to gut microbial metabolism (Esterhuizen *et al*., 2018), but now hypothesize that this metabolite could rather be a product of alanine-glyoxylate transaminase (E.C.2.6.1.44). This enzyme uses pyruvate and glycine to form alanine and glyoxylate. The formed glyoxylate could then be degraded to glycolic acid (Figure. 5.5B).

4-Pentenoic acid could only be allocated a level three identity based on the classification system of Schymanski *et al*. (2014), thus there exists doubt about the true identity of this metabolite. Although the metabolite was significantly elevated in all three phenotypes (Figure 5.4C), more research is warranted to correctly identify this metabolite, thus we can only speculate about the involvement of the metabolite in the altered metabolism observed in the m.3243A>G mutation phenotypes. Currently we hypothesize that this might be a fragment from a larger fatty acid, but this remains to be determined experimentally.

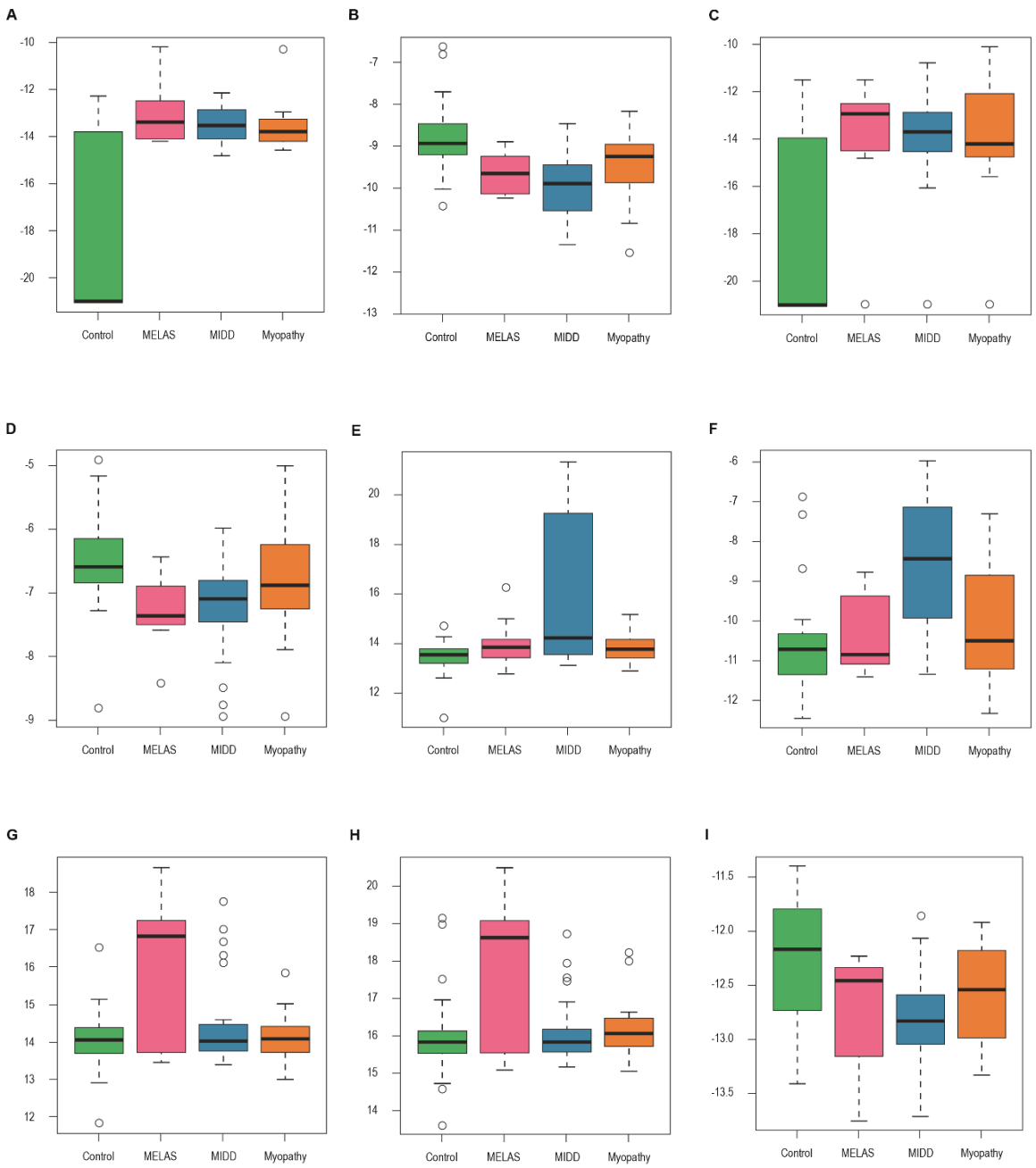

Figure 5.4. Quantitative profiling of selected metabolites. Box plots showing the median, lower and upper quartiles, as well as the minimum and maximum values. The data is expressed in arbitrary units. A) 2-hydroxyglutaric acid; B) glycolic acid; C) 4-pentenoic acid; D) pyroglutamic acid; E) glucose; F) myo-inositol; G) caproic/caprylic acid; H) butyric/valeric/2-hydroxybutyric/3-methyl-2-oxovaleric acid; I) homocysteine.

Some metabolites were only perturbed in two of the three phenotypes: 2-ethylhydracrylic acid was elevated in the myopathy and MIDD patient groups. This metabolite is known to be affected in mitochondrial disease (Reinecke *et al*., 2012) and is formed from 2-methylbutyryl-CoA, a metabolite in the isoleucine catabolism. Thus, our data indicates that isoleucine catabolism is increased in MIDD and myopathy. Pseudo-uridine, sarcosine, arabinose, pyroglutamic acid, dodecanoylcarnitine, homocysteine and 2,5-furandicarboxylic acid were

commonly affected in the MELAS and MIDD patient groups. Upon investigation of these commonly affected metabolites we were able to link most of these metabolites to possible altered redox status, as these metabolites are directly and indirectly affected by dehydrogenase enzymes. Functioning of dehydrogenase enzymes are controlled by cofactors (NAD+, FADH, NADH, FADH2), which are produced by the TCA cycle. When the OXPHOS system is disrupted due to a mitochondrial disease and flow of electrons along this chain are affected, levels of the cofactors are altered causing a redox imbalance. This redox imbalance then ultimately results in the dysfunction of the dehydrogenase enzymes (Brière *et al*., 2004; Khan *et al*., 2014; Naviaux, 2014; Reinecke *et al*., 2012; Smeitink *et al*., 2006). These results prove that there are indeed metabolic similarities between MELAS, MIDD and myopathy patients suffering from the same mutation (m.3243A>G), from a systemic point of view. However, in comparison to the number of metabolites affected, only a small overlap was seen, which might be attributed to specific tissue mainly affected by the biochemical dysfunction (as well as the cellular response of the affected tissue), contributing differently to the urinary metabolome. Nevertheless, the limited number of metabolites commonly affected by the m.3243A>G mutation support the phenotypic variance found for this mutation; and also highlight the close relationship between metabolome and phenotype (Fiehn, 2002).

5.2.2.2 Metabolic perturbation of MELAS

In comparison with the study of Hall *et al*. (2015) who investigated metabolic differences between three phenotypes associated with the m. 3243A>G mutation (MELAS, MIDD, MERRF), we were able to identify 29 perturbed metabolites in our MELAS patient group compared to the six affected metabolites Hall *et al* identified (N-methylnicotinamide, hippuric acid, creatinine, 4-cresyl sulfate, glycolic acid, 4-hydroxyphenylacetic acid). Although we were able to detect and quantify all six of these metabolites in our study, only glycolic acid was significantly decreased in the urine of our MELAS group, compared to the controls. We did, however, detect a strong metabolic perturbation in the MELAS group, as illustrated in Figure. 5.5. The discrepancy observed between the number of metabolites identified between the two studies and the fact that only one of the previously reported metabolites were altered in our patient group (glycolic acid) can be ascribed to two possible reasons. Firstly, Hall *et al*. (2015) used a single analytical platform (NMR) where as we implemented two additional analytical platforms (LC-MS/MS, GC-TOF-MS), thus enhancing the metabolome coverage (Marshall and Powers, 2017). Secondly, by using MS, with inherent higher sensitivity compared to NMR (Markley *et al*., 2017), we were theoretically able to detect lower metabolite concentrations, thus increasing our dataset. Comparing our list of perturbed metabolites to that reported by Esterhuizen *et al*. (2018) on MELAS patients,

some markers, like lactic acid and alanine, were not statistically perturbed in our study. The main reason for this is the way in which the urinary metabolomics data was normalized. Since urinary creatinine concentrations was previously reported to be affected by mitochondrial disease (Esterhuizen *et al*., 2017), and was significantly affected in our MIDD group, we normalized our data to urinary osmolality instead of creatinine. Since Esterhuizen *et al*. (2018) normalized their data to creatinine, our list of perturbed metabolites could thus not be directly compared to their list.

On closer inspection of the MELAS metabolic perturbation, several pathways were found to be disturbed. Beta-oxidation/fatty acid catabolism (glycerol, dodecanoylcarnitine, acetylcarnitine, caproic acid, propionylcarnitine, acetic acid, butyric acid) as well as an integrated group of pathways consisting of the one-carbon metabolism, methylation and transsulfuration pathway (glycine, taurine, cystathionine, cystine, homocysteine, pyroglutamic acid) were particularly striking. Previous reports hypothesized that beta-oxidation might be stalled in MELAS patients and that this is responsible for the altered levels of beta-oxidation intermediates detected (Esterhuizen *et al*., 2018). However, our data does not support this hypothesis, but rather indicates that fatty acid synthesis might be upregulated. If fatty acid catabolism was increased, increased concentrations of glycerol and long chain fatty acids should have been detected. However, glycerol and dodecanoylcarnitine (C12-carnitine) were strongly reduced in the patients (Figure 5.5A). These two metabolites indicate that fatty acid catabolism was not increased, but rather decreased. Thus, it seems like less triacylglycerols are catabolized to free fatty acids and glycerol. However, caproic acid (medium chain fatty acid), butyric acid (short chain fatty acid), as well as acetylcarnitine, propionylcarnitine and acetic acid were all increased in the MELAS patients. The only logical explanation for this increase is increased mitochondrial fatty acid synthesis. De novo fatty acids synthesis (FAS) in eukaryotes can take place in (at least) two subcellular compartments: in the cytoplasm (FAS1) and in mitochondria (FAS2), while the mitochondrial pathway for FAS is completely independent of the cytosolic FAS apparatus (Hiltunen *et al*., 2009). Although evidence on the eukaryotic system is vague, in fungi, there is good experimental support for the hypothesis that the FAS2 pathway is the sole source of octanoic acid, the precursor required for the production of lipoic acid. Lipoic acid, a potent antioxidant (Padmalayam *et al*., 2009), is an essential cofactor for pyruvate dehydrogenase (PDH), 2-ketoglutarate dehydrogenase as well as the glycine cleavage system (Hiltunen *et al*., 2009). It was shown that homozygous inactivation of the lipoic acid synthase gene in mice cause embryonic lethality, and embryo survival cannot be rescued by supplementing the diet of pregnant mothers with lipoic acid (Yi and Maeda, 2005). Thus, it seems like lipoic acid synthesis is essential for cellular survival. Our data indicates that fatty

acid synthesis is increased in the MELAS patients, and we hypothesize that it is possibly for octanoic acid synthesis, in order to ultimately produce lipoic acid in the mitochondria.

One-carbon metabolism, the methylation cycle and the transsulfuration pathway are also perturbed in the MELAS patients. Lower levels of glycine and homocysteine were detected (methylation cycle) as well cystathionine, cysteine (transsulfuration route) and pyroglutamic acid (note that cysteine was measured in the oxidized form - cystine). A recent study, using flux analyses on Deletor mice, reported glucose-driven de novo serine biosynthesis and directing of the synthesized serine to the transsulfuration pathway to synthesize glutathione (Nikkanen *et al*., 2016). This notion was confirmed in tissue cultures where EtBr-treated T-Rex-293 cells showed increased serine biosynthesis and transsulfuration as a result of mitochondrial DNA depletion (Bao *et al*., 2016), reiterating the connection between the respiratory chain and one-carbon metabolism. But our results of the MELAS patients clearly show reduced transsulfuration (reduced homocysteine, cystationine and cysteine). Therefore, we hypothesize that the methylation cycle in our MELAS patients are stalled in order to generate lipoic acid (Figure. 5.5B). S-adenosylmethionine (SAM) is used by lipoic acid synthase to form lipoic acid and methionine. This hypothesis is quite reasonable if one considers the elevated fatty acid synthesis observed in the MELAS patients. Since lipoic acid is an excellent antioxidant in the mitochondrion, the notion of increased lipoic acid synthesis in mitochondrial disease, and the accompanying interruption of the methylation cycle, is rather plausible. However, this remains to be investigated using a targeted metabolic study, focusing on specific metabolites involved in the methylation cycle, lipoic acid synthesis and transsulfuratio.

A

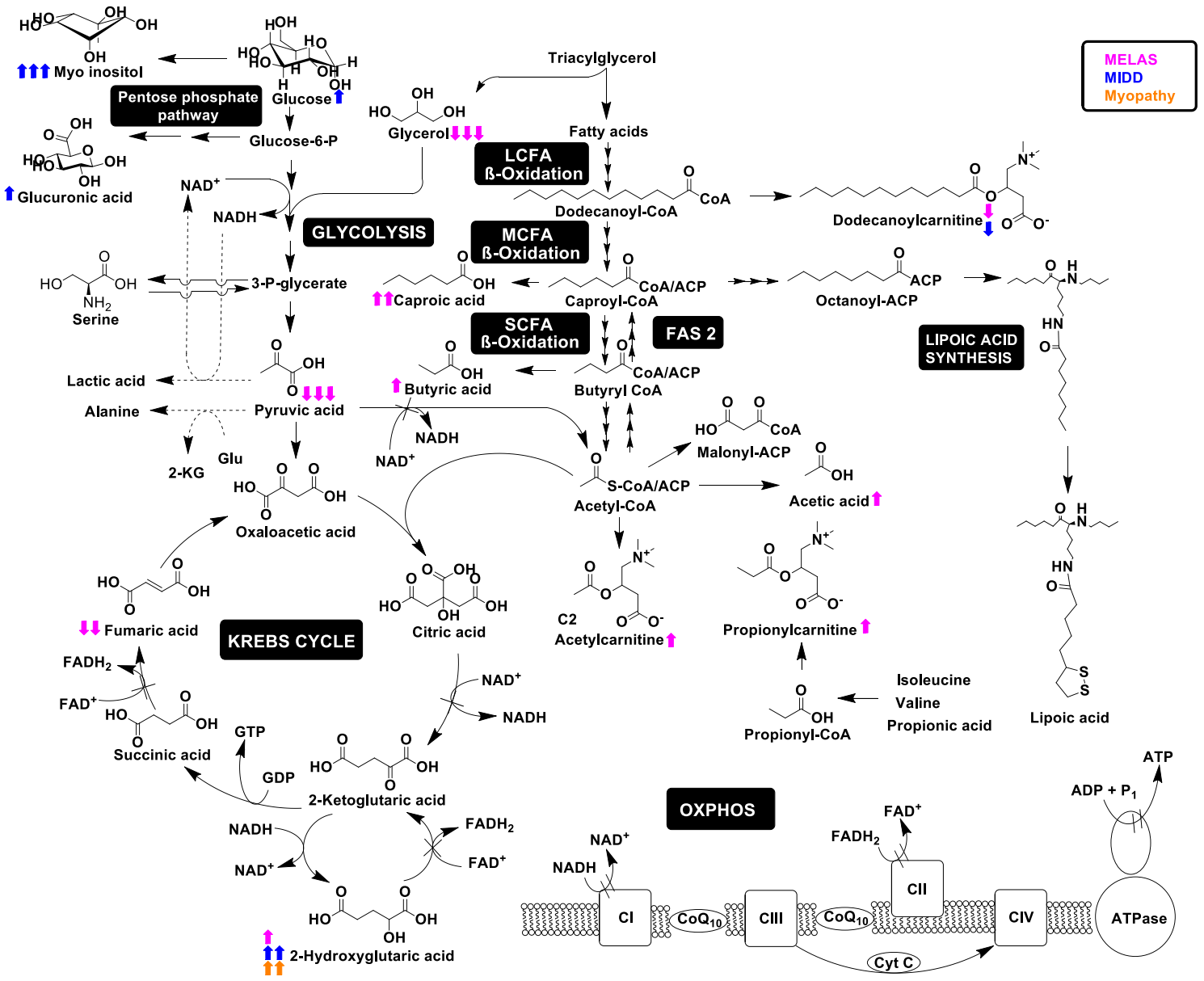
MELAS
MIDD
Myopathy
Myo inositol
Glucose
Pentose phosphate pathway
Glucose-6-P
Glucuronic acid
Triacylglycerol
Glycerol
Fatty acids
LCFA ß-Oxidation
Dodecanoyl-CoA
Dodecanoylcarnitine
NAD+
NADH
GLYCOLYSIS
MCFA ß-Oxidation
3-P-glycerate
Serine
Caproic acid
Caproyl-CoA
Octanoyl-ACP
SCFA ß-Oxidation
FAS 2
LIPOIC ACID SYNTHESIS
Lactic acid
Alanine
Pyruvic acid
Butyric acid
Butyryl CoA
Glu
2-KG
Oxaloacetic acid
Malonyl-ACP
Acetyl-CoA
Acetic acid
Citric acid
C2
Acetylcarnitine
Propionylcarnitine
Fumaric acid
KREBS CYCLE
Isoleucine
Valine
Propionic acid
Propionyl-CoA
Lipoic acid
FADH2
FAD+
Succinic acid
GTP
GDP
2-Ketoglutaric acid
2-Hydroxyglutaric acid
OXPHOS
ATP
ADP + P1
CI
CII
CIII
CIV
ATPase
CoQ10
Cyt C

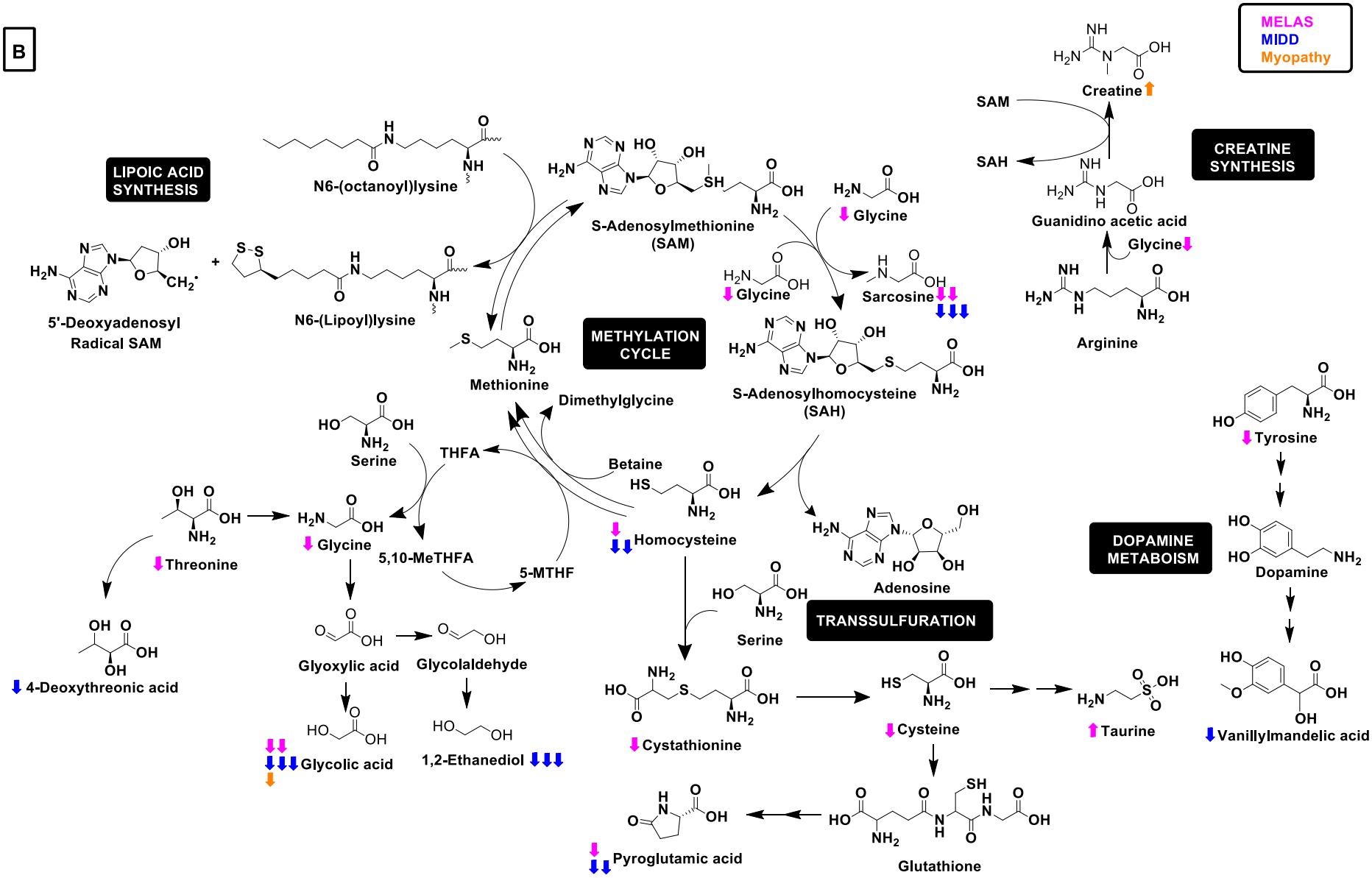
B
MELAS
MIDD
Myopathy
LIPOIC ACID SYNTHESIS
N6-(octanoyl)lysine
5'-Deoxyadenosyl Radical SAM
N6-(Lipoyl)lysine
S-Adenosylmethionine (SAM)
METHYLATION CYCLE
Methionine
Dimethylglycine
Glycine
Sarcosine
S-Adenosylhomocysteine (SAH)
CREATINE SYNTHESIS
Creatine
SAM
SAH
Guanidino acetic acid
Glycine
Arginine
Serine
THFA
Betaine
Homocysteine
Threonine
Glycine
5,10-MeTHFA
5-MTHF
Adenosine
DOPAMINE METABOISM
Tyrosine
Dopamine
Vanillylmandelic acid
TRANSSULFURATION
Serine
4-Deoxythreonic acid
Glyoxylic acid
Glycolaldehyde
Glycolic acid
1,2-Ethanediol
Cystathionine
Cysteine
Taurine
Pyroglutamic acid
Glutathione

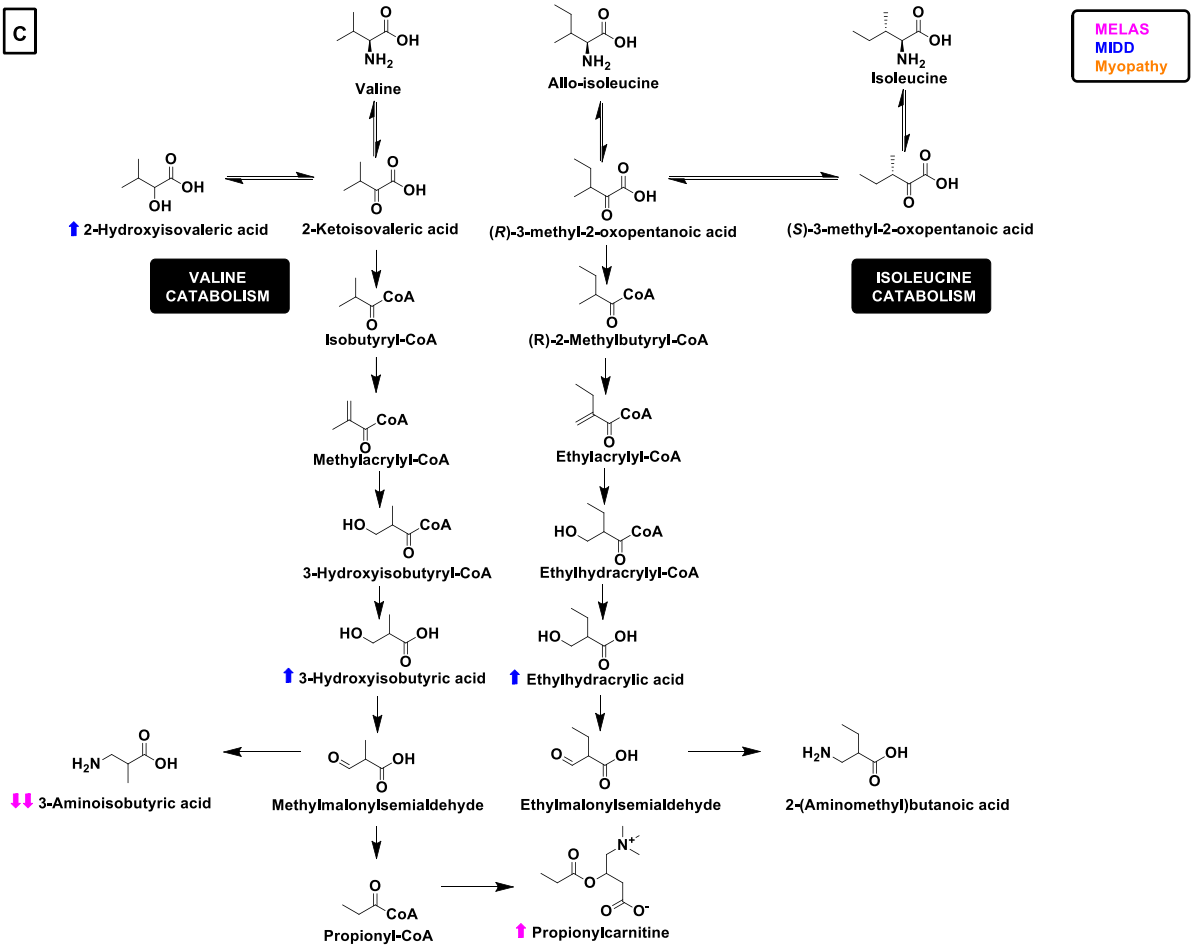

Figure 5.5. Metabolic charts of the perturbed metabolism detected in MELAS, MIDD and myopathy. Metabolites significantly altered in the MELAS group are marked with pink arrows, MIDD with blue arrows and myopathy with orange arrows. ↑ indicates that the relative concentration of the metabolite is increased in the patients, relative to the controls. ↓ indicates that the relative concentration of the metabolite is deceased in the patients, relative to the controls. A single ↑ = metabolite is increased (d < 1.0); ↑↑ = moderate increase (d < 1.2); ↑↑↑ = highly increased (d > 1.2) and, similarly, a single ↓ = metabolite is decreased (d < 1.0); ↓↓ = moderate decrease (d < 1.2); ↓↓↓ = highly decreased (d > 1.2).

5.2.2.3 Metabolic perturbation of MIDD

When comparing our MIDD VIP list to the altered metabolites identified by Hall *et al*. (2015) in their MIDD patients, we were able to identify 22 metabolites compared to their four metabolites (N-methylnicotinamide, hippuric acid, S-methyl-cysteine-sulfoxide, 4-cresyl sulfate) identified in their study. Even though we were able to measure and quantify all four these metabolites, none of them where significantly altered in our MIDD group.

The metabolic profile of the MIDD patients shows a strong perturbation of glucose metabolism, with elevated levels of glucose, myo-inositol and glucuronic acid. This was

expected, since MIDD is characterized by high blood sugar levels (hyperglycemia), resulting from a shortage of the hormone insulin, which regulates the amount of sugar in the blood. Glycolysis is the fundamental pathway for the metabolism of glucose, as well as other various carbohydrates and is also required for other critical functions such as regulation of insulin secretion in the pancreatic β-cells (Guo *et al*., 2012). When blood glucose concentrations increase, it enters the pancreatic β -cell where the plasma membrane is depolarized by closing the ATP-sensitive potassium channel; the latter is controlled by the ATP/ADP ratio. Once this channel has been closed, the calcium concentration will increase allowing insulin containing granules to merge with the plasma membrane. This will ultimately result in the secretion of the insulin to regulate the blood glucose levels. An altered ATP/ADP ratio, as observed in mitochondrial diseases patients, could affect the secretion of insulin, resulting in diabetes and could explain the results seen in our MIDD group (Kwak *et al*., 2010; Maassen at al., 2004). However, 22 of the 30 MIDD patients (73%) included in this study received insulin at the time of sample collection. Thus, the metabolic profile of these patients have to be interpreted with the insulin treatment in mind. But even with insulin treatment, the MIDD group still displayed higher levels of glucose, myo-inositol and glucuronic acid, compared to the controls. Therefore, the insulin treatment was not able to regulate the glucose metabolism to normal levels. But one should keep in mind the age difference between the MIDD patients and the controls. Since the MIDD patients were significantly older than the controls (Table 5.1), this could also have influenced the metabolic alteration observed in the patients.

Sarcosine and homocysteine were again lower in the MIDD patients, similar to that observed in the MELAS patients, indicating an altered methylation cycle in the MIDD group. However, metabolites in the transsulfuration route were not altered, only low pyroglutamic acid was observed (Figure 5.5B). The low pyroglutamic acid is possibly due to the increased use of glutathione as an anti-oxidant, thus less pyroglutamic acid is formed. Nevertheless, we could not demonstrate lower glutathione concentration in the patients, possibly because glutathione is quite unstable and our untargeted metabolomics approach is not optimal for the accurate quantification of glutathione.

Branched-chain amino acid (BCAA) metabolism was also affected in the MIDD patients, with elevated levels of 2-hydroxyisovaleric acid, 3-hydroxyisobutyric acid and 2-ethylhydracrylic acid detected. In addition to the maintenance of glucose homeostasis, insulin plays a major role in the regulation of branched-chain amino acid (BCAA) metabolism (Pisters *et al*., 1992). Thus, the increased valine and isoleucine catabolism we detected in our patients might be due to the patients being insulin resistant, or even from the insulin therapy itself. Lastly, the

lower 4-deoxythreonine levels found in the MIDD patients, have been associated with diabetes before (Kassel *et al*., 1986). Hence, the metabolic profile we detected in the MIDD patients is consistent with that of diabetes patients.

5.2.2.4 Metabolic perturbation of myopathy

For the myopathy patient group, only five important metabolites were detected. Four of these metabolites overlapped with one or more of the other phenotypes; leaving only one, unique metabolite - creatine. Even though only this one metabolite was highlighted, it still indicated the presence of the phosphocreatine shuttle in our myopathy patient group. The phosphocreatine system is a pathway that utilizes the energy generating enzyme creatine kinase to convert creatine into phosphocreatine (PCr), by dephosphorylating ATP into ADP. The latter provides immediate energy to tissues that has a high energy demand, such as skeletal muscle. This is a reversible reaction where ATP can also be generated from PCr and ADP, which allows this system to act as an energy pool for buffering and regeneration of ATP as needed. As this enzyme relies on the ATP/ADP ratio, altered ATP levels could effect this process which could explain the elevated level we detected in our myopathy patients.

5.3 CONCLUSION

A question that remains unanswered in the field of mitochondrial disease, and more specifically with regards to the m.3243A>G mutation, is: "*Why do patients present with different phenotypes although they harbor the same mutation?*" Using a multiplatform analytical approach, we investigated the m.3243A>G mutation from a metabolomics point of view and identified metabolic similarities, as well differences, for all three phenotypes investigated in this study.

In conclusion, our data confirm that there are distinct metabolic / mechanistic differences between the three phenotypes caused by the m.3243A>G mutation. Identifying these metabolic similarities and differences is the first part of the puzzle to ultimately resolve the conundrum why these patients present with such a broad spectrum of symptoms, carrying the same mitochondrial DNA mutation. Understanding this mystery may lead to better diagnostic and treatment options for these patients

5.4 EXPERIMENTAL PROCEDURES

5.4.1 PATIENTS AND ETHICS

For this study we used urine samples from a genetically confirmed m.3243A>G mutation cohort from the Radboud Centre for Mitochondrial Medicine, Nijmegen, The Netherlands. The patients were divided into a MELAS (n=9), MIDD (n=30) or a myopathy group (n=18) as well as healthy controls (n=29). To ensure homogeneity the following samples were excluded: 1) controls that received either medication or supplementation at the time of sample collection; 2) controls with a medical condition (such as diabetes, hypertension, etc.); 3) patients that received an organ transplant (kidney, liver). Due to ethical considerations, treatment (medication and supplementation) of the patients could not be stopped. Characteristics from the patient and control groups are summarized in Table 5.1. The study complied with all Institutional guidelines and terms of the Declaration of Helsinki of 1975 (as revised in 2013) for investigation of human participants. Ethical approval was obtained from the Health Research Ethics Committee (HREC) of the North-West University, South Africa (NWU-00170-13-A1) and by the Ethics Committee of the Nijmegen-Arnhem region of the Netherlands. All the patients, as well as the controls, provided written informed consent for their urine samples to be used for these research purposes.

5.4.2 METABOLIC PROFILING

We used a multiplatform metabolomics approach to investigate the urine samples of patients harboring the same m.3243A>G mutation, but presented with different phenotypes (MELAS, MIDD, myopathy) compared to healthy controls. The different platforms were considered complementary, thus increasing the metabolome coverage. Three analytical platforms were utilized in this study and can be divided into targeted and untargeted approaches. The targeted analyses consisted of liquid chromatography tandem-mass spectrometry (LC-MS/MS) while the untargeted analyses consisted of gas chromatography time-of-flight mass spectrometry (GC-TOF-MS) and nuclear magnetic resonance (NMR) spectroscopy.

5.4.3 DATA MINING AND STATISTICAL ANALYSES

The data from each analytical platform (GC-TOF-MS, LC-MS/MS and NMR) was pre-processed individually before it was merged into a single metabolomics data set (pre-processing details are given in the SI). Since urinary creatinine levels might be affected in mitochondrial disease patients (Esterhuizen *et al*., 2017), the metabolomics data was

normalized against osmolality instead of creatinine. After normalization, the data was log-transformed. To determine discriminatory features/metabolites for each of the phenotypes compared to the healthy controls, univariate statistical methods were implemented. Metabolites had to be statistically (t-test) and practically (effect size; d value of > 0.8) significant before being considered important [analyses performed in Excel 2013 (Microsoft Inc.)]. T-test p-values were evaluated at a 5% and 10% significance level (indicated by ** and * respectively in Table 5.2), after correcting for multiple testing using the Bonferroni-Holm approach (Holm, 1979; McLaughlin & Sainani, 2014). To determine the identity of the important features, the spectral information (NMR), retention time, fragmentation spectra (MS) were matched to in-house and commercial libraries as well as public databases. To identify similarities and statistically significant differences between the different phenotypes, analysis of variance (ANOVA) and post hoc analyses were also incorporated using the list of important metabolites identified for each phenotype. Multivariate analyses (principle component analyses, i.e. PCA) were performed in MetaboAnalyst 3.0 (Xia and Wishart 2016) and used to visualize the natural grouping/separation of the respective groups.

5.4.4 ACKNOWLEDGEMENTS

We would like to thank Prof. L.J. Mienie from the North-West University, Potchefstroom, South Africa, for valuable help with the interpretation of the metabolic data. The research was supported by a grant from the Technology Innovation Agency (TIA, Grant number Metabol. 01), South Africa. The research facilities were provided by the National Metabolomics Platform, North-West University, Potchefstroom Campus, Potchefstroom, South Africa.

5.4.5 SUPPLEMENTAL INFORMATION

Supplemental Information includes Supplemental Experimental Procedures as well as an additional figure.

5.4.6 AUTHOR CONTRIBUTIONS

R.L., M.J., Z.L., F.vdW. and J.S. planned and oversaw the study. K.E., Z.L. and S.M. performed all analytical work. Data mining was performed by R.L., Z.L., S.M. and K.E. The manuscript was written by K.E., R.L. and Z.L., assisted by all the authors.

5.4.7 DECLARATION OF INTERESTS

The authors declare no competing interests. Jan Smeitink is the founding CEO of Khondrion.

5.5 REFERENCES

Bao, X.R., Ong, S.E., Goldberger, O., Peng, J., Sharma, R., Thompson, D.A., Vafai, S.B., Cox, A.G., Marutani, E., Ichinose, F., Goessling, W., Regev, A., Carr, S.A., Clish, C.B., Mootha, V.K., 2016. Mitochondrial dysfunction remodels one-carbon metabolism in human cells. *eLife*. e10575.

Brière, J., Chrétien, D., Bénit, P., Rustin, P., 2004. Respiratory chain defects: what do we know for sure about their consequences in vivo? *Biochimica et Biophysica Acta (*BBA) - Bioenergetics. 1659 (2), 172–177.

Chin, R.M., Fu, X., Pai, M.Y., Vergnes, L., Hwang, H., Deng, G., Diep, S., Lomenick, B., Meli, V.S., Monsalve, G.C., 2014. The metabolite α-ketoglutarate extends lifespan by inhibiting ATP synthase and TOR. *Nature*. 510 (7505), 397.

Esterhuizen, K., van der Westhuizen, F.H., Louw, R., 2017. Metabolomics of mitochondrial disease. *Mitochondrion*. 35, 97-110.

Esterhuizen, K., Lindeque, J.Z., Mason, S., van der Westhuizen, F.H., Suomalainen, A., Hakonen, A.H., Carroll, C.J., Rodenburg, R.J., de Laat, P., Janssen, M.C.H., Smeitink, J.A.M., Louw, R., 2018. A urinary biosignature for mitochondrial myopathy, encephalopathy, lactic acidosis and stroke like episodes (MELAS). *Mitochondrion*. doi: 10.1016/j.mito.2018.02.003.

Fiehn, O., 2002. Metabolomics—the link between genotypes and phenotypes. *Plant Molecular Biology*. 48, 155-171.

Finsterer, J., 2007. Genetic, pathogenetic, and phenotypic implications of the mitochondrial A3243G tRNALeu (UUR) mutation. *Acta Neurologica Scandinavica*. 116 (1), 1-14.

Goto, Y., Nonaka, I., Horai, S., 1990. A mutation in the tRNA (Leu (UUR)) gene associated with the MELAS subgroup of mitochondrial encephalomyopathies. *Nature*. 348 (6302), 651-653.

Guo, X., Li, H., Xu, H., Woo, S., Dong, H., Lu, F., Lange, A.J., Wu, C., 2012. Glycolysis in the control of blood glucose homeostasis. *Acta Pharmaceutica Sinica B*. 2 (4) 358-367.

Hall, A.M., Vilasi, A., Garcia-Perez, I., Lapsley, M., Alston, C.L., Pitceathly, R.D., McFarland, R., Schaefer, A.M., Turnbull, D.M., Beaumont, N.J., 2015. The urinary proteome and metabonome differ from normal in adults with mitochondrial disease. *Kidney Int*. 87 (3), 610–622.

Hiltunen, J.K., Schonauer, M.S., Autio, K.J., Mittelmeier, T.M., Kastaniotis, A.J., Dieckmann, C.L., 2009. Mitochondrial fatty acid synthesis type II: more than just fatty acids. *The Journal of Biological Chemistry*. 284 (14), 9011-9015.

Holm, S., 1979. A Simple Sequentially Rejective Multiple Test Procedure. *Scandinavian Journal of Statistics*. 6 (2), 65-70.

Johnson, S.C., Yanos, M.E., Kayser, E.B., Quintana, A., Sangesland, M., Castanza, A., Uhde, L., Hui, J., Wall, V.Z., Gagnidze, A., Oh, K., Wasko, B.M., Ramos, F.J., Palmiter, R.D., Rabinovitch, P.S., Morgan, P.G., Sedensky, M.M., Kaeberlein, M., 2013. mTOR inhibition alleviates mitochondrial disease in a mouse model of Leigh syndrome. *Science*. 342 (6165), 1524-1528.

Kami, K., Fujita, Y., Igarashi, S., Koike, S., Sugawara, S., Ikeda, S., Sato, N., Ito, M., Tanaka, M., Tomita,M., 2012. Metabolomic profiling rationalized pyruvate efficacy in cybrid cells harboring MELAS mitochondrial DNA mutations. *Mitochondrion*. 12 (6), 644–653.

Kassel, D., Martin, M., Schall, W., Sweeley, C., 1986. Urinary metabolites of L-threonine in type 1 diabetes determined by combined gas chromatography/chemical ionization mass spectrometry. *Biological mass spectrometry*. 13 (10), 535-540.

Kaufmann, P., Engelstad, K., Wei, Y., Kulikova, R., Oskoui, M., Battista, V., Koenigsberger, D.Y., Pascual, J.M., Sano, M., Hirano, M., 2009. Protean phenotypic features of the A3243G mitochondrial DNA mutation. *Archives of Neurology*. 66 (1), 85-91.

Khan, N.A., Auranen, M., Paetau, I., Pirinen, E., Euro, L., Forsström, S., Pasila, L., Velagapudi, V., Carroll, C.J., Auwerx, J., Suomalainen, A., 2014. Effective treatment of

mitochondrial myopathy by nicotinamide riboside, a vitamin B3. *EMBO Molecular Medicine*. 6 (6), 721-731.

Kwak, S.H., Park, K.S., Lee, K., Lee, H.K., 2010. Mitochondrial metabolism and diabetes. *Journal of Diabetes Investigation*. 1 (5), 161-169.

Lorenzoni, P.J., Werneck, L.C., Kay, C.S.K., Silvado, C.E.S., Scola, R.H., 2015. When should MELAS (Mitochondrial myopathy, Encephalopathy, Lactic Acidosis, and Stroke-like episodes) be the diagnosis? *Arquivos de Neuro-Psiquiatria*. 73 (11), 959-967.

Maassen, J.A., 'T Hart, L.M., Van Essen, E., Heine, R.J., Nijpels, G., Jahangir Tafrechi, R.S., Raap, A.K., Janssen, G.M., Lemkes, H.H., 2004, Mitochondrial diabetes: molecular mechanisms and clinical presentation. *Diabetes*. 53 (1), 103-109.

Manwaring, N., Jones, M.M., Wang, J.J., Rochtchina, E., Howard, C., Mitchell, P., Sue, C.M., 2007. Population prevalence of the MELAS A3243G mutation. *Mitochondrion*. 7 (3), 230-233.

Markley, J.L., Brüschweiler, R., Edison, A.S., Eghbalnia, H.R., Powers, R., Raftery, D., Wishart, D.S., 2017. The future of NMR-based metabolomics. *Current Opinion in Biotechnology*. 43, 34-40.

Marshall, D.D. and Powers, R., 2017. Beyond the paradigm: Combining mass spectrometry and nuclear magnetic resonance for metabolomics. *Progress in Nuclear Magnetic Resonance Spectroscopy*. 100, 1-16.

McLaughlin, M.J. and Sainani, K.L., 2014. Bonferroni, Holm, and Hochberg corrections: fun names, serious changes to p values. *Physical Medicine and Rehabilitation*. 6 (6), 544-546.

Naviaux, R.K., 2014. Metabolic features of the cell danger response. *Mitochondrion*. 16, 7–17.

Nikkanen, J., Forsström, S., Euro, L., Paetau, I., Kohnz, R.A., Wang, L., Chilov, D., Viinamäki, J., Roivainen, A., Marjamäki, P., 2016. Mitochondrial DNA replication defects disturb cellular dNTP pools and remodel one-carbon metabolism. *Cell Metabolism*. 23 (4), 635–648.

Padmalayam, I., Hasham, S., Saxena, U., Pillarisetti, S., 2009. Lipoic acid synthase (LASY): a novel role in inflammation, mitochondrial function, and insulin resistance. *Diabetes*. 58 (3), 600-608.

Pisters, P.W., Cersosimo, E., Rogatko, A., Brennan, M.F., 1992. Insulin action on glucose and branched-chain amino acid metabolism in cancer cachexia: differential effects of insulin. *Surgery*. 111 (3), 301-310.

Reinecke, C.J., Koekemoer, G., van der Westhuizen, F.H., Louw, R., Lindeque, J.Z., Mienie, L.J., Smuts,I., 2012. Metabolomics of urinary organic acids in respiratory chain deficiencies in children. *Metabolomics.* 8 (2), 264–283.

Scaglia, F., Northrop, J.L., 2006. The mitochondrial myopathy encephalopathy, lactic acidosis with stroke-like episodes (MELAS) syndrome: a review of treatment options. *CNS Drugs*. 20 (6), 443-464.

Schymanski, E.L., Jeon, J., Gulde, R., Fenner, K., Ruff, M., Singer, H.P., Hollender, J., 2014. Identifying Small Molecules via High Resolution Mass Spectrometry: Communicating Confidence. *Environmental Science & Technology*. 48, 2097–2098.

Smeitink, J.A., Zeviani, M., Turnbull, D.M., Jacobs, H.T., 2006. Mitochondrial medicine: a metabolic perspective on the pathology of oxidative phosphorylation disorders. *Cell Metabolism*. 3 (1), 9–13.

Smuts, I., van der Westhuizen, Francois H., Louw, R., Mienie, L.J., Engelke, U.F., Wevers, R.A., Mason, S., Koekemoer, G., Reinecke, C.J., 2013. Disclosure of a putative biosignature for respiratory chain disorders through a metabolomics approach. *Metabolomics*. 9 (2), 379 391.

Xia, J., Wishart, D.S., 2016. Using MetaboAnalyst 3.0 for comprehensive metabolomics data analysis. *Current Protocols in Bioinformatics*. 55, 10-14.

Yi, X., Maeda, N., 2005. Endogenous production of lipoic acid is essential for mouse development. *Molecular and Cellular Biology*. 25 (18), 8387-8392.

Zhang, A., Sun, H., Wang, P., Han, Y., Wang X., 2012. Modern analytical techniques in metabolomics analysis. *Analyst*. 137 (2), 293-300.

5.6 SUPPLEMENTARY INFORMATION

5.6.1 QUALITY CONTROL SAMPLE AND BATCH COMPOSITION

To evaluate the quality of the urinary metabolomics analyses, quality control (QC) samples were introduced into each analytical run. These samples were obtained by preparing a stock QC sample, which consisted of urine from all the patient and control samples. This stock QC sample was then aliquoted and stored at – 80 °C. Once the patient and control sample were analyzed on each platform, a number QC aliquots were introduced into each batch and were treated in the same manner as the control and patient samples. For the targeted LC-MS/MS analyses, three QC aliquots were included in the beginning of a batch, each of them analyzed twice, and then another QC aliquot included after every five samples. For GC-TOF-MS analyses two QC aliquots were included at the beginning of a batch and then after every 10th sample. For the NMR analyses, only one QC was included in the beginning of the batch, with no other QC's included in the rest of the NMR batch as it is well-established that NMR is a highly reproducible analytical platform (Keun *et al*. 2002; Dumas *et al*. 2006; Emwas *et al*. 2013).

5.6.2 ANALYTICAL PLATFORMS AND SAMPLE ANALYSES

Sample handling, preparation and analyses are described in detail by Esterhuizen *et al*., 2018. All the samples were analyzed on three analytical platforms, namely: targeted LC-MS/MS (quantification of amino acids and acylcarnitines), untargeted GC-TOF-MS (analyzing organic acids, amino acids, sugars) and untargeted NMR (organic acids, sugars, amino acids and nucleotides), again described in detail by Esterhuizen *et al*., 2018.

5.6.3 PRE-PROCESSING, NORMALIZATION AND EXTRACTION OF DATA

Figure 5.6 shows a schematic representation of the workflow that was followed to determine metabolic similarities and differences between the different m.3243A>G mutation phenotypes. The sample groups consisted of 29 controls, 9 MELAS patients, 30 MIDD patients and 18 myopathy patients. Before analyses commenced, the samples and controls were randomized and divided into several batches. These batches included QC samples, which were used to evaluate the quality of the analyses of the samples on each analytical platform (as mentioned above). The randomized batches were then analyzed on the three analytical platforms, LC-MS/MS, GC-TOF-MS and NMR. Each analytical platform's data was extracted individually and inspected to determine if any between-batch effects occurred.

From the inspection, it was noted that no significant batch effects occurred, therefore no batch corrections were needed. Data normalization were done in two steps. First, the data was normalized against the specific internal standard used for the specific analysis. Thereafter the data was normalized against osmolality as determined by Ampath Laboratories on the Advanced Osmometer (IEPSA Diagnostics, South Africa). Since urinary creatinine levels might be affected in mitochondrial disease patients (Esterhuizen *et al*., 2017), all the data in this study was normalized against osmolality instead of creatinine.

After normalization of the data, a supervised 80% zero filter was applied, where a specific metabolite had to be detected/quantified in 80% of the samples in at least one of the sample groups (controls, MELAS, MIDD or myopathy), otherwise it was removed from the data set. This was followed by filtering the data further with a 50 % coefficient of variation (CV) filter. The QC samples were used to determine the CV of a given metabolic feature/analyte and if the CV was above 50%, the feature was consider poorly quantified under the set experimental conditions and removed from the dataset. After the 50% CV filtering, features were further excluded by applying a low variance and noise filter by using a Fisher's ratio analysis with a cutoff of $p<0.05$. With this filter, constant peaks related to chemical artefacts and noise were removed, as they carry no relevant variance for this investigation. Finally, missing/zero values were replaced by half of the lowest value in the data set after which the data was log transformed. These three individually pre-processed data sets were then combined into one single data matrix and used for all further statistical analyses.

Univariate statistical analyses were used to determine important metabolites that differed significantly between each phenotype group and the healthy controls, respectively. For a metabolite to be considered important, it had to be statistically (t-test) and practically (effect size; d value of > 0.8) significant. T-test p-values were evaluated at a 5% and 10% significance level after correcting for multiple testing using the Bonferroni-Holm approach (Holm, 1979; McLaughlin & Sainani, 2014). Multivariate analyses (principle component analyses, i.e. PCA) were then used to visualize the natural grouping/separation of the respective groups with regards to these important metabolites. Visualization of this natural separation enabled us to identify phenotypic specific metabolic perturbations. The data was also visualized with heat maps and volcano plots to highlight the metabolites most affected. Using the important metabolites identified in each phenotype, a Venn diagram was then constructed to identify metabolic similarities between the three phenotypes (MELAS, MIDD and myopathy). Finally metabolic differences were identified between the phenotypes by performing ANOVA analyses on the important metabolites. The metabolic differences were visualized in the form of metabolic pathways with box-plots highlighting specific differences.

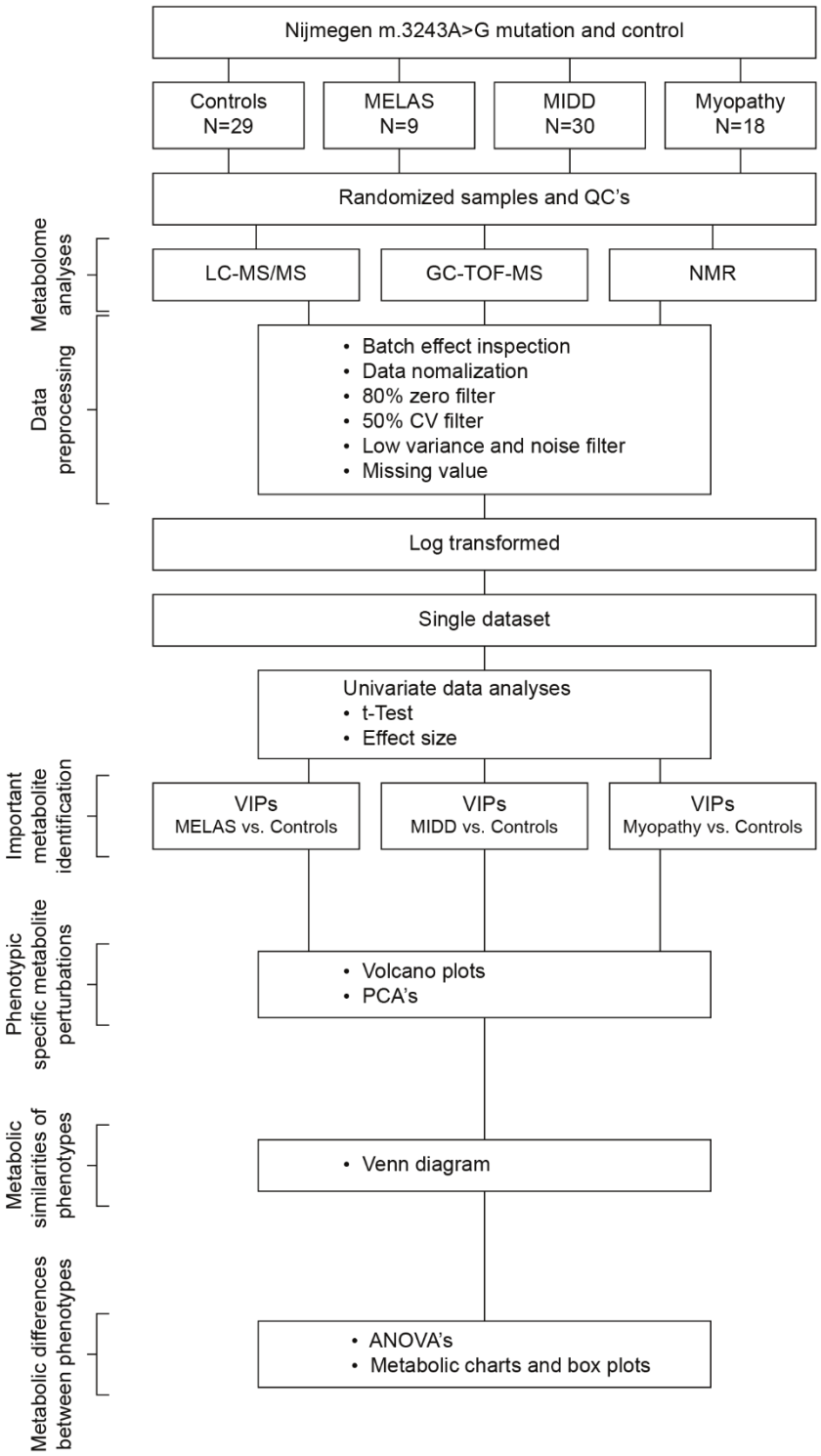

Figure 5.6. Schematic overview of the study. This scheme depicts the global workflow used for sample analysis and pre-processing, through the statistical workflow, in order to identify metabolites that discriminate the different phenotypes from the control. This workflow consisted of metabolome analyses, data pre-possessing, important metabolite identification, identification of phenotypic specific metabolic perturbations, and identification of metabolic similarities and differences.

5.6.4 REFERENCES

Dumas, M.E., Maibaum, E.C., Teague, C., Ueshima, H., Zhou, B., Lindon, J.C., Nicholson, J.K., Stamler, J., Elliott, P., Chan, Q. and Holmes, E., 2006. Assessment of analytical reproducibility of 1H NMR spectroscopy based metabonomics for large-scale epidemiological research: the INTERMAP Study. *Analytical chemistry*. 78 (7), 2199-2208.

Emwas, A.H.M., Salek, R.M., Griffin, J.L. and Merzaban, J., 2013. NMR-based metabolomics in human disease diagnosis: applications, limitations, and recommendations. *Metabolomics*. 9 (5), 1048-1072.

Esterhuizen, K., van der Westhuizen, F.H., Louw, R., 2017. Metabolomics of mitochondrial disease. *Mitochondrion*. 35, 97-110.

Esterhuizen, K., Lindeque, J.Z., Mason, S., van der Westhuizen, F.H., Suomalainen, A., Hakonen, A.H., Carroll, C.J., Rodenburg, R.J., de Laat, P., Janssen, M.C.H., Smeitink, J.A.M., Louw, R., 2018. A urinary biosignature for mitochondrial myopathy, encephalopathy, lactic acidosis and stroke like episodes (MELAS). *Mitochondrion*. doi: 10.1016/j.mito.2018.02.003.

Keun, H.C., Ebbels, T.M., Antti, H., Bollard, M.E., Beckonert, O., Schlotterbeck, G., Senn, H., Niederhauser, U., Holmes, E., Lindon, J.C. and Nicholson, J.K., 2002. Analytical reproducibility in 1H NMR-based metabonomic urinalysis. *Chemical research in toxicology*, 15 (11), 1380-1386.

Chapter 6

Summary and conclusions

6

6.1 INTRODUCTION

The inspiration for this study was derived from a series of mitochondrial disease studies done at the Centre for Human Metabolomics (North-West University), on a cohort of South African patients diagnosed with mitochondrial disease. These studies included molecular, cellular as well as metabolomics studies, all of which contributed valuable information to the field of mitochondrial disease. However, from a metabolomics point of view, various problems were encountered: 1) the group of patients were extremely heterogeneous with regard to ethnicity as well as demographics, 2) these patients were only classified as mitochondrial disease patients based on enzyme analyses done on mitochondrial respiratory chain enzyme deficiencies (complex CI–IV), 3) little information was available on the medication and/or supplements the patients were taking at the time of sample collection, 4) the control group could have been matched better to the patient group. All of these complications made a metabolomics study more complex, as each one of these problems adds variation to a metabolomic data set.

For this study, we obtained samples from two international cohorts: Nijmegen, The Netherlands and Helsinki, Finland. These samples proved to be very valuable for several reasons: 1) all of the patients were genetically screened for mtDNA mutations after they presented with symptoms associated with mitochondrial disease, 2) after genetic screening all of the patients were diagnosed with the m.3243A>G mutation, 3) each cohort was quite homogeneous, from an ethnic point of view, 4) the control groups was in most cases family members that were also genetically screened but tested negative for the m.3243A>G mutation. This provided us with control groups that were more closely matched to the patient cohorts, 5) we obtained information on additional symptoms these patients presented with, medication they used as well as supplements they were taking. All of this provided us with a more homogenous patient and control group, which eliminated the major contributors of variation that we encountered in our previous metabolomics studies on the South African cohort. Since the patients suffered from three different phenotypes, MELAS, MIDD and myopathy, it presented us with the perfect opportunity to not only investigate the metabolic

alteration caused by mitochondrial disease, but also to study possible mechanistic differences involved in the different phenotypes.

Therefore, the **aim** of this study was to investigate the urinary metabolome of three different m.3243A>G mutation phenotypes i.e. MELAS, MIDD and myopathy, using a multi-platform metabolomics approach.

The specific objectives of the study were:

a. To **analyze** all patient and control samples on five different analytical platforms.

b. To do data pre-processing and normalization for all analytical platforms before combining the different data sets to **generate a single data matrix.**

c. To perform **statistical analyses** in order to obtain a list of metabolites perturbed in each phenotype.

d. To do **biological interpretation** of the data in order to generate new knowledge on the altered metabolome of the different phenotypes.

In the first part of this study we investigated patients that specially presented with MELAS, one of the most common phenotypes associated with the m.3243A>G mutation, in an attempt to identify metabolites specifically perturbed by this phenotype. In the second part of this study we attempted to extend on these findings by investigating two additional phenotypes (MIDD and myopathy) to identify metabolic similarities as well as differences between these m.3243A>G associated phenotypes.

6.2 SUMMARY ON THE FINDINGS FROM THIS STUDY

6.2.1 CHAPTER 2 – Literature review

Although not listed as a specific objective, the first output from this study was publishing a review article (Esterhuizen *et al*., 2017) in *Mitochondrion* on the metabolomics of mitochondrial disease. This paper formed part of the literature background for this study (Chapter 2) and provides other researchers with valuable information with regards to:

1) the general applications and platforms of metabolomics. Here metabolomics is introduced to the reader who is not familiar with the technology and its application in biological studies. Concepts like targeted and untargeted metabolomics are discussed, as well as the idea of using numerous platforms to complement each other in an effort to increase the metabolome coverage.

2) different models used in mitochondrial disease studies where metabolomics was used as an investigation tool. Here numerous studies are summarized, including the use of knock-out nematodes models, different knock-out mouse models, tissue cultures as well as human skeletal muscle, plasma and urine.

3) perturbed metabolites reported in each of these studies and visualizations of these metabolites in the form of metabolic pathways. To many researchers a list of perturbed metabolites is seen as the main outcome from a metabolic study. But if one considers the very nature of a metabolomics study, where the metabolites detected and reported on is ultimately determined by the choice of analytical platforms utilized, one must keep in mind that the metabolite reported as perturbed in a study might be very limited if a single analytical platform was used to analyze the samples. This does not mean that the reported metabolites are not important, but rather that more metabolites might be perturbed in that specific samples, only that the analytical platform utilized could not detect these metabolites and therefore they were not reported in the study as perturbed. With this in mind, perhaps the biggest outcome of this paper was the combination of perturbed metabolites, from all the models and studies reported on in the paper, into metabolic charts. Thus, it brought information from numerous studies together to get a global picture of the metabolic consequence of mitochondrial disease. The discrepancies between specific studies was also highlighted: metabolites where research is not in agreement regarding its alteration in the disease. These should be followed up in new studies.

6.2.2 CHAPTER 4 – Biosignature for MELAS

Even though MELAS is the most common phenotype associated with the m.3243A>G mutation, very little metabolomics data has been reported on the phenotype prior to this study. Therefore, in this part of the study we specifically focused on the patients presenting with the MELAS phenotype in an attempt to expand this field of knowledge. This led to a publication in *Mitochondrion* (Esterhuizen *et al*., 2018). This part of the study was divided into an exploratory phase and a validation phase. During the exploratory phase, we investigated the urine metabolome of our Nijmegen MELAS patients by using a multi-

platform metabolomics approach that consisted of untargted (GC-MS, NMR, negative LC-IM-MS, and positive LC-IM-MS) and targeted analyses (LC-MS/MS). We were able to identify 36 metabolites that were altered in these patients when compared to healthy controls. Our data was linked to redox imbalance, stalled fatty acid oxidation, amino acid catabolism as well as the intricate web of pathways consisting of the one-carbon metabolism, methylation cycle and transsulfuration pathway. Even though this intricate web of pathway has previously been linked to PEO, this is the first paper associating alterations in these pathways with the MELAS phenotype.

In the validation phase, we used the 36 metabolites identified in the Nijmegen MELAS patients and extracted data on these 36 metabolites from a large dataset from the Helsinki cohort. This cohort was only used in the validation part of this study and consisted of two MELAS patients and seven controls. When visualizing the covariance of the extracted data with principle component analysis, the Helsinki MELAS patients clearly separated from their respective control group. Even though only two patients were included in this validation phase, it highlighted the applicability of a biosignature for mitochondrial disease studies and possibly even diagnostics and disease progression monitoring.

6.2.3 CHAPTER 5 – Comparing three m.3243A>G mutation phenotypes

From the results obtained in Chapter 4, it was evident that urine is a useful source for disease-specific metabolomics data. Therefore, to improve on the findings from Chapter 4, we investigated two additional phenotypes (MIDD and myopathy), also associated with the m.3243A>G mutation, presented as a manuscript prepared for submission to *Cell Reports*. We attempted to shed more light on the biochemical mechanisms involved in the three different phenotypes (MELAS, MIDD and myopathy), all in an effort to ultimately help answer the question as to why patients, harboring the same mutation, present with such a broad spectrum of symptoms. From the start, we realized that one cannot expect to solve such a complicated conundrum with a single metabolomics study, but that a metabolic comparison of the phenotypes might be the first piece of the puzzle to ultimately resolve this mystery. This part of the study was again divided in two parts. With the first part, metabolic similarities were investigated. Three metabolites, 2-hydroxyglutaric acid, glycolic acid and 4-pentenoic acid were detected as perturbed in MELAS, MIDD and myopathy. Since 2-hydroxyglutaric acid and glycolic acid have previously been reported as perturbed in mitochondrial disease, these metabolites warrant further investigation as possible universal markers for the disease. But 2-hydroxyglutaric acid is not merely a metabolite excreted in the urine, it disturbs cell signaling by inhibiting mTOR. Since mTOR regulates cell growth, cell proliferation, cell

survival, protein synthesis and autophagy, any metabolite that interferes with mTOR should set off alarm bells and warrants further investigation. With regards to 4-pentenoic acid, the true identity of this metabolite remains problematic. Currently we speculate that this metabolite is actually a fragment from another larger fatty acid, but this remains to be investigated/confirmed with future research. Only after the true identity of this metabolite is confirmed, using authentic standards, can biological information be obtained on its involvement in mitochondrial disease.

Phenotype-specific metabolic profiles (biosignatures) were obtained for MELAS, MIDD and myopathy. The most striking disturbance in MELAS was altered fatty acid synthesis, the methylation cycle and the transsulfuration pathway. Our data showed that fatty acid synthesis is increased, and we hypothesize that this is for increased octanoic acid synthesis. The formed octanoic acid is then used, along with S-adenosylmethionine from the methylation cycle, to form lipoic acid. Lipoic acid is not only an essential cofactor for pyruvate dehydrogenase, 2-ketoglutarate dehydrogenase and the glycine cleavage system, but it is also a potent antioxidant. Knock-out animal studies have shown that lipoic acid synthesis is essential for cellular survival, and that oral supplementation could not rescue embryonic lethargy. This demonstrates that lipoic acid synthesis is critical for normal cellular function and possibly strengthens our hypothesis on the altered fatty acid synthesis and methylation cycle being as a consequence of the cell's efforts to synthesize lipoic acid.

The MIDD patients show a strong perturbation of glucose metabolism, with elevated levels of glucose, myo-inositol and glucuronic acid detected. This came as no surprise as these MIDD patients suffer from high blood sugar levels as a result of an insulin shortage. Since the majority of the patients in the MIDD group received insulin at the time of sample collection, the metabolic profile of these patients had to be interpreted with the insulin treatment in mind. A metabolic disturbance in branched-chain amino acid catabolism was also detected in the MIDD patients, but again this was expected since insulin plays a major role in the regulation of branched-chain amino acid metabolism. Lastly, the myopathy patients showed only five metabolites perturbed, compared to the 29 in MELAS and 22 in MIDD. Thus, it can be argued that the metabolism in myopathy was not as disturbed or severe as that detected in MELAS and MIDD. However, creatine was detected as increased in the myopathy patients, and not in the MIDD of MELAS patients. Due to the muscle involvement of the myopathy patients, one can expect alterations in the urinary creatine levels. Creatine is one of the main energy stores in the muscle (in the form of phosphorylated creatine) and was previously reported as increased in mitochondrial disease.

6.3 STRENGTHS AND LIMTATIONS OF THE STUDY

As with any study, this study also had strengths as well as limitations that should be mentioned. These strengths and limitations proved to be valuable lessons learned for future studies and will serve as a good foundation on which similar research can be built.

6.3.1 STRENGHTS

6.3.1.1 Patient and control samples

Even though the m.3243A>G mutation is one of the most common mitochondrial disease-causing mutations, large cohorts of patients suffering from this mutation are extremely rare. Since no such cohort exists for South African patients, we had to use international collaborations to obtain samples to use in this study. Without these samples, this study would not have been possible. Thus, it is with great appreciation that we list this as a huge strength of this study. We received samples that were confirmed m.3243A>G mutated with the urinary mutation load included as well. We received detailed phenotypic information on the patients as well as lists of medication and supplementation taken by the patients and controls at the time of samples collection. Without cohorts like this, and the additional information we received on the patients, a study like this would not be possible.

6.3.1.2 Multi-platform metabolomics approach

A major strength of this study was the utilization of different analytical platforms to investigate the urine metabolome of our m.3243A>G patients and controls. The metabolomics platforms consisted of untargeted (NMR, GC-MS, negative LC-IM-MS, and positive LC-IM-MS) as well as targeted analyses (LC-MS/MS) and allowed us to analyze a larger portion of the metabolome compared to using only a single analytical platform. This is because different analytical platforms complement each other by focusing on different parts of the metabolome. For example, targeted LC-MS/MS focus on amino acid and acylcarnitine analyses (as applied here), while techniques such as untargeted GC-MS is fit for volatilized compounds such as organic acids. Thus, analyzing a larger portion of the metabolome enables us to identify metabolites that would otherwise have been missed when using only a single analytical technique. Furthermore, when using a multi-platform analytical approach, certain metabolites can be detected on more than one platform. For instance, by derivatizing the sample for GC-MS analysis, the amino acids become more volatile (as amino acid derivatives) and can thus be analyzed with GC-MS. In our study the amino acids were

detected on the GC-MS, LC-MS/MS and some of them even on the NMR (depending on the relative concentration of the amino acid). This is a huge positive – if a metabolite is detected as perturbed on more than one analytical platform, it increases the credibility of the findings drastically.

6.3.2 LIMITATIONS

6.3.2.1 Identification of features/metabolites from the untargeted metabolomics data

In the first part of the study (Chapter 4), we used five different analytical platforms to generate data on the urinary metabolome. However, after investigation of the VIP lists, it was evident that the majority of the VIPs were contributed by only three platforms (GC-MS, NMR and LC-MS/MS), with the untargeted LC-IM-MS (positive ionization) contributing only four metabolites and untargeted LC-IM-MS (negative ionization) none. Even though a large number of features were detected with the untargeted LC-IM-MS platforms, identification of the features was problematic. Very few MS/MS libraries or databases are available compared to the number of GC-MS databases. Furthermore, on the LC-IM-MS platform, one only gets high accurate mass (m/z), compared to the spectral information one receives on the GC-MS, thus identification of features remains problematic for the LC- LC-IM-MS data (Schymanski *et al*., 2014). For this reason, the unidentified features (metabolites that could not be identified) were filtered from the data set during the bioinformatics process. Therefore, for the second part of the study (Chapter 5), it was decided to only use the data from three analytical platforms (GC-MS, NMR and LC-MS/MS) and ignore the data from the LC-IM-MS (positive and negative ionization) platforms. These can be analyzed in future when better databases become commercially available.

6.3.2.2 Number of patients per phenotype

Another limitation in this study, was the limited number of samples that we had in some of our phenotype groups. For the validation part of the MELAS study (Chapter 4), only two MELAS patients were compared to 7 controls (Helsinki cohort). Even for the Nijmegen cohort, the patient numbers were relatively low (MELAS = 9, MIDD = 30, myopathy = 18). A small sample size meant that we could not be as strict with exclusion criteria, which in turn influenced the homogeneity of our groups to an extent. But even though we had a limited number of samples, the study design still enabled us to identify metabolites perturbed in each phenotype. Larger sample sizes is ideal, but one has to be realistic as well, realizing

that we are studying a rare disease and that large cohorts containing hundreds of samples is not possible to obtain.

6.3.2.3 Medication and supplements

In an attempt to improve their quality of life, the patients used various forms of medication and supplementation, which varied based on the symptoms the patient presented with. A portion of the medications and supplements are ultimately excreted in the urine after it has been metabolized. Even though sufficient information was available with regards to the medication and supplements these patients took, it is difficult to comprehend the extent to which the medication and supplementation may have affected the patient's urinary metabolome. Collecting urine samples before the patient starts treatment will be ideal, but again not realistic.

6.3.2.4 Normalization of metabolomics data

One of the important lessons learned in this study was with regards to the normalization of the data. Urine has become a popular sample of choice in metabolomic studies, as it is easy to obtain and one of the least invasive biofluids to collect. Whilst some body fluids, such as blood, forms part of a closed system where the concentrations are more controlled, the volume of urine excreted can vary considerably due to water consumption and other physiological factors (Warrack *et al*., 2009). Creatinine is a waste product that is formed during a process where creatine and creatine phosphate are catabolized (Salazar, 2014). In a healthy human, the excretion of creatinine is constant and directly proportional to muscle or lean body mass. In theory, the excretion of metabolites that are proportional to one's body size could then be normalized by using creatinine (Patel *et al*., 2013). However, in patients where the kidneys are compromised, this could become a problem, because their bodies cannot excrete creatinine at a constant rate anymore. If creatinine is used as the normalization factor, this could lead to the inaccurate normalization of urinary metabolites.

Problems with creatinine normalization could potentially occur in mitochondrial disease patients as their kidney function might be impaired due to decreased levels of ATP. If creatinine normalization is problematic, normalization with osmolality can be considered. Osmolality not only gives an indication of the urine solute concentration, but is also a direct measure of the total endogenous metabolic output. Osmolality is also usually unaffected by diet, activity, gender, age, stress, or health, which is very beneficial when compared to the use of creatinine levels (Warrack *et al*., 2009).

When investigating the MELAS patient group in Chapter 4, the urine creatinine concentrations correlated strongly with the osmolality concentrations. This indicated that either creatinine or osmolality could be used for normalization. We therefore decided to use the data normalized to creatinine, as this is the method used by most diagnostic laboratories. However, when investigating and comparing the data of all three phenotypes (Chapter 5), the creatinine values for the MIDD patient group were statistically significantly different from the controls (and the other two phenotypes). Therefore, for that part of the study, we decided to use the data normalized against osmolality rather than creatinine in order to be able to compare the data from the different phenotypes. Thus, due to different normalization strategies, the MELAS VIP list obtained in Chapter 4 differed from the VIP list obtained for MELAS in Chapter 5. This discrepancy remains to be further investigated.

It is important to realize that even though creatinine is not statistically affected in a cohort, it does not mean that it is not affected at all. One suggestion therefore is to evaluate both the creatinine and osmolality in one's study, before making decisions on the approach to normalization of one's data. Another suggestion, more in the diagnostic field, where working with individual patients, is to move away from using creatinine as a normalization technique and rather use osmolality. This would eliminate the uncertainty with regards to kidney impairment, and provide more accurate results.

6.4 FOR FUTURE STUDIES

Valuable lessons have been learned from the strengths and limitations encountered in this study. These lessons will pave the way for future studies and not only highlight areas that should be avoided or needs further investigation, but also identify areas that could be improved on.

6.4.1 PATHWAYS AFFECTED IN DIFFERENT PHENOYPES

From the results discussed in Chapters 4 and 5, it is evident that although these patients are affected by the same mutation, different pathways have been identified as perturbed in the different phenotypes. Some of the affected pathways that warrant further investigation is: 1) the group of pathways consisting of one carbon metabolism, methylation and the transsulfuration pathway (MELAS), 2) mitochondrial fatty acid synthesis (MELAS), 3) lipoic acid synthesis (MELAS), 4) carbohydrate metabolism (MIDD) and 4) phosphocreatine

metabolism (myopathy). For these follow-up studies, metabolic flux analyses using ^{13}C-glucose can be considered in tissue cultures or even mouse models.

6.4.2 REINVESTIGATE UNTARGETED LC-IM-MS DATA

Metabolomics is a rapid growing field with databases evolving at an equally fast pace. This means that something not possible a year or even a couple of months ago could be a possibility now. With this in mind it is definitely necessary to reinvestigate the untargeted metabolomics data generated in this study using positive and negative LC-IM-MS. If any additional information could be mined from the existing data, it could be beneficial for future studies.

6.5 CONCLUSION

When looking back on the discovery of the first human pathological mtDNA mutation in 1988 (Holt *et al*., 1988; Wallace *et al*., 1988), followed by the discovery of the m.3243A>G mutation in 1990 (Goto *et al*., 1990), we have come a long way with regards to diagnosis and treatment of these patients - even though no cure is available yet. There is however always room for improvement and with this study we contributed to the field of mitochondrial disease by investigating the metabolome of three m.3243A>G mutation phenotypes.

Even though several challenges were encountered during this study, all the objectives have been successfully completed. With this study, we were able to identify mechanistic differences between the phenotypes on a metabolic level. These differences highlight areas that could be investigated further, both of which could improve current diagnostic approaches as well as management of the patients' quality of life. With our metabolomic findings we were able to demonstrate the valuable information that could be gained when embracing new techniques, moving away from the more traditional approaches, and combining various analytical platforms.

The field of mitochondrial disease is like an iceberg of which barely the tip has been uncovered. With every study, we are a step closer to unraveling this mysterious group of diseases. Until then, for us as researchers, our main aim should be to ask how we can contribute to the field of mitochondrial disease and how we can help these patients improve their quality of life.

In conclusion, I end this journey with two quotes from the DIA/NORD 2012 US Conference on Rare Diseases and Orphan Products. "*If we lose focus, we become fanatics*" (Charles Mohan, CEO and executive director of the United Mitochondrial Disease Foundation) and "*People need to collaborate more and worry less about egos*" (Susan Riley Keyes, vice president Nemucore Medical Innovations Inc).

6.6 REFERENCES

Esterhuizen, K., van der Westhuizen, F.H., Louw, R., 2017. Metabolomics of mitochondrial disease. *Mitochondrion*. 35, 97-110.

Esterhuizen, K., Lindeque, J.Z., Mason, S., van der Westhuizen, Francois H, Suomalainen, A., Hakonen, A.H., Carroll, C.J., Rodenburg, R.J., de Laat, P.B., Janssen, M.C., 2018. A urinary biosignature for mitochondrial myopathy, encephalopathy, lactic acidosis and stroke like episodes (MELAS). *Mitochondrion*.

Goto, Y., Nonaka, I., Horai, S., 1990. A mutation in the tRNA (Leu (UUR)) gene associated with the MELAS subgroup of mitochondrial encephalomyopathies. *Nature*. 348 (6302), 651-653.

Holt, I.J., Harding, A.E., Morgan-Hughes, J.A., 1988. Deletions of muscle mitochondrial DNA in patients with mitochondrial myopathies. *Nature*. 331 (6158), pp. 717-719.

Patel, S.S., Molnar, M.Z., Tayek, J.A., Ix, J.H., Noori, N., Benner, D., Heymsfield, S., Kopple, J.D., Kovesdy, C.P. & Kalantar-Zadeh, K., 2013. Serum creatinine as a marker of muscle mass in chronic kidney disease: results of a cross-sectional study and review of literature", *Journal of cachexia, sarcopenia and muscle*. 4 (1), 19-29.

Salazar, J.H., 2014. Overview of urea and creatinine*. Laboratory Medicine*. 45 (1), 19-20.

Schymanski, E.L., Jeon, J., Gulde, R., Fenner, K., Ruff, M., Singer, H.P., Hollender, J., 2014. Identifying Small Molecules via High Resolution Mass Spectrometry: Communicating Confidence. *Environmental Science & Technology*. 48, 2097–2098.

Wallace, D.C., Singh, G., Lott, M.T., Hodge, J.A., Schurr, T.G., Lezza, A.M., Elsas, L.J., Nikoskelainen, E.K., 1988. Mitochondrial DNA mutation associated with Leber's hereditary optic neuropathy. *Science*. 242 (4884) 1427-1430.

Warrack, B.M., Hnatyshyn, S., Ott, K., Reily, M.D., Sanders, M., Zhang, H., Drexler, D.M. 2009. Normalization strategies for metabonomic analysis of urine samples. *Journal of Chromatography B*. 877 (5-6), 547-552.

Annexure A

A

Metabolomics of mitochondrial disease

Esterhuizen *et al*., 2017

Mitochondrion

Impact factor (2016/2017): 3.704

Mitochondrion 35 (2017) 97–110

Contents lists available at ScienceDirect

Mitochondrion

journal homepage: www.elsevier.com/locate/mito

Review

Metabolomics of mitochondrial disease

Karien Esterhuizen, Francois H. van der Westhuizen, Roan Louw*

Human Metabolomics, North-West University, Potchefstroom Campus, Potchefstroom, South Africa

ARTICLE INFO

Keywords:
Metabolomics
Mitochondrial disease
OXPHOS
Respiratory chain deficiency
Metabolism

ABSTRACT

Mitochondrial disease (MD) diagnostics and disease progression investigations have traditionally relied very little on metabolic data, due to a lack of biomarker sensitivity and specificity. The recent drive to find novel, low intervention biomarkers and new therapeutic approaches have revived an interest in what metabolic data can offer, as presented in this timely review. We review how metabolomics has been applied to MD and provide an extensive overview of the reported metabolic perturbations and common mechanistic features that may provide a basis for future research. We conclude by highlighting the substantial potential of metabolomics for future diagnostics and mitochondrial medicine.

1. Introduction

Mitochondrial disease, when defined as disorders resulting from deficiencies in the mitochondrial oxidative phosphorylation (OXPHOS) system, has a current minimum prevalence of one in every 5000 live births and is therefore considered one of the most common inborn errors of metabolism (Gorman et al., 2015; Schaefer et al., 2004). Although diagnostic methods for mitochondrial disease are available, several studies have highlighted limitations in the diagnostic approach, including overlapping phenotypes, patient selection, disease monitoring and response to treatment, to name but a few (DiMauro and Schon, 2003; Reinecke et al., 2012; Schaefer et al., 2004; Smuts et al., 2013). Metabolomics is one of the more recent additions to the "-omics" family and can be defined as the detection, quantification and identification of all small-molecule metabolites present in a biological sample (Dunn et al., 2005). Since the metabolome is at the end-point of all cellular activity, implementation of metabolomics in a study holds the potential to overcome some of the limitations currently observed in the study of mitochondrial disease. With these limitations in mind, various studies have used a metabolomics approach to study mitochondrial disease and, with significant progress made in recent years, a review of these contributions and the potential they reveal is long overdue. Here we review metabolomics as a relatively novel approach to the field of mitochondrial disease research and diagnostics, with a focus on the instrumental platforms, practicalities and future prospects.

2. Mitochondrial disease as an inherited metabolic disease

Since the first inborn error of metabolism (IEM) was identified by Archibald E. Garrod in 1904, diagnosing IEMs has evolved extensively and to date more than 500 IEMs, affecting various metabolic pathways, can be diagnosed using an array of analytical techniques (Kamboj, 2008; Martins, 1999). Diagnosing most IEMs involves targeted analyses, which measures a specific metabolite(s). Altered concentrations of a specific metabolite(s) usually results from a specific enzyme defect. An example is the case of isovaleric acidemia, in which isovaleric acid coenzyme A (CoA) dehydrogenase is defective, resulting in the accumulation of isovalerylglycine in urine. Another example is propionic acidemia, where propionyl-CoA carboxylase is defective, resulting in the accumulation of propionic acid. Thus, for many IEMs, altered levels of one (or a few) specific metabolite(s) are analyzed in a biological sample and used to diagnose the disease. In contrast, a defect of the OXPHOS system results in insufficient ATP production due to the inhibited flow of electrons through the respiratory chain, resulting in a NAD^+/NADH redox imbalance, oxidative stress and a reduction of the mitochondrial membrane potential. Compared to an IEM where fewer metabolites are usually affected, the redox imbalance ultimately results in a plethora of possible cellular responses, generally affecting a large number of metabolites (Brière et al., 2004; Naviaux, 2014; Reinecke et al., 2009; Smeitink et al., 2006).

For mitochondrial disease, the current gold standard for diagnosis is measuring the activity of the respiratory chain enzymes in tissue biopsies plus complex V and functional tests if fresh samples are available, in combination with other assessments. These assessments includes brain imaging, genetic testing for specific mutations, histochemical investigations as well as exercise stress tests to determine the arteriovenous oxygen difference (a-vO2 difference) (Haas et al., 2008; Menezes et al., 2014; Taivassalo et al., 2012). Over the past 15 years,

* Corresponding author at: North-West University, Potchefstroom Campus, Private Bag X6001, Potchefstroom 2520, South Africa.
E-mail address: Roan.Louw@nwu.ac.za (R. Louw).

http://dx.doi.org/10.1016/j.mito.2017.05.012
Received 12 August 2016; Received in revised form 8 May 2017; Accepted 26 May 2017
Available online 31 May 2017
1567-7249/ © 2017 Elsevier B.V. and Mitochondria Research Society. All rights reserved.

various scoring systems for mitochondrial disease have been developed (for both pediatric and adult patients) to assist physicians in screening patients for the disease (Bernier et al., 2002; Koene et al., 2016; Parikh et al., 2015; Phoenix et al., 2006; Schaefer et al., 2004; Wolf and Smeitink, 2002). However, the use of metabolite data is very limited in these scoring systems and includes only a few selected metabolites (lactate, pyruvate, alanine, tricarboxylic acid cycle intermediates, ethylmalonic acid, 3-methylglutaconic acid, dicarbonic acids, acylcarnitines) (Parikh et al., 2015; Phoenix et al., 2006; Rasanu et al., 2011; Schaefer et al., 2004; Wolf and Smeitink, 2002). Few studies have used semi-targeted or untargeted metabolomics to study mitochondrial disease, despite the potential of the technology to find metabolites/biomarkers not previously associated with the disease. Such an approach might be useful in understanding and diagnosing the disease, as well as screening and monitoring of patients.

3. Metabolomics: general applications and platforms

Metabolomics was first defined in 1998 (by Oliver et al., 1998) and has since become a popular investigative tool for research on biological systems and complex disease models, using a wide range of biofluids, tissues and cell cultures (Dunn et al., 2011; Nikolic et al., 2014). Metabolomics usually follow one of three approaches: a *targeted* approach where a group of small metabolites are quantified and identified, a *semi-targeted* approach that focuses on a specific class of metabolite (for example amino acids, organic acids or acylcarnitines), or an *untargeted* approach, which is the unbiased detection and quantification of all the metabolites in a sample using a single- or multiple-platform approach (Álvarez-Sánchez et al., 2010; Dunn et al., 2011; Dunn et al., 2013; Monteiro et al., 2013).

Analytical techniques used in metabolomics studies usually include a technique to separate the metabolites in the biological matrix [gas chromatography (GC), liquid chromatography (LC) or capillary electrophoresis (CE)] coupled with a detection system [mass spectrometry (MS) or nuclear magnetic resonances (NMR)]. To increase the sensitivity of the analytical technique, numerous different combinations of these components are available (Bouatra et al., 2013). It is also important to realize that the specific metabolites detected by metabolomics studies depends on various factors, for example more polar compounds are usually investigated with an LC-system, whereas a GC-system is the preferred technique for more non-polar metabolites. While NMR is not as sensitive as mass spectrometry, it is a useful technique when sample volumes are limited as it is a non-destructive technique. Another factor to take in consideration is the stability of a compound as some metabolites are unstable and therefore more difficult to detect - some of these metabolites might require a derivatization step to increase stability. Data pre-processing and clean-up can also influence the metabolites reported by a study. During the clean-up process, metabolites may be removed from the data matrix for numerous reasons (like a high coefficient of variance in the quality control samples etc.), thus a specific metabolite may not be in the data set to be considered for statistical analyses and is thus not reported on by the study. Another factor to take in account is the availability of spectral libraries for data interpretation. LC-MS and NMR has a limited number of databases available compared to GC–MS, which has a wide range of public as well as commercial spectral libraries available (Monteiro et al., 2013). To summarize, each analytical platform has both advantages and disadvantages that should be taken into account before deciding on an appropriate technique (Fang and Gonzalez, 2014). The use of different combinations of platforms is encouraged to analyze a larger portion of the metabolome, since the different analytical methods usually complement each other (Bouatra et al., 2013).

4. The application of metabolomics in mitochondrial disease research

4.1. Models

The use of metabolomics in the field of mitochondrial disease research has been very limited, compared to its use to study other human diseases, such as diabetes and cardiovascular disease. This is probably a result of the relatively small number of well-defined (phenotype–genotype) samples available in mitochondrial disease patient cohorts and the heterogeneous nature of the disease. To address this challenge, numerous models have been developed to study the disease.

One such animal model uses the nematode *Caenorhabditis elegans* (*C. elegans*). This model is favored because the *C. elegans* respiratory chain (RC) subunits are morphologically very similar to the human RC. Using these nematodes, various knockout models have been generated to mimic different mitochondrial diseases, including a complex I knockout (CI KO) model [gas-1(fc21), a complex II knockout (CII KO) model [mev-1 (kn1), a complex III knockout (CIII KO) model [isp-1(qm150), a tricarboxylic acid (TCA) cycle knockout model (idh-1(ok2832) and coenzyme Q biosynthesis knockout model [clk-1(qm30) (Butler et al., 2013; Falk et al., 2008; Morgan et al., 2015; Vergano et al., 2014). In addition to the nematode, another animal model frequently used in metabolomics studies is a mouse model such as the *Ndufs4* knockout mouse model. Due to the size of complex I, various mutations have been associated with the complex, including a mutation in the *Ndufs4* gene, which is involved in the assembly and stability of complex I. Another mouse model used is a deletor mouse model, which contains a 13 amino acid duplication situated in the mitochondrial helicase Twinkle. This deletor model is used to study adult-onset mitochondrial myopathy also known as progressive external ophthalmoplegia (PEO). Animal models such as these are currently favored in metabolomics studies to investigate the altered metabolism in mitochondrial disease, due in part to the more homogenous nature of experimental animals, compared to the more heterogeneous nature of human samples (Ahola-Erkkila et al., 2010; Leong et al., 2012; Nikkanen et al., 2016; Tyynismaa et al., 2010). Additionally, due to its controlled environment, animal models are also useful in therapeutic studies, as it is much easier to investigate the effect of potential treatment (Leong et al., 2015).

Although not as commonly used as animal models, a few studies have used cell cultures for the investigation of mitochondrial disease (Bao et al., 2016; Kami et al., 2012; Shaham et al., 2008; Shaham et al., 2010; Sim et al., 2002; Vo et al., 2007). Cell cultures are particular useful study models, as the metabolite profiling of the extracellular medium provides rich information on the uptake, metabolism and secretion of metabolites. Cell cultures used for the metabolomics investigation of mitochondrial disease includes fibroblasts to investigate Leigh's disease, human embryonic kidney cells to investigate how mitochondrial dysfunction alters the one-carbon metabolism pathways, cybrid cells from 143B osteosarcoma cells to investigate the m.A3243G MELAS mutation and muscle cells to investigate induced complex I and complex III defects with rotenone and antimycin A, respectively.

The application of metabolomics in human biofluids is a major objective of current research in the field as it holds potential to clarify the complex biochemistry and the involved diagnostics. A reason for this is that metabolites are the end products of cellular processes and the variability in their concentrations could be due to changes in biological systems, which could, in turn, be linked to phenotype. Human biofluids that have been used in metabolomics studies investigating mitochondrial disease include plasma, blood and urine. Urine samples have become a favored sample choice for investigating mitochondrial disease, as it is easy to obtain and requires minimal sample preparation (Esteitie et al., 2005; Reinecke et al., 2012; Smuts et al., 2013; Venter

et al., 2015). However, when working with human biofluids, the involvement of the gut microbiome should never be underestimated. The metabolites measured in the biofluids are not only due to the human genes, but are also influenced/metabolized by the hundreds of trillions of microbes colonizing the human body, i.e. the microbiome (Wikoff et al., 2009).

4.2. Defining patient and control groups for metabolomics investigations

The outcome of metabolomics investigations are significantly affected by the way patient and control groups are defined, as well as the phenotypic homogeneity of these groups. In most metabolomics studies on mitochondrial disease (MD), the patients were compared to healthy controls to ascertain the effects of the disease on the metabolism. Although this approach could shed light on the basic biochemistry of the disease, it would have been beneficial from a diagnostic point of view to compare patients suffering from MD to a disease control group, the latter being a group of patients with a different disease but displaying similar clinical symptoms. However, only a few metabolomics studies have used disease control groups, such as organic acidemia and fatty acid oxidation defects, to compare to their mitochondrial disease cohorts (Barshop, 2004; Sim et al., 2002). One of the latest studies involving metabolomics of mitochondrial disease implemented an alternative control group referred to as *clinically referred controls* (Venter et al., 2015), i.e. individuals who initially presented with symptoms usually associated with mitochondrial disease, but did not display a respiratory chain deficiency on enzymatic level. The use of this type of control group is of particular value due to the diverse phenotypes of mitochondrial disease, overlapping with other diseases, and the challenges of diagnosing a primary mitochondrial deficiency. In most cases, a physician will have to distinguish mitochondrial disease patients from those who present with similar symptoms, but do not have the disease (DiMauro and Schon, 2003; Schaefer et al., 2004). Due to the limited number of studies comparing other disease control groups to mitochondrial disease cohorts, the rest of this review will focus on metabolomics studies where patients/disease models with a deficient OXPHOS system is compared to healthy controls (Butler et al., 2013; Falk et al., 2008; Falk et al., 2011; Hall et al., 2015; Johnson et al., 2013; Legault et al., 2015; Leong et al., 2012; McCormack et al., 2015; Morgan et al., 2015; Reinecke et al., 2012; Shaham et al., 2008; Shatla et al., 2014; Smuts et al., 2013; Vergano et al., 2014; Vo et al., 2007).

4.3. Metabolites and pathways affected by mitochondrial disease

Considering the wide-ranging immediate and downstream cellular consequences of any of a number of possible types and levels of deficiencies of the OXPHOS system in different tissues, it is not surprising that the metabolome is not affected in a localized way, as is often the case in other inherited metabolic disorders (Brière et al., 2004; Elstner and Turnbull, 2012; Naviaux, 2014; Reinecke et al., 2009). This is clearly demonstrated by the vast number of metabolites, as summarized in Table 1, that have been reported in literature as affected by mitochondrial disease. However, an in-depth discussion or understanding of all the mechanisms regulating these metabolic pathways is beyond the scope of this review, and thus only a selected number of prominent and novel findings will further be highlighted, as well as the possible mechanisms responsible for these perturbations.

A fundamental consequence of an OXPHOS deficiency is the disturbance of the redox balance, which modulates a wide-ranging number of cellular processes. This results from a compromised electron transport through the respiratory chain (RC), resulting in leakage of electrons from the RC, poor membrane coupling (with resulting effect on nucleotide phosphorylation state) and a decreased redox state/ratio of the nicotinamide nucleotides and flavin coenzyme. The altered states of these OXPHOS electron carriers along with other nucleotides also modulate the activities of numerous dehydrogenase and other enzymes involved in metabolic reactions (Brière et al., 2004; Naviaux, 2014; Reinecke et al., 2009; Smeitink et al., 2006). The result of this shift, as well as pathways affected by other mechanisms, can be observed in a number of catabolic and anabolic pathways - the most of which are illustrated in Fig. 1, which summarizes in a number of sections (A-I) the reported perturbed metabolism in mitochondrial disease. The most well-known perturbation is the conversion of pyruvate to lactate (Fig. 1A). Under normal circumstances, pyruvate is converted to acetyl-CoA by the pyruvate dehydrogenase complex (PDHc), with the concomitant interconversion of NAD^+ to NADH. However, the decreased NAD^+/NADH ratio caused by an OXPHOS defect inhibits the conversion of pyruvate to acetyl-CoA, resulting in increased pyruvate levels. The latter is then converted to lactate by lactate dehydrogenase (LDH) with the concomitant interconversion of NADH to NAD^+. This is a classic example of how the activity of one dehydrogenase enzyme reaction (PDHc) can be inhibited, while the activity of another dehydrogenase reaction (LDH) can be increased by the same decreased NAD^+/NADH ratio, depending on the direction of the reaction. The conversion of pyruvate to lactate also results in the recycling of NAD +, which allows anaerobic glycolysis to continue in an attempt to recover ATP levels. The lactate/pyruvate ratio is also of great importance as this ratio gives an indication on the cytosolic redox state (Munnich et al., 1996). Furthermore, in the TCA cycle, three dehydrogenases (citrate synthase, isocitrate synthase and α-ketoglutarate dehydrogenase) are inhibited by a high NADH concentration, thus a lowered NAD^+/NADH ratio will lead to a congested TCA cycle, accounting for the increased levels of TCA cycle intermediates, and the metabolites they are subsequently converted to, as commonly reported by metabolomics studies (Fig. 1A).

Similarly, a frequent observation in mitochondrial disease is elevated alanine, which forms via the transamination of pyruvate by alanine aminotransferase. Together with the mentioned TCA cycle intermediates, as well as lactate (or elevated lactate/pyruvate ratio), alanine is one of the few metabolic markers used in scoring criteria for MD (Wolf and Smeitink, 2002). Thus, it is not surprising that numerous metabolomics studies also detected and reported these markers as important biomarkers as can be seen from Table 1. Noteworthy is that these “classic” metabolic markers (of albeit limited sensitivity and specificity) are reported in various models of the disease, e.g. elevated pyruvate was reported in an Ndufs4 knockout mouse model (Johnson et al., 2013), as well as in patient urine and plasma samples (Legault et al., 2015); elevated lactate was reported in a complex I knockout nematode model (Vergano et al., 2014), in addition to frequent reports in patient urine and plasma samples (Legault et al., 2015; Reinecke et al., 2012; Shaham et al., 2008; Shatla et al., 2014; Smuts et al., 2013). Furthermore, increased alanine was reported in nematode models (Falk et al., 2008; Falk et al., 2011; Vergano et al., 2014), tissue cultures (Bao et al., 2016), mouse models (Tyynismaa et al., 2010), patient plasma (Legault et al., 2015; Shaham et al., 2008; Shatla et al., 2014) and patient urine samples (Smuts et al., 2013). Although the studies listed here also identified possible novel biomarkers, they still reported the classic markers to be discriminative between MD and controls – something that bolsters the overall metabolomics methodology.

As evident from the illustrations in Fig. 1, the decreased NAD^+/NADH ratio can also account for numerous other metabolites altered by MD. One example is the ketone bodies, acetoacetate and 3-hydroxybutyric acid. Acetoacetate is formed from acetyl-CoA and is converted to 3-hydroxybutyric acid by 3-hydroxybutyric acid dehydrogenase with the concomitant conversion of NADH to NAD^+. Again the decreased NAD^+/NADH ratio can account for the increased 3-hydroxybutyric acid reported in human urine (Legault et al., 2015; Shatla et al., 2014). However, Ahola-Erkkila et al. (2010) reported decreased levels of 3-hydroxybutyric acid in a mouse model – clear discrepancies between different disease models and studies. While the lactate/pyruvate ratio provides information on the cytosolic redox state of a model,

Table 1
Metabolites associated with mitochondrial disease when compared to healthy controls.

	Falk *et al*., 2008			Falk *et al*., 2011	Butler *et al*., 2013		Vergano *et al*., 2014						Morgan *et al*., 2015		McCormack *et al*., 2015	Tyynismaa *et al*., 2005		Ahola-Erkkilä *et al*., 2010		Leong *et al*., 2012	Johnson *et al*., 2013	Nikkanen *et al*., 2016				Vo *et al*., 2007	Bao *et al*., 2016	Shaham *et al*., 2008	Reinecke *et al*., 2012	Smuts *et al*., 2013	Shatla *et al*., 2014		Legault *et al*., 2015		Hall *et al*., 2015	
	CI KO gas-1 (fc21)	CII KO mev-1 (kn1)	CIII KO isp-1 (qm150)	CIII KO isp-1 (qm150)	CII KO mev-1 (kn1)	CIII KO isp-1 (qm150)	CI KO gas-1 (fc21)	CII KO mev-1 (kn1)	CIII KO isp-1 (qm150)	Q10 KO clk-1(qm30)	Krebs KO idh-1(ok2832)	CI KO gas-1 (fc21)	CII KO mev-1 (kn1)	CI KO gas-1 (fc21)	Deletor	Deletor	Deletor	Deletor	NDUFS4 KO	NDUFS4 KO	Deletor	Deletor	PEO	PEO	Cell cultures	Cell cultures	Human Plasma	Human urine	Human urine	MD score greater than 4	MD score greater than 4	Urine	Plasma	MELAS	MIDD
	Nematode			Nematode	Nematode		Nematode						Nematode		Nematode	Mouse (Male)	Mouse (Female)	Mouse plasma	Mouse muscle	Mouse	Mouse	Mouse skeletal muscle	Mouse heart muscle	Human Plasma	Human skeletal muscle	Cell cultures	Cell cultures (spent media)	Human Plasma	Human urine	Human urine	Human urine	Human Plasma	Human urine	Human Plasma	Human urine	Human urine
Amino acids																																			
Alanine	+			+			+										+					+			–	+	+	+	+		+		+		
Alpha–amino adipic acid																							+			–				+						
Arginine	–							+												–						–	+									
Asparagine					+																	+				–	+							–		
Aspartic acid	+			+			–		–	–	+			–	–							+	+													
Betaine																						+	+											–		
Choline																						+												–		
Citruline																																		–		
Cystathionine																							+	+	+		+							–		
Cystine														–																						
Dimethylglycine																							+													
Ethanolamine					+																															
Gamma–Glutamylcysteine																							+													
Glutamic acid	–	–	–	–	+		–		–	–		–		–	–							+		+	+	–										
Glutamine	+	–	–	–							+	–										+				–	+									
Glycine	+	+	+				–		–	–	+	–		–	–			+		+		+	+			–				+		+				
Histidine												–	–													–	+									
Homocitrulline																				+																
Homocysteine																											–									
Isoleucine	+	+	+					+			+			+								+	+			–										
Kynurenine																								+			+								–	
Leucine	+	+	+											+						–		+				–	+									
Lysine	–		–					+			+															–										
Methionine												–										+				+										
N–Acetylaspartic acid																																+				
N–Narbamoyl–beta–alanine																											–									
Ornithine		–	–																				+				–									
Phenylalanine	–	+						+				–								+		+				–										
Phosphocholine																						+														
Proline												–										+	+			–					+					
Hydroxyproline																						+														
Serine											+			–	+		+					+	+	+	+	+	+			+						
Homoserine																						+														
Threonine		+	+																			+	+			–										

Table 1 *(continued)*

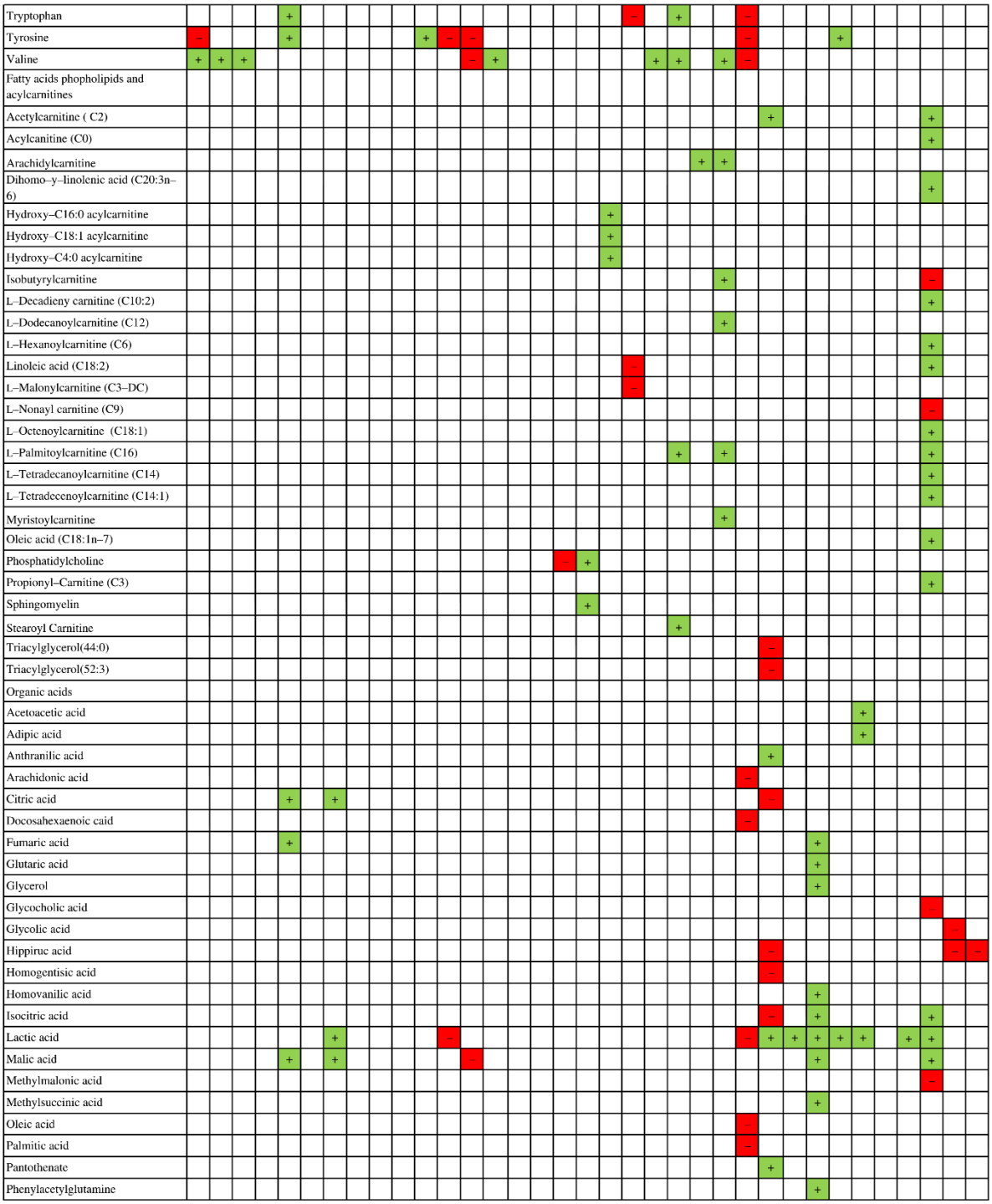

Table 1 *(continued)*

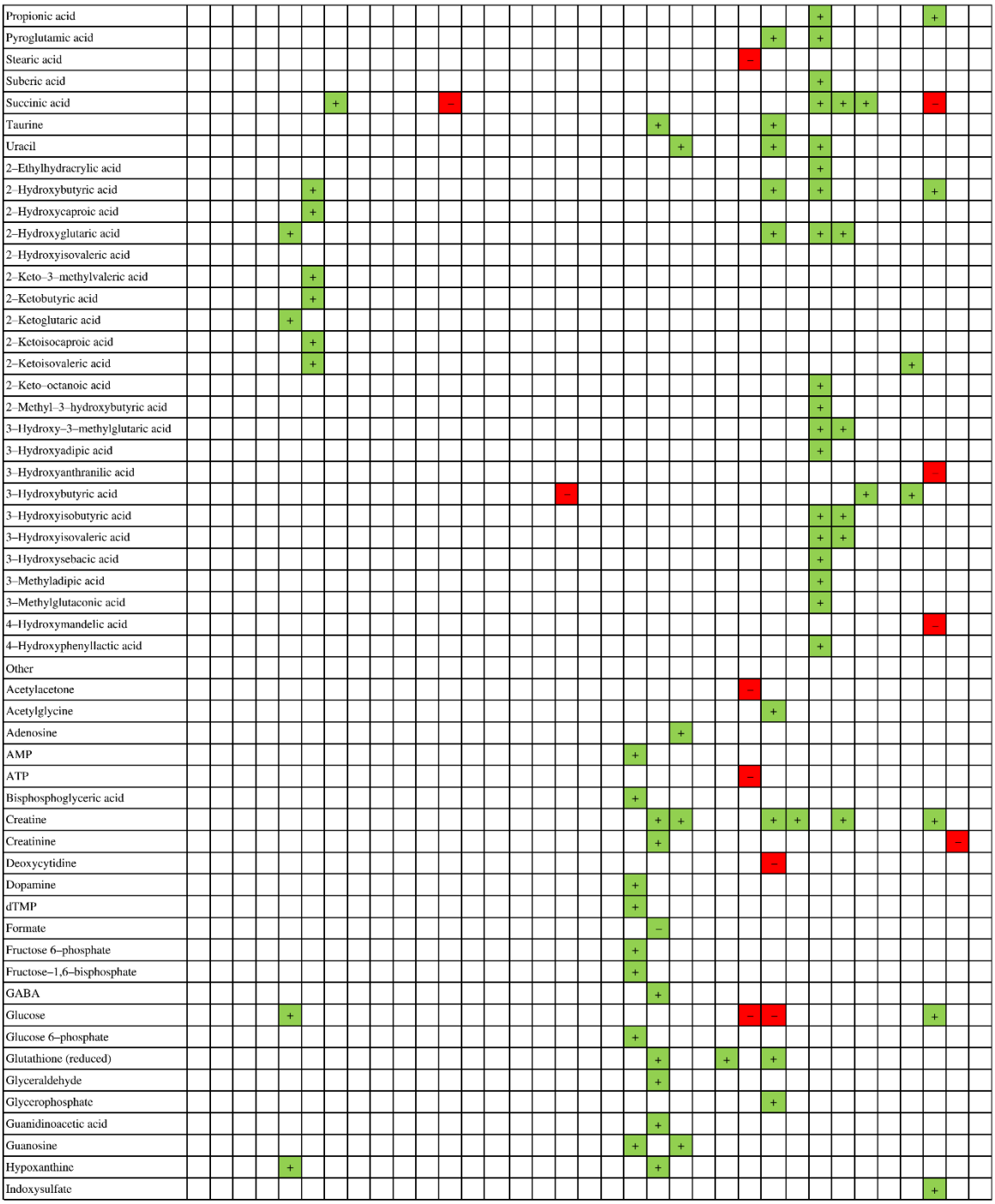

Table 1 *(continued)*

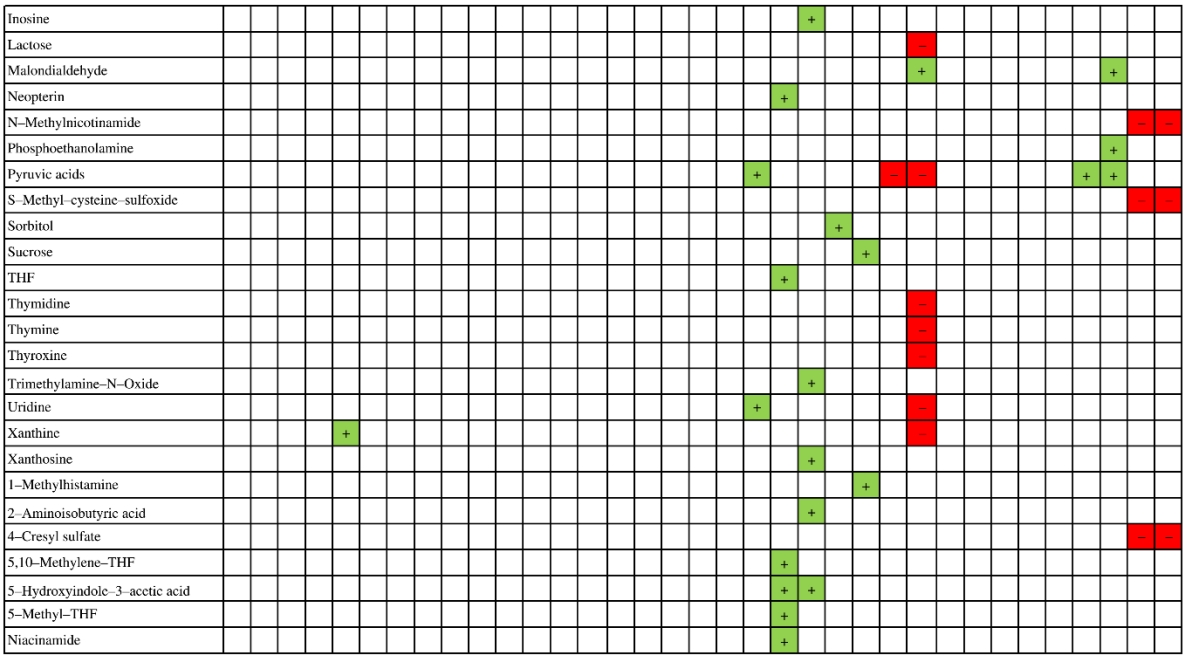

Metabolites marked as + (Green) have been reported to be elevated (in intensity) in that specific disease model/study compared to the healthy controls. Metabolites marked as - (Red) have been reported to decreased (in intensity) in that specific model/study compared to the healthy controls. Blank spaces indacate that the specific metabolite has not been reported to be significantly altered in that specific disease model/study compared to the healthy controls.

the acetoacetate/3-hydroxybutyric acid ratio is also of great importance as it reflects the mitochondrial redox state of the model (Munnich et al., 1996).

An altered redox balance can also explain observations of a perturbed catabolism of the branched chain amino acids (Fig. 1B). Firstly, the lowered NAD^+/NADH ratio inhibits the activity of the branched-chain α-ketoacid dehydrogenase complex (BCKDC) responsible for the oxidative decarboxylation of 2-ketoisocaproic acid, 2-keto-3-methylvaleric acid, 2-ketoisovaleric acid in the leucine, isoleucine and valine catabolic pathways, respectively. This leads to increased levels of 2-ketoisocaproic acid, 2-keto-3-methylvaleric acid, 2-ketoisovaleric acid and 2-hydroxycaproic acid reported in nematode models (Butler et al., 2013) and human urine (Legault et al., 2015). In addition, there is evidence that the branched-chain amino acid catabolic pathway (Fig. 1B) is dysregulated by an altered (decreased) $FAD/FADH_2$ redox state, which can be affected by deficient electron delivery to complex II. This is, for example, evident by the elevated excretion in urine of 3-hydroxyisovaleric acid in MD patients, which in these disorders would implicate a decreased $FAD/FADH_2$ ratio and subsequent inhibition of isovaleryl-CoA dehydrogenase (Reinecke et al., 2012; Smuts et al., 2013). In a similar mechanism in the isoleucine catabolism, 2-methylbutyryl-CoA has been found to be elevated, putatively due to the decreased $FAD/FADH_2$ ratio, resulting in the conversion of 2-methylbutyryl-CoA to 2-ethylhydracrylic acid and the elevated excretion of the latter in patients suffering from MD (Reinecke et al., 2012). In addition to branched-chain amino acids, the catabolism of the ketogenic amino acid, lysine (Fig. 1C), have frequently been reported in metabolomics investigations to be affected in MD via a similar regulatory mechanism (Bao et al., 2016; Falk et al., 2008; Smuts et al., 2013).

One-carbon metabolism, the methylation cycle and the transsulfuration pathway form an intricate web of pathways that are also regulated by the redox state (Fig. 1D). Although one-carbon metabolism has previously been identified as a possible cellular response to deficiencies of the OXPHOS system (Naviaux, 2014), it was not until recent metabolomics studies (Bao et al., 2016; Nikkanen et al., 2016) that altered one carbon metabolism was identified as a major consequence of mitochondrial disease. One-carbon metabolism is a process where serine acts as the major one-carbon donor to the folate cycle. During this cycle, dietary folate enters the system and is converted to tetrahydrofolate (THF). One-carbon units are donated to THF by serine, which results in the formation of 5,10-methylene-THF and glycine. The formed 5,10-methylene-THF can be reduced to 5-methyl-THF, a methyl group donor that is involved in the conversion of homocysteine to methionine in the methylation cycle, with 5-methyl-THF being converted back to THF. The one carbon cycle also forms 10-formyl THF, involved in purine synthesis (Fig. 1E) as well as 5,10-methylene-THF that is involved in pyrimidine biosynthesis (Fig. 1F). In the methylation cycle, methionine is converted to S-adenosylmethionine (SAM), a universal methyl donor to reactions that involve numerous methyltransferase reactions, including carnitine and polyamine biosynthesis as well as methylation reactions. The methylation capacity is mostly used for metabolite methylation, of which creatine and phosphatidylcholine synthesis utilizes the vast majority, up to 80% (Mudd et al., 2007). Furthermore, the folate cycle is linked to NADPH biosynthesis; therefore, serine can be considered a one-carbon donor of the generation of NADPH for antioxidant defense (Yang and Vousden, 2016). Nikkanen et al. (2016) recently reported that mitochondrial DNA replication defects disturb cellular dNTP pools and remodel one-carbon metabolism, activating de novo serine biosynthesis that ultimately drives glutathione synthesis.

Because of the central role that serine and glycine play in the one-carbon metabolism, it is not surprising that numerous metabolomics

Fig. 1. Summary of the perturbed metabolism detected in different mitochondrial disease models. a) glycolysis pathway and the TCA cycle; b) branched chain amino acids metabolism; c) tryptophan and lysine metabolism; d) one-carbon metabolism, the methylation cycle and transsulfuration pathway; e) the purine pathway; f) the urea cycle and pyrimidine pathway; g) phenylalanine and tyrosine metabolism; h) glycine, threonine and serine metabolism; i) fatty acid metabolism. This compilation of figures summarizes the findings from numerous studies on the altered metabolic profile caused by mitochondrial disease compared to healthy controls. Abbreviations used for the different models include: N = nematodes, M = mouse, C = tissue cultures, P = human plasma and U = human urine. Metabolites marked in green were reported as elevated (in intensity) in that specific disease model compared to the healthy controls. Metabolites marked in red were reported as decreased (in intensity) in that specific model compared to the healthy controls. When a metabolite is marked yellow, different studies found the specific metabolite as being increased or decreased (in intensity) in that specific disease model, thus for the yellow metabolites, current literature does not have consensus on whether the metabolite is increased or decreased in the disease model. Nicotinamide nucleotides and flavin coenzyme involved in the redox state are marked in blue.

studies reported variations in glycine and serine levels caused by MD (Table 1). Considering glycine, most studies reported that MD elevated glycine levels, including studies on nematodes (Falk et al., 2008), mouse models (Ahola-Erkkila et al., 2010; Leong et al., 2012; Nikkanen et al., 2016) and humans (Smuts et al., 2013; Shatla et al., 2014). Some studies however reported lower glycine levels in nematodes (McCormack et al., 2015; Morgan et al., 2015; Vergano et al., 2014) – again discrepancies between different studies. For serine, elevated levels were reported in nematode- and mouse models, as well as in tissue cultures and patient samples. Although serine and glycine have previously been linked to MD, it was only recently that a broader metabolomics approach (Bao et al., 2016; Nikkanen et al., 2016) identified disturbed cellular dNTP pools and remodeling of the one-carbon metabolism caused by MD and linked the altered glycine and serine levels to one-carbon metabolism. This again reiterates the value of metabolomics not only as a useful tool in identifying novel biomarkers, but also as indispensable in the elucidation of mechanistic alterations caused by mitochondrial disease.

Other notable metabolic pathways that are influenced by MD include phenylalanine and tyrosine catabolism (Fig. 1G), sphingomyelin

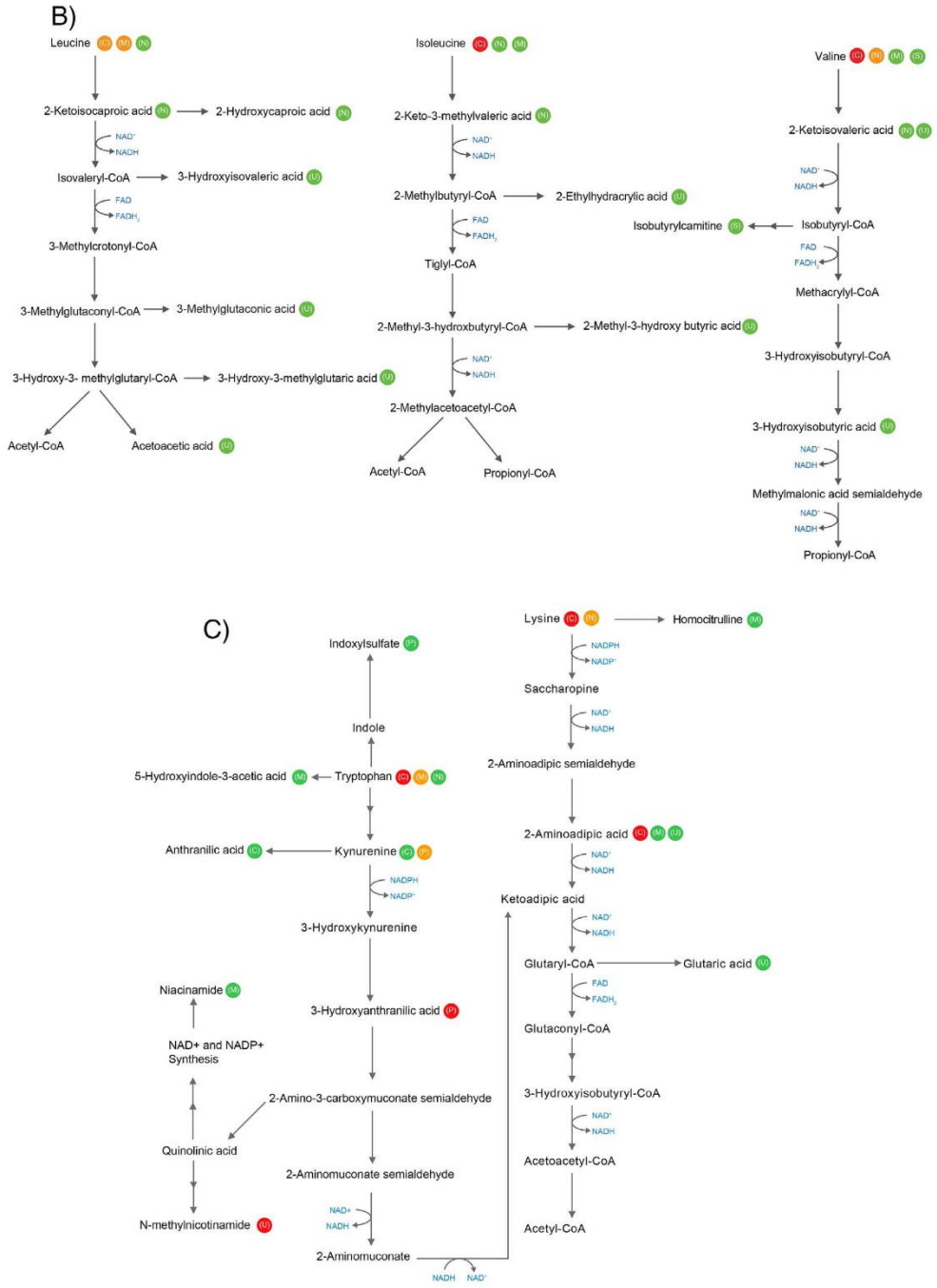

Fig. 1. (*continued*)

biosynthesis (Fig. 1H) as well as beta-oxidation (Fig. 1I), often resembling glutaric aciduria type II. Possibly also a consequence of redox shift, or in the case of phenylalanine catabolism possibly also liver dysfunction (Reinecke et al., 2012), a wide range of metabolites in these pathways have been identified to be affected by MD in numerous studies and models, including mouse models (Johnson et al., 2013; Leong et al., 2012) and patient plasma and urine (Legault et al., 2015; Reinecke et al., 2012). Several of the affected metabolites that can be attributed to increased catabolism of fatty acids and amino acids share a bioenergetics-sensing (hormone-modulated) induction pathway with the serum biomarker FGF-21 and possibly also GDF-15 (Kalko et al., 2014; Smuts et al., 2013; Suomalainen, 2011). Another consequence of phenylalanine metabolism is the formation of benzoic acid via cinnamic acid (Fig. 1G), a reaction that cannot be catalyzed by humans, but is

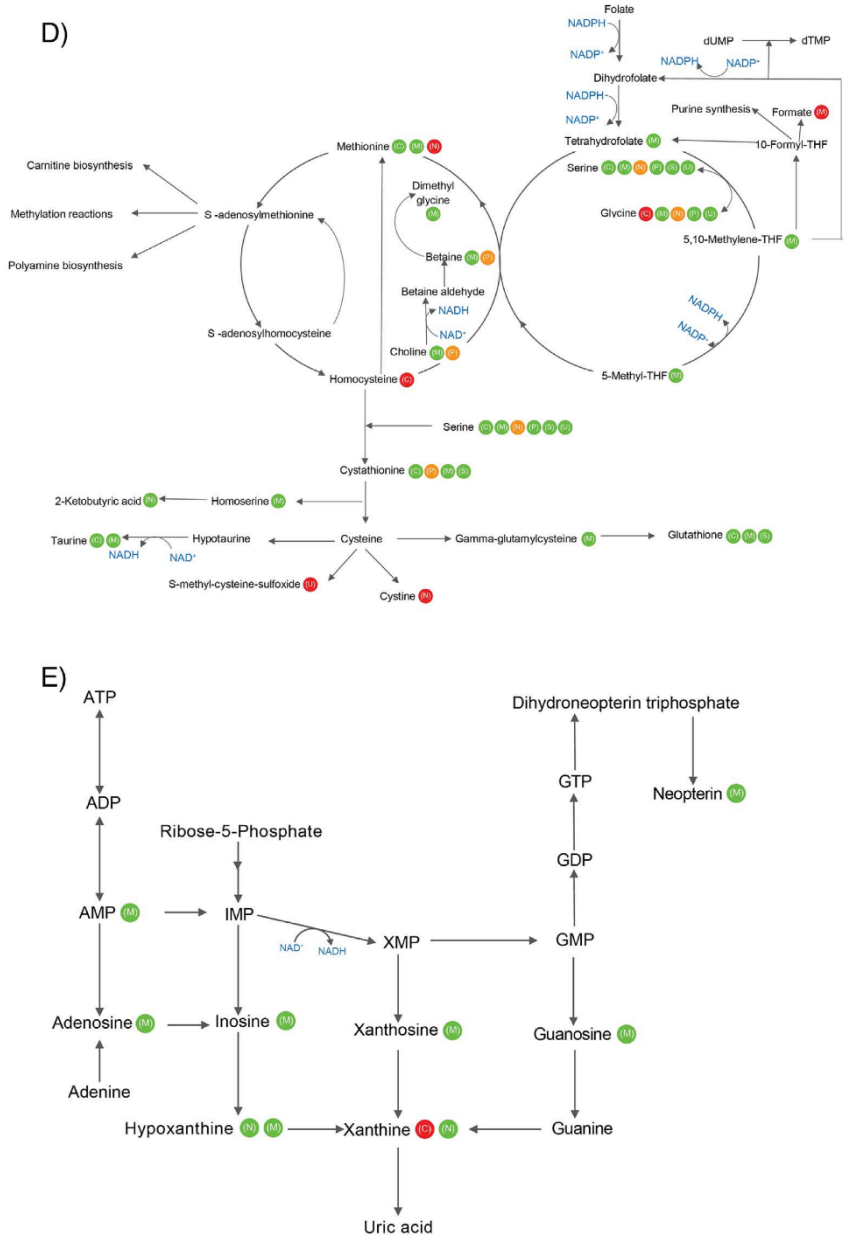

Fig. 1. (*continued*)

indeed catalyzed by the gut microbiota (Badenhorst et al., 2014). From here the benzoic acid is conjugated with glycine to form hippuric acid, another metabolite reported as perturbed by mitochondrial disease (Bao et al., 2016; Hall et al., 2015).

Clearly, in a complex disease of this kind, predicting the metabolic response in vivo at any point in time – considering the number of variables involved – is a systems biology challenge of the highest order as is evident from all the metabolic pathways affected by the disease (Fig. 1A–I). Even though some of the metabolites, such as citric acid, alanine and isoleucine, are consistently reported as elevated (Butler et al., 2013; Shaham et al., 2008; Smuts et al., 2013; Vergano et al., 2014; Vo et al., 2007), discrepancies are found for other metabolites. While glycine, lysine and glutamic acid were reported as elevated in certain studies, other studies reported decreased levels of the same metabolites (Butler et al., 2013; Falk et al., 2008; Smuts et al., 2013). These contradictions make it difficult for researchers to draw common mechanistic conclusions, as the elevation or decrease of a metabolite can change the flux of a metabolic pathway. Moreover, different altered metabolic profiles were reported for specific study models. In nematode models, Vergano et al. (2014) obtained clear metabolic separation between a complex II knockout model and nematodes with complex I and complex III knockouts, due to different metabolic alterations caused by

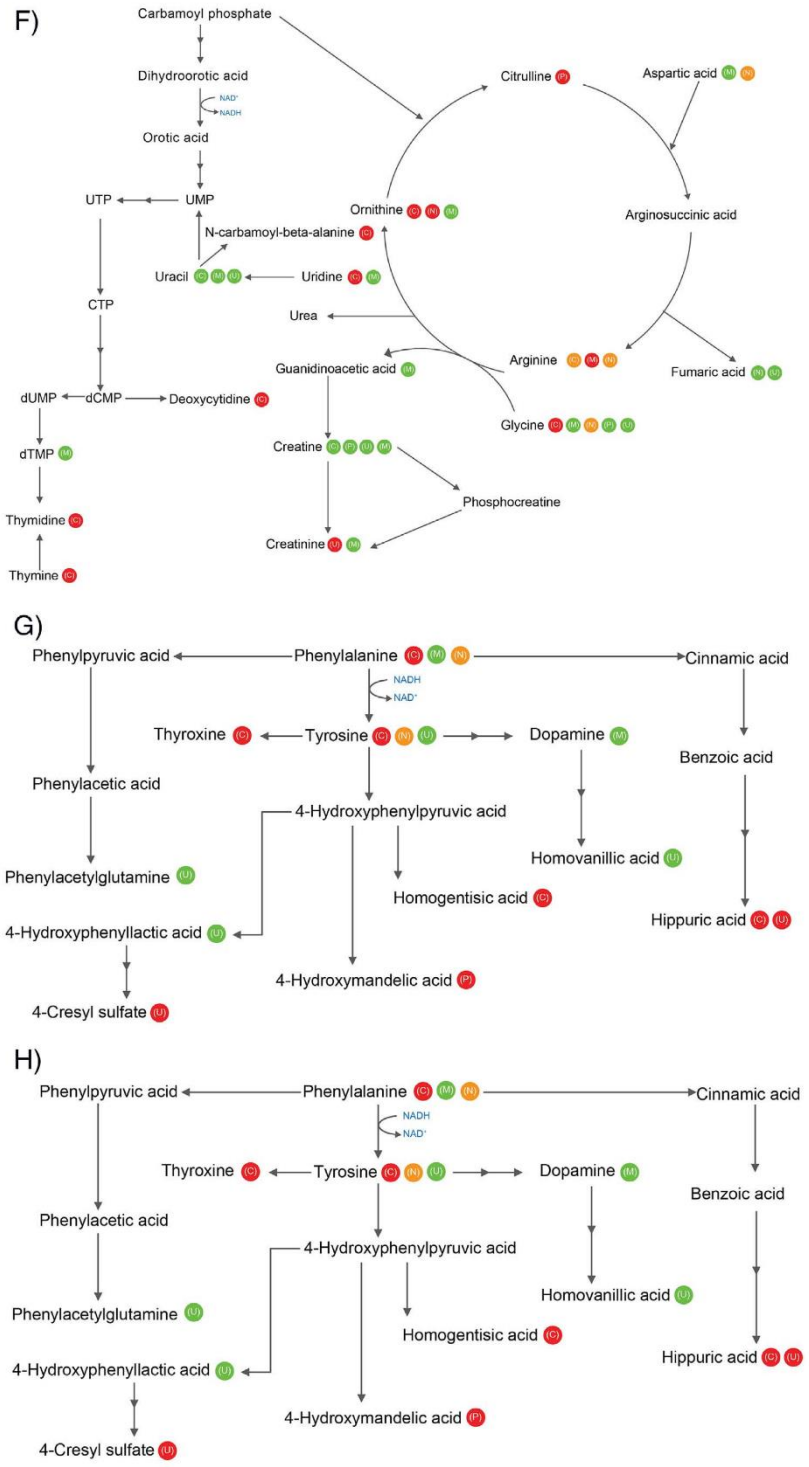

Fig. 1. (*continued*)

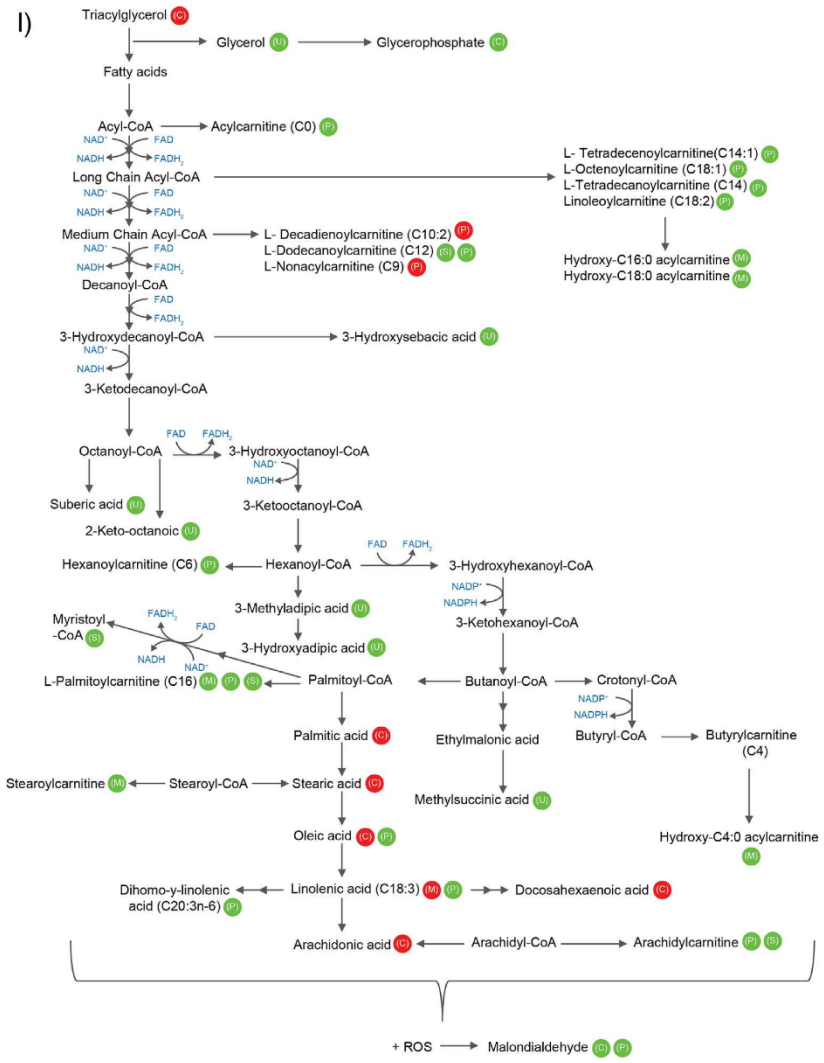

Fig. 1. (*continued*)

the knockouts. However, no metabolic separation was reported between complex I, complex III and combined complex defects when investigating human urine (Reinecke et al., 2012). Two possible explanations can be offered for this: first, it can be argued that although complex II is part of the respiratory chain, it also forms part of the TCA cycle. This could explain why a complex II metabolic profile would be more similar to the metabolic profile caused by a TCA cycle defect than an OXPHOS defect. A second argument could be that while it is possible to distinguish different mitochondrial diseases from each other in animal models, this is far more difficult to achieve in human biofluids. The reason for this is that animal models present a more controlled environment and the animals are highly inbred, while patients live in a less controlled environment where external factors could drastically influence the metabolome. Humans are also more genetically diverse, compared to animal models, adding to an increase in variation of the metabolome.

In recent studies, some of the metabolites reported in Table 1 showed promising results as potential markers to monitor MD. One example is where a ketogenic diet restored levels of 3-hydroxybutyric acid and phosphatidylcholine in deletor mice (Ahola-Erkkila et al., 2010). In another study, elevated 2-hydroxybutyrate levels in Ndufs4 knockout were restored with the help of hypoxic conditions (Jain et al., 2016). In a study using nematodes as a model, McCormack et al. demonstrated that by restoring the redox imbalance (nicotinic acid supplementation), altered sirtuin and PPAR signaling pathways were restored, which resulted in improved longevity in the nematodes with a complex I defect (McCormack et al., 2015). By administering purine or format supplementation, cells that showed growth defects as result of decreased serine levels could also be rescued (Bao et al., 2016). These studies proved that a metabolomics approach not only have the potential to identify diagnostic markers, but possibly also identify metabolic markers that can be used to monitor disease progression or even therapeutic interventions.

Lastly, normalization of metabolomics data remains problematic,

especially for urine samples. Unlike plasma, where solute concentrations are tightly controlled, urine volume can vary widely based upon water consumption and other physiological factors. Therefore, the concentrations of endogenous metabolites analyzed in urine vary widely and normalizing for these effects is necessary (Warrick et al., 2009). Normalization approaches commonly used include osmolality, creatinine concentration, and components that are common to all samples ("total useful mass spectrometry signal"). Numerous studies reported on altered creatine concentration in mitochondrial disease, including mouse models (Nikkanen et al., 2016), tissue cultures (Bao et al., 2016), plasma (Legault et al., 2015; Shaham et al., 2008) and urine (Smuts et al., 2013). Due to creatine being converted to creatinine, the use of creatinine for urine normalization in mitochondrial disease studies raises concern and should thus be reconsidered.

5. Conclusions and future prospects of metabolomics in mitochondrial disease investigations

It is evident that metabolomics, whether targeted, semi-targeted or untargeted, has been a far more successful tool for generating new information on the biochemical pathways involved in mitochondrial disease, compared to the pre-omics approach. This can be ascribed to the more holistic approach of "-omics", which focuses on all the changes in a system simultaneously to get a better idea of both the pathological and the physiological conditions (Monteiro et al., 2013). As previously mentioned, the current gold standard for diagnosing mitochondrial disease is biochemical analyses performed on muscle biopsies together with other assessments, such as clinical and histochemical assays. However, obtaining muscle biopsies requires anesthesia, is expensive and can be a very traumatic experience in pediatric patients (Smuts et al., 2013). The great strides made with high throughput molecular genetics and the reduction of its cost (notably for exome sequencing) have enabled a significant surge in identifying the mutations affecting MD, even before a patient presents with any symptoms. However, a genetics approach can be expensive, time-consuming, with numerous limitations (DaRe et al., 2013; DiMauro and Schon, 2003; Menezes et al., 2014; Schaefer et al., 2004) and thus be an unattainable process, especially in developing countries. On the other hand, a metabolic *biosignature* (a combination of biomarkers) for MD has the potential to be used as a non-invasive screening method for suspected patients, simplifying the identification of patients who require muscle biopsies (Reinecke et al., 2012; Smuts et al., 2013; Venter et al., 2015).

Another great challenge regarding mitochondrial disease is the monitoring of patients, whether for the progression of the disease or for the response to treatment (Smuts et al., 2013). A non-invasive metabolic biomarker or biosignature could fulfill this purpose, as it would not require a muscle biopsy every time information on the patient's progression or response was needed (Suomalainen, 2011; Zhang et al., 2012). This potential application is of particular interest considering the current drive to find therapeutic drugs for MD. Markers for disease progression can potentially be identified through correlation studies, where the correlation of metabolites with the deterioration of the phenotype is investigated. Once validated, these metabolites could then be used to monitor patients during or without therapies. Although possible in theory, considering its application in other diseases and with the first promising results from animal models of MD, this approach has not yet been attempted or reported in a clinical setting for MD.

In conclusion, it is clear that over a period of more than 15 years, the technology and bioinformatics tools to better identify small molecules on a comprehensive scale have evolved immensely and in a similar way to that of the other -omics tools. The implementation of these techniques in the field of mitochondrial disease has proven to be extremely beneficial and metabolomics has been able to link various potential biomarkers to mitochondrial disease. Considering the scope and mechanistic nature of the metabolic perturbations involved in MD, as reviewed here, it is more likely that a search for a combination of metabolic biomarkers, i.e. a biosignature, may present the best potential for further disclosing the cell biological consequences of this complex disease. Moreover, by targeting blood and urine metabolomics, this holistic approach is likely to provide applications of significant value to mitochondrial medicine.

References

Ahola-Erkkila, S., Carroll, C.J., Peltola-Mjosund, K., Tulkki, V., Mattila, I., Seppanen-Laakso, T., Oresic, M., Tyynismaa, H., Suomalainen, A., 2010. Ketogenic diet slows down mitochondrial myopathy progression in mice. Hum. Mol. Genet. 19 (10), 1974–1984.

Álvarez-Sánchez, B., Priego-Capote, F., Luque de Castro, M., 2010. Metabolomics analysis I. Selection of biological samples and practical aspects preceding sample preparation. TrAC Trends Anal. Chem. 29 (2), 111–119.

Badenhorst, C.P.S., Erasmus, E., van der Sluis, R., Nortje, C., van Dijk, A.A., 2014. A new perspective on the importance of glycine conjugation in the metabolism of aromatic acids. Drug Metab. Rev. 46 (3), 343–361.

Bao, X.R., Ong, S.E., Goldberger, O., Peng, J., Sharma, R., Thompson, D.A., Vafai, S.B., Cox, A.G., Marutani, E., Ichinose, F., Goessling, W., Regev, A., Carr, S.A., Clish, C.B., Mootha, V.K., 2016. Mitochondrial dysfunction remodels one-carbon metabolism in human cells. elife 5, e10575.

Barshop, B.A., 2004. Metabolomic approaches to mitochondrial disease: correlation of urine organic acids. Mitochondrion 4 (5), 521–527.

Bernier, F.P., Boneh, A., Dennett, X., Chow, C.W., Cleary, M.A., Thorburn, D.R., 2002. Diagnostic criteria for respiratory chain disorders in adults and children. Neurology 59 (9), 1406–1411.

Bouatra, S., Aziat, F., Mandal, R., Guo, A.C., Wilson, M.R., Knox, C., Bjorndahl, T.C., Krishnamurthy, R., Saleem, F., Liu, P., 2013. The human urine metabolome. PLoS One 8 (9), e73076.

Brière, J., Chrétien, D., Bénit, P., Rustin, P., 2004. Respiratory chain defects: what do we know for sure about their consequences in vivo? Biochim. Biophys. Acta Bioenergetics 1659 (2), 172–177.

Butler, J.A., Mishur, R.J., Bhaskaran, S., Rea, S.L., 2013. A metabolic signature for long life in the *Caenorhabditis elegans* Mit mutants. Aging Cell 12 (1), 130–138.

DaRe, J.T., Vasta, V., Penn, J., Tran, N.B., Hahn, S.H., 2013. Targeted exome sequencing for mitochondrial disorders reveals high genetic heterogeneity. BMC Med. Genet. 14 (1), 118.

DiMauro, S., Schon, E.A., 2003. Mitochondrial respiratory-chain disease. N. Engl. J. Med. 348 (26), 2656–2668.

Dunn, W.B., Bailey, N.J.C., Johnson, H.E., 2005. Measuring the metabolome: current analytical technologies. Analyst 130, 606–625.

Dunn, W.B., Broadhurst, D.I., Atherton, H.J., Goodacre, R., Griffin, J.L., 2011. Systems level studies of mammalian metabolomes: the roles of mass spectrometry and nuclear magnetic resonance spectroscopy. Chem. Soc. Rev. 40 (1), 387–426.

Dunn, W.B., Erban, A., Weber, R.J., Creek, D.J., Brown, M., Breitling, R., Hankemeier, T., Goodacre, R., Neumann, S., Kopka, J., 2013. Mass appeal: metabolite identification in mass spectrometry-focused untargeted metabolomics. Metabolomics 9 (1), 44–66.

Elstner, M., Turnbull, D.M., 2012. Transcriptome analysis in mitochondrial disorders. Brain Res. Bull. 88 (4), 285–293.

Esteitie, N., Hinttala, R., Wibom, R., Nilsson, H., Hance, N., Naess, K., Teär-Fahnehjelm, K., Von Döbeln, U., Majamaa, K., Larsson, N., 2005. Secondary metabolic effects in complex I deficiency. Ann. Neurol. 58 (4), 544–552.

Falk, M., Zhang, Z., Rosenjack, J., Nissim, I., Daikhin, E., Nissim, I., Sedensky, M., Yudkoff, M., Morgan, P., 2008. Metabolic pathway profiling of mitochondrial respiratory chain mutants in *C. elegans*. Mol. Genet. Metab. 93 (4), 388–397.

Falk, M.J., Rao, M., Ostrovsky, J., Daikhin, E., Nissim, I., Yudkoff, M., 2011. Stable isotopic profiling of intermediary metabolic flux in developing and adult stage *Caenorhabditis elegans*. JoVE (48), e2288.

Fang, Z., Gonzalez, F.J., 2014. LC–MS-based metabolomics: an update. Arch. Toxicol. 1–12.

Gorman, G.S., Schaefer, A.M., Ng, Y., Gomez, N., Blakely, E.L., Alston, C.L., Feeney, C., Horvath, R., Yu-Wai-Man, P., Chinnery, P.F., 2015. Prevalence of nuclear and mitochondrial DNA mutations related to adult mitochondrial disease. Ann. Neurol. 77 (5), 753–759.

Haas, R.H., Parikh, S., Falk, M.J., Saneto, R.P., Wolf, N.I., Darin, N., Wong, L., Cohen, B.H., Naviaux, R.K., 2008. The in-depth evaluation of suspected mitochondrial disease. Mol. Genet. Metab. 94 (1), 16–37.

Hall, A.M., Vilasi, A., Garcia-Perez, I., Lapsley, M., Alston, C.L., Pitceathly, R.D., McFarland, R., Schaefer, A.M., Turnbull, D.M., Beaumont, N.J., 2015. The urinary proteome and metabonome differ from normal in adults with mitochondrial disease. Kidney Int. 87 (3), 610–622.

Jain, I.H., Zazzeron, L., Goli, R., Alexa, K., Schatzman-Bone, S., Dhillon, H., Goldberger, O., Peng, J., Shalem, O., Sanjana, N.E., Zhang, F., 2016. Hypoxia as a therapy for mitochondrial disease. Eur. J. Pharmacol. 352 (6281), 54–61.

Johnson, S.C., Yanos, M.E., Kayser, E.B., Quintana, A., Sangesland, M., Castanza, A., Uhde, L., Hui, J., Wall, V.Z., Gagnidze, A., Oh, K., Wasko, B.M., Ramos, F.J., Palmiter, R.D., Rabinovitch, P.S., Morgan, P.G., Sedensky, M.M., Kaeberlein, M., 2013. mTOR inhibition alleviates mitochondrial disease in a mouse model of Leigh syndrome. Science 342 (6165), 1524–1528.

Kalko, S.G., Paco, S., Jou, C., Rodríguez, M.A., Meznaric, M., Rogac, M., Jekovec-Vrhovsek, M., Sciacco, M., Moggio, M., Fagiolari, G., De Paepe, B., De Meirleir, L.,

Ferrer, I., Roig-Quilis, M., Munell, F., Montoya, J., López-Gallardo, E., Ruiz-Pesini, E., Artuch, R., Montero, R., Torner, F., Nascimento, A., Ortez, C., Colomer, J., Jimenez-Mallebrera, C., 2014. Transcriptomic profiling of TK2 deficient human skeletal muscle suggests a role for the p53 signalling pathway and identifies growth and differentiation factor-15 as a potential novel biomarker for mitochondrial myopathies. BMC Genomics 15, 91.

Kamboj, M., 2008. Clinical approach to the diagnoses of inborn errors of metabolism. Pediatr. Clin. N. Am. 55 (5), 1113–1127.

Kami, K., Fujita, Y., Igarashi, S., Koike, S., Sugawara, S., Ikeda, S., Sato, N., Ito, M., Tanaka, M., Tomita, M., 2012. Metabolomic profiling rationalized pyruvate efficacy in cybrid cells harboring MELAS mitochondrial DNA mutations. Mitochondrion 12 (6), 644–653.

Koene, S., Hendriks, J.C.M., Dirks, I., de Boer, L., de Vries, M.C., Janssen, M.C.H., Smuts, I., Fung, C.-W., Wong, V.C.N., de Coo, I.R.F.M., Vill, K., Stendel, C., Klopstock, T., Falk, M.J., McCormick, E.M., McFarland, R., de Groot, I.J.M., Smeitink, J.A.M., 2016. International Pediatric Mitochondrial Disease Scale. J. Inherit. Metab. Dis. 39, 705–712.

Legault, J.T., Strittmatter, L., Tardif, J., Sharma, R., Tremblay-Vaillancourt, V., Aubut, C., Boucher, G., Clish, C.B., Cyr, D., Daneault, C., 2015. A Metabolic signature of mitochondrial dysfunction revealed through a monogenic form of leigh syndrome. Cell Rep. 13 (5), 981–989.

Leong, D.W., Komen, J.C., Hewitt, C.A., Arnaud, E., McKenzie, M., Phipson, B., Bahlo, M., Laskowski, A., Kinkel, S.A., Davey, G.M., Heath, W.R., Voss, A.K., Zahedi, R.P., Pitt, J.J., Chrast, R., Sickmann, A., Ryan, M.T., Smyth, G.K., Thorburn, D.R., Scott, H.S., 2012. Proteomic and metabolomic analyses of mitochondrial complex I-deficient mouse model generated by spontaneous B2 short interspersed nuclear element (SINE) insertion into NADH dehydrogenase (ubiquinone) Fe-S protein 4 (Ndufs4) gene. J. Biol. Chem. 287 (24), 20652–20663.

Leong, X.F., Ng, C.Y., Tardif, J., Jaarin, K., 2015. Animal models in cardiovascular research: hypertension and atherosclerosis. Biomed. Res. Int. 2015, 1–11.

Martins, A.M., 1999. Inborn errors of metabolism: a clinical overview. Sao Paulo Med. J. 117 (6), 251–265.

McCormack, S., Polyak, E., Ostrovsky, J., Dingley, S.D., Rao, M., Kwon, Y.J., Xiao, R., Zhang, Z., Nakamaru-Ogiso, E., Falk, M.J., 2015. Pharmacologic targeting of sirtuin and PPAR signaling improves longevity and mitochondrial physiology in respiratory chain complex I mutant *Caenorhabditis elegans*. Mitochondrion 22, 45–59.

Menezes, M.J., Riley, L.G., Christodoulou, J., 2014. Mitochondrial respiratory chain disorders in childhood: insights into diagnosis and management in the new era of genomic medicine. Biochim. Biophys. Acta Gen. Subj. 1840 (4), 1368–1379.

Monteiro, M., Carvalho, M., Bastos, M., Guedes de Pinho, P., 2013. Metabolomics analysis for biomarker discovery: advances and challenges. Curr. Med. Chem. 20 (2), 257–271.

Morgan, P., Higdon, R., Kolker, N., Bauman, A., Ilkayeva, O., Newgard, C., Kolker, E., Steele, I., Sedensky, M., 2015. Comparison of proteomic and metabolomic profiles of mutants of the mitochondrial respiratory chain in *Caenorhabditis elegans*. Mitochondrion 20, 95–102.

Mudd, S.H., Brosnan, J.T., Brosnan, M.E., Jacobs, R.L., Stabler, S.P., Allen, R.H., Vance, D.E., Wagner, C., 2007. Methyl balance and transmethylation fluxes in humans. Am. J. Clin. Nutr. 85, 19–25.

Munnich, A., Rötig, A., Chretien, D., Saudubray, J., Cormier, V., Rustin, P., 1996. Clinical presentations and laboratory investigations in respiratory chain deficiency. Eur. J. Pediatr. 155, 262–274.

Naviaux, R.K., 2014. Metabolic features of the cell danger response. Mitochondrion 16, 7–17.

Nikkanen, J., Forsström, S., Euro, L., Paetau, I., Kohnz, R.A., Wang, L., Chilov, D., Viinamäki, J., Roivainen, A., Marjamäki, P., 2016. Mitochondrial DNA replication defects disturb cellular dNTP pools and remodel one-carbon metabolism. Cell Metab. 23 (4), 635–648.

Nikolic, S.B., Sharman, J.E., Adams, M.J., Edwards, L.M., 2014. Metabolomics in hypertension. J. Hypertens. 32 (6), 1159–1169.

Oliver, S.G., Winson, M.K., Kell, D.B., Baganz, F., 1998. Systematic functional analysis of the yeast genome. Trends Biotechnol. 16 (9), 373–378.

Parikh, S., Goldstein, A., Koenig, M.K., Scaglia, F., Enns, G.M., Saneto, R., Anselm, I., Cohen, B.H., Falk, M.J., Greene, C., Gropman, A.L., 2015. Diagnosis and management of mitochondrial disease: a consensus statement from the Mitochondrial Medicine Society. Am. Coll. Med. Genet. Genomics 17 (9), 689–701.

Phoenix, C., Schaefer, A.M., Elson, J., Morava, E., Bugiani, M., Uziel, G., Smeitink, J., Turnbull, D., McFarland, R., 2006. A scale to monitor progression and treatment of mitochondrial disease in children. Neuromuscul. Disord. 16 (12), 814–820.

Rasanu, T., Mehedinti, T., Hancu, A., Damian, I., Mihailov, C., Rasanu, I., 2011. Mitochondrial myopathies: current diagnosis (ii). Rom. J. Neurol. Psychiatry 10 (1), 12.

Reinecke, F., Smeitink, J.A., Van Der Westhuizen, F.H., 2009. OXPHOS gene expression and control in mitochondrial disorders. Biochim. Biophys. Acta (BBA) - Mol. Basis Dis. 1792 (12), 1113–1121.

Reinecke, C.J., Koekemoer, G., van der Westhuizen, F.H., Louw, R., Lindeque, J.Z., Mienie, L.J., Smuts, I., 2012. Metabolomics of urinary organic acids in respiratory chain deficiencies in children. Metabolomics 8 (2), 264–283.

Suomalainen, A., 2011. Biomarkers for mitochondrial respiratory chain disorders. J. Inherit. Metab. Dis. 34, 277–282.

Schaefer, A.M., Taylor, R.W., Turnbull, D.M., Chinnery, P.F., 2004. The epidemiology of mitochondrial disorders—past, present and future. Biochim. Biophys. Acta Bioenergetics 1659 (2), 115–120.

Shaham, O., Wei, R., Wang, T.J., Ricciardi, C., Lewis, G.D., Vasan, R.S., Carr, S.A., Thadhani, R., Gerszten, R.E., Mootha, V.K., 2008. Metabolic profiling of the human response to a glucose challenge reveals distinct axes of insulin sensitivity. Mol. Syst. Biol. 4, 214.

Shaham, O., Slate, N.G., Goldberger, O., Xu, Q., Ramanathan, A., Souza, A.L., Clish, C.B., Sims, K.B., Mootha, V.K., 2010. A plasma signature of human mitochondrial disease revealed through metabolic profiling of spent media from cultured muscle cells. Proc. Natl. Acad. Sci. U. S. A. 107 (4), 1571–1575.

Shatla, H.M., Tomoum, H.Y., Elsayed, S.M., Elagouza, I.A., Shatla, R.H., Mohsen, M.M., Hamed, A.N., 2014. Role of plasma amino acids and urinary organic acids in diagnosis of mitochondrial diseases in children. Pediatr. Neurol. 51 (6), 820–825.

Sim, K.G., Carpenter, K., Hammond, J., Christodoulou, J., Wilcken, B., 2002. Acylcarnitine profiles in fibroblasts from patients with respiratory chain defects can resemble those from patients with mitochondrial fatty acid [beta]-oxidation disorders. Metabolism 51 (3), 366–371.

Smeitink, J.A., Zeviani, M., Turnbull, D.M., Jacobs, H.T., 2006. Mitochondrial medicine: a metabolic perspective on the pathology of oxidative phosphorylation disorders. Cell Metab. 3 (1), 9–13.

Smuts, I., van der Westhuizen, Francois H., Louw, R., Mienie, L.J., Engelke, U.F., Wevers, R.A., Mason, S., Koekemoer, G., Reinecke, C.J., 2013. Disclosure of a putative biosignature for respiratory chain disorders through a metabolomics approach. Metabolomics 9 (2), 379–391.

Taivassalo, T., Ayyad, K., Haller, R.G., 2012. Increased capillaries in mitochondrial myopathy: implications for the regulation of oxygen delivery. Brain J. Neurol. 135 (Pt 1), 53–61.

Tyynismaa, H., Carroll, C.J., Raimundo, N., Ahola-Erkkila, S., Wenz, T., Ruhanen, H., Guse, K., Hemminki, A., Peltola-Mjosund, K.E., Tulkki, V., Oresic, M., Moraes, C.T., Pietilainen, K., Hovatta, I., Suomalainen, A., 2010. Mitochondrial myopathy induces a starvation-like response. Hum. Mol. Genet. 19 (20), 3948–3958.

Venter, L., Lindeque, Z., van Rensburg, P.J., van der Westhuizen, F., Smuts, I., Louw, R., 2015. Untargeted urine metabolomics reveals a biosignature for muscle respiratory chain deficiencies. Metabolomics 1–11.

Vergano, S.S., Rao, M., McCormack, S., Ostrovsky, J., Clarke, C., Preston, J., Bennett, M.J., Yudkoff, M., Xiao, R., Falk, M.J., 2014. In vivo metabolic flux profiling with stable isotopes discriminates sites and quantifies effects of mitochondrial dysfunction in *C. elegans*. Mol. Genet. Metab. 111 (3), 331–341.

Vo, T.D., Lee, W.P., Palsson, B.O., 2007. Systems analysis of energy metabolism elucidates the affected respiratory chain complex in Leigh's syndrome. Mol. Genet. Metab. 91 (1), 15–22.

Warrick, B.M., Hnatyshyna, S., Otta, K., Reilya, M.D., Sandersa, M., Zhanga, H., Drexlera, D.M., 2009. Normalization strategies for metabonomic analysis of urine samples. J. Chromatogr. B 877, 547–552.

Wikoff, W.R., Anforab, A.T., Liub, J., Schultzb, P.G., Lesleyb, S.A., Petersb, E.C., Siuzdaka, G., 2009. Metabolomics analysis reveals large effects of gut microflora on mammalian blood metabolites. PNAS 106 (10), 3698–3703.

Wolf, N.I., Smeitink, J.A., 2002. Mitochondrial disorders: a proposal for consensus diagnostic criteria in infants and children. Neurology 59 (9), 1402–1405.

Yang, M., Vousden, K.H., 2016. Serine and one-carbon metabolism in cancer. Nat. Rev. Cancer 16 (10), 650–662.

Zhang, X., Clausen, M.R., Zhao, X., Zheng, H., Bertram, H.C., 2012. Enhancing the power of liquid chromatography–mass spectrometry-based urine metabolomics in negative ion mode by optimization of the additive. Anal. Chem. 84 (18), 7785–7792.

Annexure B

B

A urinary biosignature for mitochondrial myopathy, encephalopathy, lactic acidosis and stroke like episodes (MELAS)

Esterhuizen *et al*., 2018

Mitochondrion

Impact factor (2016/2017): 3.704

Mitochondrion xxx (xxxx) xxx–xxx

Contents lists available at ScienceDirect

Mitochondrion

journal homepage: www.elsevier.com/locate/mito

A urinary biosignature for mitochondrial myopathy, encephalopathy, lactic acidosis and stroke like episodes (MELAS)

Karien Esterhuizen[a], J. Zander Lindeque[a], Shayne Mason[a], Francois H. van der Westhuizen[a], Anu Suomalainen[b], Anna H. Hakonen[b], Christopher J. Carroll[b], Richard J. Rodenburg[c], Paul B. de Laat[c], Mirian C.H. Janssen[c], Jan A.M. Smeitink[c], Roan Louw[a,*]

[a] Mitochondria Research Laboratory, Centre for Human Metabolomics, North-West University, Potchefstroom, South Africa
[b] Research Programs Unit, Molecular Neurology, Biomedicum-Helsinki, University of Helsinki, Helsinki, Finland
[c] Radboud Center for Mitochondrial Medicine, Department of Pediatrics, Radboud University Nijmegen Medical Center, Nijmegen, The Netherlands

ARTICLE INFO

Keywords:
MELAS
m.3243A > G
Metabolomics
Mutation
Metabolism
mtDNA

ABSTRACT

We used a comprehensive metabolomics approach to study the altered urinary metabolome of two mitochondrial myopathy, encephalopathy lactic acidosis and stroke like episodes (MELAS) cohorts carrying the m.3243A > G mutation.

The first cohort were used in an exploratory phase, identifying 36 metabolites that were significantly perturbed by the disease. During the second phase, the 36 selected metabolites were able to separate a validation cohort of MELAS patients completely from their respective control group, suggesting usefulness of these 36 markers as a diagnostic set. Many of the 36 perturbed metabolites could be linked to an altered redox state, fatty acid catabolism and one-carbon metabolism. However, our evidence indicates that, of all the metabolic perturbations caused by MELAS, stalled fatty acid oxidation prevailed as being particularly disturbed.

The strength of our study was the utilization of five different analytical platforms to generate the robust metabolomics data reported here. We show that urine may be a useful source for disease-specific metabolomics data, linking, amongst others, altered one-carbon metabolism to MELAS. The results reported here are important in our understanding of MELAS and might lead to better treatment options for the disease.

1. Introduction

Mitochondrial diseases are one of the most common inborn errors of metabolism, with a minimum prevalence of 1:5000 (Gorman et al., 2015; Schaefer et al., 2008). Mitochondrial myopathy, encephalopathy, lactic acidosis and stroke like episodes, better known as MELAS (MIM 540000), is one such a mitochondrial disease and was first described in 1984 as a "neurodegenerative disease caused by the decreased ability of cells to produce sufficient energy in the form of ATP" (Pavlakis et al., 1984). In 1990, the MELAS phenotype was associated with a specific mutation, now known as the m.3243A > G mutation (Goto et al., 1990). This mutation is a point mutation on position 3243 of the mitochondrial DNA (mtDNA), where an adenine (A) is substituted with a guanine (G) in the MT-TL 1 gene. The latter gene encodes for a transfer ribonucleic acid (tRNA), which recognizes the codons UUA and UUG for the amino acid leucine in mitochondrial translation (Scaglia and Northrop, 2006; Kami et al., 2012). The mutation thus disturbs mitochondrial protein synthesis, ultimately affecting Complexes I, III, IV and V of the oxidative phosphorylation (OXPHOS) system. Although almost 80% of all MELAS cases are caused by the m.3243A > G mutation, other mtDNA mutations have later been associated with the MELAS phenotype, including the m.3244G > A, m.3258T > C, m.3271T > C, m.3291T > C and m.8356T > C mutation (Ruiz-Pesini et al., 2007; Scaglia and Northrop, 2006).

Patients diagnosed with MELAS can also present with a wide range of symptoms, varying in degree of prevalence and severity. However, in this study, a MELAS phenotype was defined as a patient carrying the m.3243A > G mutation AND that had at least one stroke like episode. Although late onset MELAS does occur, these patients were not included in this study. Initially, the m.3243A > G mutation was specifically associated with MELAS, however, over time various other phenotypes have also been linked to this mutation, including maternally inherited diabetes and deafness (MIDD), progressive external ophthalmoplegia (PEO) and mitochondrial recessive ataxia syndrome (MIRAS) (Scaglia and Northrop, 2006; Manwaring et al., 2007).

A recent study attempted to identify mechanistic differences

* Corresponding author at: North-West University, Potchefstroom Campus, Private Bag X6001, Potchefstroom 2520, South Africa.
E-mail address: Roan.Louw@nwu.ac.za (R. Louw).

https://doi.org/10.1016/j.mito.2018.02.003
Received 17 August 2017; Received in revised form 27 January 2018; Accepted 15 February 2018
1567-7249/ © 2018 Elsevier B.V. and Mitochondria Research Society. All rights reserved.

Please cite this article as: Esterhuizen, K., Mitochondrion (2018), https://doi.org/10.1016/j.mito.2018.02.003

between different m.3243A > G phenotypes using nuclear magnetic resonance (NMR) spectroscopy. With this single metabolomics technique, the authors were able to identify six urinary metabolites (all decreased in the patients, compared to the controls) that were able to distinguish MELAS patients from controls (Hall et al., 2015). The markers included *N*-methylnicotinamide, hippurate, creatinine, 4-cresyl sulfate, glycolate, and a marker with unconfirmed identity, possibly 4-hydroxyphenylacetic acid. Although these markers point towards altered phenylalanine and tyrosine metabolism, arginine metabolism (creatinine) and a connection to gut microbial metabolism (4-cresyl sulfate and glycolate), the exact mechanism(s) for these changes remains elusive. Here we aimed to extend these findings on MELAS by investigating the urine metabolome of MELAS patients using a multi-platform metabolomics approach. With a larger metabolome coverage, additional metabolites affected in the MELAS patients, compared to healthy controls, can potentially be identified. This can potentially provide a more extensive and improved biochemical understanding of the metabolic perturbations resulting from this specific phenotype.

2. Methods

2.1. Patients and ethics

Urine samples of two cohorts of genetically confirmed m.3243A > G MELAS patients and healthy controls were obtained from the Radboud University Medical Center in Nijmegen, The Netherlands and the University of Helsinki, Finland. To ensure group homogeneity, exclusion criteria were applied to the original cohorts, namely, 1) controls that received either medication or supplementation at the time of sample collection; 2) controls with a medical condition (such as diabetes, hypertension, etc.) Characteristics of the patients and controls are summarized in Tables 1 and 2, including data on the urinary epithelial cell m.3243A > G mutation load measured in the patients.

The study complied with all applicable institutional guidelines and terms of the Declaration of Helsinki of 1975 (as revised in 2013) for investigation of human participants. Ethical approval was obtained from the Health Research Ethics Committee (HREC) of the North-West University (NWU-00170-13-S1). All the patients as well as the controls provided written informed consent for their urine samples to be used for research purposes.

2.2. Metabolic profiling

A multi-platform metabolomics approach, which consisted of targeted as well as untargeted techniques, was used to analyze the urine samples of the MELAS patients and healthy controls in order to obtain an extensive metabolomics data set. Targeted analyses consisted of liquid chromatography tandem-mass spectrometry (LC-MS/MS) while untargeted analyses consisted of gas chromatography–mass spectrometry (GC–MS), nuclear magnetic resonance (NMR) spectroscopy and liquid chromatography mass spectrometry with ion mobility (LC-IM-MS) — in positive and negative ionization mode. The protocols for the metabolomics techniques and sample preparation used are discussed in detail in the SI.

2.3. Statistical analyses

Data matrixes obtained from the GC–MS, LC-MS/MS, NMR and the two LC-IM-MS platforms were pre-processed individually and were then combined into one single metabolomics data set (pre-processing details are given in the SI). The data were normalized to creatinine, as discussed in the SI. The data was then log-transformed before univariate and multivariate statistical analyses. Univariate analyses (student t–test and effect size) were performed in Excel 2013 (Microsoft Inc.), while the multivariate analyses [principle component analysis (PCA) and heatmaps] were done using Matlab (Mathworks, Natick, Ma) and MetaboAnalyst 3.0 (www.metaboanalyst.ca), respectively. A feature with a *t*-test P value of < 0.05 and an effect size *d* value of > 0.8 was considered important, thus showing statistical significant and practical differences between the patient group and the healthy controls. The covariance and discriminatory power of the important metabolites were visualized with PCA, heatmaps and a volcano plot. The identity of the important features were determined from matching the spectral information (NMR), retention time, high resolution mass and/or fragmentation spectra (MS) to in-house and commercial libraries as well as public databases. Confidence levels for each identity were included (Fiehn et al., 2007) as well as the analytical platform used to detect the metabolite (Table 3).

Table 1
Characteristics of the MELAS patients and healthy controls of the Nijmegen cohort used in this study (means ± standard deviation).

Characteristic	Patients	Controls
Total, N	9	29
Age, y	31.4 ± 11.6	34.8 ± 19.8
Male	6	10
Female	3	19
Creatinine (mmol/L)	7.2 ± 5.2	13.2 ± 7.1
Osmolality(mOsm/kg)	570.2 ± 279.4	765.6 ± 271.7
NMDAS Score	44.9 ± 18.7	N/A
% m.3243A > G	81 ± 0.19	N/A
Symptoms (number of patients presenting with symptoms)		
Cardiomyopathy	3 (33.3%)	N/A
Epilepsy	7 (77.8%)	N/A
Myopathy	9 (100%)	N/A
Strokes	9 (100%)	N/A
GI dysmotility	7 (77.8%)	N/A
Diabetes	5 (55.6%)	N/A
Renal insufficiency	0 (0%)	N/A
Hearing loss	9 (100%)	N/A
Medication (number of patients exposed)		
Acetylsalicylic acid	1 (11.1%)	N/A
Angiotensin-converting-enzyme inhibitor (ACE inhibitor)	1 (11.1%)	N/A
Anticoagulant	2 (22.2%)	N/A
Antiepileptic	7 (77.8%)	N/A
Angiotensin Receptor Blockers (ARBs)	1 (11.1%)	N/A
Beta blockers	2 (22.2%)	N/A
Calcium antagonist	1 (11.1%)	N/A
Diuretic	1 (11.1%)	N/A
Insulin	4 (44.4%)	N/A
Laxative	1 (11.1%)	N/A
Statin	1 (11.1%)	N/A
Sulfanylurea derivative	1 (11.1%)	N/A
Supplements (number of patients exposed)		
Arginine	2 (22.2%)	N/A
B12 carnitine	1 (11.1%)	N/A
Carnitine	1 (11.1%)	N/A
Coenzyme Q10	2 (22.2%)	N/A
Folic acid	1 (11.1%)	N/A
Riboflavin	2 (22.2%)	N/A

The m.3243A > G mutation load was determined in urinary epithelial cells as described earlier (de Laat et al., 2012).

3. Results

3.1. Exploratory phase

The Nijmegen cohort were utilized for the exploratory phase, i.e. searching for a biosignature for MELAS. Univariate measures — student's *t*-test (P < 0.05) and effect size (d > 0.8) — highlighted 36 metabolites that differed significantly between the MELAS patients and healthy controls (Table 3). All but four of the 36 urinary metabolites were increased in the MELAS patients (Fig. 1B + C), with only sarcosine, glycerol, hydroxylamine and 6-azathymine being decreased. The

Table 2
Characteristics of the MELAS patients and healthy controls of the Helsinki cohort used in this study (means ± standard deviation).

Characteristic	Patients	Controls
Total, N	2	7
Age, y	54.7 ± 2.2	38.5 ± 13.6
Creatinine (mmol/L)	7.4 ± 2.4	16.2 ± 2.9
Osmolality(mOsm/kg)	504.5 ± 187.4	755.0 ± 69.2
% m.3243A > G urine	71.5 ± 20.5	N/A
% m.3243A > G blood	21.5 ± 9.2	N/A
Symptoms (number of patients presenting with symptoms)		
Ataxia	1 (50%)	N/A
Cardiomyopathy	2 (100%)	N/A
Depression	2 (100%)	N/A
Diabetes	2 (100%)	N/A
Hearing loss	2 (100%)	N/A
Hyperaldosteronism	1 (50%)	N/A
Myopathy	1 (50%)	N/A
Migraine-type headache	1 (50%)	N/A
Ptosis	1 (50%)	N/A
Medication (number of patients exposed)		
Acetylsalicylic acid	1 (50%)	N/A
Angiotensin-converting-enzyme inhibitor (ACE inhibitor)	1 (50%)	N/A
Beta blocker	1 (50%)	N/A
Benzodiazepines	2 (100%)	N/A
Insulin	2 (100%)	N/A
Metformin	1 (50%)	N/A
Sulfanylurea derivative	1 (50%)	N/A
Supplements (number of patients exposed)		
Calcium	1 (50%)	N/A
Coenzyme Q10	1 (50%)	N/A
Iron	1 (50%)	N/A
Magnesium	2 (100%)	N/A
Omega	2 (100%)	N/A
Vitamin B	1 (50%)	N/A
Vitamin D	1 (50%)	N/A

The m.3243A > G mutation load was determined in urinary epithelial cells.

visualized covariance of these metabolites (Fig. 1A) resulted in separate grouping of the MELAS patients and controls (albeit with some overlap). The PCA scores plot show that the MELAS patients are more homogenous than the controls – indicating a more defined metabolic profile in comparison to the controls. A Venn diagram (Fig. 2) illustrates the contribution of each analytical platform used in this study towards the final 36 important metabolites detected. Although a large number of features were detected using each analytical platform, only those metabolites that differed significantly between the MELAS and control groups and could be identified/partially identified were considered — forming the final metabolic fingerprint.

3.2. Validation phase

The Helsinki cohort were used for the validation phase of this study. After identifying the 36 metabolites for MELAS using the Nijmegen cohort during the exploratory phase, data on the same 36 metabolites were extracted from the Helsinki cohort and used for the validation phase. The visualized covariance of these metabolites (Fig. 3) showed that the 36 metabolite fingerprint strongly separated MELAS patients from controls in a different sample set.

4. Discussion

We report here a multi-platform metabolomics investigation of the urinary metabolome of MELAS patients carrying the m.3243A > G mutation. We show that urine may be a useful source for disease-specific metabolomics data. Furthermore, we identified a 36 metabolite fingerprint that partially-separated the patients from the controls in two separate cohorts, suggesting usefulness of these 36 separate markers as a diagnostic set.

Several of the affected pathways identified by our metabolomics approach was disturbed by redox-status (Fig. 4), with increased levels of lactic acid, pyruvic acid, acetoacetic acid and the branched chain amino acids (leucine, isoleucine). These metabolites have previously been linked to mitochondrial diseases in various studies, using different mitochondrial disease models (Esterhuizen et al., 2017) and fits with an altered NAD^+/NADH ratio, now considered key in the development of mitochondrial disease (Khan et al., 2014). Cofactors NADH and $FADH_2$ are formed in the tricarboxylic acid (TCA) cycle and serve as electron carriers onto the complexes of the OXPHOS system. When a defect in any one of the components of the OXPHOS system occurs, the flow of electrons along this chain is hindered. This perturbed flow results in altered levels of oxidized cofactors (NAD^+, FADH) to reduced cofactors (NADH, $FADH_2$), i.e. a redox imbalance (Brière et al., 2004; Khan et al., 2014; Naviaux, 2014; Reinecke et al., 2012; Smeitink et al., 2006), affecting dehydrogenase enzymes. A redox imbalance could explain the altered lactic and pyruvic acid levels detected as lactate dehydrogenase, a redox dependent enzyme, is responsible for the interconversion of these two metabolites. The lactate/pyruvate ratio, an indicator of cytosolic redox state (Munnich et al., 1996) was slightly increased in the urine of MELAS patients, compared to the controls, although not statistically significant ($P = 0.2$). Furthermore, since branched chain amino acids are ultimately metabolized to their respective α-keto acids through the branched-chain α-keto acid dehydrogenase complex (BCKDC), altered BCKDC activity, caused by a redox imbalance, could elucidate the accumulation of the isoleucine and leucine detected in the MELAS cohort. Another point of interest was the ketone body acetoacetic acid, which is converted to 3-hydroxybutyric acid by 3-hydroxybutyric acid dehydrogenase. Since the activity of this enzyme is also dependent on the redox balance, an altered redox balance caused by MELAS could explain the increased levels of acetoacetic acid found in our MELAS patient group. Thus our findings suggest that urine reflects the overall redox-balance of the body.

Currently receiving a lot of attention in the field of mitochondrial disease research is an intricate web of pathways consisting of one-carbon metabolism, the methylation cycle and the trans-sulfuration pathway. It has been hypothesized that these pathways could be affected in defective OXPHOS systems, but it was not until recent studies that this intricate web of pathways was positively associated with the disease (Bao et al., 2016; Nikkanen et al., 2016). In addition to a redox imbalance, our data is also supportive of alterations in this cluster of pathways, with increased levels of, cysteine, trimethylglycine (betaine), taurine, and trimethylamine *N*-oxide (TMAO) detected (Fig. 4D and Table 3). Firstly, cysteine is metabolized to taurine through a cofactor-dependent reaction, thus influencing the taurine levels detected in the MELAS patients. Secondly, during the methylation cycle, homocysteine is converted to methionine through a reaction where choline is converted to trimethylglycine (betaine), ultimately producing dimethylglycine. Finally, choline additionally produces trimethylamine (TMA), which is further broken down to TMAO and dimethylamine. Thus the results reported here not only indicate affected one-carbon metabolism, but also an altered trans-sulfuration pathway and methylation cycle, explaining the altered levels of all these metabolites observed in this study.

Another component of the metabolism that seems to be strongly affected by MELAS is fatty acid oxidation. We hypothesize that stalled beta-oxidation is responsible for the altered levels of glycerol, butyric/valeric acid (short chain fatty acid), caproic/caprylic acid (medium chain fatty acid), carnitine, acetyl-carnitine (C2) and butanoyl-carnitine (C4). The altered levels of isovaleryl-carnitine (C5) and propionyl-carnitine (C3) are indicative of altered uneven-chain fatty acid and/or altered amino acid catabolism. From the volcano plot (Fig. 1C), some of the most discriminatory (statistically significant) metabolites in the MELAS patients can be linked to stalled fatty acid catabolism/beta-

Table 3
List of 36 metabolites that differed significantly between MELAS patients and controls in the Nijmegen cohort.

	Direction	P-value (Student *t*-test)	D-value (effect size)	Level of identification	Platform
Amino acids					
Alanine	↑	0.001	1.258	1	NMR (LC-MS/MS)
Arginine	↑	0.015	0.962	1	LC-MS/MS
Aspartic acid	↑	0.019	0.872	1	LC-MS/MS
Cysteine	↑	0.001	1.244	1	LC-MS/MS
Isoleucine	↑	0.001	1.050	1	NMR
Leucine	↑	0.004	1.007	1	NMR
Lysine	↑	0.014	0.895	1	NMR
N2-Succinyl-L-glutamic acid 5-semialdehyde	↑	0.004	1.052	3	LC-IM-MS (+)
N-acetyltryptophan	↑	0.003	1.118	3	LC-IM-MS (+)
Proline	↑	0.004	1.123	1	NMR
Sarcosine	↓	0.031	0.853	1	GC–MS
Taurine	↑	0.014	0.924	3	GC–MS
Trimethylglycine (betaine)	↑	0.003	1.100	1	NMR
Organic acids					
3-Hydroxybutyric acid	↑	0.011	0.993	1	GC–MS
4-Hydroxyglutaric acid	↑	0.007	1.033	3	GC–MS
Acetoacetic acid	↑	0.037	0.810	1	NMR
Butyric/valeric acid	↑	0.000	1.107	2	NMR
Caproic/caprylic acid	↑	0.000	1.225	2	NMR
Citric acid	↑	0.004	1.134	1	NMR
Glycerol	↓	0.002	1.183	3	GC–MS
Lactic acid	↑	0.004	1.085	1	GC–MS (NMR)
Pyruvic acid	↑	0.014	0.987	1	NMR (GC–MS)
Carnitines					
Carnitine	↑	0.000	1.068	1	NMR
C2-Carnitine	↑	0.000	1.083	1	LC-MS/MS
C3-Carnitine	↑	0.000	1.017	1	LC-MS/MS
C4-Carnitine	↑	0.002	0.923	1	LC-MS/MS
C5-Carnitine	↑	0.000	0.895	1	LC-MS/MS
Other					
6-Azathymine	↓	0.006	0.973	3	GC–MS
2,3-Butanediol glucoside	↑	0.002	1.139	3	LC-IM-MS (+)
Butanal	↑	0.015	0.834	3	GC–MS
Glucose	↑	0.000	1.225	1	NMR
Hydroxylamine	↓	0.002	1.081	3	GC–MS
Resolvin D2	↑	0.015	0.877	3	LC-IM-MS (+)
TMAO	↑	0.004	0.844	1	NMR
Urea	↑	0.024	0.878	1	NMR
Xanthine	↑	0.011	0.856	1	NMR

If a metabolite was detected as significant by more than one analytical platform, the second platform is indicated in the table in brackets. ↑ means the metabolite is increased in the MELAS patients, relative to the Controls. ↓ means the metabolite is decreased in the MELAS patients, relative to the Controls.

oxidation. Many carnitine conjugates also increased in the MELAS group, however, the question arose as to how free carnitine can be increased as well in the MELAS group while it is used for detoxification and hence excreted in elevated levels as conjugates. For this to be possible, increased carnitine biosynthesis is needed. However, such a scenario would require one-carbon units in the form of s-adenosylmethionine for the synthesis of carnitine via trimethyllysine. We thus speculate that due to the increased carnitine conjugates excreted in the urine of MELAS patients, one-carbon metabolism is affected in an effort to replenish the diminished carnitines. Thus, although many of the effected metabolites we report here can be linked to a redox imbalance and one-carbon metabolism, methylation and transsulfuration, our results indicate that stalled fatty acid oxidation was severely affected in this MELAS cohort.

Other metabolites detected as increased can be linked to different metabolic pathways. Increased amino acid catabolism (possibly through the activation of AMPK due to low energy levels) is supported by the increased levels of arginine, N2-succinyl-L-glutamic acid 5-semialdehyde, aspartic acid, and urea. Even though some of the patients received carnitine (n = 1) and arginine (n = 2) supplementation, our data was still supportive of stalled beta-oxidation (Fig. 4C) and increased amino acid catabolism (Fig. 4B), even when the patients receiving supplementation were excluded from the data analysis (data not shown). Altered levels of xanthine is supportive of affected purine pathway. Lastly, 2,3-butandiol would normally be associated with high level of alcohol consumption; however, this metabolite can also be expected in urine when high level of glucose (as detected in the MELAS patients) are present as it is further metabolized by the gut microbes (Elshaghabee et al., 2016; Venkataraman et al., 2014). Additionally the increased levels of 4-hydroxyvaleric acid could also be ascribed to gut microbial metabolism. Since seven of the nine MELAS patients demonstrated GI dysmotility, the altered levels of 2,3-butandiol and 4-hydroxyvaleric acid could indeed be due to altered gut metabolism on the measured urinary metabolome.

A study in 2015 (Hall et al., 2015) of renal involvement in mitochondrial disease included a cohort of 14 patients with the MELAS phenotype; NMR was utilized to identify six potential urinary markers (*N*-methylnicotinamide, hippurate, creatinine, 4-cresyl sulfate, glycolate, and a marker with unconfirmed identity, possibly 4-hydroxyphenylacetic acid). In our study, we detected and quantified N^1-methylnicotinamide, hippurate, creatinine, glycolate, but none of these markers were significantly affected by MELAS ($P > 0.05$ and $d < 0.8$) in our cohort. Lastly, our multi-platform approach resulted in the detection of 36 metabolites perturbed by MELAS compared to the six reported by Hall et al. (2015), whom only used a single analytical platform.

The strength of our study was the utilization of five different analytical platforms to generate the robust metabolomics data reported

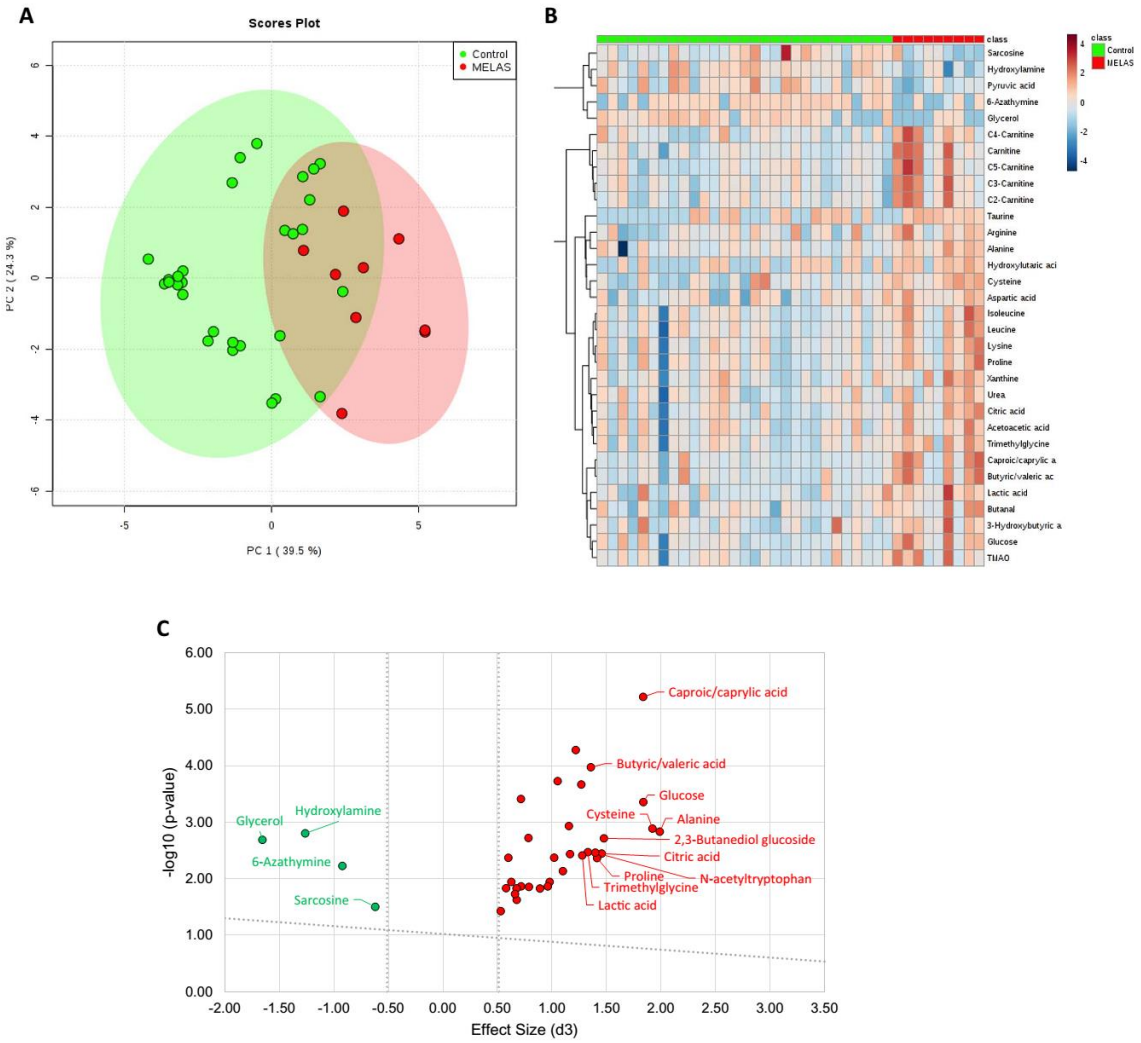

Fig. 1. Differences between Controls and MELAS patients of the exploration (Nijmegen) cohort using the 36 selected variables. A) principal component analysis score (PCA) plot. Sample grouping are shown in the PCA with 90% confidence ellipses; B) heatmap; C) volcano plot.

here. Of the five platforms employed, only three (GC–MS, NMR and LC-MS/MS) contributed to the majority of our metabolite list as illustrated in Fig. 2. Although many discriminatory features were detected with untargeted LC-IM-MS, only four metabolites (in positive ionization mode) was identified with moderate confidence while none of the discriminatory features in negative ionization mode could be identified. Nevertheless, some of the 36 important metabolites were detected and identified as important by more than one platform (Fig. 2) due to their overlapping coverage of the metabolome, giving more credibility to the metabolite as being critical in the disease. One important metabolite were detected by both the NMR and LC-MS/MS (alanine) while the overlap between the GC–MS and NMR was two metabolites (lactic acid and pyruvic acid). In the light of these findings, we recommend using a multi-platform approach to analyze the metabolome in mitochondrial disease studies as the multiple platforms complement each other, rather than substitute for each other.

5. Conclusion

We have performed a multi-platform metabolomics investigation on two MELAS cohorts in order to better understand the metabolic alterations caused by the disease. To our knowledge, this is the first multi-platform metabolomics investigation of the MELAS phenotype. By combining the metabolic data sets generated with the multi-platform analytical approach, we were able to cover a larger part of the metabolome, which led to the identification of 36 metabolites (during the exploratory phase) that differed significantly between the patient and control group, compared to the six markers previously reported for the disease (Hall et al., 2015). During the validation phase, the 36 selected metabolites were able to separate a validation cohort of two MELAS patients completely from their respective control group.

Upon further investigation of our data, most of the disturbed metabolites could be explained by a redox imbalance caused by a defective OXPHOS system while stalled fatty acid oxidation prevailed as being

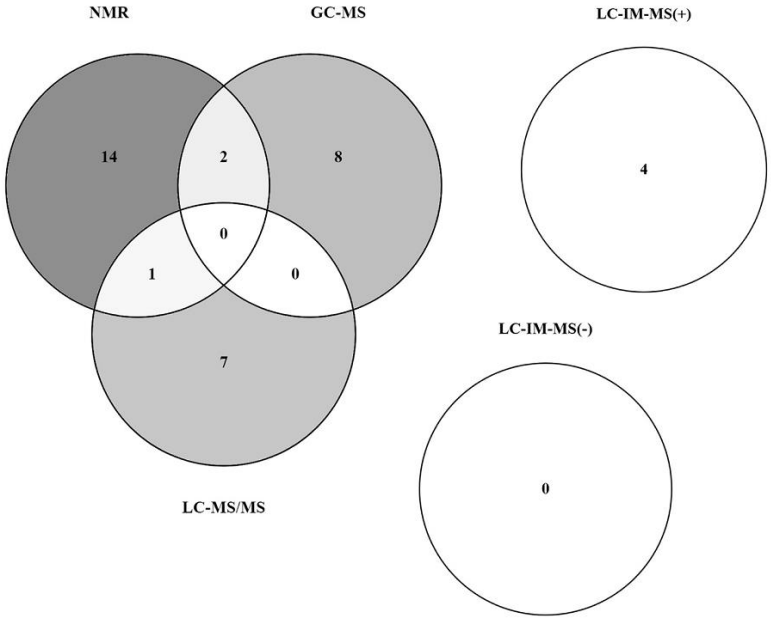

Fig. 2. Venn diagram illustrating the contribution of each analytical platform to the detection of the 36 important metabolites. Five analytical platforms were used to analyze the metabolome of the MELAS patients and controls. Although a large number of features were detected using each platform, only the metabolites that differed significantly between the MELAS and controls groups and that could be identified/partially identified were considered as "important", thus forming part of the final metabolic fingerprint consisting of 36 metabolites.

particularly perturbed in the MELAS phenotype. Furthermore the intricate web of pathways consisting of the one-carbon metabolism, methylation cycle and trans-sulfuration pathway — previously linked to PEO (Bao et al., 2016; Nikkanen et al., 2016) – can now, with our data, also be linked to the MELAS phenotype. Although redox imbalance has previously been associated with mitochondrial disease (Brière et al., 2004; Khan et al., 2014; Naviaux, 2014; Reinecke et al., 2012; Smeitink et al., 2006), our data confirms the global impact of mitochondrial disease on the metabolism, further contributing to its complexity.

The small number of MELAS patients used in this study (nine

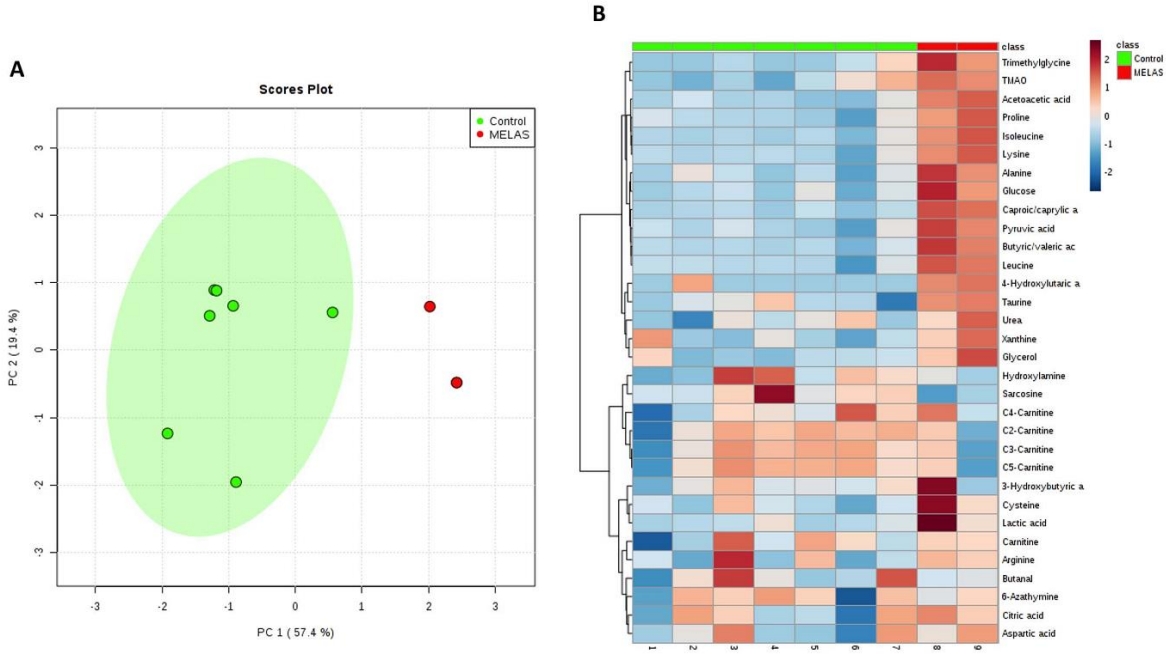

Fig. 3. Differences between Controls and MELAS patients of the validation (Helsinki) cohort using the 36 selected variables. A) principal component analysis score (PCA) - since this cohort only contains two MELAS samples, an ellipse could not be drawn for the patient group, although the two samples clearly grouped well away from the controls, indicating natural separation. Sample grouping are shown in the PCA with 90% confidence ellipses; B) heatmap.

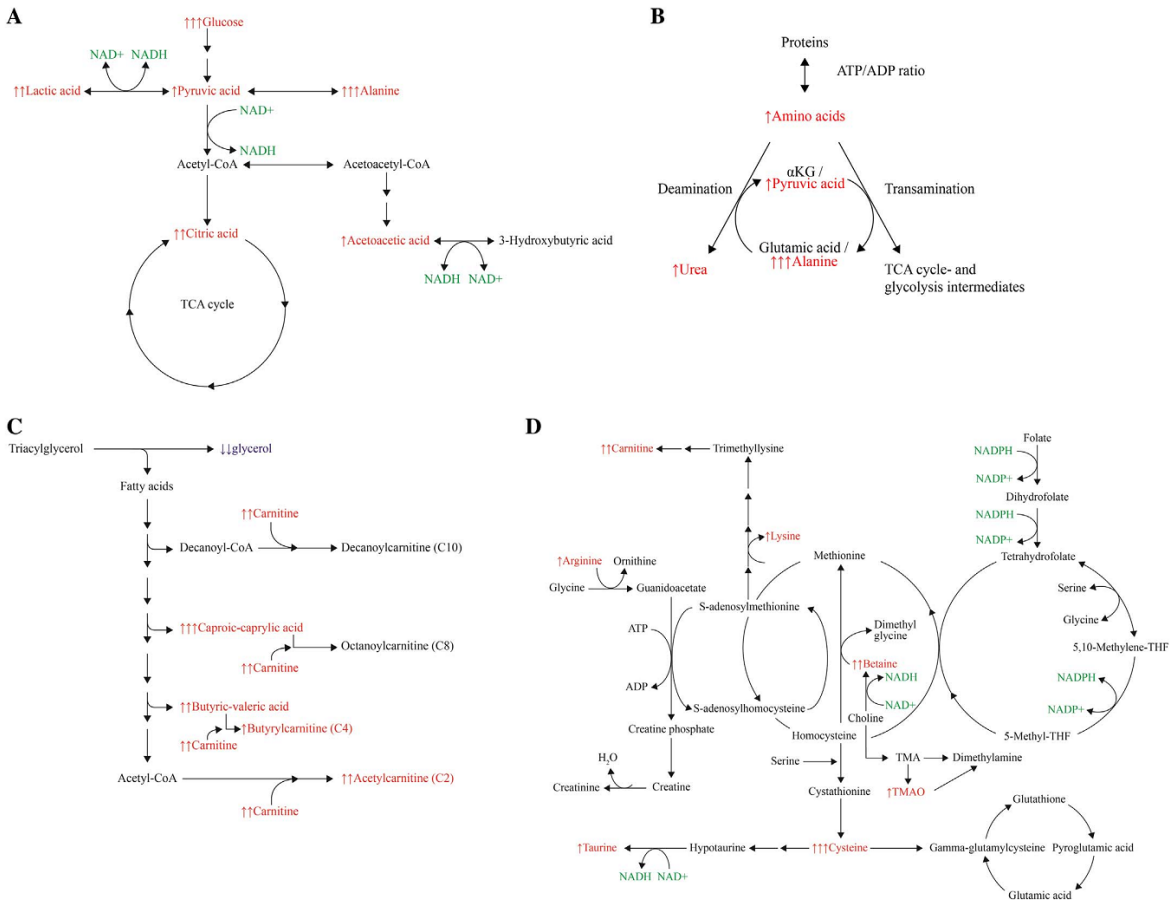

Fig. 4. Schematic representation of the altered metabolism detected in the MELAS patients compared to healthy controls. A) altered glucose metabolism, B) protein catabolism, C) lipid catabolism, D) one-carbon metabolism, methylation cycle and the transsulfuration route. Metabolites significantly increased by MELAS (compared to the controls) are indicated in red, those significantly decreased are indicated in blue. ↑ = metabolite is increased ($d < 1.0$); ↑↑ = moderate increase ($d < 1.2$); ↑↑↑ = highly increase ($d > 1.2$) and ↓↓ = moderate decrease ($d < 1.2$). Cofactor dependent reactions are indicated in green. (For interpretation of the references to colour in this figure legend, the reader is referred to the web version of this article.)

MELAS patients for the exploratory phase and only two patients for the validation phase) is a limitation of the study. Larger numbers of patients would have been preferential, although it was not available to this study. Also, all the MELAS patients used in this study had the m.3243A > G mutation – none had any of the numerous other MELAS-causing mutations. Thus the biosignature suggested here is specific for this single phenotype. Although further research is warranted, this study is the first to follow a comprehensive metabolomics analysis approach to identify metabolites altered by the MELAS phenotype. Understanding the metabolic alterations of MELAS could further our understanding of the disease and might lead to better treatment options.

Acknowledgements

The research was supported by a grant from the Technology Innovation Agency (TIA, Grant number Metabol. 01), South Africa. The research facilities were provided by the National Metabolomics Platform, North-West University, Potchefstroom Campus, Potchefstroom.

Appendix A. Supplementary data

Supplementary data to this article can be found online at https://doi.org/10.1016/j.mito.2018.02.003.

References

Bao, X.R., Ong, S.E., Goldberger, O., Peng, J., Sharma, R., Thompson, D.A., Vafai, S.B., Cox, A.G., Marutani, E., Ichinose, F., Goessling, W., Regev, A., Carr, S.A., Clish, C.B., Mootha, V.K., 2016. Mitochondrial dysfunction remodels one-carbon metabolism in human cells. elife 5, e10575.

Brière, J., Chrétien, D., Bénit, P., Rustin, P., 2004. Respiratory chain defects: what do we know for sure about their consequences in vivo? Biochim. Biophys. Acta Bioenerg. 1659 (2), 172–177.

Elshaghabee, F.M., Bockelmann, W., Meske, D., de Vrese, M., Walte, H.G., Schrezenmeir, J., Heller, K.J., 2016. Ethanol production by selected intestinal microorganisms and lactic acid bacteria growing under different nutritional conditions. Front. Microbiol. 7, 47.

Esterhuizen, K., van der Westhuizen, F.H., Louw, R., 2017. Metabolomics of mitochondrial disease. Mitochondrion 35, 97–110.

Fiehn, O., Robertson, D., Griffin, J., van der Werf, M., Nikolau, B., Morrison, N., Sumner, L.W., Goodacre, R., Hardy, N.W., Taylor, C., Fostel, J., Kristal, B., Kaddurah-Daouk, R., Mendes, P., van Ommen, B., Lindon, J.C., Sansone, S., 2007. The metabolomics standards initiative (MSI). Metabolomics 3, 175–178.

Gorman, G.S., Schaefer, A.M., Ng, Y., Gomez, N., Blakely, E.L., Alston, C.L., Feeney, C., Horvath, R., Yu-Wai-Man, P., Chinnery, P.F., 2015. Prevalence of nuclear and

mitochondrial DNA mutations related to adult mitochondrial disease. Ann. Neurol. 77 (5), 753–759.
Goto, Y., Nonaka, I., Horai, S., 1990. A mutation in the tRNA (Leu (UUR)) gene associated with the MELAS subgroup of mitochondrial encephalomyopathies. Nature 348 (6302), 651–653.
Hall, A.M., Vilasi, A., Garcia-Perez, I., Lapsley, M., Alston, C.L., Pitceathly, R.D., McFarland, R., Schaefer, A.M., Turnbull, D.M., Beaumont, N.J., 2015. The urinary proteome and metabonome differ from normal in adults with mitochondrial disease. Kidney Int. 87 (3), 610–622.
Kami, K., Fujita, Y., Igarashi, S., Koike, S., Sugawara, S., Ikeda, S., Sato, N., Ito, M., Tanaka, M., Tomita, M., 2012. Metabolomic profiling rationalized pyruvate efficacy in cybrid cells harboring MELAS mitochondrial DNA mutations. Mitochondrion 12 (6), 644–653.
Khan, N.A., Auranen, M., Paetau, I., Pirinen, E., Euro, L., Forsström, S., Pasila, L., Velagapudi, V., Carroll, C.J., Auwerx, J., Suomalainen, A., 2014. Effective treatment of mitochondrial myopathy by nicotinamide riboside, a vitamin B3. EMBO Mol. Med. 6 (6), 721–731.
de Laat, P., Koene, S., van den Heuvel, L.P.W.J., Rodenburg, R.J.T., Janssen, M.C.H., Smeitink, J.A.M., 2012. Clinical features and heteroplasmy in blood, urine and saliva in 34 Dutch families carrying the m.3243A > G mutation. J. Inherit. Metab. Dis. 35, 1059–1069.
Manwaring, N., Jones, M.M., Wang, J.J., Rochtchina, E., Howard, C., Mitchell, P., Sue, C.M., 2007. Population prevalence of the MELAS M.3243A > G mutation. Mitochondrion 7 (3), 230–233.
Munnich, A., Rötig, A., Chretien, D., Saudubray, J., Cormier, V., Rustin, P., 1996. Clinical presentations and laboratory investigations in respiratory chain deficiency. Eur. J. Pediatr. 155, 262–274.
Naviaux, R.K., 2014. Metabolic features of the cell danger response. Mitochondrion 16, 7–17.
Nikkanen, J., Forsström, S., Euro, L., Paetau, I., Kohnz, R.A., Wang, L., Chilov, D., Viinamäki, J., Roivainen, A., Marjamäki, P., 2016. Mitochondrial DNA replication defects disturb cellular dNTP pools and remodel one-carbon metabolism. Cell Metab. 23 (4), 635–648.
Pavlakis, S.G., Phillips, P.C., DiMauro, S., De Vivo, D.C., Rowland, L.P., 1984. Mitochondrial myopathy, encephalopathy, lactic acidosis, and strokelike episodes: a distinctive clinical syndrome. Ann. Neurol. 16 (4), 481–488.
Reinecke, C.J., Koekemoer, G., van der Westhuizen, F.H., Louw, R., Lindeque, J.Z., Mienie, L.J., Smuts, I., 2012. Metabolomics of urinary organic acids in respiratory chain deficiencies in children. Metabolomics 8 (2), 264–283.
Ruiz-Pesini, E., Lott, M.T., Procaccio, V., Poole, J.C., Brandon, M.C., Mishmar, D., Yi, C., Kreuziger, J., Baldi, P., Wallace, D.C., 2007. An enhanced MITOMAP with a global mtDNA mutational phylogeny. Nucleic Acids Res. 35, D823–D828.
Scaglia, F., Northrop, J.L., 2006. The mitochondrial myopathy encephalopathy, lactic acidosis with stroke-like episodes (MELAS) syndrome: a review of treatment options. CNS Drugs 20 (6), 443–464.
Schaefer, A.M., McFarland, R., Blakely, E.L., He, L., Whittaker, R.G., Taylor, R.W., Chinnery, P.F., Turnbull, D.M., 2008. Prevalence of mitochondrial DNA disease in adults. Ann. Neurol. 63 (1), 35–39.
Smeitink, J.A., Zeviani, M., Turnbull, D.M., Jacobs, H.T., 2006. Mitochondrial medicine: a metabolic perspective on the pathology of oxidative phosphorylation disorders. Cell Metab. 3 (1), 9–13.
Venkataraman, A., Rosenbaum, M.A., Werner, J.J., Winans, S.C., Angenent, L.T., 2014. Metabolite transfer with the fermentation product 2,3-butanediol enhances virulence by *Pseudomonas aeruginosa*. ISME J. 8 (6), 1210–1220.

A urinary biosignature for mitochondrial myopathy, encephalopathy, lactic acidosis and stroke like episodes (MELAS)

Online supplementary document

URINE QUALITY CONTROL SAMPLE

Quality control (QC) sample were prepared by pooling equal amounts of urine from all of the patient as well as control samples. Theses pooled urine QC sample were then aliquoted into smaller volumes, stored – 80 °C until use and were prepped in the same manner as the samples. For GC-MS analyses two QC samples were analyzed in the beginning of each batch and then after every 10 samples. For NMR analyses only one QC in the beginning of the batch, and for the LC analyses (targeted and untargeted) three in the beginning of the batch, each of them twice, and then after every 5 samples. Creatinine was determined by using the QuantiChromTM Creatinine Assay Kit from BioAssay Systems. Osmolality was determined by Ampath Laboratories on the Advanced Osmometer (IEPSA Diagnostics, South Africa).

URINE METABOLOMIC ANALYSES

Gas chromatography mass spectrometry (GC-MS)

For untargeted GC-MS analyses an adapted version of a minimal sample preparation method published by Venter el al., 2014 was used. Sample aliquots, which were stored at -80°C, were thawed over night at 4°C and centrifuged at 15 700 x g at room temperature for 2 minutes to remove any crystals. A calculated volume for each sample (totaling 0.25 µmoles of creatinine) were transferred into clean vials. To each sample, 50 µL 3-phenylbutyric acid (end concentration 50 mg/L) were added. Samples were then evaporated under a stream of nitrogen gas at 37 ˚C. Evaporated samples were derivatized using a two-step derivatization process. First samples were oximated by adding 50 µL of methoxyamine HCl (20 mg/mL pyridine), after which it was incubated at 60°C for 60

minutes. After the oximation step, samples were silylated by adding 50 µL BSTFA containing 1 % TMCS after which they were again incubated for 60°C for 60 minutes. Derivatized samples were then transferred to vials with flat bottom inserts

Samples were analyzed on a GC-TOFMS-system consisting of an Agilent 7890 GC system coupled to a Leco Pegasus HT mass analyzer and an Agilent 7693 auto sampler, with helium gas being used as carrier gas. Metabolites were separated using a Restek RXi® - 5 column (10 m X 0.2 mm X 0.18 µm). 10 µL of sample was injected per run in a 1:10 split mode at a flow rate of 1.50 mL/min, with front inlet temperature being kept at a constant 250°C. To enhance separation of metabolites the oven temperature was ramped from 70°C to 300°C over a period of 13 minutes. The initial oven temperature started at 70°C and was increased to 120 °C at a flow rate of 7°C/min. Thereafter the temperature was again increased to 230°C at 10°C / min and then to 300°C at 13°C /min. The transfer line was maintained at 225 °C, while the ion source temperature was kept at 200 °C for the entire run. Data was captured with an acquisition rate of 20 spectra (50 – 950 m/z) per second, with the detector voltage kept at 1450 V. Total run time added up to 13 minutes. For extraction of GC-MS data, ChromaTOF (Leco). To identify compounds spectral matching was done by using both a commercial library (NIST11) as well as an in-house created library (Reinecke *et al*., 2012).

Targeted LC-MS

Sample aliquots, which were stored at -80°C, were thawed over night at 4°C and centrifuged at 15 700 x g at room temperature for 2 minutes to remove any crystals. A calculated volume for each sample (totaling 0.25 µmoles of creatinine) were transferred into clean vials. To each sample 100, µL of an internal isotope solution containing phenylalanine, methionine valine C4, C8 and C 16 (end concentration 10 mg/L) as well as 50 uL 3-phenylbutyric acid (end concentration 50 mg/L) were added. Samples were then evaporated under a stream of nitrogen gas at 37 ˚C. Samples were then derivatized by adding 300 µL N-butanol:acetyl chloride after which they were incubated for 50 min

at 60°C. Samples were then again evaporated under a stream of nitrogen gas at 37 ˚C. To reconstitute samples, 100 µL mobile phase (50% acetonitrile, 50% water) were added to each sample and left at room temperature for 30 minutes to ensure that the evaporated samples was completely dissolved. The samples were then vortexed and transferred to vials with tapered inserts.

Samples were analyzed on 1290 infinity LC from the 1200 infinity series connected to a 6460 triple quadrupole mass analyzer (Agilent Technologies, Santa Clara, CA, USA) in positive ionization mode. The sample injection volume was 5 µL which was separated on a C18 column (ZORBAX SB-Aq, 2.1 x 150 mm, 3.5 µm, Agilent Technologies, Santa Clara, CA, USA), using a flow rate of 0.2 mL/min with mobile phases A (Milli-Q water and 0.1% formic acid) and B (acetonitrile and 0.1 % formic acid). To enhance separation a mobile phase gradient was used (Table S1). Samples were analyzed in multiple reaction monitoring mode (MRM) for maximum sensitivity, with specific precursor and product ions for the various amino acids and carnitines being monitored (Table S2). Gas temperature was kept at 300 °C, with a flow rate of 7.5 L/min and a capillary voltage of 3500 V. Total run time added up to 33 minutes, which included a post run time of 10 minutes.

Nuclear magnetic resonance (NMR) spectroscopy

For NMR analyses, 500 µL urine aliquots were thawed over night at 4°C and centrifuged at room temperature for 5 minutes at 12 000 x g. After the samples were centrifuged, 450 µL were aliquoted into a new micro-centrifuge tube. To the aliquoted samples 50 µL NMR buffer solution (pH 7.4, KH2PO4 with TSP, in D2O) were added. Samples were vortexed and transferred into standard 5-mm NMR tubes.

Analyses were performed at 500 MHz on a Bruker Avance III HD NMR spectrometer (Bruker Biospin, Rheinstetten, Germany), fitted with a triple resonance inverse (TXI) ^{1}H {^{15}N, ^{13}C} probe head as well as x, y, z gradient coils. ^{1}H spectra was obtained 28 transients in 32K data points, with a spectral

width of 6002 Hz. Water resonance was pre-saturated by single-frequency irradiation with a relaxation delay of 4 seconds, and a 90° excitation pulse of 8 µs. Automatic shimming occurred on the deuterium signal. Resonance widths for both the TSP and metabolite peaks were less than 1 Hz. Automatic Fourier transformation as well as phase and baseline correction was done. For NMR spectral processing Bruker Topspin, and for identification and quantification Bruker AMIX (Ellinger *et al*., 2013) was used.

Untargeted liquid chromatography – ion mobility – mass spectrometry (LC-IM-MS)

A calculated volume for each sample (totaling 0.25 µmoles of creatinine) were transferred into clean vials. To each sample 100, µL of an internal isotope solution containing stable isotopes for phenylalanine, methionine, valine, C4-, C8- and C16-carnitines (end concentration 10 mg/L) as well as 50 uL 3-phenylbutyric acid (end concentration 50 mg/L) were added and then dried under a stream of nitrogen gas. To reconstitute samples, 100 µL mobile phase (50% acetonitrile, 50% water) were added to each sample and left at room temperature for 30 minutes to ensure that the evaporated samples was completely dissolved. The samples were then vortexed and transferred to vials with tapered inserts.

Samples were also analyzed on the Synapt G2-Si (hybrid ion mobility-MS system) (Waters) containing an Acquity UPLC system equipped with ESI source. Five µL sample was injected and separated on a Waters T3 column (2.1 x 100 mm, 1.8 µm) kept at 30 °C, using water with 1 % formic acid as mobile phase A and acetonitrile with 1 % formic acid as mobile phase B. The mobile phase gradient reported elsewhere (Want *et al*., 2010) were used for LC separation. The nebulization gas was set to 650 L/min at a temperature of 500°C, and the cone gas was set to 30 L/min. The capillary voltage and cone voltage were set at 2000 V and 30 V, respectively. The Q-TOF acquisition rate was 0.1 s, with argon used as the collision gas at a pressure of 7.066 × 10−3 Pa. Data was captured in HDMSe mode where the collision-induced dissociation (CID) energy for the first (low energy) channel

was set at 0 V and those for the second (high energy) channel was set to ramp between 10 and 40 V. Leucine-encephalin (m/z 556.2771 in positive and 554.2615 in negative ionization) was used as lock mass to monitor (and correct) accurate mass measurements in positive and negative ionization modes. Collision cross section (CCS) values were automatically calculated from the ion mobility drift time based on a poly-alanine calibration. Progenesis QI (Nonlinear Dynamics) was used to process the data and to identify compounds using several public databases.

DATA PRE-PROCESSING, NORMALIZATION AND EXTRACTION

The extracted GC-MS, LC-QQQ as well as NMR data sets were inspected for between-batch effects occurring. No significant batch effects could be observed in any of the data sets, therefore no batch corrections were applied. For normalization, each data set was normalized against its own internal standard. The data was then normalized to the creatinine concentration as determined using the QuantiChromTM Creatinine Assay Kit).

The three, normalized datasets were then combined to generate a single data matrix. Using this combined data set, an 80% zero filter rule was applied, where a metabolite had to be present in 80% of the controls and/or patients sample, otherwise it was removed from the data set. Next, zero values were replaced by half of the lowest value in the data set after which it was log transformed. This log transformed data set was then used for all further statistical analyses (Student t-test, effect size and PCA).

Annexure C

C

Guide to Authors

MITOCHONDRION

Official Journal of the Mitochondria Research Society

AUTHOR INFORMATION PACK

TABLE OF CONTENTS

- **Description** **p.1**
- **Audience** **p.1**
- **Impact Factor** **p.2**
- **Abstracting and Indexing** **p.2**
- **Editorial Board** **p.2**
- **Guide for Authors** **p.4**

ISSN: 1567-7249

DESCRIPTION

Mitochondrion is a definitive, high profile, peer-reviewed international research journal. The scope of *Mitochondrion* is broad, reporting on basic science of mitochondria from all organisms and from basic research to pathology and clinical aspects of mitochondrial diseases. The journal welcomes original contributions from investigators working in diverse sub-disciplines such as evolution, biophysics, biochemistry, molecular and cell biology, genetics, pharmacology, toxicology, forensic science, programmed cell death, aging, cancer and clinical features of mitochondrial diseases.

Mitochondrion includes:
***MitoMatters*:** Editorial and news of general interest invited by Editorial Office.
***Profiles and Perspectives*:** Invited by Editorial Office and written by senior investigators in the field.
***The Mito Mew*:** Editorial and news of general interest.
***Review Articles*:** Reviews of major importance in mitochondrial biology. These articles will be peer-reviewed. Articles may be of any length; however, unusually long articles should be discussed with the editor before submission.
***Fast Track Articles*:** Peer-reviewed, short studies that are refereed rapidly and published generally within 10 weeks. These papers should be a concise complete piece of work of special significance and timeliness and should not exceed 4 printed pages (i.e., 10 pages of double-spaced typescript, including tables and figures up to a total number of 4).
***Original Articles*:** Peer-reviewed, high-quality, concise research investigations that represent new and significant contributions to science.
***Letters to the Editor*:** Comments on papers published in the Journal and on other matters of interest to mitochondria researcher.
***Book Reviews*:** invited by the editorial office.
***Announcements and Calendar*:** Providing notices of forthcoming meetings, courses, and other events relevant to mitochondria researchers.

AUDIENCE

Investigators working in diverse sub-disciplines such as evolution, biophysics, biochemistry, molecular and cell biology, genetics, pharmacology, toxicology, forensic science, programmed cell death, aging, cancer and clinical features of mitochondrial diseases.

IMPACT FACTOR

2016: 3.704 © Clarivate Analytics Journal Citation Reports 2017

ABSTRACTING AND INDEXING

EMBiology
MEDLINE®
Current Contents/Clinical Medicine
BIOBASE
EMBASE
Science Citation Index Expanded
Research Alert
CAS

EDITORIAL BOARD

Editor-in-Chief:

Keshav K. Singh, Joy and Bill Harbert Endowed Chair and Professor of Genetics and Pathology
Department of Genetics, School of Medicine
University of Alabama at Birmingham
Kaul Genetics Building, Suite 620
720 20th St. South
Birmingham, AL 35294
USA

Phone: +1 205-934-2750
Fax: +1 205-934-2766

Honorary Editor:

Anthony W. Linnane, Epworth Medical Centre, Richmond (Melbourne), Victoria, Australia

Editorial Board Members:

Susanne Arnold, Radboudumc, Nijmegen, Netherlands
Narayan Avadhani, University of Pennsylvania, University Park, Pennsylvania, USA
Yidong Bai, University of Texas Health Sciences Center at San Antonio, San Antonio, Texas, USA
Vilhelm Bohr, National Institute of Aging (NIA), Baltimore, Maryland, USA
Richard Boles, Children's Hospital Los Angeles, Los Angeles, California, USA
Paul Brookes, University of Rochester Medical Center, Rochester, New York, USA
Craig Cameron, Pennsylvania State University, University Park, Pennsylvania, USA
Maria Louisa Campo, University of Extremadura, Cáceres, Spain
Xin Jie Chen, State University of New York (SUNY) Upstate Medical University, Syracuse, New York, USA
Patrick F. Chinnery, Newcastle University, Newcastle upon Tyne, UK
Bruce H. Cohen, Akron Children's Hospital, Akron, Ohio, USA
William C. Copeland, National Institute of Environmental Health Sciences (NIEHS), Research Triangle Park, North Carolina, USA
Salvatore DiMauro, Columbia University, New York, New York, USA
Francoise Foury, Université Catholique de Louvain, Louvain-la-Neuve, Belgium
Erich Gnaiger, Medizinische Universität Innsbruck, Innsbruck, Austria
Yu-ichi Goto, National Center of Neurology & Psychiatry (NCNP), Tokyo, Japan
Lawrence I. Grossman, Wayne State University School of Medicine, Detroit, Michigan, USA
Min-Xin Guan, Cincinnati Children's Hospital Medical Center, Cincinnati, Ohio, USA
Maureen R. Hanson, Cornell University, Ithaca, New York, USA
Charles L. Hoppel, Case Western Reserve University School of Medicine, Cleveland, Ohio, USA
Paul M. Hwang, National Institutes of Health (NIH), Bethesda, Maryland, USA
Grazia Isaya, Mayo Clinic, Rochester, Minnesota, USA
Naoaki Ishii, Tokai University School of Medicine, Kanagawa, Japan
Laura S. Kaguni, Michigan State University, East Lansing, Michigan, USA
Konstantin Khrapko, Beth Israel Deaconess Medical Center, Boston, Massachusetts, USA
Kiyoshi Kita, Nagasaki University, Nagasaki, Japan
John J. Lemasters, Medical University of South Carolina (MUSC), Charleston, South Carolina, USA
Alfred Lewin, University of Florida College of Medicine, Gainesville, Florida, USA
Jiankang Liu, Xi'an Jiaotong University, Xi'an, China

Hideyuki J. Majima, Kagoshima University Graduate School of Medical & Dental Sciences, Kagoshima, Japan
Dan Mishmar, Ben-Gurion University of the Negev, Beer Sheva, Israel
Max Møller, Aarhus University, Slagels, Denmark
Carlos T. Moraes, University of Miami, Miller School of Medicine, Miami, Florida, USA
Arnold Munnich, Hôpital Necker - Enfants Malades, Paris, France
Robert K. Naviaux, University of California at San Diego (UCSD), San Diego, California, USA
Thomas O'Brien, University of Florida, Gainesville, Gainesville, Florida, USA
Shigeo Ohta, Nippon Medical School, Kawasaki City, Kanagawa, Japan
Debkumar Pain, University Medical & Dental School of New Jersey, Newark, New Jersey, USA
Sergio Papa, Università degli Studi di Bari Aldo Moro, Bari, Italy
Peter L. Pedersen, Johns Hopkins University School of Medicine, Baltimore, Maryland, USA
George Perry, University of Texas at San Antonio, San Antonio, Texas, USA
Cal Pinkert, University of Alabama, Tuscaloosa, Alabama, USA
Mark Prescott, Monash University, Victoria, Australia
Lene Juel Rasmussen, University of Copenhagen, Copenhagen, Denmark
Rodrigue Rossignol, Institute for Health and Medical Research, Bordeaux, France
Michael Sack, National Institutes of Health (NIH), Bethesda, Maryland, USA
Russell P. Saneto, Seattle Children's Hospital Research Institute, Seattle, Washington, USA
Hiromi Sesaki, Johns Hopkins University School of Medicine, Baltimore, Maryland, USA
Gerald S. Shadel, Yale University School of Medicine, New Haven, Connecticut, USA
Jan Smeitink, Radboudumc, Nijmegen, Netherlands
Linda L. Spremulli, University of North Carolina at Chapel Hill, Chapel Hill, North Carolina, USA
Daret St. Clair, University of Kentucky, Lexington, Kentucky, USA
Masashi Tanaka, Tokyo Metropolitan Institute of Gerontology, Tokyo, Japan
Mark Tarnopolsky, McMaster University Medical Center, Hamilton, Ontario, Canada
Kumarasamy Thangaraj, Centre for Cellular and Molecular Biology, Hyderabad, India
David R. Thorburn, Murdoch Childrens Research Institute, Parkville, Victoria, Australia
Douglas C. Wallace, University of California at Irvine, Irvine, California, USA
Yau-Huei Wei, National Yang Ming University, Taipei, Taiwan, ROC
Lee-Jun Wong, Baylor College of Medicine, Houston, Texas, USA
Michael P. Yaffee, University of California at San Diego (UCSD), La Jolla, California, USA
Massimo Zeviani, National Neurological Institute “Carlo Besta”, Milano, Italy

GUIDE FOR AUTHORS

Your Paper Your Way

We now differentiate between the requirements for new and revised submissions. You may choose to submit your manuscript as a single Word or PDF file to be used in the refereeing process. Only when your paper is at the revision stage, will you be requested to put your paper in to a 'correct format' for acceptance and provide the items required for the publication of your article.
To find out more, please visit the Preparation section below.

INTRODUCTION

Mitochondrion is a definitive, high profile, peer-reviewed international research journal. The scope of *Mitochondrion* is broad, reporting on basic science of mitochondria from all organisms and from basic research to pathology and clinical aspects of mitochondrial diseases. The journal welcomes original contributions from investigators working in diverse sub-disciplines such as evolution, biophysics, biochemistry, molecular and cell biology, genetics, pharmacology, toxicology, forensic science, programmed cell death, aging, cancer and clinical features of mitochondrial diseases.

Types of paper

Original Articles
Peer-reviewed, high-quality, concise research investigations that represent new and significant contributions to science.

Fast Track Articles
Peer-reviewed, short studies that are refereed rapidly and published generally within 10 weeks. These papers should be a concise complete piece of work of special significance and timeliness and should not exceed 4 printed pages (i.e., 10 pages of double-spaced typescript, including tables and figures up to a total number of 4).

Review Articles
Reviews of major importance in mitochondrial biology. These articles will be peer-reviewed. Articles may be of any length; however, unusually long articles should be discussed with the editor before submission.

MitoMatters
Editorial and news of general interest invited by Editorial Office. Profiles and Perspectives: Invited by Editorial Office and written by senior investigators in the field.

The Mito Mew
Editorial and news of general interest.

Letters to the Editor
Comments on papers published in the Journal and on other matters of interest to mitochondria researchers. These should be less than 400 words and may include one illustration or table.

Book Reviews
Invited by the editorial office.

Announcements and Calendar
Providing notices of forthcoming meetings, courses, and other events relevant to mitochondria researchers.

Contact details for submission

Please submit manuscripts intended for Mitochondrion via the journal's online editorial and submission system available at http://ees.elsevier.com/mitoch.

Customer support is available 24/7:
Please use our help site at: http://service.elsevier.com/. Here you will be able to learn more about EES via interactive tutorials, explore a range of online submission solutions via our knowledgebase, and find answers to frequently asked questions. You will also find our 24/7 support contact details should you need any assistance from one of our customer service representatives.

For questions regarding the reviewing process, please contact the Editor-in-Chief, Dr. Keshav K. Singh at mitochondriona@roswellpark.org or at

Keshav K. Singh, Ph.D Department of Cancer Genetics Roswell Park Cancer Institute Cell and Virus Building, Room 247 Elm and Carlton Streets Buffalo, NY 14263 USA

Submission checklist

You can use this list to carry out a final check of your submission before you send it to the journal for review. Please check the relevant section in this Guide for Authors for more details.

Ensure that the following items are present:

One author has been designated as the corresponding author with contact details:
• E-mail address
• Full postal address

All necessary files have been uploaded:
Manuscript:
• Include keywords
• All figures (include relevant captions)
• All tables (including titles, description, footnotes)
• Ensure all figure and table citations in the text match the files provided
• Indicate clearly if color should be used for any figures in print
Graphical Abstracts / Highlights files (where applicable)
Supplemental files (where applicable)

Further considerations
• Manuscript has been 'spell checked' and 'grammar checked'
• All references mentioned in the Reference List are cited in the text, and vice versa
• Permission has been obtained for use of copyrighted material from other sources (including the Internet)
• A competing interests statement is provided, even if the authors have no competing interests to declare
• Journal policies detailed in this guide have been reviewed
• Referee suggestions and contact details provided, based on journal requirements

For further information, visit our Support Center.

BEFORE YOU BEGIN

Ethics in publishing

Please see our information pages on Ethics in publishing and Ethical guidelines for journal publication.

Policy and ethics

When conducting scientific research using human tissue and which is intended for publication in Mitochondrion, authors should follow procedures that are in accordance with the ethical standards as formulated in the Helsinki Declaration of 1975 (revised 1983). When conducting experiments on animals, authors should adhere to the local or national requirements for the care and use of laboratory animals.

Declaration of interest

All authors must disclose any financial and personal relationships with other people or organizations that could inappropriately influence (bias) their work. Examples of potential conflicts of interest include employment, consultancies, stock ownership, honoraria, paid expert testimony, patent applications/ registrations, and grants or other funding. Authors must disclose any interests in two places: 1. A summary declaration of interest statement in the title page file (if double-blind) or the manuscript file (if single-blind). If there are no interests to declare then please state this: 'Declarations of interest: none'. This summary statement will be ultimately published if the article is accepted. 2. Detailed disclosures as part of a separate Declaration of Interest form, which forms part of the journal's official records. It is important for potential interests to be declared in both places and that the information matches. More information.

Submission declaration and verification

Submission of an article implies that the work described has not been published previously (except in the form of an abstract, a published lecture or academic thesis, see 'Multiple, redundant or concurrent publication' for more information), that it is not under consideration for publication elsewhere, that its publication is approved by all authors and tacitly or explicitly by the responsible authorities where the work was carried out, and that, if accepted, it will not be published elsewhere in the same form, in English or in any other language, including electronically without the written consent of the copyright-holder. To verify originality, your article may be checked by the originality detection service Crossref Similarity Check.

Changes to authorship

Authors are expected to consider carefully the list and order of authors **before** submitting their manuscript and provide the definitive list of authors at the time of the original submission. Any addition, deletion or rearrangement of author names in the authorship list should be made only **before** the manuscript has been accepted and only if approved by the journal Editor. To request such a change, the Editor must receive the following from the **corresponding author**: (a) the reason for the change in author list and (b) written confirmation (e-mail, letter) from all authors that they agree with the addition, removal or rearrangement. In the case of addition or removal of authors, this includes confirmation from the author being added or removed.

Only in exceptional circumstances will the Editor consider the addition, deletion or rearrangement of authors **after** the manuscript has been accepted. While the Editor considers the request, publication of the manuscript will be suspended. If the manuscript has already been published in an online issue, any requests approved by the Editor will result in a corrigendum.

Copyright

Upon acceptance of an article, authors will be asked to complete a 'Journal Publishing Agreement' (see more information on this). An e-mail will be sent to the corresponding author confirming receipt of the manuscript together with a 'Journal Publishing Agreement' form or a link to the online version of this agreement.

Subscribers may reproduce tables of contents or prepare lists of articles including abstracts for internal circulation within their institutions. Permission of the Publisher is required for resale or distribution outside the institution and for all other derivative works, including compilations and translations. If excerpts from other copyrighted works are included, the author(s) must obtain written permission from the copyright owners and credit the source(s) in the article. Elsevier has preprinted forms for use by authors in these cases.

For gold open access articles: Upon acceptance of an article, authors will be asked to complete an 'Exclusive License Agreement' (more information). Permitted third party reuse of gold open access articles is determined by the author's choice of user license.

Author rights

As an author you (or your employer or institution) have certain rights to reuse your work. More information.

Elsevier supports responsible sharing

Find out how you can share your research published in Elsevier journals.

Role of the funding source

You are requested to identify who provided financial support for the conduct of the research and/or preparation of the article and to briefly describe the role of the sponsor(s), if any, in study design; in the collection, analysis and interpretation of data; in the writing of the report; and in the decision to submit the article for publication. If the funding source(s) had no such involvement then this should be stated.

Funding body agreements and policies

Elsevier has established a number of agreements with funding bodies which allow authors to comply with their funder's open access policies. Some funding bodies will reimburse the author for the gold open access publication fee. Details of existing agreements are available online.

Open access

This journal offers authors a choice in publishing their research:

Subscription
• Articles are made available to subscribers as well as developing countries and patient groups through our universal access programs.
• No open access publication fee payable by authors.
• The Author is entitled to post the accepted manuscript in their institution's repository and make this public after an embargo period (known as green Open Access). The published journal article cannot be shared publicly, for example on ResearchGate or Academia.edu, to ensure the sustainability of peer-reviewed research in journal publications. The embargo period for this journal can be found below.
Gold open access
• Articles are freely available to both subscribers and the wider public with permitted reuse.
• A gold open access publication fee is payable by authors or on their behalf, e.g. by their research funder or institution.

Regardless of how you choose to publish your article, the journal will apply the same peer review criteria and acceptance standards.

For gold open access articles, permitted third party (re)use is defined by the following Creative Commons user licenses:

Creative Commons Attribution (CC BY)
Lets others distribute and copy the article, create extracts, abstracts, and other revised versions, adaptations or derivative works of or from an article (such as a translation), include in a collective work (such as an anthology), text or data mine the article, even for commercial purposes, as long as they credit the author(s), do not represent the author as endorsing their adaptation of the article, and do not modify the article in such a way as to damage the author's honor or reputation.

Creative Commons Attribution-NonCommercial-NoDerivs (CC BY-NC-ND)
For non-commercial purposes, lets others distribute and copy the article, and to include in a collective work (such as an anthology), as long as they credit the author(s) and provided they do not alter or modify the article.

The gold open access publication fee for this journal is **USD 2400**, excluding taxes. Learn more about Elsevier's pricing policy: https://www.elsevier.com/openaccesspricing.

Green open access
Authors can share their research in a variety of different ways and Elsevier has a number of green open access options available. We recommend authors see our green open access page for further information. Authors can also self-archive their manuscripts immediately and enable public access from their institution's repository after an embargo period. This is the version that has been accepted for publication and which typically includes author-incorporated changes suggested during submission, peer review and in editor-author communications. Embargo period: For subscription articles, an appropriate amount of time is needed for journals to deliver value to subscribing customers before an article becomes freely available to the public. This is the embargo period and it begins from the date the article is formally published online in its final and fully citable form. Find out more.

This journal has an embargo period of 12 months.

Language (usage and editing services)
Please write your text in good English (American or British usage is accepted, but not a mixture of these). Authors who feel their English language manuscript may require editing to eliminate possible grammatical or spelling errors and to conform to correct scientific English may wish to use the English Language Editing service available from Elsevier's WebShop.

Submission
Our online submission system guides you stepwise through the process of entering your article details and uploading your files. The system converts your article files to a single PDF file used in the peer-review process. Editable files (e.g., Word, LaTeX) are required to typeset your article for final publication. All correspondence, including notification of the Editor's decision and requests for revision, is sent by e-mail.

Referees
Please submit, with the manuscript, the names, addresses and telephone, fax and e-mail details (where possible) of five suitable, potential reviewers. If there are compelling reasons for excluding some individuals as potential reviewers, these may be mentioned. However, the ultimate reviewer selection is at the discretion of the Editor-in-Chief.

Additional Information
After final acceptance of an article, only corrections to the title and list of authors as they appear on the accepted article will be permitted, not changes; particularly, no author names may be added to or deleted from the accepted lists.

The Editor-in-Chief is responsible for the professional review of the manuscripts. Receipt of manuscripts by the Editor-in-Chief will be acknowledged.

All materials submitted become the property of *Mitochondrion*. In the case of rejection of a paper, manuscripts will not be returned to authors.

Mitochondrion is the Official Journal of the Mitochondria Research Society. The journal is included as a part of the annual subscription to the society. Information regarding the society can be obtained from The Mitochondria Research Society, P.O. Box 306, Riderwood, MD 21139-0306, USA or visit the society's web site at http://www.mitoresearch.org.

PREPARATION

NEW SUBMISSIONS
Submission to this journal proceeds totally online and you will be guided stepwise through the creation and uploading of your files. The system automatically converts your files to a single PDF file, which is used in the peer-review process.
As part of the Your Paper Your Way service, you may choose to submit your manuscript as a single file to be used in the refereeing process. This can be a PDF file or a Word document, in any format or lay-out that can be used by referees to evaluate your manuscript. It should contain high enough quality figures for refereeing. If you prefer to do so, you may still provide all or some of the source files at the initial submission. Please note that individual figure files larger than 10 MB must be uploaded separately.

References
There are no strict requirements on reference formatting at submission. References can be in any style or format as long as the style is consistent. Where applicable, author(s) name(s), journal title/book title, chapter title/article title, year of publication, volume number/book chapter and the pagination must be present. Use of DOI is highly encouraged. The reference style used by the journal will be applied to the accepted article by Elsevier at the proof stage. Note that missing data will be highlighted at proof stage for the author to correct.

Formatting requirements
There are no strict formatting requirements but all manuscripts must contain the essential elements needed to convey your manuscript, for example Abstract, Keywords, Introduction, Materials and Methods, Results, Conclusions, Artwork and Tables with Captions.
If your article includes any Videos and/or other Supplementary material, this should be included in your initial submission for peer review purposes.
Divide the article into clearly defined sections.

Figures and tables embedded in text
Please ensure the figures and the tables included in the single file are placed next to the relevant text in the manuscript, rather than at the bottom or the top of the file. The corresponding caption should be placed directly below the figure or table.

Peer review
This journal operates a single blind review process. All contributions will be initially assessed by the editor for suitability for the journal. Papers deemed suitable are then typically sent to a minimum of two independent expert reviewers to assess the scientific quality of the paper. The Editor is responsible for the final decision regarding acceptance or rejection of articles. The Editor's decision is final. More information on types of peer review.

REVISED SUBMISSIONS

Use of word processing software
Regardless of the file format of the original submission, at revision you must provide us with an editable file of the entire article. Keep the layout of the text as simple as possible. Most formatting codes will be removed and replaced on processing the article. The electronic text should be prepared in a way very similar to that of conventional manuscripts (see also the Guide to Publishing with Elsevier). See also the section on Electronic artwork.
To avoid unnecessary errors you are strongly advised to use the 'spell-check' and 'grammar-check' functions of your word processor.

Article structure

Subdivision - numbered sections
Divide your article into clearly defined and numbered sections. Subsections should be numbered 1.1 (then 1.1.1, 1.1.2, ...), 1.2, etc. (the abstract is not included in section numbering). Use this numbering also for internal cross-referencing: do not just refer to 'the text'. Any subsection may be given a brief heading. Each heading should appear on its own separate line.

Introduction
State the objectives of the work and provide an adequate background, avoiding a detailed literature survey or a summary of the results.

Material and methods
Provide sufficient details to allow the work to be reproduced by an independent researcher. Methods that are already published should be summarized, and indicated by a reference. If quoting directly from a previously published method, use quotation marks and also cite the source. Any modifications to existing methods should also be described.

Results
Results should be clear and concise.

Discussion
This should explore the significance of the results of the work, not repeat them. A combined Results and Discussion section is often appropriate. Avoid extensive citations and discussion of published literature.

Conclusions
The main conclusions of the study may be presented in a short Conclusions section, which may stand alone or form a subsection of a Discussion or Results and Discussion section.

Essential title page information

• ***Title.*** Concise and informative. Titles are often used in information-retrieval systems. Avoid abbreviations and formulae where possible.
• ***Author names and affiliations.*** Please clearly indicate the given name(s) and family name(s) of each author and check that all names are accurately spelled. You can add your name between parentheses in your own script behind the English transliteration. Present the authors' affiliation addresses (where the actual work was done) below the names. Indicate all affiliations with a lower-case superscript letter immediately after the author's name and in front of the appropriate address. Provide the full postal address of each affiliation, including the country name and, if available, the e-mail address of each author.
• ***Corresponding author.*** Clearly indicate who will handle correspondence at all stages of refereeing and publication, also post-publication. This responsibility includes answering any future queries about Methodology and Materials. **Ensure that the e-mail address is given and that contact details are kept up to date by the corresponding author.**
• ***Present/permanent address.*** If an author has moved since the work described in the article was done, or was visiting at the time, a 'Present address' (or 'Permanent address') may be indicated as a footnote to that author's name. The address at which the author actually did the work must be retained as the main, affiliation address. Superscript Arabic numerals are used for such footnotes.

Abstract should not exceed **100** words.

Keywords

Immediately after the abstract, provide a maximum of 6 keywords, using American spelling and avoiding general and plural terms and multiple concepts (avoid, for example, 'and', 'of'). Be sparing with abbreviations: only abbreviations firmly established in the field may be eligible. These keywords will be used for indexing purposes.

Abbreviations
Define abbreviations that are not standard in this field in a footnote to be placed on the first page of the article. Such abbreviations that are unavoidable in the abstract must be defined at their first mention there, as well as in the footnote. Ensure consistency of abbreviations throughout the article.

Acknowledgements
Collate acknowledgements in a separate section at the end of the article before the references and do not, therefore, include them on the title page, as a footnote to the title or otherwise. List here those individuals who provided help during the research (e.g., providing language help, writing assistance or proof reading the article, etc.).

Formatting of funding sources
List funding sources in this standard way to facilitate compliance to funder's requirements:

Funding: This work was supported by the National Institutes of Health [grant numbers xxxx, yyyy]; the Bill & Melinda Gates Foundation, Seattle, WA [grant number zzzz]; and the United States Institutes of Peace [grant number aaaa].

It is not necessary to include detailed descriptions on the program or type of grants and awards. When funding is from a block grant or other resources available to a university, college, or other research institution, submit the name of the institute or organization that provided the funding.

If no funding has been provided for the research, please include the following sentence:

This research did not receive any specific grant from funding agencies in the public, commercial, or not-for-profit sectors.

Math formulae
Please submit math equations as editable text and not as images. Present simple formulae in line with normal text where possible and use the solidus (/) instead of a horizontal line for small fractional terms, e.g., X/Y. In principle, variables are to be presented in italics. Powers of e are often more conveniently denoted by exp. Number consecutively any equations that have to be displayed separately from the text (if referred to explicitly in the text).

Footnotes
Footnotes should be used sparingly. Number them consecutively throughout the article. Many word processors build footnotes into the text, and this feature may be used. Should this not be the case, indicate the position of footnotes in the text and present the footnotes themselves separately at the end of the article.

Artwork

Electronic artwork
General points
• Make sure you use uniform lettering and sizing of your original artwork.
• Preferred fonts: Arial (or Helvetica), Times New Roman (or Times), Symbol, Courier.
• Number the illustrations according to their sequence in the text.
• Use a logical naming convention for your artwork files.
• Indicate per figure if it is a single, 1.5 or 2-column fitting image.
• For Word submissions only, you may still provide figures and their captions, and tables within a single file at the revision stage.
• Please note that individual figure files larger than 10 MB must be provided in separate source files.
A detailed guide on electronic artwork is available.
You are urged to visit this site; some excerpts from the detailed information are given here.
Formats
Regardless of the application used, when your electronic artwork is finalized, please 'save as' or convert the images to one of the following formats (note the resolution requirements for line drawings, halftones, and line/halftone combinations given below):
EPS (or PDF): Vector drawings. Embed the font or save the text as 'graphics'.
TIFF (or JPG): Color or grayscale photographs (halftones): always use a minimum of 300 dpi.
TIFF (or JPG): Bitmapped line drawings: use a minimum of 1000 dpi.
TIFF (or JPG): Combinations bitmapped line/half-tone (color or grayscale): a minimum of 500 dpi is required.
Please do not:

• Supply files that are optimized for screen use (e.g., GIF, BMP, PICT, WPG); the resolution is too low.
• Supply files that are too low in resolution.
• Submit graphics that are disproportionately large for the content.

Color artwork
Please make sure that artwork files are in an acceptable format (TIFF (or JPEG), EPS (or PDF), or MS Office files) and with the correct resolution. If, together with your accepted article, you submit usable color figures then Elsevier will ensure, at no additional charge, that these figures will appear in color online (e.g., ScienceDirect and other sites) regardless of whether or not these illustrations are reproduced in color in the printed version. **For color reproduction in print, you will receive information regarding the costs from Elsevier after receipt of your accepted article**. Please indicate your preference for color: in print or online only. Further information on the preparation of electronic artwork.

Figure captions
Ensure that each illustration has a caption. A caption should comprise a brief title (**not** on the figure itself) and a description of the illustration. Keep text in the illustrations themselves to a minimum but explain all symbols and abbreviations used.

Tables

Please submit tables as editable text and not as images. Tables can be placed either next to the relevant text in the article, or on separate page(s) at the end. Number tables consecutively in accordance with their appearance in the text and place any table notes below the table body. Be sparing in the use of tables and ensure that the data presented in them do not duplicate results described elsewhere in the article. Please avoid using vertical rules and shading in table cells.

References

Citation in text
Please ensure that every reference cited in the text is also present in the reference list (and vice versa). Any references cited in the abstract must be given in full. Unpublished results and personal communications are not recommended in the reference list, but may be mentioned in the text. If these references are included in the reference list they should follow the standard reference style of the journal and should include a substitution of the publication date with either 'Unpublished results' or 'Personal communication'. Citation of a reference as 'in press' implies that the item has been accepted for publication.

Web references
As a minimum, the full URL should be given and the date when the reference was last accessed. Any further information, if known (DOI, author names, dates, reference to a source publication, etc.), should also be given. Web references can be listed separately (e.g., after the reference list) under a different heading if desired, or can be included in the reference list.

Data references
This journal encourages you to cite underlying or relevant datasets in your manuscript by citing them in your text and including a data reference in your Reference List. Data references should include the following elements: author name(s), dataset title, data repository, version (where available), year, and global persistent identifier. Add [dataset] immediately before the reference so we can properly identify it as a data reference. The [dataset] identifier will not appear in your published article.

References in a special issue
Please ensure that the words 'this issue' are added to any references in the list (and any citations in the text) to other articles in the same Special Issue.

Reference management software
Most Elsevier journals have their reference template available in many of the most popular reference management software products. These include all products that support Citation Style Language styles, such as Mendeley and Zotero, as well as EndNote. Using the word processor plug-ins from these products, authors only need to select the appropriate journal template when preparing their article, after which citations and bibliographies will be automatically formatted in the journal's style. If no template is yet available for this journal, please follow the format of the sample references and citations as shown in this Guide. If you use reference management software, please ensure that you remove all field codes before submitting the electronic manuscript. More information on how to remove field codes.

Users of Mendeley Desktop can easily install the reference style for this journal by clicking the following link:
http://open.mendeley.com/use-citation-style/mitochondrion
When preparing your manuscript, you will then be able to select this style using the Mendeley plug-ins for Microsoft Word or LibreOffice.

Reference formatting
There are no strict requirements on reference formatting at submission. References can be in any style or format as long as the style is consistent. Where applicable, author(s) name(s), journal title/book title, chapter title/article title, year of publication, volume number/book chapter and the pagination must be present. Use of DOI is highly encouraged. The reference style used by the journal will be applied to the accepted article by Elsevier at the proof stage. Note that missing data will be highlighted at proof stage for the author to correct. If you do wish to format the references yourself they should be arranged according to the following examples:

AudioSlides

The journal encourages authors to create an AudioSlides presentation with their published article. AudioSlides are brief, webinar-style presentations that are shown next to the online article on ScienceDirect. This gives authors the opportunity to summarize their research in their own words and to help readers understand what the paper is about. More information and examples are available. Authors of this journal will automatically receive an invitation e-mail to create an AudioSlides presentation after acceptance of their paper.

Data visualization

Include interactive data visualizations in your publication and let your readers interact and engage more closely with your research. Follow the instructions here to find out about available data visualization options and how to include them with your article.

Research data

This journal encourages and enables you to share data that supports your research publication where appropriate, and enables you to interlink the data with your published articles. Research data refers to the results of observations or experimentation that validate research findings. To facilitate reproducibility and data reuse, this journal also encourages you to share your software, code, models, algorithms, protocols, methods and other useful materials related to the project.

Below are a number of ways in which you can associate data with your article or make a statement about the availability of your data when submitting your manuscript. If you are sharing data in one of these ways, you are encouraged to cite the data in your manuscript and reference list. Please refer to the "References" section for more information about data citation. For more information on depositing, sharing and using research data and other relevant research materials, visit the research data page.

Data linking
If you have made your research data available in a data repository, you can link your article directly to the dataset. Elsevier collaborates with a number of repositories to link articles on ScienceDirect with relevant repositories, giving readers access to underlying data that gives them a better understanding of the research described.

There are different ways to link your datasets to your article. When available, you can directly link your dataset to your article by providing the relevant information in the submission system. For more information, visit the database linking page.

For supported data repositories a repository banner will automatically appear next to your published article on ScienceDirect.

In addition, you can link to relevant data or entities through identifiers within the text of your manuscript, using the following format: Database: xxxx (e.g., TAIR: AT1G01020; CCDC: 734053; PDB: 1XFN).

Mendeley Data
This journal supports Mendeley Data, enabling you to deposit any research data (including raw and processed data, video, code, software, algorithms, protocols, and methods) associated with your manuscript in a free-to-use, open access repository. During the submission process, after uploading your manuscript, you will have the opportunity to upload your relevant datasets directly to *Mendeley Data*. The datasets will be listed and directly accessible to readers next to your published article online.

For more information, visit the Mendeley Data for journals page.

Data in Brief
You have the option of converting any or all parts of your supplementary or additional raw data into one or multiple data articles, a new kind of article that houses and describes your data. Data articles ensure that your data is actively reviewed, curated, formatted, indexed, given a DOI and publicly available to all upon publication. You are encouraged to submit your article for *Data in Brief* as an additional item directly alongside the revised version of your manuscript. If your research article is accepted, your data article will automatically be transferred over to *Data in Brief* where it will be editorially reviewed and published in the open access data journal, *Data in Brief*. Please note an open access fee of 500 USD is payable for publication in *Data in Brief*. Full details can be found on the Data in Brief website. Please use this template to write your Data in Brief.

Data statement
To foster transparency, we encourage you to state the availability of your data in your submission. This may be a requirement of your funding body or institution. If your data is unavailable to access or unsuitable to post, you will have the opportunity to indicate why during the submission process, for example by stating that the research data is confidential. The statement will appear with your published article on ScienceDirect. For more information, visit the Data Statement page.

AFTER ACCEPTANCE

Online proof correction
Corresponding authors will receive an e-mail with a link to our online proofing system, allowing annotation and correction of proofs online. The environment is similar to MS Word: in addition to editing text, you can also comment on figures/tables and answer questions from the Copy Editor. Web-based proofing provides a faster and less error-prone process by allowing you to directly type your corrections, eliminating the potential introduction of errors.
If preferred, you can still choose to annotate and upload your edits on the PDF version. All instructions for proofing will be given in the e-mail we send to authors, including alternative methods to the online version and PDF.
We will do everything possible to get your article published quickly and accurately. Please use this proof only for checking the typesetting, editing, completeness and correctness of the text, tables and figures. Significant changes to the article as accepted for publication will only be considered at this stage with permission from the Editor. It is important to ensure that all corrections are sent back to us in one communication. Please check carefully before replying, as inclusion of any subsequent corrections cannot be guaranteed. Proofreading is solely your responsibility.

Offprints
The corresponding author will, at no cost, receive a customized Share Link providing 50 days free access to the final published version of the article on ScienceDirect. The Share Link can be used for sharing the article via any communication channel, including email and social media. For an extra charge, paper offprints can be ordered via the offprint order form which is sent once the article is accepted for publication. Both corresponding and co-authors may order offprints at any time via Elsevier's Webshop. Corresponding authors who have published their article gold open access do not receive a Share Link as their final published version of the article is available open access on ScienceDirect and can be shared through the article DOI link.

AUTHOR INQUIRIES

Visit the Elsevier Support Center to find the answers you need. Here you will find everything from Frequently Asked Questions to ways to get in touch.
You can also check the status of your submitted article or find out when your accepted article will be published.

© Copyright 2018 Elsevier | https://www.elsevier.com

Information for Authors

This page describes our policies and provides information that we think will be helpful to you as you prepare manuscripts for submission and publication. If you have submitted a paper and want information about the status of the paper, please log in to our online manuscript submission system, Editorial Manager (EM). If you run into any problems or if you have specific questions, you can always e-mail us at reports@cell.comor call +1-617-386-2190.

About the Journal

Cell Reports is an open-access journal from Cell Press that publishes high-quality papers across the entire spectrum of the life sciences. The primary criterion for publication in *Cell Reports*, as for all Cell Press journals, is new biological insight. *Cell Reports* publishes thought-provoking, cutting-edge research, with a focus on a shorter, single-point story, called a Report, in addition to a longer Article format. *Cell Reports* also publishes Resources, which highlight significant technical advances and/or major informational data sets.

Editorial Evaluation Timeline

We read and evaluate every submission, and we try our best to get back to you quickly. We are mindful of how long it can take to publish a paper, so we work with authors and reviewers to minimize that time. Here's how long each step in the process usually takes:

Initial decision to review	3–5 days after submission
Decision after review	3–4 weeks after submission
Anticipated timeframe for suggested revisions	2–3 months (with flexibility if needed)
Time to online publication	3–5 weeks after acceptance

Presubmission Inquiries

Unsure if your paper is suitable for *Cell Reports*? Send us a presubmission inquiry at reports@cell.com, and we'll let you know what we think in 2–5 business days. Please include a title, an abstract, and an explanation of why your paper is significant and broadly interesting.

Relationship between Cell Press Journals

Cosubmission

If you think your paper might be suitable for two Cell Press journals, you can submit the paper for joint consideration. To do this, upload your manuscript to one of the journals. In your cover letter, indicate that you are seeking co-consideration and mention the name of the other journal. Each journal will evaluate the paper independently. If both journals decide to review the paper, they will agree on reviewers and will make independent decisions based on feedback from those reviewers.

Transfer of Papers between Cell Press Journals

We know it can be time consuming to serially submit your paper to multiple journals, restarting the review process each time. Cell Press publishes many journals, and we give you the opportunity to transfer your paper, along with the reviews and the reviewers' identities, from one journal to another. If you have questions about the suitability of your paper for transfer, please contact the editor of the receiving journal. If you have general questions about the transfer process, please refer to our FAQs on article transfers. Often, the Editor of the target journal will be able to reach a decision based on the existing reviews. The Editors may seek comments from additional reviewers, but we will make every effort to expedite the decision. If you transfer your paper using our online system, you will have a chance to edit your files before they are sent to the receiving journal. You can always submit your paper to another Cell Press journal without mentioning the first review process. In this case, the manuscript will be evaluated as a regular new submission.

Editorial Policies

Preprint Servers

We will consider papers previously posted on preprint servers like arXiv, bioRxiv, BioRN, ChemRxiv, or ChemRN. To make the submission process easier, we are also participating in the bioRxiv direct journal submission program. We are very interested to hear from researchers about their motivations for posting and to discuss with them whether it is the best approach for their paper, so we strongly encourage authors who are planning to submit to us to contact the editors first to discuss their specific paper and situation. This policy only applies to the original submitted version of the paper; we do not support posting of revisions that respond to editorial input and peer review or posting of the final published version to preprint servers. Also, our prepublication publicity policies with regard to coverage in the broader media still apply to studies posted on preprint servers. For more information about preprint servers and the discussions related to them, please see this blog post.

Related Manuscripts

If you or your coauthors have any related papers submitted or in press elsewhere, you need to let us know and include them with your initial submission (or with your revision if they were submitted during revision). We ask this because having access to related papers often helps us (and reviewers) to assess the submitted work, and it can help prevent potentially difficult scenarios down the road. Failure to provide copies of related manuscripts may delay the review process and may be grounds for rejection. As a matter of publishing ethics, we cannot consider any paper that contains data that have been published or submitted for publication elsewhere.

Authorship

Our authorship policy accommodates diverse types of research, providing a framework that makes clear the contributions of each author.

Author Contributions Section: To make author contributions transparent, all research articles should include an Author Contributions section. Please describe the contributions concisely and use initials to indicate author identity. We encourage you to use the CRediT taxonomy, which offers standardized descriptions of author contributions. An Authors Contributions section is not required for front-matter articles.

Corresponding Author and Lead Contact: You must designate at least one corresponding author and only one lead contact.

Corresponding Author: We prefer that each paper have a single corresponding author because we think that the ownership and responsibility that are inherent in corresponding authorship will promote best practices in design and performance of experiments, analysis of results, organization and retention of original data, and preparation of figures and text.

That said, we understand that, for some studies, particularly for interdisciplinary ones, multiple authors may bear the responsibilities of a corresponding author. If you feel strongly and have compelling reasons, you may include additional corresponding authors. We may ask you to explain your rationale and to verify that all corresponding authors understand their responsibilities (listed below). We ask that you describe each corresponding author's specific contributions in the Author Contributions section.

Lead Contact: The lead contact is the corresponding author who is also responsible for communicating with the journal (before and after publication) and accountable for fulfilling

requests for reagents and resources and for arbitrating decisions and disputes. For research papers with multiple corresponding authors, please designate one (and only one) corresponding author as the lead contact. If there is only one corresponding author, then that author is automatically also the lead contact. You should denote the lead contact with a footnote in the author list (e.g., "[5]Lead Contact").

Responsibilities of the Corresponding Author and Lead Contact: All corresponding authors bear responsibilities 1–8 below; the lead contact additionally bears responsibility 9.

1. Supervising the work
2. Being responsible for all data, figures, and text
3. Ensuring that authorship is granted appropriately to contributors
4. Ensuring that all authors approve the content and submission of the paper
5. Ensuring adherence to all editorial and submission policies
6. Identifying and declaring conflicts of interest on behalf of all authors
7. Identifying and disclosing related work by any co-authors under consideration elsewhere
8. Archiving unprocessed data and ensuring that figures accurately present the original data (see Data Archiving section)
9. Communicating with the journal (before and after publication), being accountable for fulfilling requests for reagents and resources, and arbitrating decisions and disputes

Equal Contributions: The lead contact is the only designation that we strictly limit to one author. In addition to noting corresponding authors with an asterisk, you may use numbered footnotes to designate senior authors and otherwise equally contributing authors. The following footnote should be used for authors who have made equal contributions: "[6]These authors contributed equally". Senior authors can be designated with a footnote, e.g., "[6]Senior author". Please use the Author Contributions section of the manuscript to more fully describe each author's specific contributions.

Authorship Disputes: All authors should discuss and agree on author order and authorship designations. We expect that everyone listed as an author contributed substantively to the paper.

We do not adjudicate authorship disputes. These disputes should be resolved by the researchers involved and/or their institutions. If we become aware of a dispute we will suspend consideration of the paper until the dispute is resolved. In this case (and when authors request changes to authorship) authorship should be approved in writing by all authors.

Competing Interests

Transparency is essential for a reader's trust in the scientific process and for the credibility of published articles. At Cell Press, we feel that disclosure of competing interests is a critical aspect of transparency. Therefore, we ask that all authors disclose any financial or other interests related to the submitted work that (1) could affect or have the perception of affecting the author's objectivity, or (2) could influence or have the perception of influencing the content of the article.

Prior to acceptance, author groups of all article types (front or back matter) are asked to complete and submit a "Declaration of Interests" form. We also ask that authors disclose any competing interests in the article in a dedicated Declaration of Interests section (see below). Complete details of our Declaration of Interests policy and additional author instructions are available here.

Data and Image Processing

Data processing is sometimes necessary. When it is, please keep it minimal and ensure that the final figures accurately reflect the original data. In general, please make all processing transparent. Here are some specific guidelines:

1. Any alterations should be applied to the entire image. When this is impossible (e.g., when a single color channel on a microscopy image is altered), please clearly explain the alteration in the figure legend.
2. If you remove lanes from gels and blots or consolidate your data in any way, you must make the alterations obvious.
3. Only compare data that are appropriate to compare (e.g., data from the same experiment).
4. Individual images should not be used in multiple figures unless the figures describe different aspects of the same experiment (e.g., multiple experiments were performed simultaneously with a single control experiment). If an image is used in multiple figures, please clearly state the reason in the legend.

Image Screening

We screen all accepted papers for image irregularities. If there is a question about a figure, either throughout this process or during the review process, we will work with the lead contact to resolve the issue. This is done on a case-by-case basis, but generally, we'll ask you to supply the original, unprocessed data, along with descriptions of how the experiments were performed and how the figures were prepared. Based on this, we will let you know if the current form of the figure is OK or if we'll need a revised figure. If the problem is more

serious, we may need to delay publication while we work through the issues, or we may decide not to publish the paper. Before you submit a new paper, a revision, or the final paper, it is critically important that you check the original data and make sure you know and are happy with how the figures were prepared from them. We view this as the responsibility of the corresponding author(s). As the final step before submission, we encourage you to go over all of the figures once more and connect all of the data in the figures to the original, unprocessed data. You might find our blog post on avoiding common mistakes in figure preparation helpful.

Data Archiving

We may ask you for your original, unprocessed data, so please take appropriate steps to preserve your data. We recommend that you save all unprocessed data related to your paper and distribute copies of that data to all co-authors. We also strongly encourage you to upload your original data to Mendeley Data, Dryad, or other appropriate figure/data repositories, because access to original data can increase reader confidence in the findings. If issues with your findings arise, failure to produce original data will make resolving those issues much more difficult and can be grounds for retraction.

Process for Post-Publication Issues

We will thoroughly investigate any issues with data or figures that we publish. While we do not monitor the internet or social media, we follow up on all clearly documented concerns that are directly brought to our attention (from authors or concerned readers, named and anonymous). If we think that there is reason to investigate, we will discuss the concerns with the lead contact. This process generally involves asking for the original, unprocessed data, along with descriptions of how the experiments in question were performed and how the figures were prepared. We will assess these materials, and we may consult with reviewers or other experts. There are several potential outcomes of the process. First, we may take no further action; in this case, we may publish an Editorial Note to describe the process and explain why we are taking no further action. Second, if we think the issues are resolvable with a Correction, we may ask the authors to prepare a Correction statement. Third, if we uncover serious issues, we may ask the authors to retract the paper and we will work with them to prepare a Retraction statement. Fourth, if the timeline to a potential resolution seems long, we might publish an Editorial Expression of Concern to alert the community that an investigation is ongoing. At any point during this process, if our analysis uncovers potentially serious issues, we will generally ask authors to alert their institution and funding bodies.

Correcting the scientific record is a priority for us. Because we consider the investigation process confidential, we don't report back in detail to the person who contacted us with the concern. As the process can include gathering and evaluating original data, discussing with authors, and collaborating with institutional investigations, it can take some time. We are committed to making sure that the investigation moves forward quickly, but as these are serious and important matters, we prioritize reaching the outcome that best serves the scientific community over reaching the fastest outcome.

Studies Involving Humans and Animals

For manuscripts reporting studies involving human subjects, statements identifying the committee approving the studies and confirming that informed consent was obtained from all subjects must appear in the Experimental Procedures. All experiments on live vertebrates or higher invertebrates must be performed in accordance with relevant institutional and national guidelines and regulations. In the manuscript, a statement identifying the committee approving the experiments and confirming that all experiments conform to the relevant regulatory standards must be included in the Experimental Procedures. The sex and gender, or both, must be reported for human subjects, and the sex of animal subjects and cells must be provided. In cases where this is appropriate, the influence (or association) of sex, gender, or both on the results of the study must be reported. Reporting of the age or developmental stage of subjects is also required. The editors reserve the right to seek comments from reviewers or additional information from authors on any cases in which concerns arise. We suggest that researchers carrying out experiments with animals refer to the ARRIVE guidelines and recommendations from an NIH-sponsored workshop regarding experimental design and reporting standards.

Chemical Compounds

If your paper reports a new chemical compound, you must provide the exact structure of the compound. We also encourage you to provide data to support the reported structure. If the compound was synthesized, please include details of the synthesis in the Experimental Procedures. You should submit small-molecule crystallographic data to the Cambridge Structural Database (CSD) and deposit relevant information to PubChem. Database IDs should be included in the final version of the manuscript.

In naming chemical compounds, you can use either IUPAC conventions or informal common names like rapamycin, cholesterol, and penicillin. For displaying chemical structures, please follow the IUPAC conventions. Chemical structures should be included as high-resolution files according to Cell Press Figure Guidelines.

Distribution of Materials and Data

If you publish at Cell Press, you must be willing to distribute materials and protocols to qualified researchers, with minimal restrictions and in a timely manner. Any restrictions must be disclosed in the cover letter and in the Experimental Procedures at the time of submission. You may request reasonable payment for maintenance and transport of materials. Materials include but are not limited to cells, DNA, antibodies, reagents, organisms, and mouse strains or, if necessary, the relevant ES cells.

Datasets must be made freely available to readers at the time of publication and must be provided to editors and peer reviewers at submission.

We encourage you to provide one-click access to your data by linking your article with external databases. When you provide accession numbers for your data, please use the following format: "Database: xxxx" for single accession numbers and "Database: xxxx, yyyy, zzzz" for multiple accession numbers (e.g., "Genbank: NM_000492"; "GEO: GSE6364"; "PDB: 1TUP, 1KW4, 3H5X"). See http://www.elsevier.com/books-and-journals/content-innovation/data-base-linking for more information and a full list of supported databases.

Data sets must be made freely available to readers from the date of publication and must be provided to editors and peer reviewers at submission for the purposes of evaluating the manuscript. In addition, we offer the opportunity for authors to make underlying data not included in the paper itself or deposited in a database available to the scientific community by posting them on Mendeley Data and then including a link in the published paper. For more detailed instructions, click here.

Mandatory Data Deposition

For the following types of data, submission of the full dataset to a community-endorsed, public repository is mandatory. Accession numbers must be provided in the Data and Software Availability section. Examples of appropriate public repositories include:

Protein Sequences: Uniprot

DNA and RNA Sequences: Genbank/European Nucleotide Archive (ENA)/DDBJ,Protein DataBank,UniProt

DNA Sequencing Data (traces and short reads): NCBI Trace and Short-Read Archive, ENA's Sequence Read Archive

Deep Sequencing Data: Deposit in GEO or ArrayExpress upon submission to the journal

The sequences of all RNAi, antisense, and morpholino probes must be included in the paper or deposited in a public database with the accession number provided in the paper.

Human Genomic Data Reporting Newly Described SNPs and CNVs Identified in Control Samples: dbSNP, the Database of Genomic Variants Archive (DGVa), or the Database of Genomic Structural Variation (dbVAR)

Human Sequence Data: dbGaP or similar repository. If, due to IRB restrictions, data collected for the paper cannot be made accessible in a public repository or shared upon legitimate request, please let us know in the cover letter at the stage of submission. If there are no IRB restrictions to sharing, we expect data deposition in a public repository.

Microarray Data: GEO or ArrayExpress upon submission to the journal. Data must be MIAME compliant, as described at the MGED website specifying microarray standards.

Structures of Biological Macromolecules: The atomic coordinates and related experimental data (structure factor amplitudes/intensities and/or NMR restraints) must be deposited at a member site of the Worldwide Protein Data Bank. Electron microscopy-derived density maps must be deposited into the EMDB through one of the partner sites (Protein Data Bank in Europe or EMDataBank). Atomic coordinates fitted to EM maps must also be deposited to a wwPDB member site. The corresponding database IDs must be included in the manuscript. Authors must agree to release the atomic coordinates and experimental data when the associated article is published. Additionally, when your paper is selected for external peer review, we will ask you to provide the PDB Validation Report(s) if your paper reports any structure(s) determined by X-ray crystallography before we contact reviewers. We will use these reports for peer review purposes, and they will not be part of the final published paper. You can read more about this requirement here.

Non-mandatory Data Deposition

We encourage you to submit the following types of data to public databases. Some of these databases allow anonymous referees the ability to access the data. When there is no public repository or if your dataset is too large to submit to the journal online, please contact us for advice.

Proteomics Data: PRIDE, PeptideAtlas

Protein Interaction Data: IMEx consortium of databases, including DIP, IntAct, and MINT

Chemical Compound Screening and Assay Data: PubChem

Flow Cytometry Data: Flow Repository

Rights, Sharing, and Embargoes

An overview of the rights that Cell Press authors retain, the options for sharing articles at various stages, and the duration of embargo periods, as well as open access options, is available at http://www.cell.com/rights-sharing-embargoes.

Funding Bodies

In compliance with the public access policies of various funding bodies, Cell Press deposits accepted, peer-reviewed manuscripts on authors' behalf to PubMed Central (PMC). Please see our Funding Bodies Policies page for complete information.

Publication Fee

To provide open access, expenses are offset by a publication fee of $5,000 (USD) that will allow *Cell Reports* to support itself in a fully sustainable way. This publication charge is the only fee that is requested. *Cell Reports* will consider reducing or waiving author fees for those who have difficulties with the fee, on a case-by-case basis.

Some universities have signed the Compact for Open-Access Publishing Equity (COPE): "the timely establishment of durable mechanisms for underwriting reasonable publication charges for articles written by its faculty and published in fee-based open-access journals and for which other institutions would not be expected to provide funds." More information about COPE and the list of signatories can be found at http://www.oacompact.org.

A list of institutions that provide funding for open access can be found at http://www.sparc.arl.org/sites/default/files/OA Funds in Action attachment 2014 %281%29.pdf.

Permissions

You do not need to ask our permission to use images or information that you have previously published in a Cell Press journal; we ask only that you cite the original publication. For information on how to request permission to use previously published work, please see our Permissions page. If excerpts from other copyrighted works are included in your manuscript, you must obtain written permission from the copyright owners and credit the sources in the article. To obtain permission to use material from Cell Press and Elsevier journals and books, e-mail permissions@elsevier.com. If you have adapted a figure from a published figure, please check with the copyright owners to see if permission is required and include a complete citation/reference for the original article. Obtaining permissions can take up to several weeks. As lack of appropriate permissions can delay publication, we recommend that you request permission at the time of submission.

Prepublication Publicity

We want to make sure that your paper gets the attention it deserves, so we work with the popular and scientific media to promote coverage of your paper. As part of this process, we ask that you refrain from talking to the media until one week prior to the online publication date of the paper. If you do speak with the media at that time, please inform them that the paper is under media embargo until 11 AM US east coast time on the date of publication. We encourage you to present your work at scientific meetings, but we ask that you not discuss the findings with the media beyond the formal presentation. This policy covers work that is intended for submission, currently under consideration, or in press at a Cell Press journal.

Additionally, before your paper is published, please do not discuss it or cite it as in press in review articles. However, you can discuss your embargoed paper with other scientific journals if the paper will be covered in review or news material that is intended to coincide or follow publication of your paper.

If you have any questions about our prepublication policies or if your institutional press office wishes to issue a press release, please contact our Press Officer Joseph Caputo (jcaputo@cell.com).

How to Prepare and Submit Research Articles

You can submit your manuscript using our online submission system, Editorial Manager (EM). For assistance, please contact us at reports@cell.com or +1-617-386-2190.
Editorial Manager will send all communications (including the request for final approval and the confirmation of submission) to the person who is selected as corresponding author at submission or, if no name is designated, to the person whose account is used to submit the manuscript. If you want to specify a different author for correspondence after submission, please contact the Journal Associate at reports@cell.com.

Cover Letter

In your cover letter, please explain what was previously known, the conceptual advance provided by your work, and the significance to a broad readership. You may suggest appropriate reviewers and make up to three requests for reviewer exclusions. Please use the cover letter to notify us of information that is relevant to our handling and evaluation your paper (e.g., related work, time constraints, competition). The cover letter is confidential and will not be seen by reviewers.

Initial Submissions

For initial submissions, you do not need to strictly adhere to our formatting guidelines below. You also do not need to provide a graphical abstract, highlights, or an eTOC paragraph. However, we do ask that you stay close to our length restrictions, adhere to figure limitations, and use page numbers. For information about length/figure restrictions for specific article types, please see our Article Types page.

Also, for initial submissions, you can upload your paper as a single PDF (using the "combined manuscript file" designation in EM). In doing this, you can intersperse the figures and figure legends within the Results section to aid evaluation of your paper. If you choose the single PDF option, please keep the PDF under 20 MB, and please separately upload the cover letter and any special file types such as videos and spreadsheets. If you do not choose the single PDF option, EM will build a composite PDF file of individually uploaded items. This PDF will contain links that editors and reviewers can use to download individual high-resolution files. The composite PDF will not contain the cover letter.

Formatting Guidelines

All research article formats at Cell Press generally contain the following sections in this order: title, authors, affiliations, author list footnotes, corresponding author(s) e-mail address(es), Summary, Introduction, Results, Discussion, Experimental Procedures, Author Contributions, Acknowledgments, References, figure titles and legends, tables with titles and legends, and Supplemental Information titles and legends. The text (title through supplemental legends) should be provided as one document. Figures, Supplemental Information, Graphical Abstract, and the Key Resources Table should be provided separately.

Gene symbols should be italicized; protein products of the loci are not italicized. Nonstandard abbreviations should be defined when first used in the text. Use of abbreviations should be kept at a minimum.

Title

The title should capture the conceptual significance for a broad audience. The most effective titles are no more than 10–12 words and provide an overall view of the paper's significance rather than the detailed contents of the paper, which can be elaborated upon in the Summary. Titles should avoid use of jargon, uncommon abbreviations, and punctuation. They should be no more than 150 characters total, including spaces, and must be able to be separated onto three lines of no more than 50 characters each (including spaces).

Authors/Affiliations

Author names should be spelled out. Institutional affiliations should be signified with footnotes. Affiliations should contain the following information: department(s)/subunit(s); institution; city, state/region, postal code; country. Please check author names carefully, as we cannot amend or correct these sections after publication without publishing a formal Correction.

Author List Footnotes

Footnotes are only allowed on page 1 of the text (and in tables). The only required footnote is the Lead Contact footnote. Additional footnotes may note a present address or may indicate equally contributing or senior authors. For more on designations of author contributions, please see the Authorship section.

Contact Info

Corresponding authors should be noted with an asterisk in the author list. The e-mail address(es) of the corresponding author(s) should be listed after the author list footnotes, e.g., "*Correspondence: john_doe@cell.com." Corresponding author(s) may additionally include Twitter handles as a means of contact.

Summary

The Summary is a single paragraph no longer than 150 words. An effective Summary includes the following elements: (1) a brief background of the question that avoids statements about how a process is not well understood; (2) a description of the results and approaches/model systems framed in the context of their conceptual interest; and (3) an indication of the broader significance of the work. We discourage novelty claims (e.g., use of the word “novel”) because they are overused, tend not to add meaning, and are difficult to verify. Please do not include references in the Summary.

Keywords

We encourage you to include up to ten keywords with your paper. These keywords will be associated with your paper on Cell Press platforms and on PubMed. These keywords should be listed in the manuscript after the Summary, separated by commas.

Introduction

Good introductions are succinct, presenting only the background information needed for readers to understand the motivation for the study and the results. No subheadings, please.

Results

This section should be divided with subheadings. In our view, good subheadings convey information about the findings, so we encourage you to be specific. For example, say "Factor X requires Factor Y to function in Process Z" rather than "Analysis of Factors X and Y using Approach Q." We recommend that you use similar language in your figure titles for clarity and structural harmony.

Discussion

The Discussion should explain the significance of the results and place them into a broader context. It is often helpful to the reader to indicate the directions in which the work might be built on going forward. It should not be redundant with the Results. The Discussion may contain subheadings and can be combined with the Results section.

Acknowledgments

Use this section to acknowledge contributions from non-authors, list funding sources, and declare any conflicts of interest. As this section contains important information and many funding bodies require inclusion of grant numbers here, please check it carefully.

Author Contributions

This section is required for all papers. Please use it to concisely describe each author's contributions, using initials to indicate each author's identity. We encourage you to use the CRediT taxonomy, but you can also use a traditional format (e.g., "A.B. and C.D. conducted the experiments; E.F. designed the experiments and wrote the paper.").

Declaration of Interests

This section is required for all papers. Please use it to disclose any competing interests, in accordance with Cell Press's Declaration of Interests policy. If there are no interests to declare, please note that with the following wording: "The authors declare no competing interests." The text in this section should match the text provided in the Declaration of Interests form.

References

References should include only articles that are published or in press. For references to in press articles, please confirm with the cited journal that the article is in fact accepted and in press, and include a DOI number and scheduled online publication date. Unpublished data, submitted manuscripts, abstracts, and personal communications should be cited within the text only and not included in the References list. Personal communication should be

documented by a letter of permission. Submitted articles should be cited as unpublished data, data not shown, or personal communication.

In-text citations should be written in Harvard style and not numbered, e.g., "Smith et al., 2015; Smith and Jones, 2015."

Please use the style shown below for references. Note that "et al." should only be used after ten authors.

Article in a periodical: Sondheimer, N., and Lindquist, S. (2000). Rnq1: an epigenetic modifier of protein function in yeast. Mol. Cell *5*, 163–172.

Article in a book: King, S.M. (2003). Dynein motors: Structure, mechanochemistry and regulation. In Molecular Motors, M. Schliwa, ed. (Weinheim, Germany: Wiley-VCH Verlag GmbH), pp. 45–78.

An entire book: Cowan, W.M., Jessell, T.M., and Zipursky, S.L. (1997). Molecular and Cellular Approaches to Neural Development (New York: Oxford University Press).

Figure Legends

Legends should be included in the submitted manuscript as a separate section. Each figure legend should have a brief title that describes the entire figure without citing specific panels, followed by a description of each panel. In writing the figure title, we encourage you to re-use the subheadings of the Results section to make the relationship clear. For any figures presenting pooled data, the measures should be defined in the figure legends (for example, "Data are represented as mean ± SEM."). Each legend should refer to any supporting items in the Supplemental Information (e.g., "See also Figure S1.").

Tables

Please use the Microsoft Word Table function to make tables; you may need to revise any tables that are not created using this function. Tables should include a title, and footnotes and/or legend should be concise. Include tables in the submitted manuscript as a separate section.

When creating tables, please adhere to the following guidelines:

- Do not submit tables in Excel or PDF format. Do not place an Excel table in a Word document.
- Format tables with Word's Table function; do not use tabs or spaces to create a table.

- Tables should be in black and white; rows and columns should not be shaded.
- Do not use line breaks or spaces to separate data within a cell. Use separate cells for all discrete data elements within a table.
- Number distinct tables as Table 1, Table 2, Table 3, etc., rather than as Table 1a, Table 1b, Table 1c, etc.
- If bold or italic font is used within a table to indicate some feature of the data, please give an explanation of its usage in the legend.
- All abbreviations within a table must be defined in the table legend or footnotes.
- Footnotes should be listed with superscript lowercase letters, beginning with “a.” Footnotes may not be listed with numbers or symbols.

Experimental Procedures

The Experimental Procedures should, at minimum, include enough detail to allow the reader to understand the general experimental design and to be able to assess the data presented in the figures. More detailed protocols and procedures needed for readers to reproduce experiments should be included in the Supplemental Experimental Procedures. Any supplemental tables that list materials used in the study (oligonucleotides, strains, etc.) should be included within the relevant section of the Supplemental Experimental Procedures; these tables should have a title but should not be numbered. If your paper contains Supplemental Experimental Procedures, please make sure that they are referred to within the main Experimental Procedures so that it is clear to the reader that additional details are available online. This section should also include a description of any statistical methods employed in the study. A more detailed version of the procedures and details such as oligo sequences, strains, and specifics of how constructs were made can be included in the Supplemental Information, but it is not appropriate to move the majority of the Experimental Procedures to Supplemental Information in order to shorten the text. Please see our complete Supplemental Information Guidelines for more information.

Supplemental Information

In general, please limit Supplemental Information to data and other materials that directly support the main conclusions of your paper but cannot be included in the main paper due to space or file format restrictions. SI should not be used to present data that are preliminary or that conceptually go beyond the main point of the paper.

Before submitting your supplemental materials, please refer to our complete instructions in the Supplemental Information guidelines. This page also contains information on submitting movie and other multimedia files.

How to Prepare and Submit Revised/Final Files

In addition to the sections required for initial submissions, revised manuscripts must also contain a detailed point-by-point response to the comments of the reviewers and/or editors. The cover letter should briefly summarize how the revised manuscript addresses these comments. In general, we allow 2–3 months for revision; if you think you might need more time, please contact the handling editor for guidance.

The final submission should also contain Highlights, an eTOC blurb, and a Graphical Abstract. These items will appear with the online version of the paper and on the PDF cover page. We have provided a handy checklist for preparing the final version of your paper.

Highlights and eTOC Blurb

Highlights are bullet points that convey the core findings of your paper. You may include up to four highlights. The length of each highlight cannot exceed 85 characters (including spaces).

The eTOC blurb is a short summary that describes the context and significance of the findings in your paper. It is widely seen, as it is included in the Table of Contents, so it should aim to showcase your findings in a way that is accessible to our very broad readership. Please see the "In Brief" links in the Table of Contents for examples. The blurb should be 50 words or less.

On the EM page where you are asked to upload your files, please choose "Highlights and eTOC Blurb" and upload a single Word document containing both items.

Graphical Abstract

A graphical abstract is an image that summarizes the main findings of a paper. It adds a rich, visual component to the start of a paper, helping readers to quickly appreciate and understand the central message.

Graphical abstracts may be submitted at any stage but are only required with the final submission. The image should be 5.5 inches square at 300 dpi, using Arial font with a size of 10–16 points; smaller fonts will not be legible online. Please refer to our graphical abstract guidelines for more details and recommendations.

Figures

Digital figure files submitted through Editorial Manager must conform to our digital figure guidelines or you will be asked to revise them. Please be aware that we may resize figures during the production process.

If you have any questions about figures, please contact Julie Fiorilla, Managing Editor of *Cell Reports*, at jfiorilla@cell.com.

Figure360

Figure360 is a 2- to 3-minute video that helps readers to grasp the major points of a figure, quickly and effectively. Given their utility, we encourage you to prepare F360 videos for your paper. Each F360 video covers one figure and is published alongside that figure. You may submit one video for each figure in your paper. For additional information, examples, and instructions on how to create a Figure360 video, please visit our Figure360 page for authors.

Cover Submissions

After acceptance, authors are welcome to submit potential cover images related to their manuscript. Cover submissions should be informative and may be based on or resemble figures in the article. But they should be creative and artistic. Authors may submit several different images for consideration. The editors make their selection based on the aesthetic quality of the image and the scientific scope of the study. For more information, see our Cover Submission Guidelines.

Methods Videos

We encourage you to make a Methods Video for your paper if you report any methods that are challenging or nuanced, or if you have an experimental setup that is hard to describe. These videos are short (≤1 min) and are intended to improve reproducibility and transparency. For examples and guidelines, go here.